

JAERI - M
86-029

NEANDC(J)117/U
INDC(JPN)103/L

PROCEEDINGS OF SPECIALISTS' MEETING
ON NUCLEAR DATA FOR FUSION NEUTRONICS

March 1986

(Ed.) Sin-iti IGARASI and Tetsuo ASAMI

日本原子力研究所
Japan Atomic Energy Research Institute

JAERI-Mレポートは、日本原子力研究所が不定期に公刊している研究報告書です。
入手の間合わせは、日本原子力研究所技術情報部情報資料課（〒319-11茨城県那珂郡東海村）
あて、お申しこしてください。なお、このほかに財団法人原子力弘済会資料センター（〒319-11茨城
県那珂郡東海村日本原子力研究所内）で複写による実費頒布をおこなっております。

JAERI-M reports are issued irregularly.
Inquiries about availability of the reports should be addressed to Information Division, Department
of Technical Information, Japan Atomic Energy Research Institute, Tokai-mura, Naka-gun,
Ibaraki-ken 319-11, Japan.

© Japan Atomic Energy Research Institute, 1986

編集兼発行 日本原子力研究所
印刷 日立高速印刷株式会社

Proceedings of Specialists' Meeting
on Nuclear Data for Fusion Neutronics

(Ed.) Sin-iti IGARASI and Tetsuo ASAMI

Nuclear Data Center

Tokai Research Establishment

Tokai-mura, Naka-gun, Ibaraki-ken

(Received January 31, 1986)

This report is the Proceedings of the Specialists' Meeting on the Nuclear Data for Fusion Neutronics. The meeting was held in July 23-25 1985 at Tokai Research Establishment of Japan Atomic Energy Research Institute, under the participation of twenty-odd specialists who were the members of Working Group on Nuclear Data for Fusion in Japanese Nuclear Data Committee and a part of the members of Subcommittee on Fusion Reactor in Japanese Committee on Reactor Physics. Review papers were presented for the evaluated data in JENDL-3PR1 and -3PR2, the data needs in the fusion reactor blanket design, the status of experimental and evaluated data for fusion neutronics, and the analyses of integral experiments. In a final stage of this meeting, the discussions were made in three working groups and the recommendations were reported from these three groups. The outlines of the discussions and the recommendations are also included in the Proceedings.

The texts are reproduced directly from the Author's manuscripts without any editing.

Keywords: Nuclear Data, Fusion Neutronics, Fusion Reactor,
Evaluation, Measurements, Data File, DDX, Integral
Experiment

核融合ニュートロニクスにおける核データ検討会報告書

日本原子力研究所東海研究所物理部

(編) 五十嵐信一・浅見 哲夫

(1986年1月31日受理)

この報告書は、“核融合ニュートロニクスにおける核データ検討会”の報文および討議内容をまとめたものである。検討会は1985年7月23日～25日の3日間、日本原子力研究所東海研究所の第5会議室において20数名の専門家の出席のもとに開催された。出席した専門家は主にシグマ研究委員会の核融合核データ・ワーキンググループのメンバーおよび炉物理研究委員会の核融合部会の一部のメンバーであった。この検討会の主要目的は、核融合ニュートロニクスの研究分野における核データ利用上の問題を検討し、それを整理してJENDL-3作成にフィードバックさせるとともに今後の研究に役立てることにある。とくに、核融合ニュートロニクス用として急遽用意されたJENDL-3PR1、PR2の核データの現状、問題点、それをを用いた積分実験の解析等が討議された。また、検討会の後半は、3つのサブグループ、A) JENDL-3に対するデータリクエスト、B) 実験解析への適用上の問題点、群定数化、フォーマット、C) 実験解析結果の核データへのフィードバックでの討論に当てられ、それぞれのグループからのまとめ、勧告等が出された。これらの討議内容も本報告書に収録されてある。

各報文は、早く刊行するために著者の原稿からそのまま直接に写真印刷を行い、編集の手を加えてない。

CONTENTS

Scope of the Meeting	S. Igarasi (JAERI).....	1
I. Nuclear Data Evaluation		
1. Review on Nuclear Data for Fusion Reactors		
	Y. Kanda (Kyushu Univ.).....	3
2. Status of JENDL-3PR1 and -3PR2	T. Asami (JAERI).....	15
3. Revision of the Neutron Nuclear Data of Lithium		
	S. Chiba (JAERI).....	32
4. On the Format of JENDL	T. Nakagawa (JAERI).....	41
II. From the Standpoints of Nuclear Design		
1. Nuclear Data and Integral Experiments Required for Fusion Reactor Nuclear Design		
	Y. Seki (JAERI).....	52
2. A High Tritium Breeding Ratio(TBR) Blanket Concept and Requirements for Nuclear Data relating to TBR		
	K. Maki (Hitachi Ltd.).....	57
3. On the Processing of the Nuclear Data File and the Problems of the JENDL		
	A. Hasegawa (JAERI).....	68
4. Double Differential Neutron Emission Cross Sections at 14 MeV Measured at OKTAVIAN		
	A. Takahashi (Osaka Univ.).....	99
5. Measurements of Double-Differential Neutron Emission Cross Sections at Tohoku University		
	M. Baba (Tohoku Univ.).....	119
III. Integral Experiments: Experimental Results and Analyses		
1. Nuclear Data Testing on Integral Experiments of Lithium Spheres		
	K. Sugiyama (Tohoku Univ.), J. Yamamoto (Osaka Univ.) and T. Iguchi (Univ. of Tokyo).....	141

2.	14 MeV Integral Experiment at OKTAVIAN to Check Differential Data of Secondary Neutrons	J. Yamamoto (Osaka Univ.).....	149
3.	Comparison between Measurements of the Neutron Spectra from Materials used in Fusion Reactors and Calculations using JENDL-3P1	H. Hashikura, Y. Oka and S. Kondo (Univ. of Tokyo).....	160
4.	Clean Benchmark Experiments and Analyses at FNS	H. Maekawa (JAERI).....	171
5.	Fusion Blanket Engineering Benchmark Experiments	T. Nakamura (JAERI).....	183
IV. Conclusions			
1.	Report of Subgroup A: Data Request for the JENDL-3.....		192
2.	Report of Subgroup B: The Problems of JENDL Encountered in the Experimental Analysis, in the Processing of Group Constants and of the Format Specifications.....		196
3.	Report of Subgroup C: The Feedback of Information from Neutronics Experiments and Their Analyses.....		203
4.	Discussions.....		207

Scope of the Meeting

S. Igarasi

Japan Atomic Energy Research Institute
Tokai-mura, Naka-gun, Ibaraki-ken

Study of the nuclear data pertaining to the fusion reactors has grown to be one of the smart and interesting fields. It is due to many fruits of studies obtained by engineers in the fusion reactor blanket design, reactor physicists making the computer codes for fusion neutronics calculations and group cross-section sets, evaluators of the nuclear data, and experimentalists concerned.

Nuclear data required by the engineers in the fusion reactor design field are diverse, and the requirements have become severe. To satisfy them, many measurements and evaluations for the nuclear data have been performed in the various countries. In Japan, measurements of the nuclear data have been made at Osaka University, University of Tokyo, Tohoku University, JAERI, etc. Nuclear data evaluation for JENDL-3 is now in progress, and is planned to complete by the end of 1986 fiscal year.

Prior to completion of the JENDL-3, the JENDL-3PR1 was tentatively prepared for analyses of the Japan-US cooperative experiments in simulated fusion blanket assemblies using the JAERI Fusion Neutronics Source (FNS). It was used successfully for the analyses not only of the integral experiments in JAERI but of the double differential neutron emission cross sections measured in the Universities.

Many reports related to the subject of the fusion neutronics experiments and analyses have been presented in the various meetings, such as annual meeting of Atomic Energy Society of Japan. Researchers used the JENDL-3PR1 in most cases in their calculations, when they compared their results with the theoretical calculations. They showed various questions about the nuclear data, and stimulated the evaluators to advance their work. Communications between nuclear data suppliers and users seem to be fairly good in this field.

Through discussions, however, it was sometimes found that they had misunderstanding or disagreed with each other about utilization or process of the nuclear data. There are, in particular, some anxieties in the connection between evaluated data files and data processing method for group cross sections, group cross-section sets and transport calculation codes, etc. These must be solved by spending enough time of discussions. Fortunately, knowledges of the experimental and evaluated data, of the merit and defect of the present evaluated data formats, and of the design calculations of the fusion reactor blanket are so accumulated recently that they can discuss these matters in detail. Hence, it is reasonable time to convene such a meeting as it focuses discussions on the boundaries between different aspects of researches.

This specialists' meeting aims to discuss problems concerning the nuclear data of the JENDL-3PR1, to make any vague points such as those in data formats, data utilization procedures, etc. clear, and to make recommendations for future studies of the related matters. Lectures and discussions in this meeting will be applied to the JENDL-3.

The meeting consists of lectures and group discussions. The latter is made in the following three working groups:

- (A) Data Request for the JENDL-3,
- (B) Problems of JENDL Encountered in the Experimental Analysis, in the Processing of Group Constants and of the Format Specifications,
- (C) Feedback of Information from Neutronics Experiments and Their Analyses.

The summaries of the group discussions as well as the lectures are presented in this Proceedings.

I. Nuclear Data Evaluation

1. Review on Nuclear Data for Fusion Reactors

Yukinori KANDA

Department of Energy Conversion Engineering

Kyushu University

Kasuga, Fukuoka 816, Japan

Abstract

Present status of fusion nuclear data is briefly reviewed taking account of the relation among differential experiment, evaluation, and integral experiment. It is emphasized that covariances should be introduced to the comparison between calculations and experiments and that model calculation should be effectively used in the evaluation of the fusion nuclear data. Preparation of reference data set is proposed to improve model calculation for neutronics.

1. Introduction

Recent development of plasma confinement technique stimulates experiments and plannings on blankets of fusion reactors. Neutron nuclear data are essential for these studies. In a D-T fusion reactor which is a first target in the program of fusion reactor development. Demand of tritium breeding from lithium in the blanket is one of the most marked characteristic of the D-T fusion reactor. Important data are the cross sections for ${}^6\text{Li}(n,\alpha)$ and ${}^7\text{Li}(n,n'\alpha)$ and for double differential cross sections of structural materials. The latter are used in calculation of neutron transport in the blanket.

In these studies, the computer codes developed for fast reactor calculation are applied to estimate neutron flux and tritium breeding ratio. However, nuclear data compiled for the fast reactor studies are insufficient to divert them to the fusion reactor calculation. Although typical data to be urgently improved for this application are ones described in the last paragraph, the elements of interest in fusion reactor technology are enumerated as showing in Table 1.

2. Improvement of Evaluated Nuclear Data

In the program of the fast reactor development, it has been recognized that the nuclear data are fundamental data base. For thermal reactors, they do not appear directly in planning of the system; briefly speaking, the four-factors of reactor physics are basic data. They are measured in integral experiments. Table 2 shows relation between the reactors and the nuclear data.

Neutronic studies for the fusion reactor have followed the manner of the fast reactor. It is seen in Fig. 1. Differential experiments and nuclear model calculation are referred to evaluate the nuclear data which are compiled as an evaluated nuclear data file such as JENDL or ENDF/B. Neutronic calculations are compared with integral experiments. The comparison indicates the points to be improved. In the integral experiment for the fusion reactor, relation of both the results is simple than for the fast breeding reactor, because fissile and fertile nuclides are not included and a neutron source is outside of the assembly in the former. This makes it easy to find how neutron cross sections should be modified in order to improve the ratio of calculation to experiment (C/E) for the integral experiment.

Absence of radionuclides in the integral experiment for the fusion reactor is favourable for experimenters because of easy sample handling. This is one of the reasons why the experiment is actively conducted in Japan. Especially, present works are concentrated on measurements of Tritium breeding ratio and neutron spectra in assemblers simulating the blanket

of the fusion reactor. Major neutron nuclear data in regard to these subjects are the tritium production cross section of Li and energy-angle differential neutron emission cross section (or called double differential cross section, DDX) $\sigma_n, em(E: E', \theta)$ of structural materials. However, there are many kinds of the neutron cross-section data demanded in the design applications for the fusion reactor. They are presented in Table 3 cited from Jarvis' report ¹⁾. Their data available at present have not always sufficient accuracy to use in design of the fusion reactor. Status of them are summarized in Table 4 ¹⁾.

The evaluated data will be gradually improved by these studies. However, target accuracies for the data should be considered on the basis of the present method which is performed qualitatively comparing calculations and experiments. There are three elements, the differential experiment, evaluation, and integral experiment. Their results must be consistent. Since they have proper uncertainties, reasonable data must be determined by taking account of them. An application of covariances in these procedures is an useful way to solve the problem, although estimation of the covariances for the data is very hard practically. The covariances for the evaluated data are given for some neutron data: for example, those of 15 nuclides are presented in ENDF/B-V.

The evaluated data have been revised referring comparison between the calculation and the integral experiment; the result depends on models of the neutronic calculation. In order to examine validity of the model, the evaluated data

having small uncertainties should be used in analysis of the integral experiment. For the purpose, it is intensively suggested to prepare a reference nuclear data set for a nuclide which has small variances for every cross section. Carbon-12 is to be a candidate nuclide for this proposal.

International fusion data meeting was held at Santa Fe on May 18, 1985. The scientists attending the meeting discussed and recommended that cooperation should be increased through evaluator-to-evaluator contact. A meeting synopsis was written by F. M. Mann. ²⁾ One can find the present activities for the fusion nuclear data in the world in his report.

3. Next subjects in fusion nuclear data

As presenting in the last section, there are many kinds of nuclear data demanded in application to design of the fusion reactor. Available differential experiments for them are scarce because of insufficiency of experimental facilities. It is the most severe condition to have no intense neutron source. It can not be expected to be improved the experimental condition in the near future. Therefore, the evaluation of the fusion nuclear data should be conducted using nuclear model calculation. Fortunately, the computer codes of the sophisticated model have been developed and also reasonable parameters used in the calculation have been studied. They can sufficiently compliment the scarcity of the experiment. Examples are the calculations of neutron induced reaction cross section for Cu, Ni and Cr by D. M. Hetrick et al. ³⁾ and of DDX by Y. Kikuchi et al. ⁴⁾.

Application of the covariances for the nuclear data and experiment should be promoted in this field to obtain the efficient nuclear data.

A proposal to evaluate the reference nuclear nuclear data set is presented in the last paragraph. It will be valuable to improve the model of the neutronic calculation.

The author deeply appreciate the members of the fusion nuclear data working group in Japan Nuclear Data Committee for their discussion.

References

- 1) O. N. Jarvis, European Appl. Res. Rept-Nucl. Sci. Technol. 3, 127 (1985)
- 2) M. Mann, Private Communication (1985)
- 3) D. M. Hetrick et al., Int'l Conf. Nuclear Data for Basic and Applied Science, Santa Fe, May 1985, JB-32.
- 4) Y. Kikuchi et al., J. Nucl. Sci. Tech. 22, 499 (1985)

Table 1 A list of the elements of interest in fusion reaction technology.

T Breeder	${}^6\text{Li}$, ${}^7\text{Li}$, ${}^{10}\text{B}$, ${}^{11}\text{B}$, ${}^3\text{He}$, ${}^9\text{Be}$
Neutron Multiplier	Be, Mo, Pb
Coolant	He, Li, F, Be, Na, Pb
Structural Material	Nb, Mo, V, Fe, Ni, Cr, Al, Ta, Si, C, Ti, Zr
Reflector	C, Fe, Ni, Cr, Be, Al, O
Shielding Material	H, O, ${}^{10}\text{B}$, Ca, Pb, Fe, C, Ta, W
Magnet	Al, Cu, Nb, Ti, Sn, V, Ga
Fission-Fusion Hybrid	Th, U, Pu

Table 2 Correlation of nuclear data and experiments for types of reactors.

Reactor	Differential Experiment	Evaluation	Integral Experiment	Cross Section
Thermal Reactor	Thermal neutron, Resonance region	World Value at 0.025 eV	4-factors	(n,f), Resonance integral
Fast Breeding Reactor	Many nuclides, Wide range of En, Extreme expectation (early stage)	Many studies, Discrepancy of experimental data, Difficulty of experiment	Utilization of 14 MeV neutron as an intense source, Reaction rate	(n,f), (n, γ), Scattering
Fusion Reactor	Can be expected more measurements? Hard experiments.	Extrapolation of works.	14 MeV neutron itself, Tritium breeding ratio	T- production, Anisotropy, Gas production, γ production, Activation

Table 3 Neutron cross-section data for CTR design applications.¹⁾

Reaction Cross-Section	Formulation	TRANSPORT						
		TRITIUM			HEATING DAMAGE (dpa + gas)	ACTIVATION SHIELDING	DOSIMETRY	
		PRODUCTION	NEUTRON MULT.	PARASTIC ABS.				
Total Absorption	$\sigma_{n,T}(E)$ $\sigma_{n,A}(E)$	✓			✓	✓	✓	✓
Differential elastic Total elastic	$\sigma_{n,n}(E; \theta)$ $\sigma_{n,n}(E)$	✓	✓	✓	✓	✓		✓
Energy-angle diff. inel. Energy diff. inel. Angular diff. inel. Total inelastic ³⁾	$\sigma_{n,n'}(E; E', \theta)$ $\sigma_{n,n'}(E; E')$ $\sigma_{n,n'}(E; \theta)$ $\sigma_{n,n'}(E)$	✓	✓	✓	✓	✓		✓
Capture Photon prod. in inel. scatt. Energy-angle diff. photon prod. ¹⁾ Energy diff. Photon prod. Total photon prod. Photon prod. in reactions ²⁾	$\sigma_{n,\gamma}(E)$ $\sigma_{n,n'}(E; E_{\gamma})$ $\sigma_{\gamma,em}(E; E_{\gamma}, \theta_{\gamma})$ $\sigma_{\dot{\gamma},em}(E; E_{\gamma})$ $\int \sigma_{\gamma,em}(E; E_{\gamma}) dE_{\gamma}$ $\sigma_{n,x}(E; E_{\gamma})$ $\sigma_{n,n'x}(E; E_{\gamma})$			✓	✓	✓	✓	✓
⁶ Li(n,α)T, ⁷ Li(n,n'α)T								
Energy-angle diff. neutron emission ¹⁾	$\sigma_{n,em}(E; E', \theta)$	✓			✓			
Energy-angle diff. neutron prod. (n,2n) (n,3n) (heavy elements)	$\sigma_{n,2n}(E; E', \theta)$ $\sigma_{n,2n}(E)$ $\sigma_{n,3n}(E)$		✓		✓	✓		✓
Charged particle emitting reactions ²⁾	$\sigma_{n,x}(E)$			✓	✓	✓		✓
Energy-angle charged particle ²⁾	$\sigma_{n,x}(E; E_x, \theta)$				✓	✓		
Neutron and charged particle emitting reactions ²⁾	$\sigma_{n,n'x}(E)$		✓		✓	✓	✓	✓
Energy-angle n + chgd. particle ²⁾	$\sigma_{n,n'x}(E; E_n, \theta)$				✓	✓		
Fission	$\sigma_{n,f}(E)$		✓		✓		✓	✓

Note: 1. The emission cross-sections are not reaction-type specific
 2. x ≡ p, d, t, α or ³He
 3. Isomeric states only

Table 4 Materials versus Transport Calculation Data Needs and Status. ¹⁾

	$\sigma_{n,T}(E)$	$\sigma_{n,em}(E;E',\theta)$	$\sigma_{n,2n}(E)$	$\sigma_{n,\gamma}(E;E\gamma)$	$\sigma_{\gamma,em}(E;E\gamma)$
H	S.	S.			S.
D	S.	U.	S.		
T	U.	U.			
He	S.	S.			
⁶ Li	S.	U.			
⁷ Li	S.	S.			S.
Be	S.	S.	U.		S.
¹⁰ B	S.	U.			A.
¹¹ B	S.	U.			A.
C	S.	S.			S.
N	S.	S.	S.		S.
O	S.	S.			U.
F	S.	U.	S.		S.
Na	S.	U.	S.		S.
Al	S.	S.	U.		S.
Si	S.	S.			S.
K	S.	U.	S.		U.
Ca	S.	U.			S.
Ti	S.	A.	U.		S.
V	S.	U.	U.		S.
Cr	U.	U.	U.		S.
Mn	S.	U.	S.		S.
Fe	S.	U.	S.		S.
Ni	S.	U.	U.		S.
Cu	S.	S.	S.		S.
Zr	S.	U.	S.		U.
Nb	S.	S.	S.	S.	S.
Mo	A.	U.	U.	S.	S.
Sn	S.	U.	U.		S.
Ta	S.	U.	U.	S.	U.
W	A.	U.	U.	S.	S.
Pb	S.	U.	U.		S.
Bi	S.	U.	U.		U.
²³² Th	S.	U.	U.		S.
²³⁸ U	S.	U.	A.		S.

Legend: Blank - no data needed
 S - present data appears satisfactory
 A - acceptable data anticipated soon
 U - uncertain; data inadequate, no work known in progress

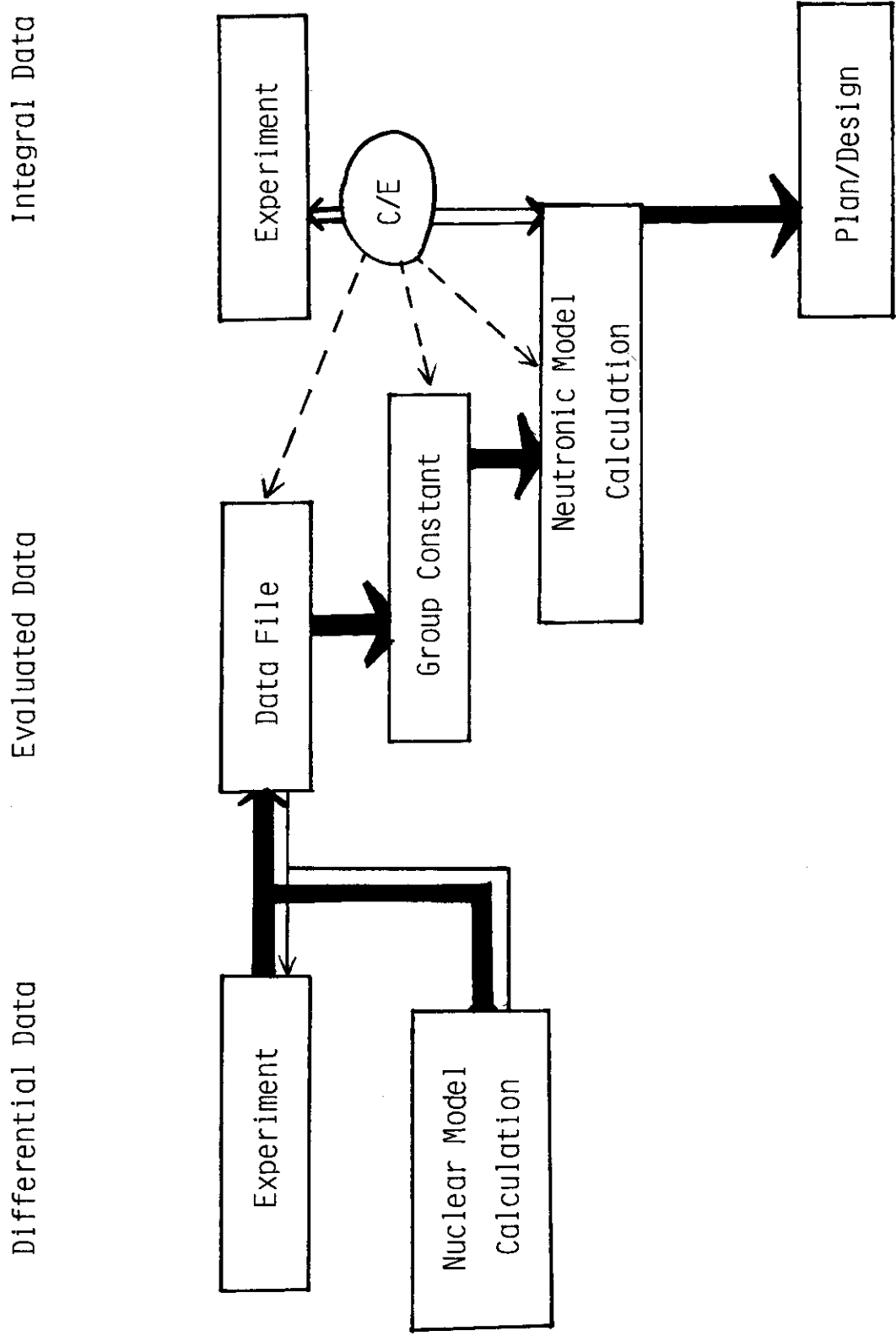


Fig.1 Flow chart of nuclear data in producing and improving.

2. Status of JENDL-3PR1 and 3PR2

Tetsuo ASAMI

Nuclear Data Center
Japan Atomic Energy Research Institute

Abstract

The compilation of JENDL-3PR1 and -3PR2 was made urgently to use their evaluated data for analyses of integral experiments for fusion neutronics. These files include the evaluated data for eight nuclides important for fusion neutronics, i.e., ${}^6\text{Li}$, ${}^7\text{Li}$, ${}^9\text{Be}$, ${}^{12}\text{C}$, ${}^{16}\text{O}$, Cr, Fe and Ni. The data for these nuclides except for ${}^{16}\text{O}$ were obtained by revising the JENDL-2 ones temporarily, and the ${}^{16}\text{O}$ data were evaluated newly. The outline and special features of these evaluated data are described briefly.

1. Introduction

The compilation of JENDL-2¹⁻²⁾ was completed in April 1983. From the benchmark tests and several analyses, the JENDL-2 data have been confirmed to be applicable to calculations for cores and shieldings of fission reactors³⁾. For the use in fusion research, however, it was pointed out that some data in JENDL-2 were generally not so good in the neutron energies higher than 5 MeV. In particular, the double differential cross section (DDX) deduced from the JENDL-2 data were insufficient for requirements from fields of fusion neutronics. In addition, JENDL-2 did not include the data of some nuclides which are important for fusion researches. In order to response an urgent requests from the fusion neutronics group in JAERI, we decided to

evaluate early for some nuclides important for fusion neutronics before the compilation of JENDL-3.

The evaluated data for eight nuclides (${}^6\text{Li}$, ${}^7\text{Li}$, ${}^9\text{Be}$, ${}^{12}\text{C}$, ${}^{16}\text{O}$, Cr, Fe and Ni) were compiled in the end of 1983. This temporary file is called JENDL-3PR1 (JENDL-3 Preliminary Version 1). The data for ${}^6\text{Li}$, ${}^7\text{Li}$, ${}^9\text{Be}$ and ${}^{12}\text{C}$ were reevaluated wholly aside of JENDL-2. The ${}^{16}\text{O}$ data were newly evaluated for this file. The some data for Cr, Fe and Ni were revised. Moreover, a part of the data for ${}^6\text{Li}$, ${}^7\text{Li}$ and ${}^{12}\text{C}$ were revised based on recent experimental data. These data are referred as JENDL-3PR2. Table 1 lists the nuclides of which data are stored in JENDL-3PR1 and 3PR2, and their evaluators. The status of the evaluated data included in these JENDL-3PR1 and -3PR2 is described briefly except for ${}^6\text{Li}$ and ${}^7\text{Li}$. The description for the latter two nuclides will be given by S. Chiba in this meeting later.

Table 2 through 7 show the changes of the contents for the evaluated data from JENDL-2 to JENDL-3PR1 and -3PR2 for ${}^9\text{Be}$ through Ni, respectively, using the definition of the ENDF/B format.

2. Evaluated data for ${}^9\text{Be}$

Since the ${}^9\text{Be}$ data⁷⁾ in JENDL-2 were estimated mainly from experimental data, some important data of which experimental ones did not exist and scarce, for example the evaluated data for the inelastic scattering, were not given in the file. The data of ${}^9\text{Be}$ in JENDL-3PR1, as shown in Table 2, were reevaluated by Shibata⁸⁾. The inelastic scattering cross sections and its angular distributons were estimated with the statistical model code CASTHY. The cross-section data for the (n,p), (n,d), (n,t) and (n, a_0) reactions were sharply modified based on the recent measurements. The evaluated data of the photon production were also given.

The DDX data deduced from the evaluated data of ^9Be in JENDL-3PR1 were compared with the experimental ones at OKTAVIAN in Osaka University⁹⁾ and with that of Tohoku University¹⁰⁾, as shown in Figs. 1 and 2, respectively. Generally the ^9Be data in JENDL-3PR1 reproduce the measured spectra in the lower energy region of secondary neutrons.

3. Evaluated data for ^{12}C

The whole reevaluation of the ^{12}C data was made by Shibata¹¹⁾ for JENDL-3PR1, since the inelastic scattering data of ^{12}C in JENDL-2¹²⁾ were insufficient for applications to fusion neutronics. Generally the data evaluation was made mainly based on the experimental data asking for help of theoretical estimations. The data for inelastic scattering leading to three discrete levels of 4.44, 7.65 and 9.63 MeV were estimated from the experimental ones. The total cross section in the range of 10 eV to 4.8 MeV and the angular distributions for elastic scattering were obtained based on the R-matrix theory using the RESCAL code. The angular distributions for inelastic scattering with the excitations of the 2nd and 3rd levels were obtained from the calculations with DWBA.

In order to fit further to the measured data of Osaka University¹³⁾, inelastic scattering with the excitation of the 3rd level (9.63 MeV) were revised, and the elastic scattering cross sections were modified to keep the evaluated total cross sections constant. The angular distributions for inelastic scattering leading to the 2nd and 3rd levels were also revised based on the measured data of Osaka University^{9,13)}. These data were compiled in JENDL-3PR2.

4. Evaluated data for ^{16}O

The ^{16}O data in JENDL-3PR1 were newly evaluated by JNDC Working Group on Nuclear Data for Fusion. The total and elastic scattering cross sections below 3 MeV were evaluated with R-matrix theory using RESCAL code. Above 3 MeV, the total cross section was estimated from the experimental data. The inelastic scattering cross sections exciting the discrete levels and their angular distributions were calculated with the statistical model code CASTHY. Only for the 2nd level the angular distribution was estimated with the coupled-channel calculation. The (n,p), (n,d) and (n,a) reaction cross sections were estimated based on the experimental data. The capture cross section was assumed to follow a $1/v$ law.

The evaluation of the photon production data are now in progress and the angular distributions for inelastic scattering with the excitation of the discrete levels are going to revise referring to recent measured data.

5. Evaluated data for Cr, Fe and Ni

As described above the high-energy data of the inelastic scattering cross sections of Cr, Fe and Ni in JENDL-2 were insufficient, in particular for the applications to fusion researches, because of the ignorance of the direct process. Therefore, the inelastic scattering data above about 5 MeV were revised and some related ones were changed somewhat. The data modifications were made in about the same way among these nuclides¹⁴⁾. For urgent and temporary modifications, this processes were done for their principal isotopes, namely ^{52}Cr (83.79%), ^{56}Fe (91.7%) and ^{58}Ni (67.76%), and the figures in the above parentheses denote their abundances in the elements. These isotopic data were used

as their elemental ones. The direct process in inelastic scattering was estimated from the calculation with a coupled-channel optical model using the ECIS code. The pre-compound effect for a whole of the discrete levels was estimated using the GNASH code and its contribution for each level was shared equally. The double differential neutron emission cross sections reproduced from these revised data were compared with the data measured at OKTAVIAN in Osaka University, as shown in Figs. 3, 4, and 5 for Cr, Fe and Ni, respectively. In general, the data in JENDL-3PR1 were fairly improved comparing with that in JENDL-2. The Cr data of JENDL-3PR1 are also fairly good compared with the ENDF/B-IV data. The Ni data in JENDL-3PR1 are somewhat good than that of ENDF/B-IV. The Fe data have a nearly same trend between JENDL-3PR1 and ENDF/B-IV. For Cr, Fe and Ni for JENDL-3, the more detailed evaluations are now in progress.

6. Conclusions

The status of the evaluated data in JENDL-3PR1 and -3PR2 was described above. The special features of these data are summarized briefly as follows:

- 1) Revised the data for high-energy neutrons whose leading parts are 14-MeV neutrons.
- 2) Evaluated the nuclear data for light nuclides in detail.
- 3) Taking account of the double differential cross sections (DDX) for neutron emission, in the data evaluation.

The data evaluations for JENDL-3 are now going on mainly in JNDC Working Groups aiming at the accomplishment in March 1987. Before the compilation of JENDL-3, some modifications will be also given for the data in JENDL-3PR1 and -3PR2. In JENDL-3, the data for photon

production will be newly given for some important nuclides, and DDX data also will be examined in detail to give a good fitting to experimental data.

References

- 1) Nakagawa, T. (ed.): Summary of JENDL-2 General Purpose File, JAERI-M 84-103(1984).
- 2) Asami, T. and Narita, T. (ed.): Graphs of Evaluated Neutron Cross Sections in JENDL-2, JAERI-M 84-052(1984).
- 3) For example:
Kikuchi, Y., Narita, T. and Takano, H.: Nucl. Sci. Tech. 17, 567 (1980); Kawai, M., Yamano, N., Hashikura, H., Minami, K., Sasaki, K., Mandai, S. and Kikuchi, Y.: Proc. 6th Intern. Conf. Radiation Shielding, Tokyo, 1983, Vol.1, p.428 (1983).
- 4) Shibata, K.: Evaluation of Neutron Nuclear Data of ${}^6\text{Li}$ for JENDL-3, JAERI-M 84-198 (1984).
- 5) Shibata, K.: Evaluation of Neutron Nuclear Data of ${}^7\text{Li}$ for JENDL-3, JAERI-M 84-204 (1984).
- 6) Chiba, S. et al.: Interaction of Fast Neutrons with ${}^{6,7}\text{Li}$, presented at Intern. Conf. Nuclear Data for Basic and Applied Science, Santa Fe, May 1985.
- 7) Shibata, K. and Ioki, K.: Neutron Nuclear Data of ${}^9\text{Be}$ Adopted in JENDL-2, JAERI-M 84-226 (1984).
- 8) Shibata, K.: Evaluation of Neutron Nuclear Data of ${}^9\text{Be}$ for JENDL-3, JAERI-M 84-226 (1984).
- 9) Takahashi, A. et al.: Proc. of Intern. Conf. on Nuclear Data for Science and Technology, Antwerp 1982, 360 (1983).

- 10) Baba, M. et al.: Proc. of Intern. Conf. on Neutron Physics and Nuclear Data for Reactors and Other Applied Purposes, Harwell 1978, 198 (1979).
- 11) Shibata, K.: private communication (1985).
- 12) Shibata, K.: Evaluation of Neutron Nuclear Data for ^{12}C , JAERI-M 83-221 (1983).
- 13) Ono, M. et al.: private communication (1984).
- 14) Kikuchi, Y., Shibata, K., Asami, T., Sugi, T. and Yamakoshi, H.: J. Nucl. Sci. Tech. 22, 499(1985).

Table 1 The nuclides instored in JENDL-3PR1 and 3PR2
and the data evaluators.

JENDL-3PR1		-3PR2	
(July 1984)		(March 1985)	
${}^6\text{Li}$	} Reevaluated by K. Shibata ^{4),5)}	${}^6\text{Li}$	} Revised by S. Chiba ⁶⁾
${}^7\text{Li}$		${}^7\text{Li}$	
${}^9\text{Be}$	Reevaluated by K. Shibata ⁷⁾		
${}^{12}\text{C}$	Reevaluated by K. Shibata ¹²⁾	${}^{12}\text{C}$	Revised by K. Shibata ¹¹⁾
${}^{16}\text{O}$	Newly Evaluated by JNDC WG on Nuclear Data For Fusion		
Cr	} Revised by Y. Kikuchi et al. ¹⁴⁾		
Fe			
Ni			

Table 2 The contents of the ^9Be evaluated data for JENDL-2, JENDL-3PR1 and -3PR2 in the ENDF/B definitions.

^9Be			
JENDL-2		JENDL-3PR1 & -3PR2	
MF	MT	MF	MT
3	1	<u>3</u>	<u>1</u>
	2		<u>2</u>
	16		<u>4</u>
	102		<u>6-9</u>
	103		<u>16</u>
	104		<u>24</u>
	105		<u>46-49</u>
	107		<u>51</u>
			<u>52</u>
			<u>102</u>
		<u>103</u>	
		<u>104</u>	
		<u>105</u>	
		<u>107</u>	
		<u>740(n, t₀)</u>	
		<u>741(n, t₁)</u>	
4	2	<u>4</u>	<u>2</u>
	16		<u>6-9</u>
			<u>16</u>
			<u>24</u>
			<u>46-49</u>
			<u>51</u>
			<u>52</u>
5	16	<u>5</u>	<u>16</u>
			<u>24</u>
			<u>46-49</u>
		<u>12</u>	<u>102</u>
			<u>741</u>
		<u>14</u>	<u>102</u>
			<u>741</u>

The underlines show some change or addition in the evaluated data in the course from JENDL-2 to JENDL-3PR1.

Table 3 The contents of the ^{12}C evaluated data for JENDL-2, JENDL-3PR1 and -3PR2 in the ENDF/B definitions.

^{12}C

JENDL-2		JENDL-3PR1		JENDL-3PR2	
MF	MT	MF	MT	MF	MT
3	1	<u>3</u>	<u>1</u>	<u>3*</u>	<u>1</u>
	2		<u>2</u>		<u>2*</u>
	4		<u>3</u>		<u>3*</u>
	51		<u>4</u>		<u>4*</u>
	91		<u>51(4.44)</u>		<u>51</u>
	102		<u>52(7.65)</u>		<u>52</u>
	107		<u>53(9.63)</u>		<u>53*</u>
			<u>91</u>		<u>91</u>
			<u>102</u>		<u>102</u>
			<u>103</u>		<u>103</u>
		<u>104</u>		<u>104</u>	
		<u>107</u>		<u>107</u>	
4	2	<u>4</u>	<u>2</u>	<u>4*</u>	<u>2</u>
	51		<u>51</u>		<u>51</u>
	91		<u>52</u>		<u>52*</u>
			<u>53</u>		<u>53*</u>
			<u>91</u>		<u>91*</u>
5	91	<u>5</u> Z <u>91</u>		<u>5</u>	<u>91</u>
		<u>12</u>	<u>51</u>	<u>12</u>	<u>51</u>
			<u>102</u>		<u>102</u>
		<u>14</u>	<u>51</u>	<u>14</u>	<u>51</u>
			<u>102</u>		<u>102</u>

The underlines show some change or addition in the evaluated data in the course from JENDL-2 to JENDL-3PR1. The asterisks show further modifications.

Table 4 The contents of the ^{16}O evaluated data for JENDL-3PR1 in the ENDF/B definitions.

^{16}O

JENDL-2	JENDL-3PR1 & -3PR2		
	MF	MT	
none	<u>3</u>	<u>1</u>	
		<u>2</u>	
		<u>3</u>	
		<u>4</u>	
		<u>16</u>	
		<u>51-79</u>	
		<u>91</u>	
		<u>102</u>	
		<u>103</u>	
		<u>104</u>	
		<u>107</u>	
		<u>4</u>	<u>2</u>
			<u>16</u>
			<u>51-79</u>
			<u>91</u>
	<u>5</u>	<u>16</u>	
		<u>91</u>	

Table 5 The contents of the Cr evaluated data for JENDL-2, JENDL-3PR1 and -3PR2 in the ENDF/B definitions.

Cr

JENDL-2		JENDL-3PR1 & -3PR2	
MF	MT	MF	MT
3	1	<u>3</u>	1
	2		<u>2</u>
	4		<u>4</u>
	16		16
	28		28
	51-90		<u>51-90</u>
	91		<u>91</u>
	102		102
	103		103
	107		107
4	2	<u>4</u>	<u>2</u>
	16		16
	28		28
	51-90		<u>51-90</u>
	91		91
5	16	<u>5</u>	<u>16</u>
	28		<u>28</u>
	91		<u>91</u>

The underlines show some modification in the evaluated data in the course from JENDL-2 to JENDL-3PR1.

Table 6 The contents of the Fe evaluated data for JENDL-2,
JENDL-3PR1 and -3PR2 in the ENDF/B definitions.

Fe

JENDL-2		JENDL-3PR1 & -3PR2	
MF	MT	MF	MT
3	1	<u>3</u> Z	1
	2		<u>2</u>
	4		<u>4</u>
	16		16
	51-83		<u>28</u>
	91		<u>51-83</u>
	102		<u>91</u>
	103		102
	107		103
			107
4	2	<u>4</u>	<u>2</u>
	16		16
	51-83		<u>51-83</u>
	91		91
5	16	<u>5</u>	<u>16</u>
	91		<u>28</u>
			<u>91</u>

The underlines show some modification in the evaluated data
in the course from JENDL-2 to JENDL-3PR1.

Table 7 The contents of the Ni evaluated data for JENDL-2, JENDL-3PR1 and -3PR2 in the ENDF/B definitions.

Ni

JENDL-2		JENDL-3PR1 & -3PR2	
MF	MT	MF	MT
3	1	<u>3</u>	1
	2		<u>2</u>
	4		<u>4</u>
	16		16
	17		17
	22		22
	28		28
	51-90		<u>51-90</u>
	91		<u>91</u>
	102		102
	103		103
	107		107
	4	2	<u>4</u>
16			16
17			17
22			22
28			28
51-90			<u>51-90</u>
91			91
5	16	<u>5</u>	<u>16</u>
	17		17
	22		22
	28		<u>28</u>
	91		<u>91</u>

The underlines show some modification in the evaluated data in the course from JENDL-2 to JENDL-3PR1.

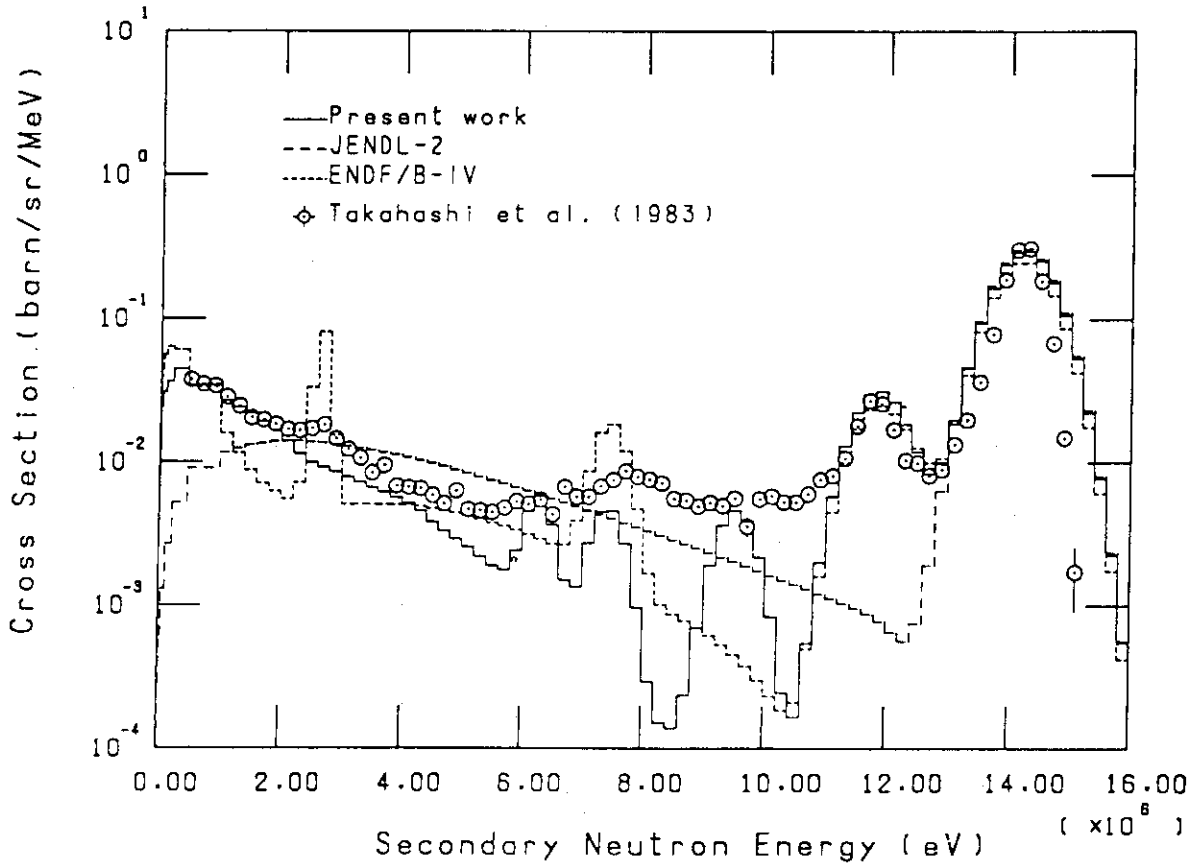


Fig.1 DDX of Be-9 (32 deg.) (Ref(8))

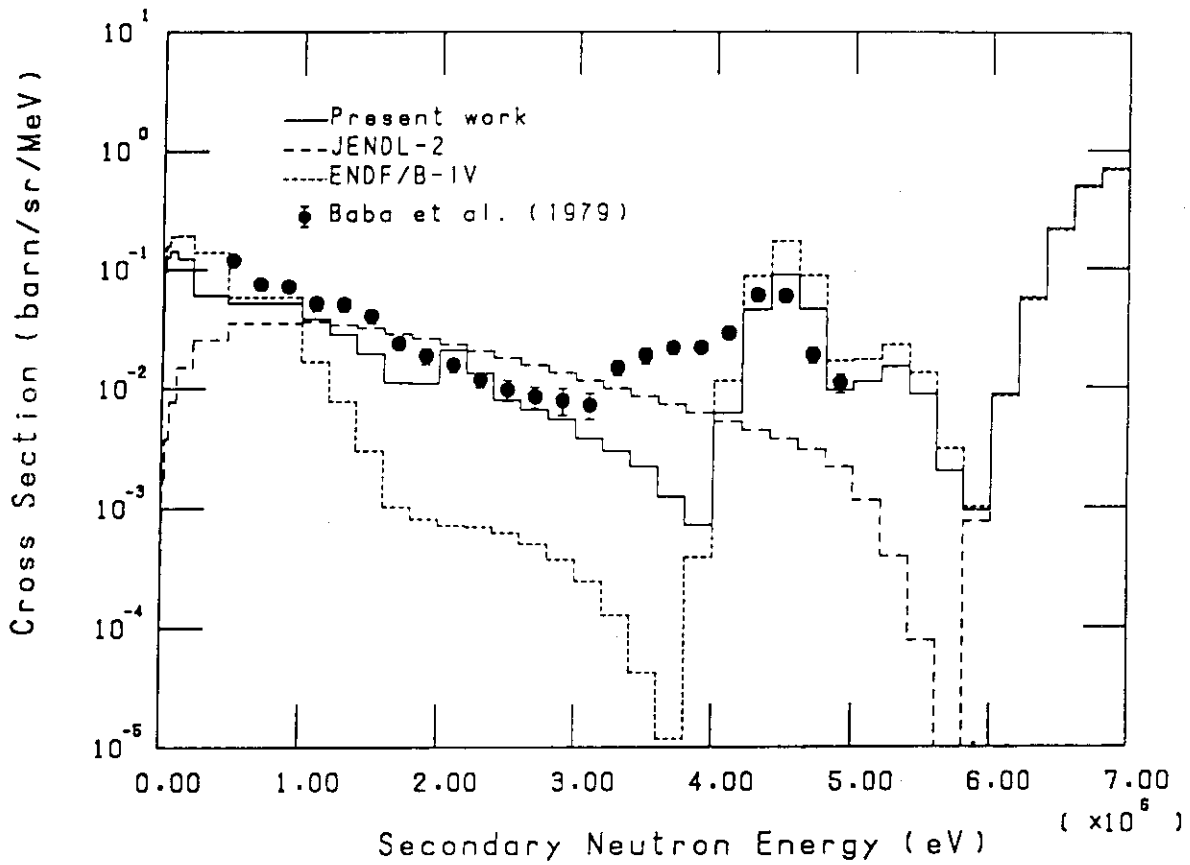


Fig.2 DDX of Be-9 (25.9 deg.) at 7.05 MeV (Ref(8))

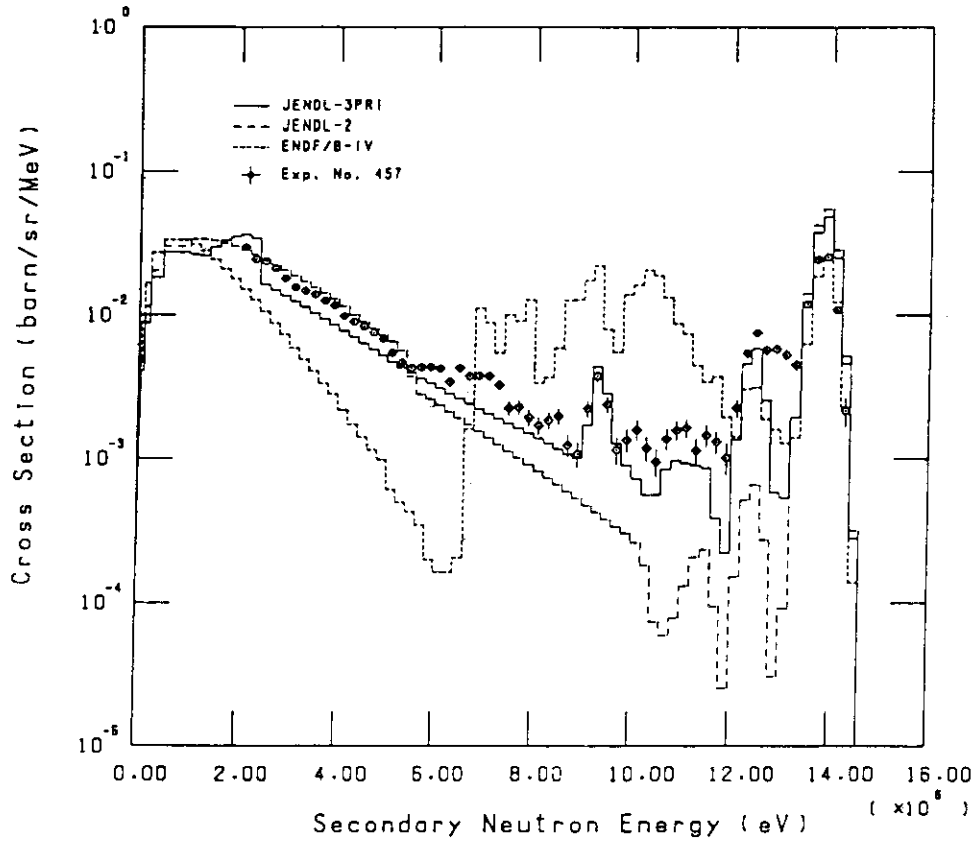


Fig.3 Comparison between DDX Files of Nat. Cr (80 deg.) (Ref(14))

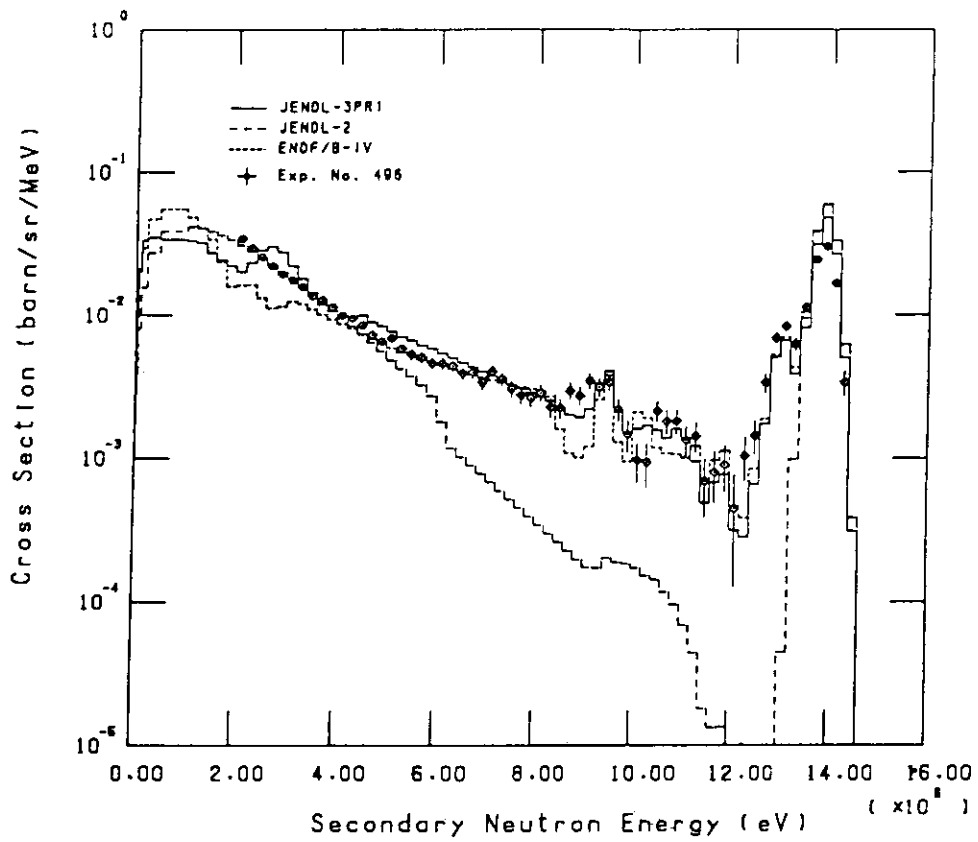


Fig.4 Comparison between DDX Files of Nat. Fe (80 deg.) (Ref(14))

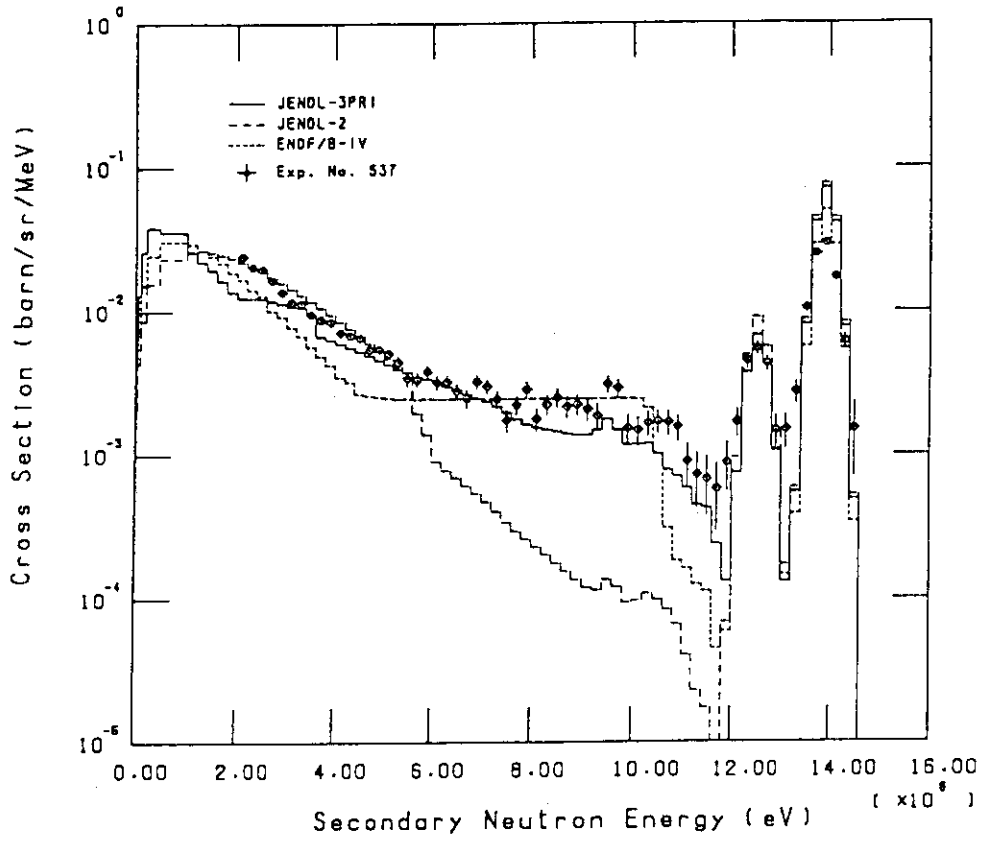


Fig.5 Comparison between DDX Files of Nat. Ni (80 deg.) (Ref(14))

3. Revision of the Neutron Nuclear Data of Lithium

Satoshi Chiba

Japan Atomic Energy Research Institute

Abstract

Neutron nuclear data of ${}^6\text{Li}$ and ${}^7\text{Li}$ stored in JENDL-3PR1 were revised, mainly on the basis of the double differential cross sections measured at Osaka and Tohoku Universities. Results of the analyses of some integral experiments were also taken into consideration. The present revision was restricted to the neutron emitting reactions. The revised data reproduce well the measured double differential cross sections.

1. Introduction

Since the evaluation for JENDL-3PR1, the first preliminary version of JENDL-3, was finished, many differential and integral neutron experiments have been done so far and JENDL-3PR1 has been compared with them. There are many evidences that the data in JENDL-3PR1 are superior to the JENDL-2 data. With regard to the data of lithium^{1).2)}, however, several problems were pointed out^{3).4).5)}:

- 1) Some higher levels not considered in the JENDL-3PR1 evaluation should be treated as discrete levels.
- 2) The elastic scattering cross section of ${}^7\text{Li}$ is overestimated as much as 10% at high energies.
- 3) The energy distributions of the continuum neutrons emitted from the ${}^6\text{Li}(n,n'd)\alpha$, ${}^7\text{Li}(n,n't)\alpha$ and ${}^6,7\text{Li}(n,2n)$ reactions are not appropriate.
- 4) The cross section of the ${}^6\text{Li}(n,2n)$ reaction is also overestimated.

These suggestions should be highly reliable, because they were commonly made from both of the differential and integral experiments. Therefore we decided to revise the data of ${}^6\text{Li}$ and ${}^7\text{Li}$. The revision was mainly based on the double differential cross sections (DDX) measured at Osaka⁶⁾ and Tohoku⁴⁾ Universities.

This paper describes the procedure and the results of the revision work for both nuclei. The evaluated data were compiled in the ENDF/B-V format.

2. Elastic and Inelastic Scattering to Discrete Levels

For each nucleus, two discrete levels (4.31 and 5.71 MeV for ${}^6\text{Li}$, and 6.68 and 7.467 MeV for ${}^7\text{Li}$) were newly considered. The excitation functions and angular distributions of neutrons for these levels were calculated with the coupled-channel model, except the 7.467-MeV level of ${}^7\text{Li}$. The coupling schemes and the optical potential parameters of Chiba et al.⁷⁾ were used in this calculation. The parameters are listed in Table 1.

The calculated excitation functions of the newly considered levels were normalized to the experimental data^{4),6)}. The 7.467-MeV level of ${}^7\text{Li}$ was assumed to have the same excitation function as that of the 6.68-MeV level.

The angular distribution for the 5.71-MeV level of ${}^6\text{Li}$ was assumed to be isotropic in the center-of-mass system.

For the first (0.478 MeV) level of ${}^7\text{Li}$, the angular distributions were calculated with the R-matrix theory adopting the parameters of Knox and Lane⁸⁾ below 10 MeV. Above 10 MeV, the coupled-channel calculation was performed. For the second (4.63 MeV) level, the R-matrix calculation was used below 8 MeV. The experimental data of Hogue et al.⁹⁾ were adopted in the energy range between 8 and 14 MeV. Above 14 MeV, the coupled-channel calculation was adopted. The angular distribution for the 7.467-MeV level was assumed to be isotropic in the center-of-mass system.

The angular distributions of the elastically scattered neutrons were also replaced with the calculated values above 14 MeV.

The elastic scattering cross section of ${}^7\text{Li}$ was reduced by 5% at 14 MeV. This reduction caused decrement of the total cross section by 3.5% at this energy.

The angular distributions of the elastically and inelastically scattered neutrons from ${}^7\text{Li}$ around 14 MeV were displayed in Figs. 1 and 2. Fig. 3 shows the total cross section of ${}^7\text{Li}$ between 10 and 20 MeV.

3. ${}^6\text{Li}(n,n'd)\alpha$ and ${}^7\text{Li}(n,n't)\alpha$ reactions

In the evaluation for JENDL-3PR1, the cross sections of the newly considered discrete levels were included in those for the ${}^6\text{Li}(n,n'd)\alpha$ and ${}^7\text{Li}(n,n't)\alpha$ reactions. Therefore the cross sections for the

${}^6\text{Li}(n,n'd)\alpha$ and ${}^7\text{Li}(n,n't)\alpha$ reactions were reduced by the contributions of the newly added levels.

The energy-angle distributions of the continuum neutrons were evaluated with the model of Holland et al.²⁰⁾:

$$\frac{d^2\sigma}{dEcd\Omega} \propto C_0^2 \cdot \rho, \quad (1)$$

$$C_0^2 = \frac{2\pi\eta}{\exp(2\pi\eta) - 1}, \quad (2)$$

$$\eta = \frac{Z_2 Z_3 e^2}{\hbar v_{23}}, \quad (3)$$

$$\rho = [E(E_{\max} - E)]^{1/2}, \quad (4)$$

where E is the energy of the secondary neutrons in the center-of-mass system and E_{\max} is its kinematically allowed maximum value. Subscript 2 means d for ${}^6\text{Li}$ and t for ${}^7\text{Li}$, and 3 means α . v_{23} is the relative velocity of particles 2 and 3 in the final state. ρ stands for the three body phase space distribution adopted in JENDL-3PR1. Eq. (1) gives a spectrum softer than ρ .

In the present evaluation, pseudo levels were used to express Eq. (1). The excitation energies of the pseudo levels were given by 0.5 MeV intervals. Cross section for each level could be calculated by integrating Eq. (1) in corresponding energy interval, because E is directly related to the excitation energy. Sum of the cross sections of these levels were normalized to the ${}^6\text{Li}(n,n'd)\alpha$ and ${}^7\text{Li}(n,n't)\alpha$ reaction cross sections.

For the angular distributions of the pseudo levels of ${}^7\text{Li}$, that of the continuum neutrons measured by Chiba et al.⁴⁾ were given. For ${}^6\text{Li}$, they were treated as isotropic in the center-of-mass system.

4. The (n,2n) Reactions

The energy distributions of the secondary neutrons from the ${}^6,7\text{Li}(n,2n)$ reactions were evaluated by the conventional evaporation model. For the evaporation temperatures, the data of Chiba et al.⁴⁾ were adopted. The angular distributions of neutrons emitted from these reactions were also replaced by the data in Ref. 4. In addition to these

modifications, the ${}^6\text{Li}(n,2n)$ reaction cross section was reduced by 20% in the whole energy range so as to reproduce the experimental data^{4),21),22)}. Fig. 4 shows the ${}^6\text{Li}(n,2n)$ reaction cross section.

5. Double Differential Cross Sections (DDX)

In Figs. 5 to 7, the DDX reproduced from the present evaluation are compared with those from JENDL-3PR1, ENDF/B and the experimental data^{4),6)}. The lines representing the evaluated data were calculated from the data in the MT numbers of 3, 4 and 5. As seen, the present evaluation reproduces the measured data very well. In the present evaluation, the energy-angle correlation of the continuum neutrons was easily taken into account, because of introduction of pseudo levels.

6. Concluding Remarks

The neutron nuclear data of ${}^6\text{Li}$ and ${}^7\text{Li}$ stored in JENDL-3PR1 have been revised. The revision was restricted to the neutron emitting reactions. The present work has been performed taking account of the measurements of the differential and integral data available at March, 1985.

With regard to discrete levels, the results of the R-matrix and coupled-channel calculations were utilized. Consideration of the two higher levels for both nuclei remarkably improved the evaluated data.

Concerning the continuum neutrons, cross sections and energy-angle distributions of the secondary neutrons were expressed by the pseudo-levels spaced by 0.5 MeV interval.

The energy distributions of the ${}^{6,7}\text{Li}(n,2n)$ reactions were evaluated with the conventional evaporation model. The cross section for the ${}^6\text{Li}(n,2n)$ reaction was reduced by 20% in the whole energy range.

The elastic scattering cross section of ${}^7\text{Li}$ was reduced by 5% at 14 MeV. This reduction caused decrement of the total cross section by 3.5% at 14 MeV. This total cross section might be underestimated, as seen in Fig. 3. This problem is left for future work.

Acknowledgement

The author would like to thank Dr. K. Shibata for his helpful discussion and advice throughout this work. He is also grateful to Dr. T. Nakagawa for his advice in making data files. He also thanks to Drs. S. Igarasi and Y. Kikuchi for their valuable advice.

References

- 1) K. Shibata, "Evaluation of Neutron Nuclear Data of ${}^6\text{Li}$ for JENDL-3", JAERI-M 84-198(1984).
- 2) K. Shibata, "Evaluation of Neutron Nuclear Data of ${}^7\text{Li}$ for JENDL-3", JAERI-M 84-204(1984).
- 3) K. Sugiyama et al., "Neutronic Experiments in a 120 cm Lithium Sphere", presented at the 13th SOFT on September 24-28, 1984, at Varese, Italy.
- 4) S. Chiba et al., to be published in J. Nucl. Sci. Technol.
- 5) H. Hashikura et al., private communication (1984).
- 6) A. Takahashi, private communication (1984), and J. Yamamoto et al., "Measurement and Analysis of Leakage Neutron Spectra from Lithium Sphere with 14MeV Neutrons", Int. Conf. Nucl. Data for Basic and Applied Sciences, Santa Fe, USA, May 1985, JA36.
- 7) S. Chiba et al., "Interaction of Fast Neutrons with ${}^{6,7}\text{Li}$ ", *ibid.*, JA50.
- 8) H.D. Knox and R.O. Lane, Nucl. Phys., A359(1981)131.
- 9) H.H. Hogue et al., Nucl. Sci. Eng., 69(1979)22.
- 10) C. Wong et al., Nucl. Phys., 33(1962)680.
- 11) A.H. Armstrong et al., Nucl. Phys., 52(1964)505.
- 12) F. Merchez et al., "Etude de la Diffusion Elastique et Inelastique des Neutrons de 14 MeV par les Noyaux ${}^6\text{Li}$, ${}^7\text{Li}$ et ${}^9\text{Be}$ ", Nuclear Data for Reactors, Vol. 1, 393(1967).
- 13) M. Hyakutake et al., J. Nucl. Sci. Technol., 11(1974)407.
- 14) J.H. Coon et al., Phys. Rev., 88(1952)562.
- 15) A. Bratenahl et al., Phys. Rev., 110(1958)927.
- 16) J.M. Peterson et al., Phys. Rev., 120(1960)521.
- 17) D.G. Foster Jr. et al., Phys. Rev., C 3(1971)576.
- 18) C.A. Goulding et al., EXFOR10251002 (1972).
- 19) G.P. Lamaze et al., Bull. Am. Phys. Soc., 24(1979)862.
- 20) R.E. Holland et al., Phys. Rev., C 19(1979)592.
- 21) V.J. Ashby et al., Phys. Rev., 129(1963)1771.
- 22) D.S. Mather et al., "Measurement of (n,2n) and (n,3n) Cross Sections at 14 MeV Incident Energy", AWRE-O-47/69(1969).

TABLE 1 Optical potential and deformation parameters

	V(MeV)	r(fm)	a(fm)	W_s (MeV)	r_1 (fm)	a_1 (fm)	β_2
${}^6\text{Li}$	45.08	1.188	0.5734	0.4432E-1.163	1.611	0.2674	1.1395
${}^7\text{Li}$	49.62-0.3622E	1.280	0.6198	1.8797E-13.24	1.338	0.1039	0.9521

E=Incident neutron energy in the laboratory system (MeV)

$V_{so}=5.5$ MeV, $r_{so}=1.15$ fm, $a_{so}=0.5$ fm

Coupling Schemes:

${}^6\text{Li}$; 1^+ (G.S.) - 3^+ (2.185) - 2^+ (4.31) - 1^+ (5.7)

${}^7\text{Li}$; $3/2^-$ (G.S.) - $1/2^-$ (0.478) - $7/2^-$ (4.63) - $5/2^-$ (6.68)

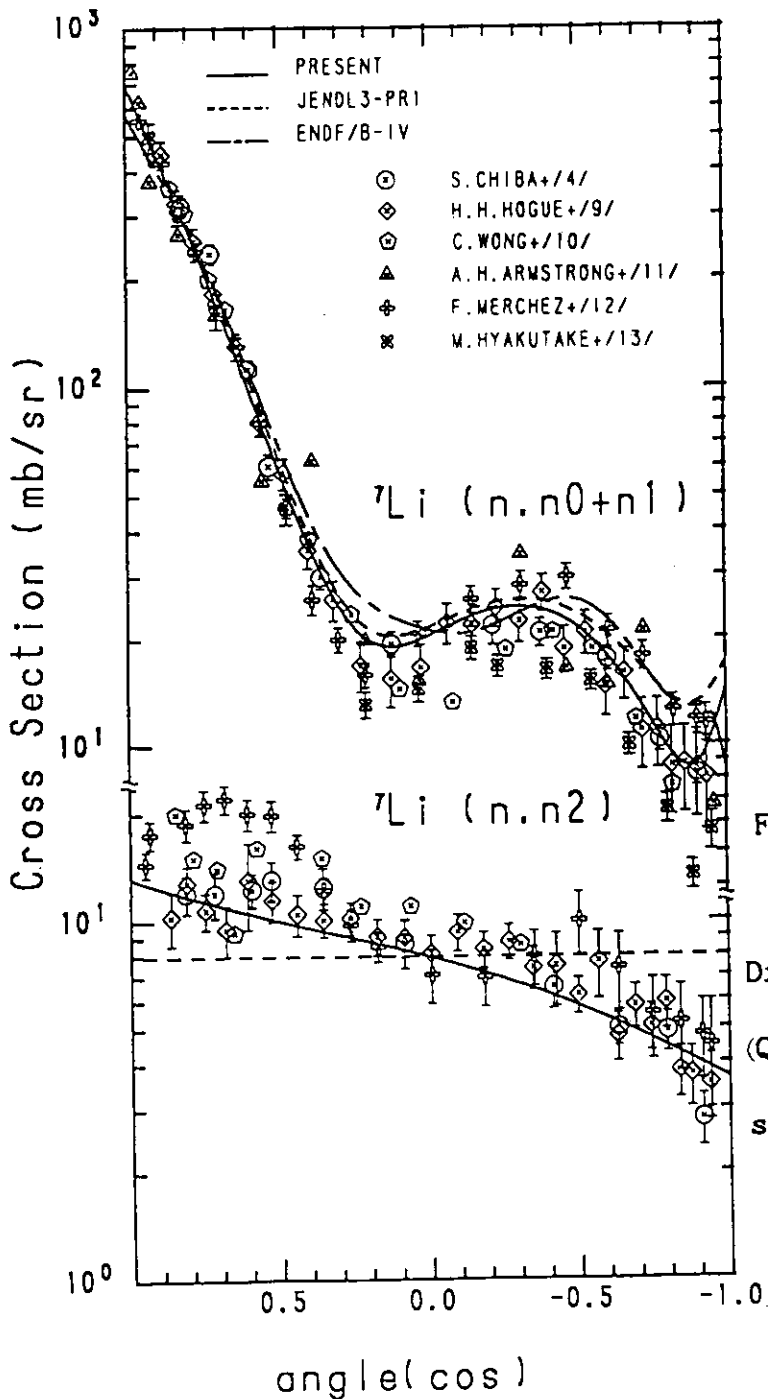


Fig.1

Differential elastic and inelastic
($Q=-4.63$ MeV) scattering cross
sections of ${}^7\text{Li}$ around 14 MeV

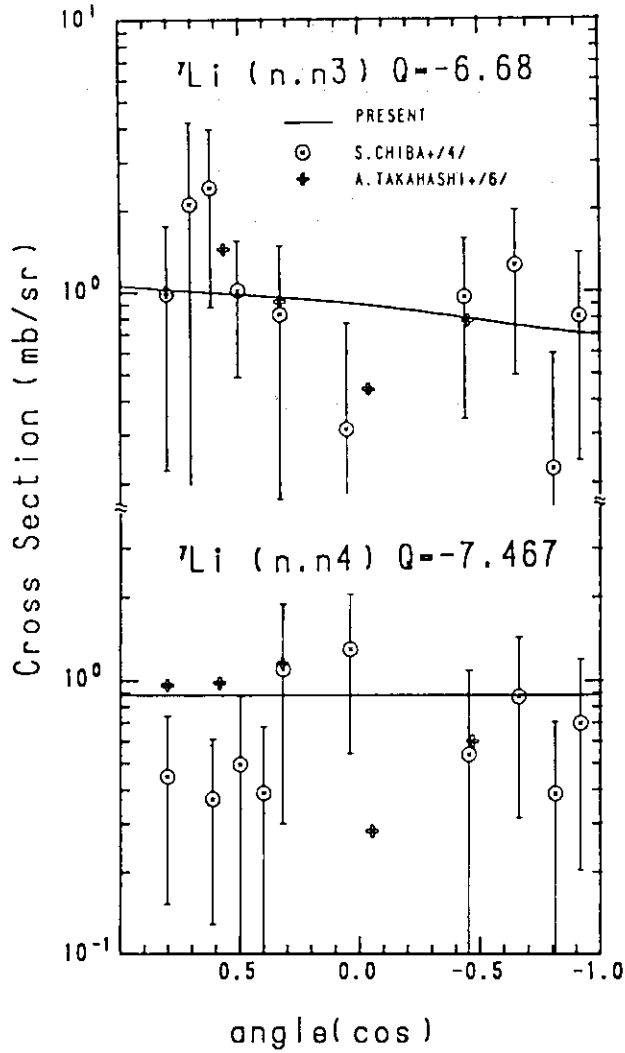


Fig.2

Differential inelastic scattering cross sections of ${}^7\text{Li}$ around 14 MeV

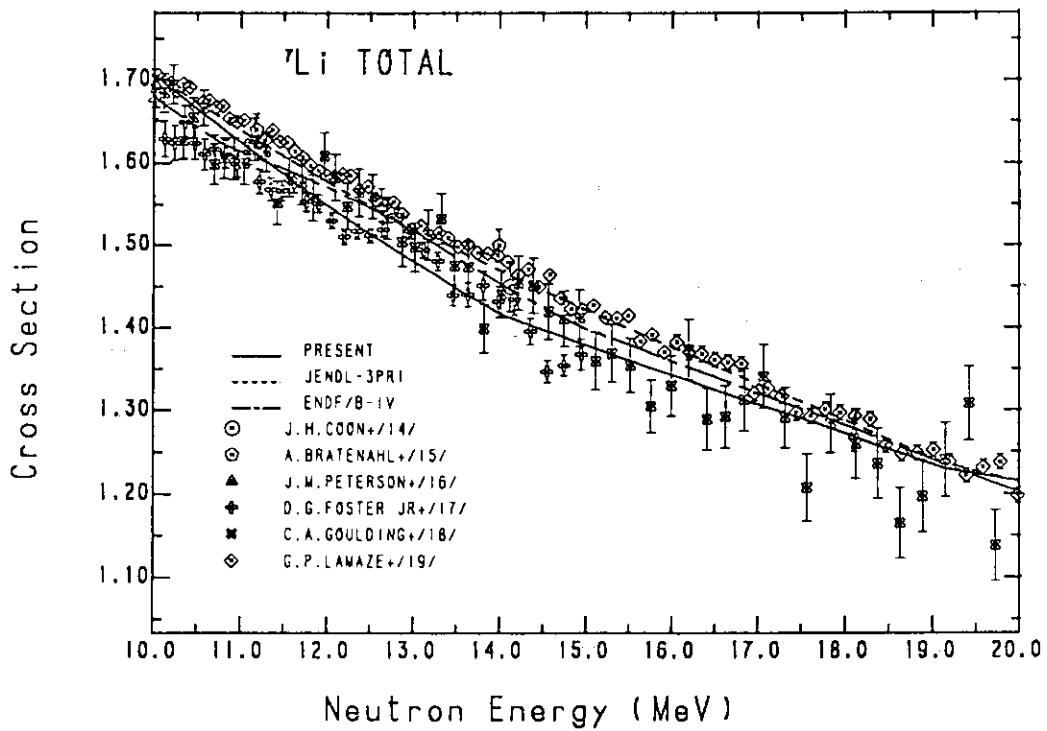


Fig.3 Total Cross Section of ${}^7\text{Li}$

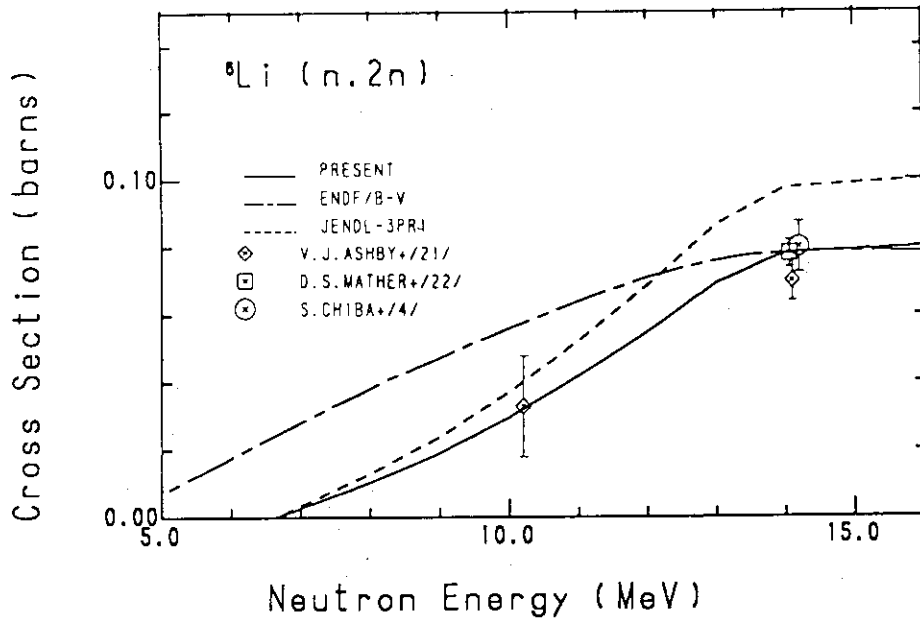


Fig.4 The ${}^6\text{Li}(n,2n)$ reaction cross section

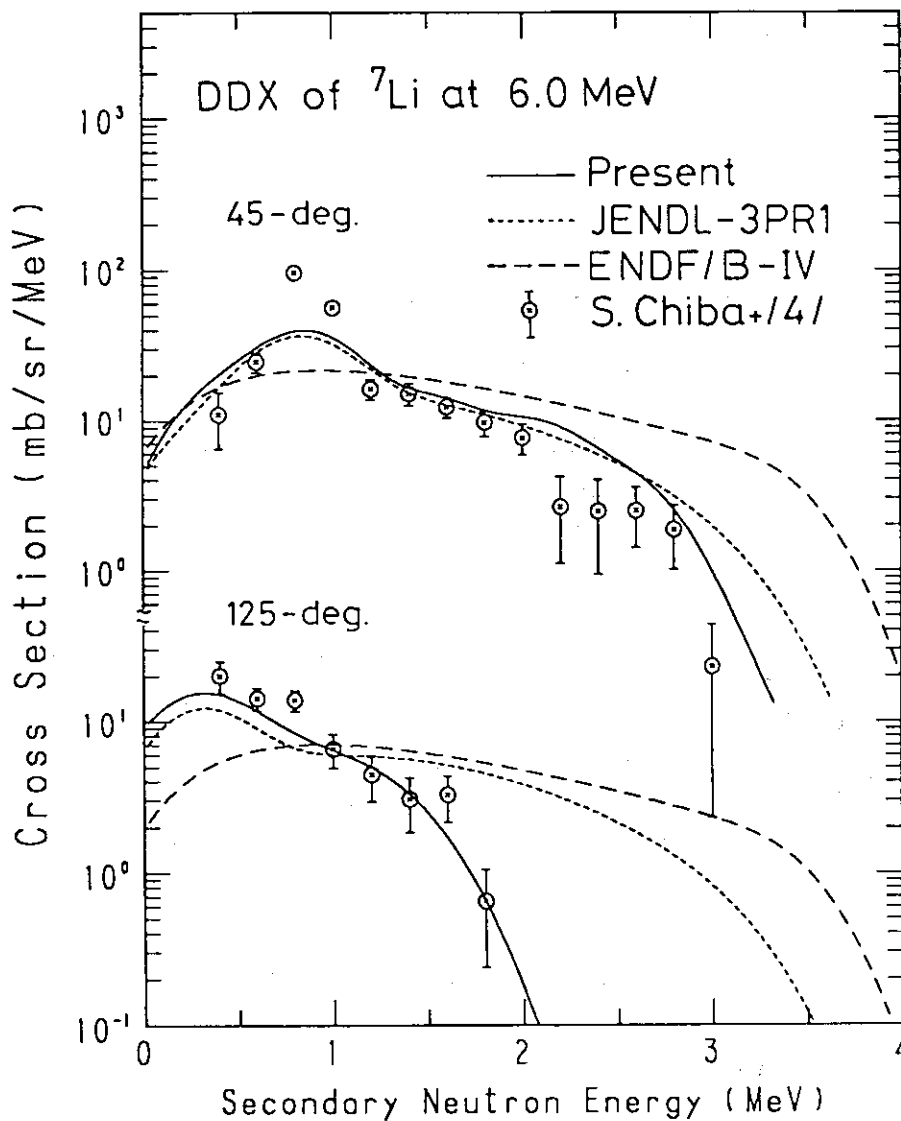


Fig.5 DDX of ${}^7\text{Li}$ at $E_{in} = 6.0$ MeV

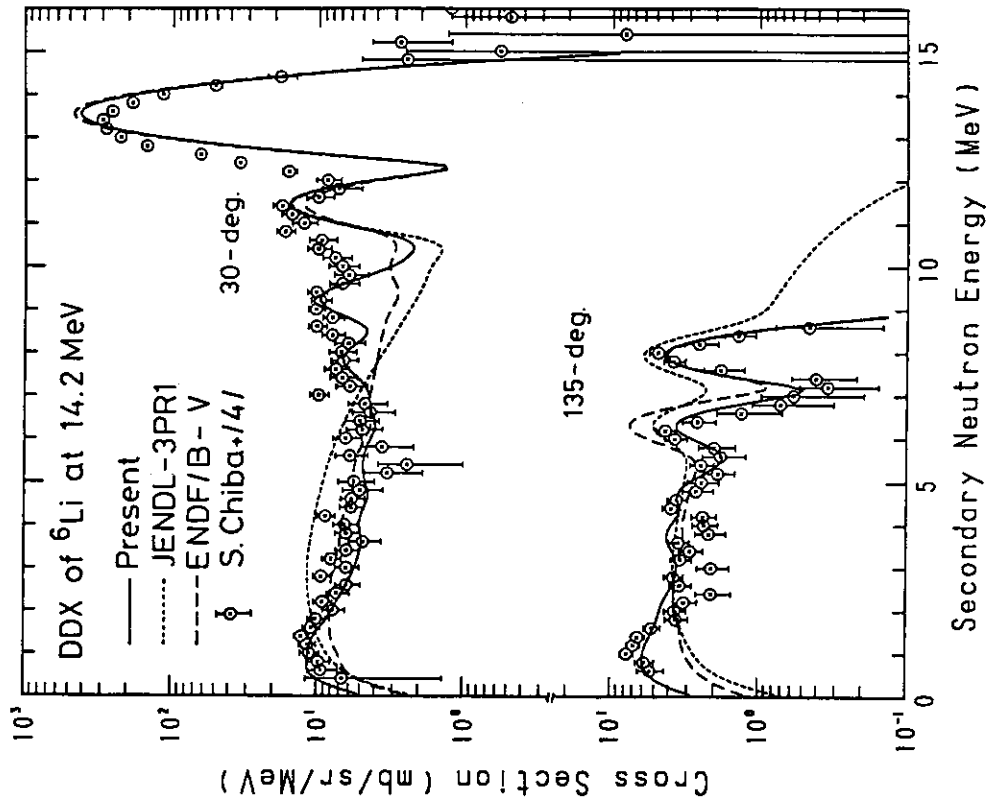


Fig.7 DDX of ${}^6\text{Li}$ at $E_{in} = 14.2$ MeV

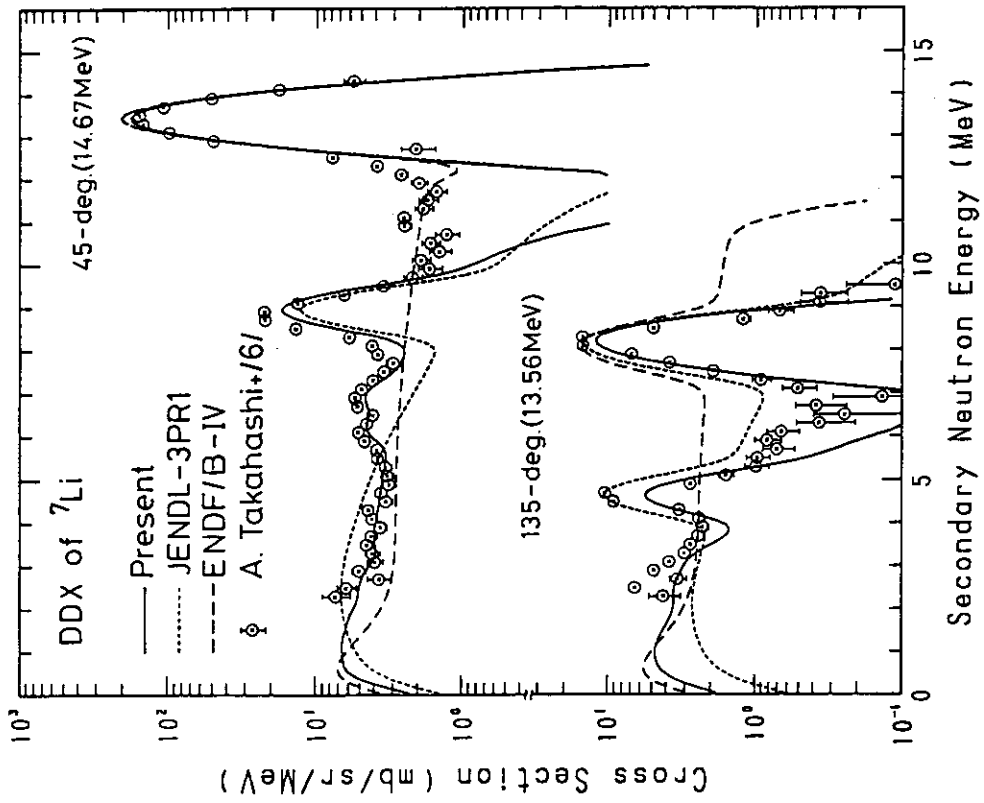


Fig.6 DDX of ${}^7\text{Li}$ around 14 MeV

4. On the Format of JENDL

Tsuneo Nakagawa
Japan Atomic Energy Research Institute
Tokai-mura, Naka-gun, Ibaraki-ken

The ENDF/B format is adopted for JENDL. In this paper, the basic things of the ENDF/B format are explained and differences among recent versions of the ENDF/B format are summarized.

1. Introduction

After evaluation, the evaluated nuclear data must be compiled in a suitable format so as to be used with various computer programs in their application fields. Among several formats developed so far, the ENDF/B format is most commonly used for many evaluated nuclear data libraries and many processing programs have been made. Japanese Evaluated Nuclear Data Library, JENDL, is also compiled by adopting the ENDF/B format. This format has several versions. The ENDF/B-IV format was adopted for JENDL-1 and JENDL-2. JENDL-3PR1 and JENDL-3PR2 were compiled in the ENDF/B-V format.

Since the purpose of this summary was to give fundamental knowledge on the format of JENDL to the attendance of this specialists' meeting, basic things of the ENDF/B format were explained by referring to Ref. 1.

2. Basic Formats

In the ENDF/B format, both of card-image and binary formats are defined. However the card-image format is more often used than the binary one. Each record of the card-image format consists of 80 columns. In the columns from 67 to 75, three identification numbers are stored as follows;

Columns 67 - 70, MAT (I4) = an identification number of material.

For final data of each version of JENDL, MAT numbers were determined as VZZY. V stands for a version of JENDL, e.g. V=2 for JENDL-2. ZZ is an atomic number. Y is an isotopic order in the same atomic number. In the case of natural element, Y is zero. For example, the data of ${}^6\text{Li}$ and ${}^7\text{Li}$ are stored in JENDL-2. Therefore

the MAT numbers of 2031 and 2032 were assigned to ${}^6\text{Li}$ and ${}^7\text{Li}$, respectively. In the case of preliminary data like those in JENDL-3PR1 or JENDL-3PR2, MAT numbers are simply given as (atomic number $\times 100 +$ last two digits of mass number).

Columns 71 - 72, MF (I2) = an integer to classify evaluated data into several files.

Table 1 gives meaning of MF numbers to be used for JENDL-3. In the case of JENDL-1 and JENDL-2, MF numbers from 1 to 5 were used, because fission-yield data could be stored into MF=1 of the ENDF/B-IV format. In JENDL-3, higher MF numbers will be used for storing energy-angular distributions, gamma-ray production data and covariance matrices of cross-section data.

Columns 73 - 75, MT (I3) = a type of reaction.

Frequently used MT numbers for JENDL are listed in Table 2.

From 76th column to the last, sequential numbers of records for each material are stored. Columns from 1 to 66 are divided into six fields. An example of data in the ENDF/B format is shown in Fig. 1. The smallest group of data has the same MAT, MF and MT numbers and it is called 'section'. A record with MT=0 always follows each section, and it is called 'SEND record'. The last record of data with the same MF numbers is 'FEND record' with MF=0 and MT=0. The data for each material is ended by 'MEND record' with MAT=0, MF=0 and MT=0.

The ENDF/B format is constructed from the following basic formats.

1) CONT record

This is a record with two floating numbers and four integers and is written as follows in this paper.

CONT / C1, C2, L1, L2, N1, N2

MAT, MF and MT numbers are not explicitly written in this manner. The first record of each section has the same structure as CONT record, and is called HEAD record.

HEAD / ZA, AWR, L1, L2, N1, N2

ZA = atomic number $\times 1000.0 +$ mass number

AWR = weight of material in the ratio to the neutron mass

2) LIST record

Stored in this record is a string of floating numbers such as coefficients of Legendre polynomial expansion.

LIST / C1, C2, L1, L2, NP, N2

(P(I), I=1, NP)

NP = number of parameters

3) TAB1 record

One-dimensional functions such as cross-section data are stored in this record.

TAB1 / C1, C2, L1, L2, NR, NP

(NBT(I), INT(I), I=1, NR)

(X(I), Y(I), I=1, NP)

NR = number of interpolation ranges

NP = number of data points

NP data points given in the TAB1 record and interpolation scheme specified in (NBT(I), INT(I), I=1, NR) represent one-dimensional function. Shape of the curve is obtained by method of interpolation defined in the ENDF/B format is so-called 'section-paper interpolation'. The data users have to pay attention to the interpolation schemes because the shape of the curve is very dependent on them.

4) TAB2 record

Two-dimensional functions, $y(x, z)$, are represented with TAB2 records.

TAB2 / C1, C2, L1, L2, NR, NZ

(NBT(I), INT(I), I=1, NR)

NR = number of interpolation ranges

NZ = number of values of secondary variable z

This TAB2 record is followed by NZ times of TAB1 or LIST records which represent $y(x, z_1)$, $y(x, z_2)$, and so on.

3. Format of each MF

Evaluated data are represented with combinations of the above mentioned basic formats. Some examples are given below.

3.1 MF=1, MT=451 (Descriptive Information)

This section must be the first one of data for each material. Descriptive information and some important characteristics of the

material are given as follows in the ENDF/B-V format.

```
HEAD / ZA , AWR , LRP , LFI , NLIB, NMOD
CONT / ELIS, STA , LIS , LISO, 0, 0
CONT / 0.0 , 0.0 , 0, 0, NWD , NXC
      ----- NWD records of descriptive information -----
CONT / 0.0 , 0.0 , MF , MT , NC , NMOD
      (repeated NXC times as index of stored data)
```

LRP = flag for resonance parameters
 LFI = flag for fissionable material
 NMOD= modification number
 ELIS= excitation energy of target material
 STA = flag for stability of material
 LIS = state number of target material
 LISO= isomeric state number

In the case where some part of data is modified, NMOD's of HEAD record and corresponding index record (CONT record) are increased by 1. The user should refer to the data with their MAT number and NMOD.

3.2 MF=2 (Resonance Parameters)

Resolved and unresolved resonance parameters are stored in the MT=151. In the evaluation for JENDL, the multi-level Breit-Wigner (MLBW) formula is very frequently used. However, the value of total spin J was assumed sometimes to be the same as the target spin in the case where J was unknown. For such cases, the use of RESENDD²⁾ is strongly recommended for reconstruction of pointwise cross sections. This problem will be solved in JENDL-3 by assuming physically correct J values to all resonances.

3.3 MF=3 (Cross Sections)

Cross sections, $\sigma(E)$, are represented in the following very simple format.

```
HEAD / ZA , AWR , LIS , LFS , 0, 0
TAB1 / S , Q , LT , LR , NR , NP
      (NBT(I), INT(I), I=1,NR)
      (E(I),  $\sigma(E(I))$ , I=1,NP)
```

LIS/LFS = initial/final state numbers
 S = temperature or break-up energy
 Q = reaction Q value

LR = emitted particles after the (n,n') reaction.

In this format, a LR flag is important for light nuclides. Examples of LR flags are given in Table 3. By using MT numbers and LR flags, break-up reactions are represented, for example, as follows,

Li-6(n,n ₁)Li-6(dα)	MT=51	LR=32
Li-7(n,n ₂)Li-7(tα)	MT=91	LR=33
B-10(n,n ₁₂)B-10(d2α)	MT=62	LR=35

In the case where resonance parameters are given in MF=2, background cross sections are given in the resonance energy region for the total, elastic scattering, fission and capture cross sections. Actual cross sections are sum of pointwise cross sections calculated from the resonance parameters and those in MF=3. If the data are also given for the nonelastic scattering, (n,f), absorption and/or neutron disappearance cross sections, they must be also modified by resonance cross sections.

3.4 MF=4 (Angular Distributions of Secondary Neutrons)

Angular distributions are always given as the following normalized function.

$$\int_{-1}^1 p(\mu, E) d\mu = 1,$$

$$\frac{d\sigma(\Omega, E)}{d\Omega} = \frac{\sigma(E)}{2\pi} p(\mu, E).$$

Two ways of representation of $p(\mu, E)$ exist by specifying the flag LTT. If LTT=1, $p(\mu, E)$ is expanded into the Legendre polynomials.

$$p(\mu, E) = \frac{1}{2} + \sum_{l=1}^{NL} \frac{(2l+1)}{2} f_l(E) P_l(\mu).$$

The coefficients, $f_l(E)$, are stored in LIST records. If LTT=2, $p(\mu, E)$ are represented with TAB1 records.

3.5 MF=5 (Energy Distributions of Secondary Neutrons)

Energy distributions are also given as the following normalized function.

$$\int_0^{E'_{max}} p(E \rightarrow E') dE' = 1.$$

By using this function, actual energy distributions are calculated as follows:

$$\frac{d\sigma(E \rightarrow E')}{dE'} = m\sigma(E)p(E \rightarrow E'),$$

where multiplicity m is implicitly given, cross section $\sigma(E)$ is given in MF=3 and the normalized distribution $p(E \rightarrow E')$ in MF=5. Five kinds of spectrum can be used depending on the control flag of LF.

- LF = 1 Tabulated functions
- LF = 5 General evaporation
- LF = 7 Fission spectrum
- LF = 9 Evaporation spectrum
- LF = 11 Energy dependent Watt spectrum

In the ENDF/B-IV format, LF=10 (energy independent Watt spectrum) is defined in the place of LF=11. For JENDL, LF's = 7 and 9 are most frequently used.

3.6 MF=6 (Energy Angular Distributions of Secondary Neutrons)

Energy-angular distributions, so-called double differential cross sections (DDX), are also given as a normalized function, $p(E \rightarrow E', \mu)$. DDX are written as follows by using the normalized function.

$$\frac{d\sigma(E \rightarrow E', \mu)}{d\Omega dE'} = m \frac{\sigma(E)}{2\pi} p(E \rightarrow E', \mu).$$

It is also possible to give them in the form of Legendre expansion.

$$p(E \rightarrow E', \mu) = \sum_{l=0}^{NL} \frac{(2l+1)}{2} f_l(E \rightarrow E') P_l(\mu).$$

In both cases, angles must be given in the laboratory system.

This MF is not often used in JENDL. In the case of JENDL-2, only the data of D has DDX.

4. Differences among Recent Versions of ENDF/B Format

The formats are different more or less among versions of the ENDF/B format. For example, the format of MF=1, MT=451 is as follows in the ENDF/B-IV format.

```

HEAD / ZA , AWR , LRP , LFI ,    0 , NXC
CONT / 0.0 , 0.0 , LDD , LFP , NWD ,    0
      ----- NWD records of descriptive information -----
CONT / 0.0 , 0.0 , MF , MT , NC ,    0
      (repeated NXC times)
LDD = flag for decay data
LFP = flag for fission product yield data

```

This format is different from the ENDF/B-V format described in Section 3.1. In the ENDF/B-VI format³⁾, further improvement will be made as follows:

```

HEAD / ZA , AWR , LRP , LFI , NLIB, NMOD
CONT / ELIS, STA , LIS , LISO, 0, NFOR
CONT / AWRI, 0.0 , 0, 0, NSUB, NVER
CONT / TEMP, 0.0 , LDRV, 0, NWD , NXC
----- NWD records of descriptive information -----
CONT / 0.0 , 0.0 , MF , MT , NC , NMOD
(repeated NXC times)

```

NFOR= format number (4, 5 or 6)

NSUB= sublibrary number (=10 for neutron-data file)

NVER= version of library

TEMP= temperature

AWRI= weight of incident particle

LRP = flag for resonance parameters. If LRP=2, resonance contributions should not be added to cross sections.

LDRV= flag for derived libraries

The following are other important differences.

Decay and fission product yields

They are stored in MF=1 until the ENDF/B-IV format. From version V, they are moved to new MF=8.

Resonance parameters

Use of the Reich-Moore formula is not allowed in the ENDF/B-V format, but allowed in the ENDF/B-IV and VI formats. From the ENDF/B-V format, widths of competing reactions can be taken into account. The format of energy dependent scattering radius is newly introduced for the ENDF/B-VI format.

Angular distributions

A simple format for isotropic distributions were introduced from the ENDF/B-V format.

Energy distributions

The energy independent Watt spectrum is no longer used from the ENDF/B-V format, and the energy dependent Watt spectrum is available instead. Furthermore, the Madland-Nix type spectrum is allowed in the ENDF/B-VI format.

Energy-angular distributions

The format is completely changed from the ENDF/B-VI format.

Covariance matrices

The format of covariance matrices were clearly defined in the ENDF/B-V format.

5. Conclusion

It is very important that the both of nuclear-data evaluators and users understand well the format of the evaluated nuclear data library. Otherwise, the evaluated data might not be properly used. In this lecture, the basic things of the ENDF/B format were explained, and some differences of the ENDF/B-VI, -V and -VI formats were summarized.

We have already decided that JENDL-3 will be compiled in the ENDF/B-V format. However, the ENDF/B-VI will be released in almost the same year as JENDL-3. Therefore JENDL Compilation Group is now investigating the possibilities of adopting the ENDF/B-VI format for JENDL-3.

References

- 1) Revised by Kinsey: "Data Format and Procedures for the Evaluated Nuclear Data File, ENDF", BNL-NCS-50496 (ENDF 102), (1979).
- 2) Nakagawa, T.: "Program RESEND (Version 84-07)", JAERI-M 84-192 (1984).
- 3) Private communication (1985)

Table 1 Definition of MF Numbers

MF	Descriptions
1	General information and some fission quantities
2	Resonance parameters
3	Neutron cross sections
4	Angular distributions of secondary neutrons
5	Energy distributions of secondary neutrons
6	Energy-angular distributions of neutrons
7	Thermal neutron scattering law
8	Radioactive decay and fission product yields
12	Photon production multiplicities and transition probabilities
13	Photon production cross sections
14	Photon angular distributions
15	Photon energy spectra
31	Covariances of $\bar{\nu}$
32	Covariances of resonance parameters
33	Covariances of neutron cross sections

Table 2 Definition of Frequently used MT Numbers

MT	Descriptions
1	Total
2	Elastic scattering
4	Total inelastic
16	(n,2n)
17	(n,3n)
18	Total fission
22	(n,n' α)
28	(n,n'p)
51-90	(n,n') to the 1st to 40th levels
91	(n,n') to the continuum level
102	Radiative capture
103	(n,p)
104	(n,d)
105	(n,t)
107	(n, α)
151	Resonance parameters
251	$\bar{\mu}_L$
451	Descriptive information
452	$\bar{\nu}$
454	Independent fission product yields
455	Delayed neutrons from fission
456	Prompt neutrons from fission

Table 3 Definition of LR Flags

LR	Particles
22	α
23	3 α
24	n α
30	n2 α
32	d
33	t
34	^3He
35	d2 α
36	t2 α

9.22380+	4	2.36006+	2	0	99	0	02925	3	16	312				
0.0	+	0-6.14367+	6	0	0	1	202925	3	16	313				
	20		2	0	0	0	02925	3	16	314				
6.16970+	6	0.0	+ 0	6.50000+	6	1.40000-	1	7.00000+	6	4.23000-	12925	3	16	315
7.50000+	6	9.15000-	1	8.00000+	6	1.13100+	0	8.50000+	6	1.26000+	02925	3	16	316
9.00000+	6	1.34400+	0	9.50000+	6	1.38500+	0	1.00000+	7	1.40200+	02925	3	16	317
1.10000+	7	1.41700+	0	1.15000+	7	1.42000+	0	1.20000+	7	1.42100+	02925	3	16	318
1.30000+	7	1.26100+	0	1.40000+	7	9.10000-	1	1.50000+	7	5.60000-	12925	3	16	319
1.60000+	7	3.00000-	1	1.70000+	7	1.22000-	1	1.80000+	7	2.20000-	22925	3	16	320
1.90000+	7	0.0	+ 0	2.00000+	7	0.0	+ 0				2925	3	16	321
											2925	3	0	322
9.22380+	4	2.36006+	2	0	99	0	02925	3	17	323				
0.0	+	0-1.12683+	7	0	0	1	102925	3	17	324				
	10		2	0	0	0	02925	3	17	325				
1.13161+	7	0.0	+ 0	1.20000+	7	4.50000-	2	1.30000+	7	3.38000-	12925	3	17	326
1.40000+	7	5.00000-	1	1.50000+	7	5.58000-	1	1.60000+	7	5.70000-	12925	3	17	327
1.70000+	7	5.67000-	1	1.80000+	7	4.90000-	1	1.90000+	7	3.71000-	12925	3	17	328
2.00000+	7	2.62000-	1								2925	3	17	329
											2925	3	0	330
9.22380+	4	2.36006+	2	0	99	0	02925	3	18	331				
0.0	+	0 1.94900+	8	0	0	1	832925	3	18	332				
	83		2	0	0	0	02925	3	18	333				
1.00000-	5	0.0	+ 0	2.53000-	2	0.0	+ 0	4.00000+	3	0.0	+ 02925	3	18	334
4.50000+	3	0.0	+ 0	5.50000+	3	0.0	+ 0	6.50000+	3	0.0	+ 02925	3	18	335
7.50000+	3	4.20000-	4	8.50000+	3	0.0	+ 0	9.50000+	3	5.00000-	52925	3	18	336
1.50000+	4	1.33000-	4	2.50000+	4	8.60000-	5	3.50000+	4	2.00000-	52925	3	18	337
4.50000+	4	8.80000-	5	5.50000+	4	9.90000-	5	6.50000+	4	8.04000-	52925	3	18	338
7.50000+	4	4.13000-	5	8.50000+	4	1.84000-	5	9.50000+	4	4.21000-	52925	3	18	339
1.50000+	5	9.90000-	5	2.50000+	5	8.80000-	5	3.50000+	5	1.99000-	42925	3	18	340
4.00000+	5	2.40000-	4	4.50000+	5	3.20000-	4	5.00000+	5	4.30000-	42925	3	18	341
5.50000+	5	6.00000-	4	6.00000+	5	8.20000-	4	6.50000+	5	1.20000-	32925	3	18	342
7.00000+	5	1.75000-	3	7.50000+	5	2.70000-	3	8.00000+	5	4.60000-	32925	3	18	343
8.50000+	5	8.20000-	3	9.00000+	5	1.25000-	2	9.50000+	5	1.60000-	22925	3	18	344
1.00000+	6	1.70000-	2	1.10000+	6	3.10000-	2	1.20000+	6	4.10000-	22925	3	18	345
1.30000+	6	8.20000-	2	1.40000+	6	2.20000-	1	1.50000+	6	3.60000-	12925	3	18	346
1.60000+	6	4.21000-	1	1.70000+	6	4.52000-	1	1.80000+	6	5.02000-	12925	3	18	347
1.90000+	6	5.35000-	1	2.00000+	6	5.48000-	1	2.10000+	6	5.53000-	12925	3	18	348
2.20000+	6	5.56000-	1	2.30000+	6	5.57000-	1	2.40000+	6	5.56000-	12925	3	18	349
2.50000+	6	5.54000-	1	2.60000+	6	5.51000-	1	2.70000+	6	5.47000-	12925	3	18	350
2.80000+	6	5.44000-	1	2.90000+	6	5.42000-	1	3.00000+	6	5.39000-	12925	3	18	351
3.20000+	6	5.40000-	1	3.40000+	6	5.51000-	1	3.50000+	6	5.55000-	12925	3	18	352
3.80000+	6	5.61000-	1	4.00000+	6	5.62000-	1	4.20000+	6	5.62000-	12925	3	18	353
4.50000+	6	5.59000-	1	5.00000+	6	5.50000-	1	5.50000+	6	5.58000-	12925	3	18	354
6.00000+	6	6.26000-	1	6.50000+	6	8.38000-	1	7.00000+	6	9.67000-	12925	3	18	355
7.50000+	6	1.00000+	0	8.00000+	6	1.00200+	0	8.50000+	6	1.00400+	02925	3	18	356
9.00000+	6	1.00300+	0	9.50000+	6	1.00100+	0	1.00000+	7	9.98000-	12925	3	18	357
1.10000+	7	9.97000-	1	1.15000+	7	9.98000-	1	1.20000+	7	9.99000-	12925	3	18	358
1.30000+	7	1.01000+	0	1.40000+	7	1.11700+	0	1.50000+	7	1.20400+	02925	3	18	359
1.60000+	7	1.22700+	0	1.70000+	7	1.19500+	0	1.80000+	7	1.22400+	02925	3	18	360
1.90000+	7	1.30400+	0	2.00000+	7	1.39300+	0				2925	3	18	361
											2925	3	0	362
9.22380+	4	2.36006+	2	0	1	0	02925	3	51	363				
0.0	+	0-4.47000+	4	0	0	1	912925	3	51	364				
	91		2	0	0	0	02925	3	51	365				
4.48894+	4	0.0	+ 0	4.50000+	4	0.0	+ 0	5.00000+	4	1.10000-	12925	3	51	366
5.50000+	4	2.01000-	1	6.00000+	4	2.72000-	1	6.50000+	4	3.42000-	12925	3	51	367
7.00000+	4	3.99000-	1	7.50000+	4	4.41000-	1	8.00000+	4	4.81000-	12925	3	51	368
8.50000+	4	5.12000-	1	9.00000+	4	5.44000-	1	9.50000+	4	5.70000-	12925	3	51	369
1.00000+	5	5.96000-	1	1.20000+	5	6.95000-	1	1.48627+	5	7.96149-	12925	3	51	370
1.50000+	5	8.00882-	1	2.00000+	5	9.58593-	1	2.12500+	5	9.91008-	12925	3	51	371

Fig. 1 Example of data in the ENDF/B format

II. From the Standpoints of Nuclear Design

1. Nuclear Data and Integral Experiments

Required for Fusion Reactor Nuclear Design

Yasushi Seki

Japan Atomic Energy Research Institute

Naka-machi, Naka-gun, Ibaraki-ken

Nuclear data required for the nuclear design of fusion reactors are described very briefly. The ${}^7\text{Li}$ cross sections in the GICX40 library which had been derived from ENDF/B-3 were replaced by those derived from JENDL-3PR1. The effects of the replacement on tritium breeding ratios of two types of blankets are shown. Integral experiments useful for the validation of the data and methods used in the nuclear design are described.

1. Introduction

Major tasks of the nuclear design of a fusion reactor are as follows:

- i) Achieve the net tritium breeding ratio greater than one,
- ii) Estimate nuclear heating in the components,
- iii) Protect radiation sensitive components, e.g. superconducting magnet (SCM),
- iv) Protect public and personnel from irradiation during reactor operation and at shutdown,
- v) Analyze fusion neutrons for plasma diagnostics.

The target accuracy and the estimation of the presently achievable accuracy of the quantities related to the above tasks are presented in Table 1 with some comments on the limiting factors of accuracy and the cause of uncertainty. It should be noted that there is still a large difference between the target accuracy and the estimated uncertainty.

To improve the accuracy of tritium breeding ratio, the nuclear data improvement and the heterogeneity treatment of the breeding blanket composition are requested. Especially the improvement of energy and angular distribution data of secondary neutrons for the constituent nuclides of the blanket is in need.

In the calculation of neutron transmission through bulk shielding, the accuracy of neutron transport cross sections seems to be the limiting factor.

The gamma-ray production data should be improved for the calculation of nuclear heating in superconducting magnets and cryopanel.

For the induced activity calculation, the accurate activation cross sections are needed not only for the major component elements but also for impurity elements.

2. ${}^7\text{Li}$ Cross Section Replacement⁽¹⁾

In the nuclear design of fusion reactors in Japan, the GICX40 cross section library⁽²⁾ is widely used. The ${}^7\text{Li}$ cross sections in the GICX40 library were derived from the ENDF/B-3⁽³⁾ in 1975. These cross sections were replaced by those derived from the newly evaluated JENDL-3PRI⁽⁴⁾. The effects of the replacement on the tritium breeding ratios in the two types of blankets, namely Li_2O blanket and Li blanket are shown in Fig. 1 together with the calculational models of the blankets. Figure 1 shows that the effect of the replacement results in the decrease of the tritium breeding by the ${}^7\text{Li}(n, n'\alpha)t$ reaction, T_7 of about 20% for both blankets. But due to the difference in the absolute values of T_7 , the reduction of the total tritium breeding ratio, T is about 7% for the Li blanket and 3.4% for the Li_2O blanket.

3. Integral Experiments Required for Nuclear Design

Integral experiments conducted mostly in the Fusion Neutronics Source Facility (FNS) which are useful in the validation of the data and methods used in the nuclear design of fusion reactors, are listed in Table 2. The experiments which are desired from the nuclear design are also listed in the table.

REFERENCES

- (1) Mori, S. and Mohri, K.: private communication
- (2) Seki, Y. and Iida, H.: JAERI-M 8818 (1980)
- (3) Drake, M.K. (edited): BNL-50274 (T-601, TID-4500), ENDF 102, Vol. 1 (1970)
- (4) Shibata, K.: JAERI-M 84-204 (NEANDC(5), 109/V) (1984)
- (5) Maekawa, H. et al.: J. Nucl. Sci. Technol., 16, 377 (1979)
- (6) Maekawa, H. et al.: JAERI-M 83-196 (1983)
- (7) Nakamura, T. et al.: to be published
- (8) Tanaka, S. et al.: JAERI-M 82-130 (1982)

- (9) Ikeda, Y. et al.: to be published in JAERI-M report
 (10) Seki, Y. et al.: JAERI-M 84-193 (1984)
 (11) Ikeda, Y. et al.: JAERI-M 83-177 (1983)
 (12) Ogawa, Y. et al.: J. Nucl. Sci. Technol., 21, 561 (1984)
 (13) Nakamura, T. et al.: Nucl. Sci. Eng.

Table 1 Target accuracy and the estimated uncertainty
of the quantities related to nuclear design

Quantity	Target accuracy	Estimated uncertainty	Major limiting factors and cause of uncertainty
a. Tritium breeding ratio	1%	10%	Nuclear data, heterogeneity
b. Nuclear heating rate			
Vacuum vessel	20%	100%	Transport calculation
Tritium breeder	5%	50%	Heterogeneity
c. Bulk shielding			
Superconducting magnets	10%	100%	Nuclear data, design criteria
Biological shield	50%	350%	Nuclear data, skyshine
d. Streaming effect			
SCM(Cu, insulator)	10%	500%	
NBI(Insulator)	20%	100%	Transport calculation
Instrumentation (window, semiconductor)	10%	100%	Gamma-ray production data
Cryopanel (heating)	20%	100%	
e. Induced activity			
NBI	50%	200%	Activation cross sections
Instrumentations	50%	200%	Impurity content
Dose rate distribution	50%	500%	Transport calculation Corrosion products

Table 2 Integral Experiments Required for Nuclear Design
of Fusion Reactors

Quantities and Objective	Experiments conducted mostly at FNS
Tritium breeding ratio	Li ₂ O-C Sphere ⁽⁵⁾ , Li ₂ O Slab, ⁽⁶⁾ Engineering Benchmark Experiment ⁽⁷⁾
Nuclear heating	Measurement using TLD ?
Radiation damage	Organic(Inorganic) insulators Copper dpa at 4°K
Validation of streaming calculation	Concrete bent duct in FNS ⁽⁸⁾ Gap streaming Duct Streaming
Induced activity	SUS-316 ⁽¹¹⁾ , Al alloys ⁽¹²⁾ , shutdown dose
Skyshine dose	OKTAVIAN ⁽¹³⁾

Lithium Oxide Blanket

Plasma	
200	Scrape-off layer
220	First wall SS(0.9) H ₂ O(0.1)
221.5	
Breeder Li ₂ O(0.623)	
265	SS(0.024) H ₂ O(0.044)
270	End wall SS(0.9) H ₂ O(0.1)
Shield	

Local Tritium Breeding Ratio

	T6	T7	Total
GICX40	0.809	0.343	1.152
GICXNEW	0.835	0.278	1.113

+3.2% -19.0% -3.4%

Liquid Lithium Blanket

Plasma	
200	Scrape-off layer
220	First wall V(1.0)
220.5	
Breeder Li(0.925)	
275	V(0.075)
280	End wall V(1.0)
Shield	

Local Tritium Breeding Ratio

	T6	T7	Total
GICX40	0.844	0.631	1.475
GICXNEW	0.876	0.493	1.370

+3.8% -21.9% -7.1%

Fig.1 Change in Tritium Breeding Ratios by the Replacement of ⁷Li Cross Sections

2. A High Tritium Breeding Ratio (TBR) Blanket Concept and Requirements for Nuclear Data relating to TBR

Koichi Maki

Energy Research Laboratory, Hitachi Ltd.
1168 Moriyama-cho, Hitachi-shi, Ibaraki, 316 Japan

Abstract

Significance of developing a blanket having a sufficiently larger tritium breeding ratio (TBR) than 1.0 is discussed. For this purpose, a high TBR blanket with a front breeder zone just before the multiplier is introduced together with conventional blankets. From discussion of TBR characteristics in these blankets, the necessity of improving on nuclear data, i.e. reducing uncertainties is presented as follows; σ_s , σ_{np} and $\sigma_{n\alpha}$ of structural and coolant materials, and σ_{n2n} of the multiplier at higher energies above several MeV, and $\sigma_{n\gamma}$ of these materials and $\sigma_{n\alpha T}$ of ${}^6\text{Li}$ at energies from several hundred keV to thermal energy.

1. Introduction

In calculation of a tritium breeding ratio (TBR), neutron transport codes and nuclear cross-sectional data are used. The uncertainties of these nuclear data bring about an uncertainty in the TBR. The purpose of the present paper is to require the nuclear data to be improved in their own uncertainties so as to reduce the TBR uncertainty.

In order to determine the nuclear data to be required, the present paper takes the following approach. At first, the importance of increasing the TBR above 1.0 is emphasized and the required value of a local TBR is predicted. Then, a high TBR blanket concept presented by Maki¹⁾ is introduced. The effects of cooling channels and SUS for spacers in the neutron multipliers on the TBR, and characteristics of the TBR are discussed for the blanket. Moreover, nuclear data relating to, and having large effects on, the TBR are discussed. Based on these discussions, the requirements for reducing uncertainties in nuclear data are presented.

2. Importance of Tritium Breeding and Local TBR

Tritium consumption rate C_T by D-T burning in a plasma is represented as,

$$\begin{aligned} C_T &= P_F \cdot f_d / 17.6 \times 1.6021 \times 10^{-19} \quad (\text{n/s}) \\ &= 0.0557 P_F \cdot f_d \quad (\text{kg/yr}) \end{aligned} \quad (1)$$

where P_F is fusion power in megawatts and f_d is load factor. The amount of tritium consumed during one year's operation is estimated for the following two cases.

Case 1. A proto type fusion reactor with $P_F=2500\text{MWt}$ and $f_d=0.8$:
If $\text{TBR}=0$, the tritium consumption in one year is 111 kg. Even if $\text{TBR}=0.9$,

the consumption is 11 kg.

Case 2. The FER²⁾ (Fusion Experimental Reactor being developed by JAERI) with $P_f=440\text{MW}$ and $f_d=0.25$: If $\text{TBR}=0$, the tritium consumption in one year is 6 kg. For $\text{TBR}=0.9$, the consumption is 0.6 kg.

When $\text{TBR}=0.9$ in Case 1 and $\text{TBR}=0$ in Case 2, the amounts of tritium consumption can be supplied by existing facilities, such as light water reactors for lithium irradiation, listed in Table 1³⁾. But, comparing the fusion powers with the powers of these facilities, we see easily that the powers in the latter need to be larger than 10 times of those in the former to supply the tritium for consumption by the former. This means that the share of electric power by fusion reactors cannot be increased to more than 1/10 of that by fission reactors. In other words, the significance of developing fusion reactors is lost, if it is impossible to increase the TBR sufficiently above 1.0. Therefore, one of the most important requisites for deciding success or failure of D-T fusion reactors is whether blankets having a TBR sufficiently larger than 1.0 can be developed or not.

The TBR calculated by a one-dimensional model corresponds to a local TBR. The local TBR must exceed the value including margins due to doubling time and nuclear data uncertainties, and effects by divertors, shell coils and several ports.

Maki¹⁾ derived the TBR margin, ΔTBR , due to the doubling time in consideration of the tritium inventory, fusion power and the tritium reduction by β decay, as follows,

$$\Delta\text{TBR} \approx \frac{N_T}{P_f} [1 - e^{-\lambda t_2}]^{-1} \quad (2)$$

where λ means a decay constant ($=0.05653\text{yr}^{-1}$); N_T , tritium inventory (in kilograms); P_f , fusion power (in megawatts); and t_2 , doubling time (in years). Values calculated by Eq. (2) are shown in Fig. 1. When we used the doubling time of 2 to 10 years assumed by Abdou⁴⁾, a mean TBR margin of about 0.05 was obtained from this figure by assuming $N_T/P_f \approx 0.01$.

Tobias and Steiner⁵⁾ estimated the TBR uncertainty due to nuclear data uncertainties as about 0.05. According to recent estimations, uncertainties due to nuclear data are higher and depend on the blanket concepts^{6,7)}. Considering these predictions, we assumed the TBR uncertainty due to nuclear data uncertainties of about 0.05 as a conservative value.

The TBR margin due to divertors and shell coils has been estimated as about 0.12 for the FER reference design of Ref.1. We applied that value to the TBR margin. The TBR margin due to several ports has also been estimated as about 0.07¹⁾ for the FER. We also applied that value to the TBR margin.

Consequently, the four margins had a summed value of about 0.29. Therefore, the local TBR was assumed to be 1.3.

3. High TBR Blanket Concept

Most methods proposed to increase the TBR have been based on using a neutron multiplier in the blanket region nearest the plasma⁶⁻¹²⁾. In these methods neutrons are multiplied by the $(n,2n)$ reaction of beryllium, lead, etc., before reacting with lithium. There is no increase in the TBR above the local value of 1.3 in the blanket separated from the

first wall such as shown in Fig. 2.

In the blanket, shown in Fig. 2, however, back scattering neutrons from the multiplier are absorbed by the first wall structural materials, for instance SUS, in the low energy absorption range. The neutron multiplying effect is, therefore, compensated by this absorption. Consequently, to prevent neutrons from being absorbed and to increase the TBR, we recommended a blanket with a thin breeder zone (designated the front breeder zone) on the plasma side just before the multiplier¹⁾.

A suitable thickness for the front breeder zone is about 1 cm for ⁶Li enrichment of 50%¹⁾, while a suitable thickness of the beryllium neutron multiplier is ten odd centimeters.

Considering these factors, a blanket with the front breeder zone and beryllium multiplier was designed as shown in Fig. 3. Then, we investigated the following two items which have large effects on the TBR.

3.1 Cooling channels in the multiplier

The actual multiplier has cooling channels, which consist of SUS cooling tubes and H₂O coolant. In this section, the effects of SUS and H₂O effective thickness on the TBR were estimated. Their effective thickness is from 0 to 0.6 cm to allow for the cooling channels. The TBRs are estimated as a function of SUS and H₂O effective thicknesses in Fig. 4. Sensitivities of the SUS thickness to the TBR are obtained as -0.35 and -0.15 Δ TBR/cm for 10- and 15-cm- thick beryllium multipliers, respectively. Sensitivities of the H₂O thickness to the ratio are obtained as -0.2 and -0.12 Δ TBR/cm for the same respective thicknesses.

The average nuclear heating density in the beryllium multiplier is several watts per cubic centimeter. One line of cooling channels arranged every 6 cm is equipped in the multiplier to remove the nuclear heat. The 0.25-cm-thick tube has a 1-cm inner diameter. The effective thicknesses of both the SUS and H₂O in these channels are estimated to be about 0.15 cm. From Fig. 4, the effects of 0.15-cm-thick SUS and H₂O on the TBR are -0.1 and -0.05 Δ TBR for 15- and 10-cm-thick beryllium multipliers, respectively. Therefore, the TBRs are predicted to be reduced by the cooling channels in the multiplier from 1.72 to 1.62 and from 1.60 to 1.55 for 15- and 10-cm-thick beryllium, respectively.

These effects of SUS and H₂O for cooling channels on the TBR are due mainly to a decrease of the Be(n,2n) reaction by their neutron-showing-down cross-sections.

3.2 Structural materials for spacers in the multiplier

In the previous discussion, only the cooling channels in the multiplier were taken into consideration for the effect on the TBR. In the actual multiplier, however, structural materials for spacers such as SUS are used to support the cooling channels and the multiplier itself. When the effective thickness of both the SUS and H₂O for the cooling channels is 0.15 cm in the multiplier, the changes of the TBRs are described as a function of the changes in thickness of the beryllium multiplier, including various compositions of SUS, as shown in Fig. 5. In this figure, SUS 0% corresponds to the multiplier taking only the cooling channels into consideration as mentioned previously. From this figure, as the SUS composition becomes larger, the beryllium multiplier thickness giving the maximum TBR is reduced. The thickness is 16 cm for an SUS composition of 0%, 13 cm for 2%,

11 cm for 5% and 10 cm for 10%. Also, the maximum TBR is reduced to 1.62, 1.52, 1.45 and 1.38 for SUS compositions of 0, 2, 5 and 10%, respectively. Therefore, it is necessary to decrease the SUS composition in the multiplier by improving the blanket concepts.

Also this TBR reduction by increasing the SUS composition are due mainly to a decrease in the $\text{Be}(n,2n)$ reaction due to its neutron-slowing-down cross section.

Even if the previous effects are taken into consideration, the blanket with the front breeder zone is shown to have a larger TBR than the local TBR of 1.3.

4. Nuclear Data Relating to TBR

In discussing the behaviors of neutrons, produced by D-T fusion reaction, flying from the first wall to the tritium production region, we present nuclear data having large effects on the TBR in this section.

4.1 Neutrons through first wall to the multiplier

In order to enhance the TBR, it is necessary to increase the neutrons multiplying reaction. From the first wall to the neutron multiplier regions, it is sufficient to take the neutrons having higher energies than the threshold energy of the $(n,2n)$ reaction into consideration. Making the slowing-down of neutrons as small as possible and preventing neutrons from being lost by a charged-particle production reaction are indispensable to increasing the neutron multiplying reaction. Therefore, nuclear data having large effects on the TBR in these regions are the slowing-down cross-sections, such as σ_{in} and σ_{el} , and charged-particle production cross-sections, such as σ_{np} and $\sigma_{n\alpha}$.

4.2 Neutrons in the multiplier before $(n,2n)$ reaction

Before the neutron multiplying reaction, it is necessary to make the slowing-down of neutrons as small as possible and to prevent neutrons from being lost by a charged-particle production reaction, just as cited in the previous subsection. In this region, therefore, the nuclear data having large effects on the TBR are slowing-down cross-sections, such as σ_{in} and σ_{el} , and charged-particle production cross-sections, such as σ_{np} and $\sigma_{n\alpha}$. In addition to these, the neutron multiplying cross-section, σ_{n2n} , is important to reduced the TBR uncertainty.

4.3 Neutrons in the multiplier after $(n,2n)$ reaction

After the neutron multiplying reaction, not slowing-down, but absorption of neutrons must be taken into consideration. Neutrons having the energy from several hundred kilo-electron-volts to thermal energy play an important part for the TBR. In the multiplying region, therefore, absorption cross sections in the energy range described above have large effects on the TBR.

4.4 Neutrons from the multiplier

Some of the neutrons from the multiplier are absorbed before the tritium production reaction. As this absorption decreases the TBR, blanket concepts must be devised to reduce it. Therefore, capture cross sections, $\sigma_{n\gamma}$, of structural materials, between the multiplier and the tritium production region, and in the tritium production region have large effects on the TBR.

The TBR contribution from neutrons of less than 100eV is more than 70% as shown in Fig. 6. From this, the tritium production cross-section, $\sigma_{n\alpha T}$ of ${}^6\text{Li}$, which has a large thermal value of 940 barns and $1/\sqrt{E_n}$ energy dependence, is important. On the other hand, the tritium production cross-sections of ${}^7\text{Li}$ have little importance; their contributions to the TBR is only several percent especially when using beryllium is used as a neutron multiplier. Even if lead is used as a neutron multiplier, tritium production by ${}^7\text{Li}$ makes a contribution to the TBR of less than 10%.

5. Requirements for Nuclear Data

In this section, materials proposed for blankets are listed and discussed. Considering the nuclear data having large effects on the TBR investigated in Sections 3 and 4, the requirements for improving nuclear data by reducing their uncertainties are presented.

5.1 Materials proposed for blankets

Material of SUS, the most commonly used material in reactors, was proposed for the first wall materials and its protectors. In addition to this, a molybdenum alloy and a vanadium alloy were proposed for the first wall materials. A ceramic SiC was proposed for the protectors.

For the structural materials of the blanket vessels, SUS is used in most blanket designs. A molybdenum alloy and a vanadium alloy were further proposed for the materials of the blanket vessels.

For the neutron multipliers, beryllium and lead, the most commonly used species, were employed in the blanket design (cf. section 3). In addition to these, their oxides or alloys were proposed for the neutron multipliers.

Lithium metal, Li_2O , LiAlO_3 , Li_2SiO_3 etc. were presented for the tritium production materials. Material of Li_2O was used in the blanket as shown in Section 3.

For the cooling channel tube materials, SUS, molybdenum alloy, vanadium alloy etc. were presented. And for the coolant, H_2O , helium gas etc. were proposed.

For the other structural materials, SUS, a molybdenum alloy, vanadium alloy etc. were presented.

The above materials are listed in Table 2.

5.2 Requirements for improving the nuclear data

In Section 3, the slowing-down of neutrons by cooling channels and the spacers in the multiplier was shown to reduce the neutron multiplying reaction. Therefore, the slowing-down cross-sections of the materials in

the multiplier were suggested to have large effects on the TBR.

In Section 4, the slowing-down and charged-particles production of neutrons at energies higher than several million-electron-volts of threshold energy in the $(n,2n)$ reaction were suggested to be important for the TBR before the multiplying reaction. And, the neutron multiplying reaction itself was shown to be important. After the multiplying reaction, the absorption and tritium production reaction were suggested as important for the TBR.

In Subsection 5.1, materials proposed for blankets were listed in Table 2.

Considering these discussions, requirements for nuclear data to lower their own uncertainties are clarified as follows.

5.2.1 Higher than several MeV

The slowing-down cross-sections, such as σ_{in} and σ_{el} , of first wall and structural materials, for example SUS, SiC, H₂O, molybdenum alloy, etc., should be improved in their uncertainties. And the charge-particle production cross-sections, such as σ_{np} , $\sigma_{n\alpha}$ etc., of these materials are required to be improved. Further, the neutron multiplication cross-sections, σ_{n2n} , of beryllium and lead should be improved.

For blankets without a neutron multiplier, the tritium production cross-section, $\sigma_{n\alpha T}$, of ⁷Li should probably be added the list of required nuclear data.

5.2.2 Several hundred keV to thermal energy

The capture cross-sections, $\sigma_{n\gamma}$, of structural materials, coolants and tritium production materials must be improved. The tritium production cross-section, $\sigma_{n\alpha T}$, of ⁶Li should be improved.

6. Conclusion

A blanket having a sufficiently larger TBR than 1.0 must be developed, in order to make D-T fusion reactors significant as electric power plants. For this purpose, a high TBR blanket having a front breeder zone just before the beryllium neutron multiplier was introduced together with conventional blankets. Based on these blankets, requirements for improving nuclear data were discussed. From this discussion, we drew the following conclusions.

(1) At higher neutron energies than several million-electron-volts, slowing-down cross-sections, such as σ_{in} and σ_{el} , and charged-particle production cross-section, such as σ_{np} and $\sigma_{n\alpha}$, of structural and coolant materials, for instance SUS, Mo alloy, SiC and H₂O, must have their uncertainties reduced. Further, σ_{n2n} of beryllium and lead should be improved.

(2) At neutron energies from several hundred kilo-electron-volts to thermal energy, capture cross-sections, $\sigma_{n\gamma}$, of structural, coolant and tritium production materials should be improved. Moreover, $\sigma_{n\alpha T}$ of ⁶Li was also required.

References

- 1) K. Maki, "Increase of Tritium Breeding Ratio by Blankets Having Front Breeder Zone in Fusion Reactors," Fusion Technology, 8 to be published.
- 2) Fusion Reactor System Laboratory, Department of Large Tokamak Development, "Conceptual Design of Fusion Experimental Reactor (FER) (Option A)," JAERI-M83-213, Japan Atomic Energy Research Institute (Nov. 1983) (in Japanese).
- 3) M. Sugiura, Handbook of Nuclear Engineering, (Ohmu-sha Tokyo), 899, (Nov. 1976).
- 4) M. Abdou, "Tritium Breeding Issue and Breeding Neutronic Problem," presented at U.S./Japanese Workshop on Breeder Neutronic Experiment, December 6-17, 1982, Japan Atomic Energy Research Institute.
- 5) M. Tobias and D. Steiner, Proc. 1st Topl. Mtg. Technology of Controlled Nuclear Fusion, San Diego, California, April 16-18, 1974, CONF-740402-P2 Vol.III, P.185. U.S. Atomic Energy Commission (1974).
- 6) J. Huang and M. Sawan, "Tritium Breeding Benchmark Calculations for a $\text{Li}_{17}\text{Pb}_{83}$ Blanket with Steel Structure," Fusion Technol., 6, 240 (1984).
- 7) E.T. Chen and J.H. Huang, "A Nuclear Data Library Comparison Study for Tritium Breeding in Helium Cooled Fusion Blankets," Trans. Am. Nucl. Soc., 46, 279 (1984).
- 8) K. Maki and T. Okazaki, "Effect of Blanket Structure on Tritium Breeding Ratio in Fusion Reactors," Nucl. Technol./Fusion, 4, 468 (1983).
- 9) C.C. Baker et al., "STARFIRE-A Commercial Tokamak Fusion Power Plant Study," ANL/FPP-80-1, P.10, Argonne National Laboratory (Sep. 1980).
- 10) M. Abdaou et al., "Demonstration Tokamak Fusion Power Plant Study (DEMO)," ANL/FPP-82-1, Argonne National Laboratory (1982).
- 11) "International Tokamak Reactor-Phase I, :International Atomic Energy Agency, Vienna (1982).
- 12) J. Jung and M. Abdou, "Assessments of Tritium Breeding Requirements and Breeding Potential for the STARFIRE/DEMO Design," Nucl. Technol./Fusion, 4, 361 (1983).

Table 1 Amount of tritium produced by various fission facilities³⁾

facility	amount of production/year	comments
light water reactor	1-3g/1GWe	produced by ternary fission
reprocessing facility	130g/1500t·U	for reprocessing capacity of 5t/day
heavy water reactor	20g/550Mwt	produced by thermal neutron capture of deuterium
moltensalt reactor	700g/1GWe	produced by reaction of neutron and lithium
lithium irradiation by light water reactor	450g/1kg· ⁶ Li	4×10^{13} (n/cm ² ·s) and load factor 80%

Table 2 Materials proposed for blankets

items	materials
first wall	SUS, Mo alloy, V alloy, SiC, etc.
blanket vessel	SUS, Mo alloy, V alloy, etc.
neutron multiplier	Be, Pb, Be alloy, Pb alloy, etc.
tritium breeder	Li, Li ₂ O, LiAlO ₃ , Li ₂ SiO ₃ , etc.
cooling channels	SUS, Mo alloy, V alloy, H ₂ O, He(gas), etc.
the other structural materials	SUS, Mo alloy, V alloy, etc.

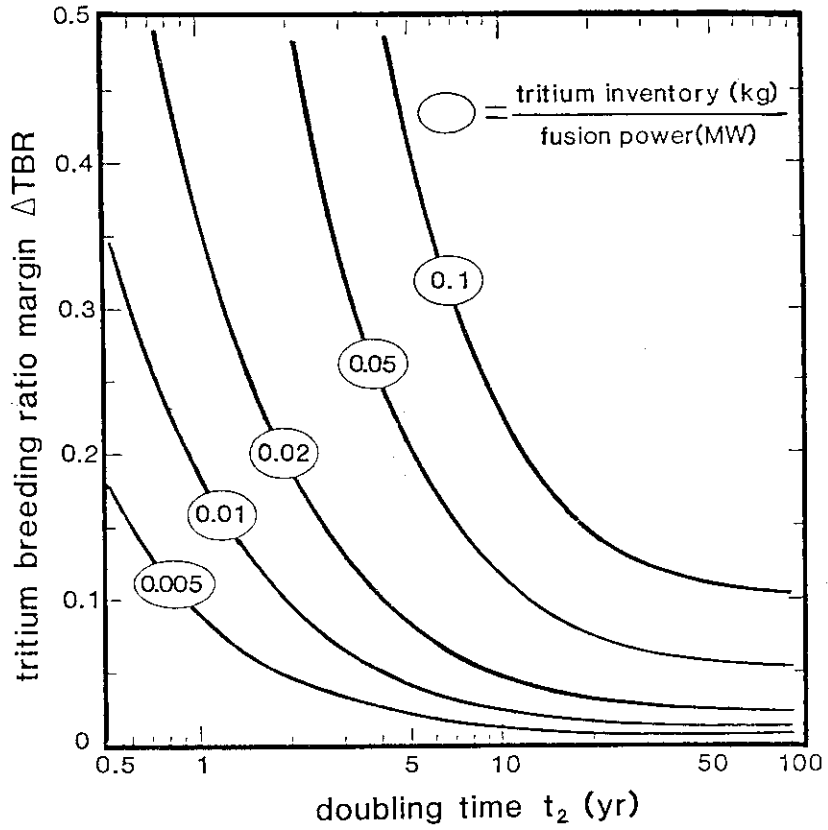


Fig. 1 Relationship between doubling time and TBR margin.¹⁾

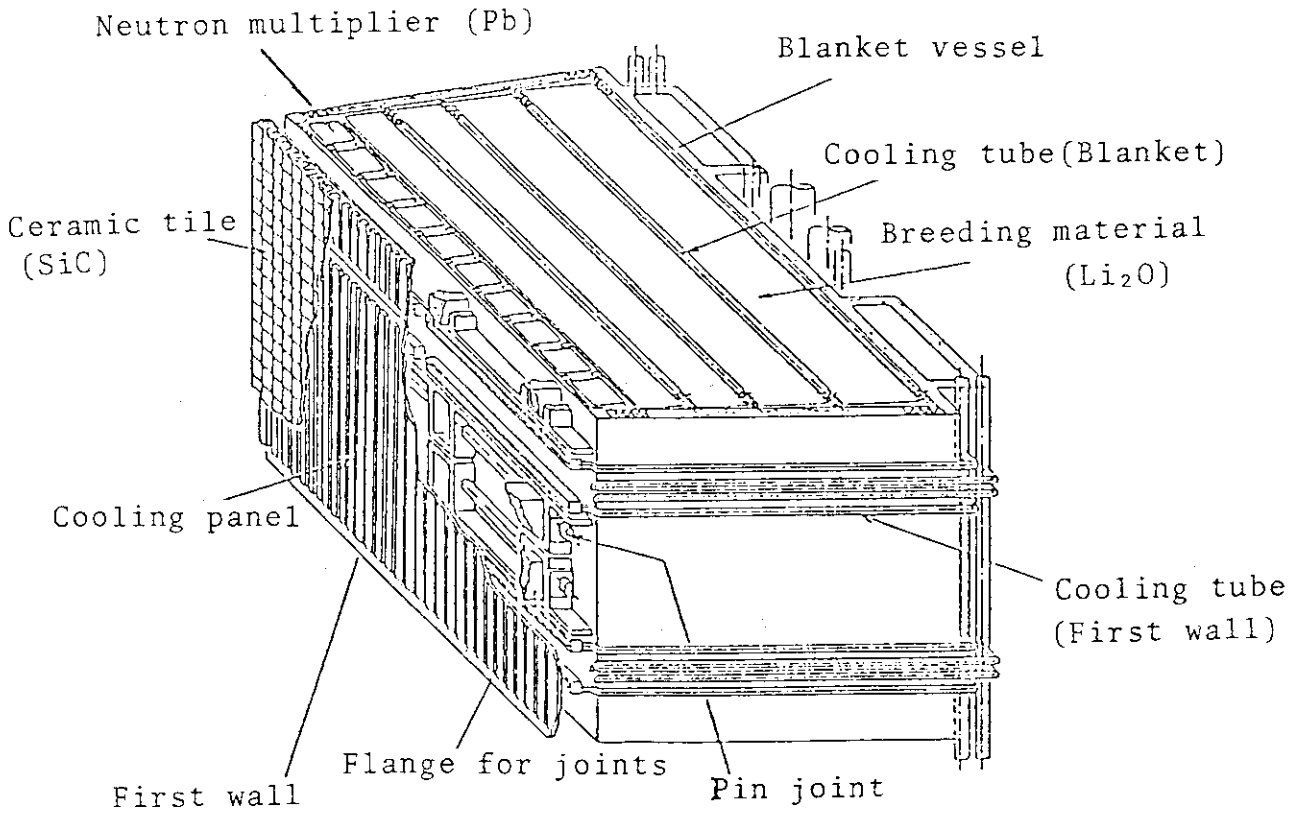


Fig. 2 Blanket concept with first wall separated from breeder zone and using a lead neutron multiplier.²⁾

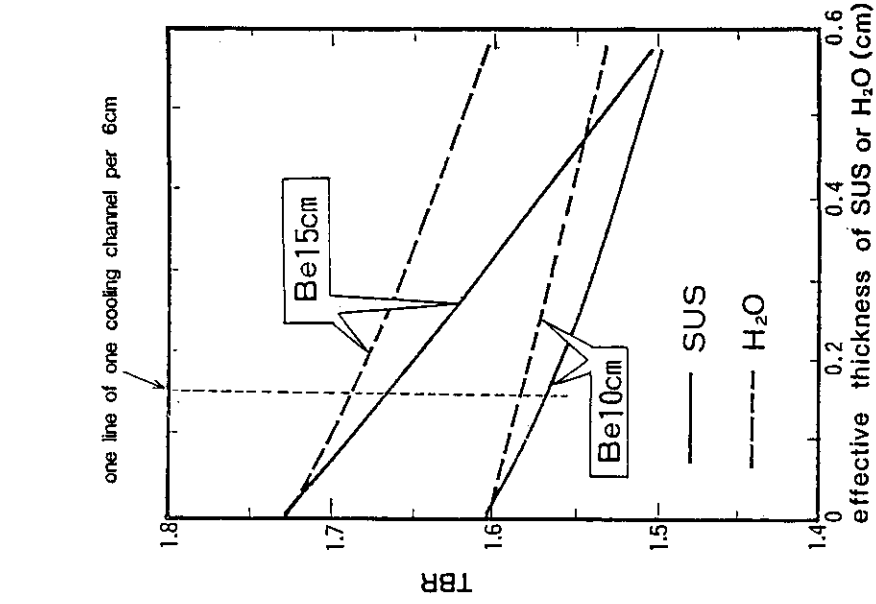


Fig. 4 Relationship between SUS or H₂O effective thickness in the beryllium multiplier and the TBR.

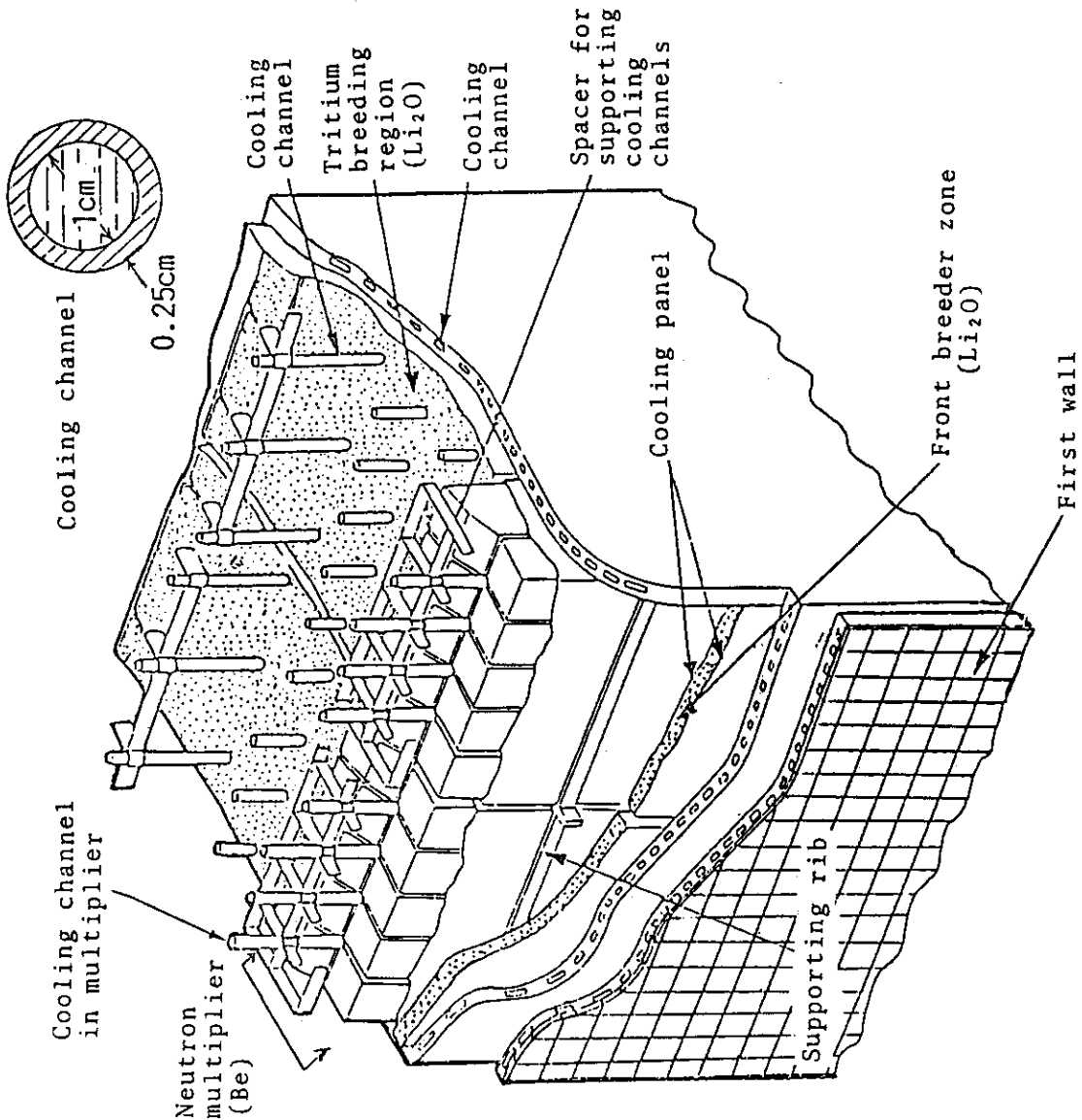


Fig. 3 Blanket concept with front breeder zone and beryllium neutron multiplier.

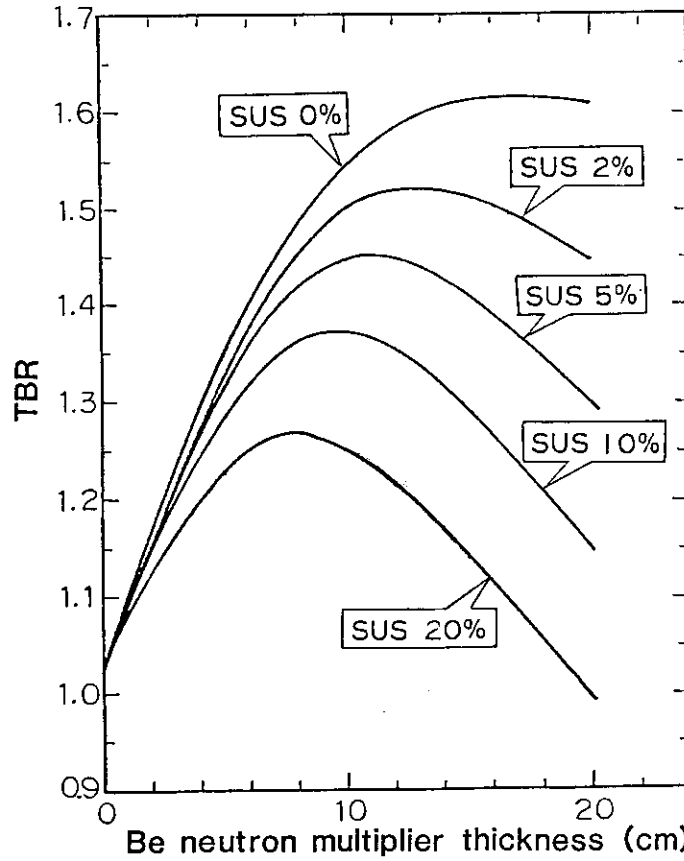


Fig. 5 Relationship between the beryllium multiplier thickness and the TBR for various SUS compositions in the multiplier besides the cooling channels (cooling channel: 0.15-cm SUS effective thickness and 0.15-cm H₂O effective thickness).

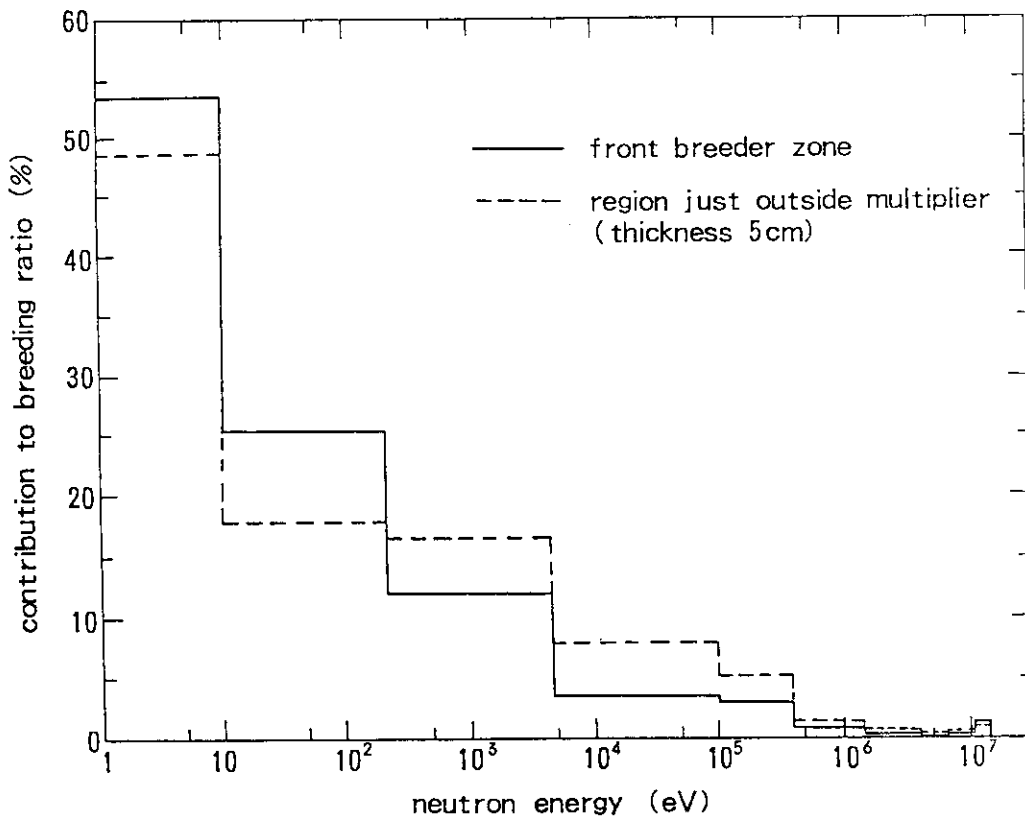


Fig. 6 Neutron energy dependency contribution to the TBR for the blanket with a 1-cm-thick front breeder zone and a 15-cm-thick beryllium multiplier.

3. On the Processing of the Nuclear Data File and the
Problems of the JENDL

Akira HASEGAWA

Japan Atomic Energy Research Institute
Tokai, Ibaraki, Japan

Summary

Brief outlines about the processing of the nuclear data files are described. Particularly stresses are placed on the problems encountered on the processing of the JENDL2, JENDL-3PR1 and PR2 (Japanese Evaluated Nuclear Data File version 2, version 3 preliminary-1 and -2 files.) Some recommendations to resolve the problems are also made.

Contents

1. Relation between Processing and the Design Concepts of Evaluated Nuclear Data File
 2. Evaluated Nuclear Data Files and Processing Codes Available in JAERI
 3. On the Details of the Processing of the Nuclear Data File and Encountered Problems of JENDL-2, -3 PR1 and PR2.
 4. Miscellaneous Comments on the JENDL
 5. Conclusions
- References

1. Relation between Processing and the Design Concepts of Evaluated Nuclear Data File

What should be considered for the conveniences of the users of the evaluated nuclear data files at the processing stage such as group constants production or general utilization of their data? They are expressed as 'completeness' and 'compactness' of the data.

'Completeness'

The data file should cover all nuclides (MAT), all data categories (MF) and all reactions (MT) with no energy range deficit. If an evaluator evaluates the data of one nuclide, he should give the data of all reactions in all energy range, i.e., even if no experimental value exists, the data should be supplied using the systematics or theoretical calculations. And the value should be defined in a unique way and if deduced value data exist they should be existent in a consistent way each others.

In JENDL-1, it happened several times that elastic cross-section data (MF=3,MT=2) are given but their angular distribution data (MF=4,MT=2) are not supplied. This incomplete data presentation is completely forbidden. For such a case, the processing code cannot process the group to group transfer matrices.

Completeness:

All MAT ; material,
 All MF ; data category,
 All MT ; reaction,
 All Energy Range; energy.

'Compactness'

The data represented in a evaluated data file should be given as practical/simple as possible. i.e., don't give the data in a complicate way.

For examples, the resonance cross-sections are usually given as resonance parameters. This is just the case for the 'compactness'. If the data are presented as point-wise basis, the data points required to represent the shape of each resonances easily exceeds 100,000 points for heavy nuclides such as U-238, Pu-239. In contrast to this, at most hundreds of resonance parameteres are sufficient for the exact

representations of these cross-sections.

However, sometimes it may happen that this practical and simplest representation causes some ambiguities for the constructed cross-sections due to the intervention of the resonance construction processing code. In this mean, the point data representation is unique but the resonance parameters representation is not. Therefore some differences are inevitably associated in the generated cross-sections. We cannot be free from these differences as far as the resonance parameter representations are taken.

For another example of simple data presentation, the manual of ENDF/B-V says that the presentation of angular distribution of inelastically scattered neutron should be given as anisotropic data when the anisotropy exceeds 5 %, others the data should be given as isotropic.

As seen from these examples, it is not always the best to give the data as detail as possible. The data should be given as the simplest way considering the accuracy of the original data and the required accuracy when the data are applied. For this point I want to draw attention of the evaluators of the data. Recently the evaluated data issued have the tendency of the expansion both in their volume and in the complicateness due to the utilization of the theoretical calculations in the evaluation steps. Sometimes it happened that almost isotropic data (very slight anisotropy) are given as anisotropic ones in the angular distribution data by using the direct output from the theoretical calculations. These data are inutile, it results in the wast of computer resources for the processing or in the confusion of the data.

Based on these two conception i.e., 'completeness' and 'compactness' of the nuclear data file, the nuclear data processing procedure can be realized.

2. Evaluated Nuclear Data Files and Processing Codes Available in JAERI

Available evaluated nuclear data files in JAERI are listed in Table 2.1.

Table 2.1 Available Evaluated Nuclear Data Files in JAERI

#	File Name	Release Date	Country	FORMAT
1	UKNDL-2	1981	U.K	UK
2	KEDAK-4	1983	F.R.G	KEDAK
3	ENDF/B-IV	1974	U.S	ENDF/B
4	+ ENDF/B-V	1979	U.S	ENDF/B
5	JENDL-2	1983	JAPAN	ENDF/B
6	ENDL-82	1982	U.S(LLNL)	TRANSMITTAL
7	JENDL-3 PR1/2	1983	JAPAN	ENDF/B
8	* JEF	(1982--	NEA(OECD)	ENDF/B
9	* EFF	(1983--	EC	ENDF/B

N.B., + : partial files only.

* : not yet available.

(: now under development.

Above data files except JEF and EFF, we can easily manipulate all of these data using EDFSRS (Evaluated Data File Storage and Retrieval System) /1/.

Available processing codes for the evaluated nuclear data files in JAERI are listed in the followings;

(1) Codes Developed in JAERI

There are two main flows for the development of the processing codes, one is a PROF-GROUCH series and the other is a RAD-HEAT series. The former is developed for the preparation of the 'JAERI-Fast Set' a group constants for the FBR core neutronic calculations. The latter is developed mainly for the shielding calculations.

A: PROF-GROUCH series

- | | | |
|----------------------|-------------|-----------------|
| 1. PROF-GROUCH-M | S.Kasturagi | JAERI (---1968) |
| 2. PROF-GROUCH-G | T.Tone | JAERI (1970) |
| 3. PROF-GROUCH-G/II | A.Hasegawa | JAERI (1974) |
| 4. PROF-GROUCH-G/II' | Y.Ishiguro | JAERI (1981) |
| 5. PROF-DDX | M.Nakagawa | JAERI (---1981) |
| 6. PROF-GROUCH-G/B | A.Hasegawa | JAERI (1984--) |

B: RADHEAT series

- | | | |
|----------------|----------|----------------|
| 1. RADHEAT-V.3 | K.Koyama | JAERI (--1977) |
| 2. RADHEAT-V.4 | N.Yamano | JAERI (1983) |

(2) Imported Codes

- | | | |
|-------------------|----------------|-------------------------------|
| 1. NJOY | R.E.MacFarlane | LANL (1982) |
| 2. MINX | C.R.Weisbin | LANL (1974) |
| 3. AMPX | N.M.Green | ORNL (1976) |
| 4. ETOE/MC2-2/SDX | H.Henryson II | ANL (1976) |
| 5. ETOX | R.E.Schenter | Battelle Northwest Lab (1969) |
| 6. ETOG | D.E.Kusner | Westing House Electric (1969) |
| 7. SUPERTOOG | R.Q.Wright | ORNL (1969) |

General comments for the processing code.

- a. Processing code and the evaluated data file are now tight coupled. It is evident that the processing code depends on the format system adopted in the evaluated files, i.e., ENDF/B, UK, KEDAK and TRANSMITTAL one. But it is not always possible that a processing code designed for an evaluated data file could correctly work for the other evaluated file of the same format system. For example, NJOY processing code is widely used in the world for the ENDF/B-V /IV processing, but it could not be applied to JENDL-2 file due to the special definition for the contents of resonance parameters. That is, the processing code and the evaluated data file becomes tight coupled ones. In this mean, there is no almighty code now. The creation philosophy of the evaluated data file is different from file to file. And the method of the data presentation is somewhat dependent on the file itself.

For example: special data definition in the evaluated data file;

JENDL-2:

There are three resonance region, i.e., 2 resolved and 1 unresolved range for Fe.

J-unknown state assignment data presentation is taken in the resolved resonance parameters.

In File-5 many partial sections are used but no co-energy mesh data presentation is taken.

File-6 (energy-angle correlated data) data presentation and double definition by File-4 and File- 5 data.

ENDL-82:

No resonance parameters data presentation method is taken. Therefore no possibility for Doppler coefficients calculation in the unresolved resonance energy range.

Energy distribution data are given roughly both of the incident energy mesh and the exit energy mesh.

3. On the Details of the Processing of the Nuclear Data File and Encountered Problems of JENDL-2, -3 PR1 and PR2.

Here I describe the details of the processing method taken in our laboratory stressing the encountered problems on the processing of JENDL-2 ,JENDL-3 PR1 or PR2. In Fig.3.1, our processing system is shown. The processing can be divided into two parts, pre-processing and processing. The former is for the preparation of energy dependent cross-section and the latter is for the group averaging process of the pre-processed one.

Outlines of the processing

A. pre-processing

The pre-processing step is introduced in order to generate energy dependent point cross-sections prior to the next averaging step. For this purpose, as shown in Fig.3.1, we use following codes.

(1) LINEAR /2/

This code is used to select out one nuclide from the evaluated file and to give the linear-linear interporable (INT=2) cross-sections (file3 data) from general interpolation data as defined in ENDF/B. This process is always necessary because the processing code PROF-GROUCH-G/B /3/ accepts only linearly interporable cross-sections(INT=2).

General interpolation data defined in ENDF/B

INT Interp.SCHEME CROSS-SECTION vs ENERGY

1	constant	constant	
2	lin-lin	linear	linear
3	lin-log	logn	linear
4	log-lin	linear	logn
5	log-log	logn	logn

(2) RECENTJ /4/

We use this code for the reconstruction of energy dependent neutron total, elastic, capture and fission cross-sections from a combination of resonance parameters and tabulated floor cross sections. These four reaction cross sections are replaced in the output file from input file.

RECENTJ /4/ is a slightly modified version of RECENT /5/. The modifications are made because of the acceptance of JENDL-2 evaluated nuclear data file as input file (J-unknown resonances in Multi-level Breit-Wigner formula) and the preparation for the calculation of self-shielding factor of unresolved resonance region by PROF.GROUCH-G/B.

In this step, cold (T=0. degree in Kelvin) cross-sections are generated.

Resonance formulae defined in ENDF/B.

a. Resolved Resonances

1. SLBW : single-level Breit-Wigner
2. MLBW : multi-level Breit-Wigner
3. Reick-Moore : R-matrix (Reich-Moore) multi-level
4. Adler: Adler-Adler multi-level

b. Unresolved Resonances

1. SLBW : single-level Breit-Wigner

An example of the processing in this step is shown in Fig.3.2 and 3, the former is floor cross-sections defined in File3 and the latter is resonance reconstructed cross-sections (floor + generated cross-sections from resonance parameters) of natural Iron of ENDF/B-IV (MAT=1192). That is, the former is input data for the code RECENTJ and the latter is the output ones. In these figures,

total (MT=1), elastic scattering (MT=2), (n,gamma) (MT=102) and total inelastic (MT=4) cross-sections are displayed.

(3) SIGMA1 /6/

For the preparation of the temperature dependent cross-sections, we use SIGMA1 /6/ code. The method taken in this code is kernel broadening method and it is regarded as fully accurate method for Doppler broadening. Usually required data points for representing cross sections are greatly reduced when temperature increases as seen in Table 3.1 for the case of Na-23 (n,gamma). An example of Doppler broadened cross-sections is shown in Fig.3.4 for Na-23 (n,gamma) of ENDF/B-IV (MAT=1156) at temperatures 0. k (cold), 300. k, and 2100. k.

But only for the unresolved range, this code can not be applied. Therefore we had to use other code for the effective cross-section calculations for this unresolved energy range.

Table 3.1 Generated data points for Na-23 (n,gamma) cross-sections of ENDF/B-IV (MAT=1156)

temperature	points	ratio to 0.k points
1 0. k	4320	1.00
2 300. k	2399	0.55
3 600. k	1930	0.45
4 900. k	1805	0.42
5 2100. k	1629	0.38

(4) UNRESR /7/

For the self-shielding factor calculations of unresolved region, we adopt UNRESR code of NJOY /7/. In the averaging process of PROF-GROUCH-G/B, processing for the self-shielding factor calculation in this unresolved range is not intended at the first stage of the development. Because for this energy range, TMS-1 code has been used. But it consumes a lot of computing time and the results shows some odd behaviour for heavy elements of JENDL-2. Thus we had to abandon that code and decided to import the UNRESR. And for the convenience of the one-through calculation, this code is directly

coupled to PROF-GROUCH-G/B to evade the separate run and resulting data merge process.

B. Processing

(5) PROF-GROUCH-G/B /3/

This code is used for the cross-section averaging process using any weight specified by the user. Processing will be performed for the following quantities for each file categories;

File1: nu, delayed chi,
 File2: unresolved range effective cross-sections (by UNRESR),
 File3: resolved range and smooth cross sections,
 File4: energy transfer matrices in P1 expansion
 and aveage of P1 coefficients for scattering reactions,
 File5: energy transfer matrices in P0 order for scattering or
 fission reactions,
 File6: energy transfer matrices in P1 expansion.

This code output group averaged cross-sections in ENDF/B Format. The calculated quantities are infinite dilution cross-sections, effective cross-sections, self-shielding factors, average weights, energy transfer matrices in P1 expanded form, average of P1 coefficients and group average of fission spectrum. These data are sufficients not only for the usual anisotropic transport code ANISN or DOT but also for the transport code of direct integration method such as PALLAS or BERMUDA.

Problems encountered for the processing of JENDL-2, JENDL-3 PR1 and PR2

(i) Selection of the energy dependent point-wise cross-section generation code

For the resonance cross-section construction process, the quality of the generated cross-sections depends on the code used. In order to improve the quality of the processing code for the resonance reconstruction, a benchmark test was performed by IAEA /8/. And the results were presented at the sixth international conference of radiation shielding held in Tokyo (May, 1983).

Summary results are shown in Table 3.2. Where the comparisons are made for the following conditions. At first point energy cross-sections are generated at cold (0.k) temperature for the ENDF/B-V

dosimetry files, next their values are regrouped to 620-group SAND-II energy structures in flat weights. Thus obtained values are compared to the reference ones. The acceptable error limit is thought as 0.5 % in every energy groups. From this table, at initial stage great divergences are found in most of the codes and after this bench mark test the results are remarkably improved. Now the codes ENTOSAN, RECENT, RESEND clear the test, and the codes AMPX, MINX, NJOY follows. When using those codes, it is very important to check the version number of the code intending to use. Otherwise you can get wrong cross-sections of more than 50 times larger values in the worst case. An examples of the comparisons between RECENT, RESEND and RESEND /9/ is shown in Fig.3.5 and 6, the former is the cross-section ratio and the latter is the generated cross-sections of each codes between 1 to 4 keV for Th-232 (n,gamma) cross-sections of ENDF/B-V. So many resonances are involved in this energy range, the differences can not find out from the resonance shape comparison as in Fig.3.6.

In Table 3.3, an example of cost performances of the energy point cross-section generation codes is shown /9/. As clearly known from U-238 case, required cpu time and generated points number depend on the code significantly. Original RESEND requires nearly 2 hours even if using 10 % error tolerable limit. RECENT generates more than 230000 points and it takes 40 min.

Even by this benchmark test all of the problems hidden in the code are not revealed. Some problems might still exist in the codes. Under the other conditions for example for the other objective file other than ENDF/B-V DOSIMETRY FILE the different conclusions might come. Especially in the benchmark test so performed only limited combinations between resonance formulae (SLBW, MLBW) and floor cross-sections had been made. That is, for other formulae, Adler-Adler, Reich-Moore, conclusions are still the status of 'open question'.

Table 3.2 Summary of initial and current maximum
per-cent differences for each code

code	initial maximum difference	current maximum difference
ENTOSAN	3 %	agreement
RESEND	2000 %	abandoned
RECENT	6 %	agreement
FOURACES	2700 %	1135 %
RESCAL	113 %	80 %
RESEDD	5000 %	agreement
FEDGROUP-3	187 % **	16 % **
FEDGROUP-C	27 % **	23 % **
NJOY (CDC)	18 % *	no additional result
NJOY (IBM)	100 % *	18 %
AMPX	24 %	1.6 %
MINX	15 % **	no additional result

* -- this ignores large per-cent differences for small cross sections near threshold.

** -- comparison based on only a portion of ENDF/B-V dosimetry library

N.B.1

code name	Participants
ENTOSAN	----- Petten, Netherlands
RESEND	----- BNL, U.S.A.
RECENT	----- N.D.S., IAEA
FOURACES	----- Bologna, Italy
RESCAL	----- Greenwood, ANL, U.S.A.
RESEDD	----- JAERI, Japan
FEDGROUP-3	----- CRI, Budapest, Hungary
FEDGROUP-C	----- IJS, Ljubljana, Yugoslavia
NJOY (CDC)	----- LANL, U.S.A.
NJOY (IBM)	----- NEADB, Saclay, FRANCE

AMPX ----- ORNL, U.S.A.
 MINX ----- ORNL, U.S.A.

N.B.2 This table was borrowed from reference /8/.

Table 3.3 Running performance of processing codes.

CPU time and generated data points.

No.	Nuclide	MAT	CPU-time (sec)			Generated Points Number		
			RECENT	RESEND (ORIG.)	RESEND (REV-2)	RECENT	RESEND (ORIG.)	RESEND (REV-2)
1	Na-23	6311	7	10	11	5155	3973	4438
2	Np-237	6337	145	146	141	33066	32308	32897
3	Au-197	6379	601	440	519	106530	54439	71515
4	Th-232	6390	1685	724	938	216435	67167	104116
5	U-235	6395	50	55	48	13000	13422	12982
6	U-238	6398	2353	960	1275	231798	74069	118914
7	Pu-239	6399	110	89	90	33485	23892	25498
8	Sc-45	6426	204	186	200	45462	27573	32146
9	Fe-58	6432	40	32	35	20535	13082	14776
10	Cu-63	6435	8	10	11	5836	5356	5428
11	In-115	6437	201	131	168	62391	34637	44205

Running conditions:

RECENT: LINEAR: 0.1 % ERR: 0.1 %

RESEND (ORIG.): ERR: 0.1 % AVERR: 0.0 LSIG: 1.0E-10

RESEND (REV-2): ERR: 0.1 % AVERR: 0.0 LSIG: 0.0

N.B.1 This table was borrowed from reference /9/.

(ii) Special treatments for JENDL-2 File in the resonance range

(a) Special treatment of J-unknown state for JENDL-2 file

In the JENDL-2 file, for the index of 'J-unknown state' un-allowed J value is assigned in the multi-level Breit-Wigner formula. This convention is restricted to JENDL-2. Therefore usual codes assuming ENDF/B convention might cause serious problems. For the processing for this 'J-unknown state' resonance level, the processed results by the processing codes are summarized as follows;

1. calculation is performed correctly by the JENDL-2 convention;
RESEND0, (RECENTJ,)
2. calculation stopped by producing some error messages;
MINX, RECENT,
3. calculation is performed with no message using invalid J values, thus the result is wrong and the values are not guaranteed; NJOY.

The nuclides list of JENDL-2 whose resonance parameters of MLBW (multi-level Breit-Wigner) contain J-unknown states is shown in Table 3.4. From this Table, it is seen that relatively important nuclides for the fusion neutronics are concerned. At present for these nuclides we have not many choices for the processing code. And in some codes like NJOY, the results cannot be guaranteed even if no error message generated in the processed output. Thus the user should pay attention for the processing of these J-unknown state assigned nuclides.

Table 3.4 Nuclides list of JENDL-2 whose resonance parameters of
MLBW(multi-level Breit-Wigner) contain J unknown
states

Nuclide	MAT	Tape	Resolved Res. Range	Unresolved Range
21-Sc- 45	2211	201	1.0E-5 eV to 90. KeV	not given
23-V - 51	2231	201	1.0E-5 eV to 100. keV	not given
26-Fe- 0	2260	202	1.0E-5 eV to 250. keV	not given
26-Fe- 57	2263	202	1.0E-5 eV to 200. keV	not given
27-Co- 59	2271	202	1.0E-5 eV to 100. keV	not given
28-Ni- 0	2280	202	1.0E-5 eV to 600. keV	not given
28-Ni- 61	2283	202	1.0E-5 eV to 61.52keV	not given
29-Cu- 0	2290	203	1.0E-5 eV to 35. keV	not given
29-Cu- 63	2291	203	1.0E-5 eV to 35. keV	not given
29-Cu- 65	2292	203	1.0E-5 eV to 35. keV	not given
41-Nb- 93	2411	203	1.0E-5 eV to 7. keV	to 50. keV
42-Mo- 0	2420	203	1.0E-5 eV to 50. keV	to 100. keV
42-Mo- 95	2423	203	1.0E-5 eV to 2. keV	to 100. keV
42-Mo- 97	2425	203	1.0E-5 eV to 1.8 keV	to 100. keV
72-Hf-177	2723	204	0.5 eV to 250. eV	to 50. keV
72-Hf-179	2725	204	0.5 eV to 250. eV	to 50. keV
73-Ta-181	2731	204	1.0E-5 eV to 1. keV	to 50. keV
94-Pu-239	2943	206	1.0 eV to 598. eV	to 30. keV
95-Am-241	2951	206	1.0E-5 eV to 150. eV	to 30. keV
95-Am-243	2954	206	1.0E-5 eV to 215. eV	to 30. keV

- (iii) Problems of the UNRESR /7/ for the processing of unresolved resonance range

In the course of importing of UNRESR module/7/ in PROF-GROUCH-G/B /3/ code, several problems are revealed.

- (1) Floor cross-sections definition for fission cross-section.

For the floor cross-sections of fission reaction, UNRESR treats MT=19 (1-st chance fission reaction) data only. Therefore if the floor cross-section of fission is given by MT=18 (total fission reaction) as the case for JENDL-2, no floor cross-sections are added for the fission cross-section. This produce serious problems for the generated fission cross-sections for JENDL-2. Thus we had to changed the original flow to add the MT=18 floor contributions to the fission cross-sections.

- (2) Selection of energy grids in the generation of the unresolved resonance cross-sections

The energy points of the cross-sections generations in the unresolved range should be defined as the same energy nodes as given in the unresolved resonance parameters with the same cross-section interpolation law defined in the resonance parameters. Thus the cross-section values between the energy grids are defined by the interpolation of th grids cross-sections generated at these points and never defined by the interpolation of the resonance parameters themselves.

For the UNRESR code, when the node energy points are relatively distante (i.e. $E \geq 3.0 E'$, E & E' are node energy), the code generate finer mesh grids cross-sections by the interpolation of the resonance parameters. This processing is completely forbidden as already stated above. An example of wrong treatment is shown in Fig.3.7 for the case of Eu-153 ENDF/B-IV (MAT=1291). And at the same time generated cross-section is given in Table 3.5.

Table 3.5 Calculated infinite dilution cross-sections of
Eu-153 (MAT=1291) ENDF/B-IV by UNRESR code

TEMPERATURE = 300.0 KELVIN

SIGMA-0 = 1.0E+50 BARN

ENERGY (EV)	TOTAL (BARN)	ELASTIC (BARN)	CAPTURE (BARN)
97.220 *	114.8	25.84	88.92
121.52	103.7	25.42	78.23
151.91	93.73	24.98	68.74
189.88	84.84	24.53	60.31
237.35	76.89	24.05	52.84
296.69	69.78	23.56	46.22
370.86	63.42	23.05	40.37
463.58	57.73	22.53	35.20
579.48	52.63	21.99	30.64
724.34	48.07	21.44	26.62
905.43	43.98	20.89	23.10
1000.0 *	42.30	19.50	22.81
1250.0	38.82	19.03	19.79
1562.5	35.70	18.55	17.15
1953.1	32.90	18.07	14.84
2441.4	30.39	17.58	12.81
3051.8	28.14	17.09	11.05
3814.7	26.11	16.60	9.515
4768.4	24.29	16.10	8.185
5960.5	22.64	15.61	7.033
7450.6	21.16	15.12	6.040
9313.2	19.81	14.63	5.186
10000.0 *	19.41	14.47	4.940

* THIS POINT IS ENERGY NODE POINT WHERE UNRESOLVED
RESONANCE PARAMETRE IS GIVEN IN FILE-2.

The code had to be changed to follow the correct processing indications. That is, firstly the code generate the cross-sections at the node energy points, and the next if the generated ones are not linearly interpolable according to the interpolation code assigned to this energy range then it generate the linearly interpolable cross-sections using the generated cross-sections at the first step.

(3) Relations between the node energy points of the resonance parameters and the energy points of the floor cross-sections

The energy points of the cross-sections generated in the unresolved range are the same as the node energy points in principle, although in some cases finer mesh cross-sections might be generated as stated in the previous section. For the case when the node energy points and floor cross-section energy points are coincide, this is for the case of ENDF/B, there are no problems. But, when they are not coincide, this may happen frequently in the case of JENDL, we found a big problem. In JENDL library, to represent the fine structure of unresolved range cross-sections, detailed structured data are usually defined by the floor cross-sections. Thus the coincidence between the unresolved resonance energy nodes and the floor cross-section grids is not always expected, more over it is better to think that the two grids are defined independently in JENDL. For such a case, the code UNRESR could not treat the floor cross-sections correctly. UNRESR add floor cross sections only at the unresolved resonance energy node, and neglect other energy points data of the fine floor cross-sections. An example for this case is given in Fig.3.8 for the total cross-sections of U-235 of JENDL-2 (MAT=2923). In this figure, UNRESR generated cross sections are shown by a line with circular marks and the RECENTJ's ones are shown by a line with triangular marks. Obviously UNRESR generated ones have a lesser points and it comes from neglect of the finer floor cross-sections as seen in Fig.3.9 and 10. Thus We changed the processing logics of the UNRESR at this point.

(4) Energy range problem of the individual nuclides for the natural elements.

For the natural elements for which several nuclides are contributing, especially Mo 0 of JENDL-2 data, the different unresolved energy range definition of each nuclides produces a large difficulty for the processing by UNRESR.

Table 3.6 Energy range defined for unresolved resonances of each nuclides for Mo-0 (natural) of JENDL-2

Isotope	Unresolved Energy Range	
Mo-92	50 keV	100 keV
Mo-94	20 keV	100 keV
Mo-95	2 keV	50 keV
Mo-96	19 keV	100 keV
Mo-97	18 keV	50 keV
Mo-98	32 keV	100 keV
Mo-100	26 keV	100 keV

For such case, UNRESR treats as the unresolved range for the first encountered one, i.e., in this case 50 to 100 keV, this produces miss-constructed cross-sections. But such data representation is also forbidden in ENDF/B convention. It is highly requested to represent the same energy range for the resonance range, i.e., lower limit of the resolved range and upper limit of the unresolved range should coincide. For this case upper limit of each nuclides should be the same, in this sense the data is not valid.

In any way, it does not produce correct cross-sections. For such nuclides, we have to calculate each isotope separately and to sum up them with their abundances after the processing.

(iv) Problems of the JENDL-2, -3 PR1 and PR2 encountered for the processing by PROF-GROUCH-G/B code /3/.

Here main discussions are placed on the processing for the energy transfer matrices.

(1). too much precise File4 angular distribution data

In the cross-section evaluation for the energy range where the experimental data are not available, theoretical calculation is usually applied. Some times evaluator use the direct output from the theoretical code not considering the output quality. In such a case, very slight anisotropic data are introduced as the file4 data. These

data are not useful but rather harmful for the actual data. Because in effect they are not so different from the isotropic one but the processing code could not recognize it and the code process them as if anisotropic case. As a result relatively large amounts of the computer resources are thrown away for the anisotropic treatment.

Thus it is recommended in inelastic case that if anisotropy is less than 5 %, give them as isotropic one. That is, it is requested to use the simple expression considering the data quality.

(2). wrong data representation for File5 energy distributions

JENDL-2 data sometimes violate the ENDF/B format regulation for FILE5: energy distribution data. Thus it resulted in the unacceptance of the JENDL file for the usual ENDF/B processing code like MINX or NJOY other than PROF-GROUCH-G/B.

a. Consistency between the energy mesh in the partial sections

In JENDL file, the energy distribution data are frequently represented by several partial sections, and the energy mesh for each partial sections is given rather arbitrary. But such definition of the energy mesh is not supported by the regulation. That is, it is requested that the same energy mesh should be used in each sections. JENDL violate this law several times.

b. Representation for the exit neutron energy distribution function

All secondary energy distribution must start and end with zero values for the distribution function in order to define the distribution in a consistent way. JENDL file sometimes violate this regulation, and this leads to miss-interpolation of exit function between the incident energy meshes and thus normalized exit function is no more guaranteed.

(3). problems relating to the adoption of File6: energy-angular co-related distributions

In JENDL-2, -3 PR1 and PR2 files, the adoption of FILE6 data is actualized for the first time in the world. For the processing of this data, a module of FILE6 processing has been developed for PROF-GROUCH-G/B /3/. Up to now, there are very few of the code available for FILE6 processing. This is one of the problems. Even if the data are prepared in JENDL, no processing code for this data results in the same result as no evaluation for this data. The available data in the world for FILE6 format is shown in Table 3.7.

Table 3.7 Available data of FILE6 energy-angular distributions
in the evaluated data files in the world

	Evaluated File	MAT	Z-A	MT
1	ENDL-82	9003	1H2	16 (n,2n)
2	JENDL-2	2012	1H2	16 (n,2n)
3	JENDL-3 PR1	306	3Li6	16 (n,2n)
4	" "	306	3Li6	91 (n,n')
5	" "	307	3Li7	16 (n,2n)
6	" "	307	3Li7	91 (n,n')
7	JENDL-3 PR2	306	3Li6	16 (n,2n)

As seen from above table, very few data are available. Probably it will not produce the strong intention for the development of file6 processing module from such a scarce file6 data in the world.

Instead of the adoption of FILE6, product data presentation by FILE4 and FILE5 was usually taken for this purpose up to now. But by using this FILE6 format, rigorous treatments are now possible for the many body break-up process of light nuclides such as Li-6 (n,2n) case. From the situation of the present possibility for the un-availability of the FILE6 processing code, JENDL gives also the FILE4 and FILE5 data at the same time for the reactions to which the FILE6 data are given.

But this is a violation to the rule of data uniqueness. Which one should be used FILE6 or FILE4 & FILE5 for this reaction? In some processing code, the possibility for double counts comes out for the reactions where FILE6 and FILE4 & FILE5 data are given. Therefore if the FILE6 data are given for some reactions, no data should be given for FILE4 and FILE5.

4. Miscellaneous Comments on the JENDL

Here I give some comments on the JENDL file.

(1). MT reaction assignment for Li-6(n,alpha)t cross-sections

In JENDL file, Li-6(n,alpha)t reactions is assigned to MT=107, but it is recommended to be assigned MT=105 for that reaction, i.e., Li-6(n,t)alpha. This is the result from the fact that the reaction products should be ordered as ascending mass number by EXFOR rule.

Examples of current MT assignment for Li-6(n,t)alpha reactions in the evaluated nuclear data files are listed in Table 3.8.

Table 3.8 Current MT assignment for Li-6(n,t)alpha reactions in the evaluated nuclear data files

	Evaluated file	MT
1	JENDL-2	107
2	JENDL-3 PR1	107
3	JENDL-3 PR2	107
4	ENDF/B-4	107
5	ENDF/B-5	105
6	ENDL-78	105
7	ENDL-82	105
8	UKNDL	107

As seen from above table, newly evaluated ones except JENDL are adopting MT=105 assignment for Li-6(n,t)alpha reaction.

(2). MAT number assignment procedure for JENDL-3 PR1 file

After the opening of the JENDL 3PR1 data, Li-6 or -7 data (MAT=306, 307) have been revised several times up to now but no explicit trace for the revision are assigned. Thus it is very difficult to identify what version was used especially for the already processed data as the group constants.

To evade such confusion it is recommended to assign another MAT number for the every revised one or to assign a special index for the trace of the revision.

(3). Mixed use of FILE6 and FILE4 & FILE5 for the same reaction data

Mixed use of FILE6 and FILE4 & FILE5 for the same reaction is completely forbidden by the violation of the uniqueness of the representation of the process. But in JENDL-3 PR1 and PR2, this mixed use is taken. This may come from the problem of the scarce availability for the FILE6 processing code. In this mean it has the reason. But in some case double counts problem may come out for the code with the capability of FILE6 processing.

It is recommended that mixed use should be avoided. For the convenience for no FILE6 processing capability code, two version of JENDL-3 PR1 and PR2 should be supplied, one is a formal version with FILE6 data and the other is a supplementary version without FILE6 i.e., composed from FILE4 & FILE5 data.

(4). Necessity for the information center of the evaluated data

The evaluation and utilization of JENDL-3 PR1 and PR2 are almost performed by private basis and thus the information such as 'when the evaluation finished?' , 'is it revised again?' , 'availability of the file ' , 'contents and their feature' etc... are not known to the general users outside of the small private community. From these facts it is highly recommended for Nuclear Data Center of JAERI to strengthen the functions as the information center for the publicity of these data and also for giving the information about the status of these data between users and evaluaters.

5. Conclusions

Brief outlines about the processing of the nuclear data files were described. And at the same time encountered problems on the processing of the JENDL2, JENDL-3 PR1 and -3 PR2 (Japanese Evaluated Nuclear Data File version 2, version 3 preliminary-1 and 2 file) were discussed. Some recommendation to resolve the problems were also shown. It was stressed that the coupling between the processing code and the evaluated nuclear data file becomes very tight and there are no almighty code applicable to all evaluated files even if for the same format system files.

References

- /1/ Hasegawa A.: "Development of EDFSRs: Evaluated Data Files Storage and Retrieval System," JAERI, JAERI-1295 (1985).
- /2/ Cullen D. E.: "Program LINEAR(Version 79-1): linearize data in the evaluated nuclear data file/version B (ENDF/B) format," Lawrence Livermore Laboratory, UCRL-504000, vol.17, Part A, Rev.2 (1979).
- /3/ Hasegawa A.: to be published as JAERI-report.
- /4/ Hasegawa A. and Kaneko K. : internal memo (1985).
- /5/ Cullen D. E.: "Program RECENT(Version 79-1): reconstruction of energy-dependent neutron cross sections from resonance parameters in the ENDF/B Format," Lawrence Livermore Laboratory, UCRL-504000, vol.17, Part C (1979).
- /6/ Cullen D. E.: "Program SIGMA1(Version 79-1): Doppler broaden evaluated cross sections in the evaluated nuclear data file/version B (ENDF/B) format," Lawrence Livermore Laboratory, UCRL-504000, vol.17, Part B, Rev.2 (1979).
- /7/ MacFarlane R. E., Muir D. W., and Boicourt R. M. : "The NJOY Nuclear Data Processing System, Volume I: User's Manual," Los Alamos National Laboratory, LA-9303-M, Vol. I (ENDF-324) (1982).
MacFarlane R. E., Muir D. W., and Boicourt R. M. : "The NJOY Nuclear Data Processing System, Volume II: The NJOY, RECONR, BROADR, HEATR, and THERMR Modules," Los Alamos National Laboratory, LA-9303-M, Vol. I (ENDF-324) (1982).
- /8/ Cullen D.E., Green N.M., Hasegawa A., Sartori E. and Panini G.C : "The IAEA Cross Section Processing Code Verification Project as it Applies to Shielding Data," Proc. of sixth Int. Conf. on Radiation Shielding, vol.1, p.118, Tokyo, May 16-20 (1983).
- /9/ Hasegawa A. and Narita T.: "Comparisons of Energy Dependent Point-wise Cross-Section Generation Codes: RESEND, RESEND, RECENT ,," Japan Atomic Energy Research Institute, JAERI-M 82-128 (1982).

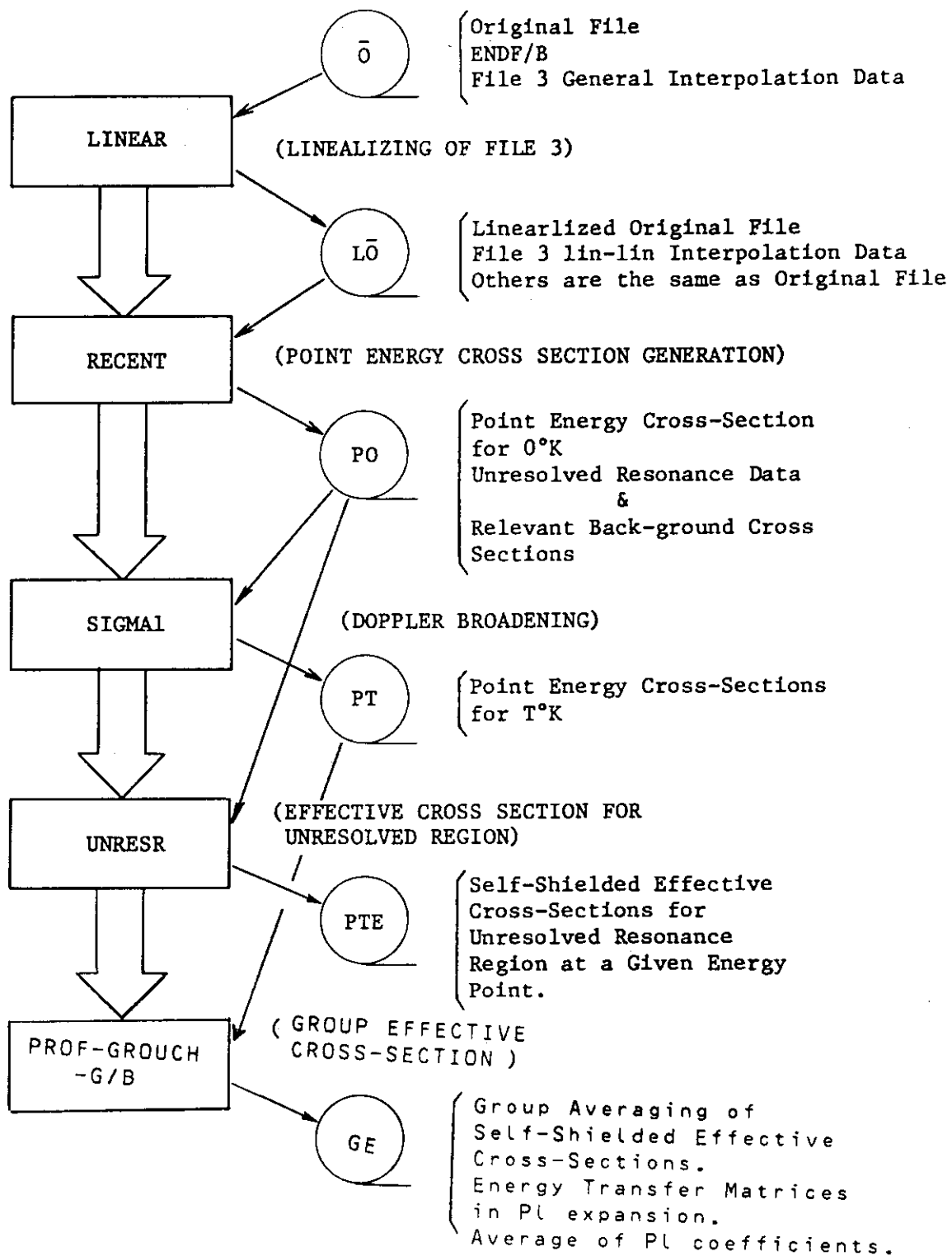


Fig. 3.1 Pre-processing and processing system flow

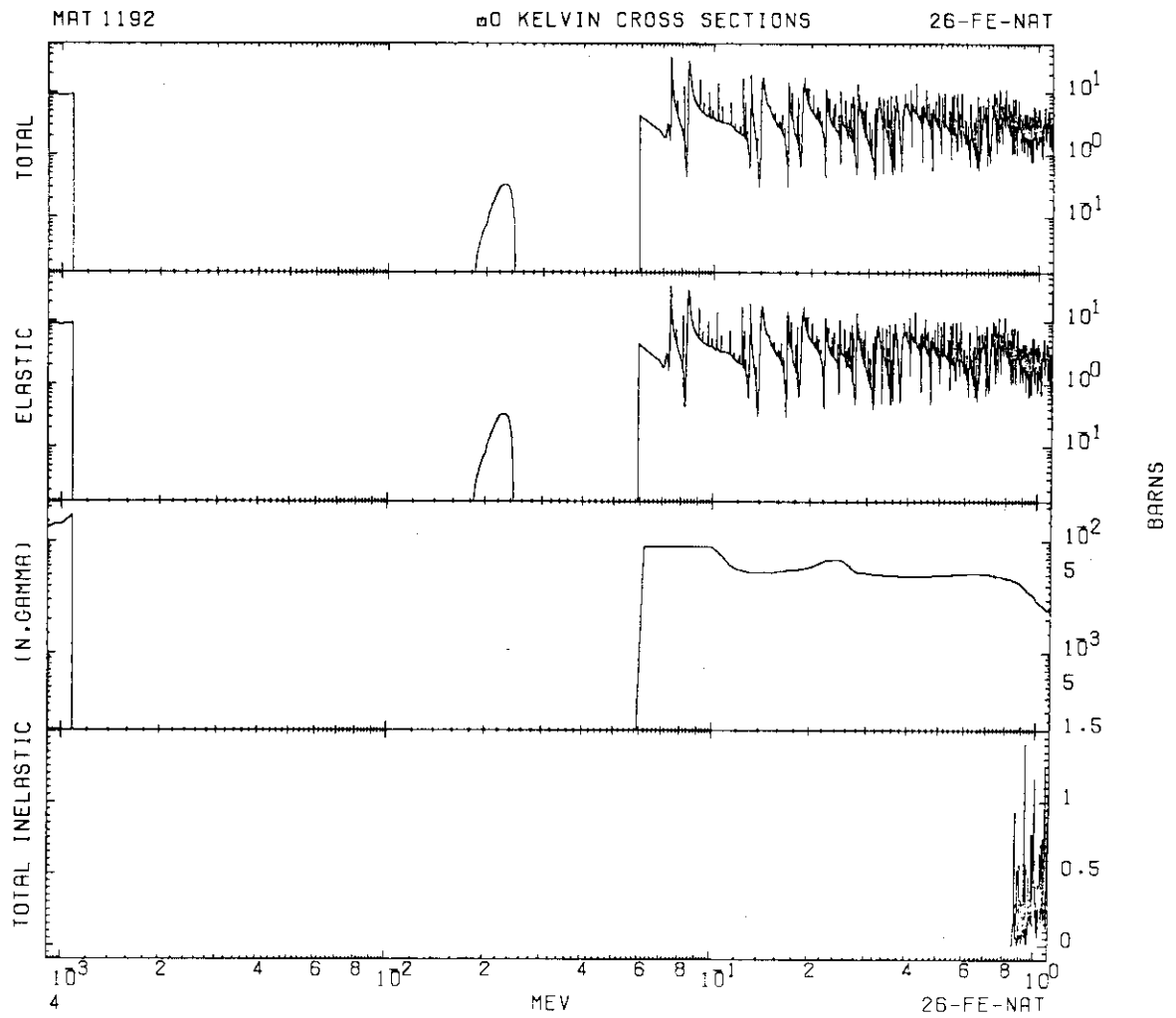


Fig. 3.2 Floor cross-section defined in FILE3 for natural Iron of ENDF/B-IV (MAT=1192)

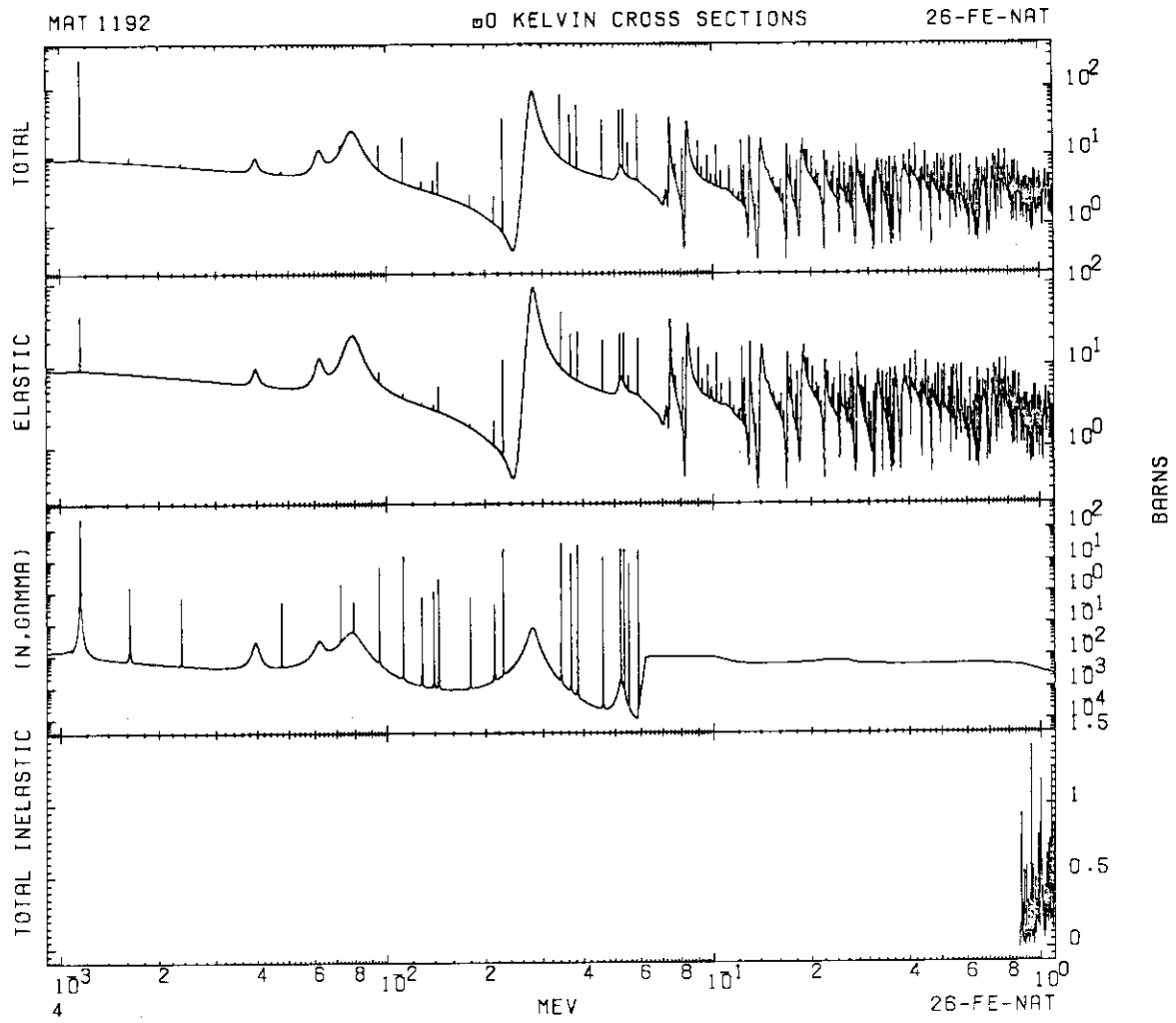


Fig. 3.3 Resonance reconstructed cross-sections for natural Iron of ENDF/B-IV (MAT=1192)

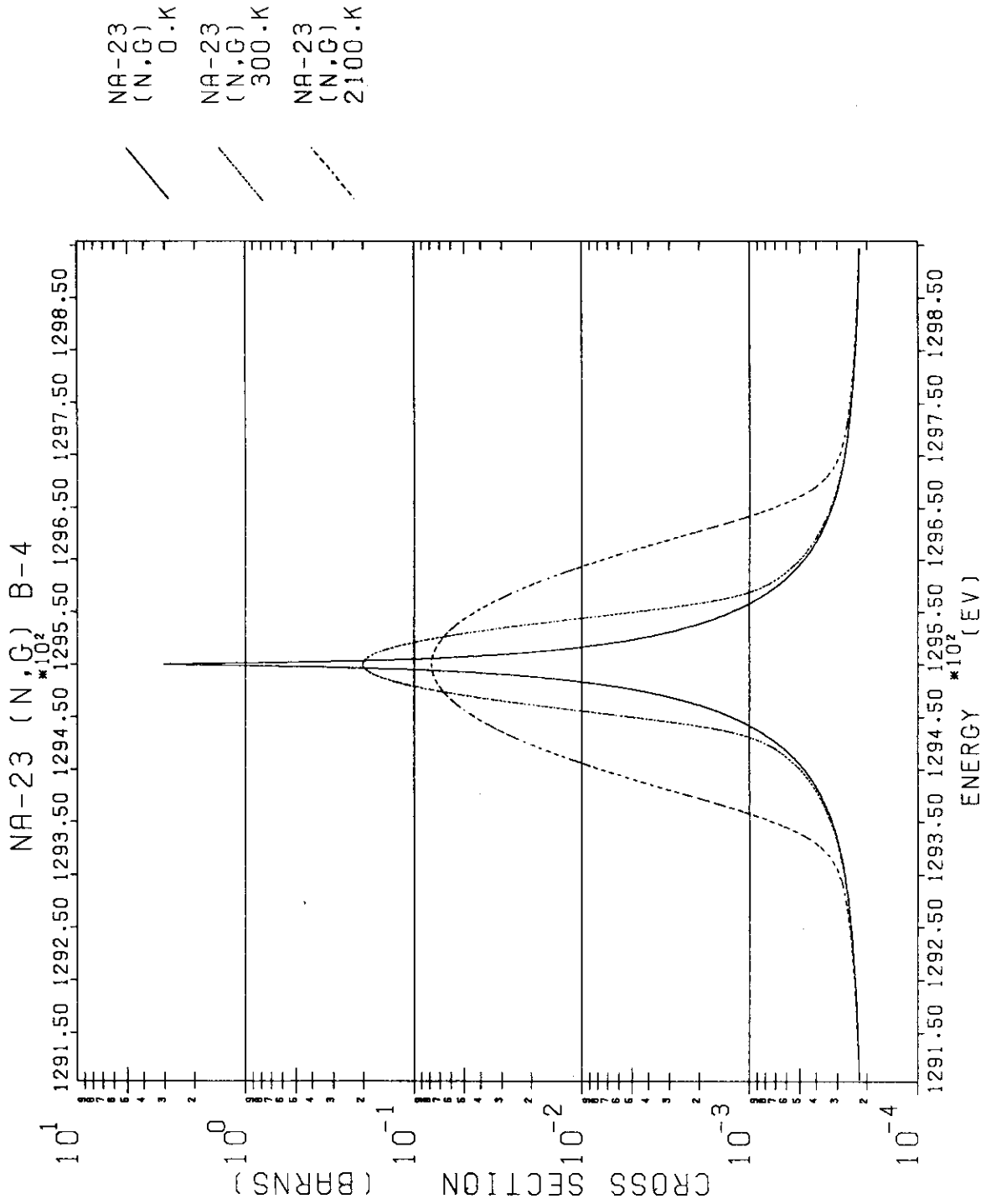


Fig. 3.4 Doppler broadened cross-section of Na-23 (n,gamma) of ENDF/B-IV (MAT=1156) for T=0., 300., 2100.kelvin degree

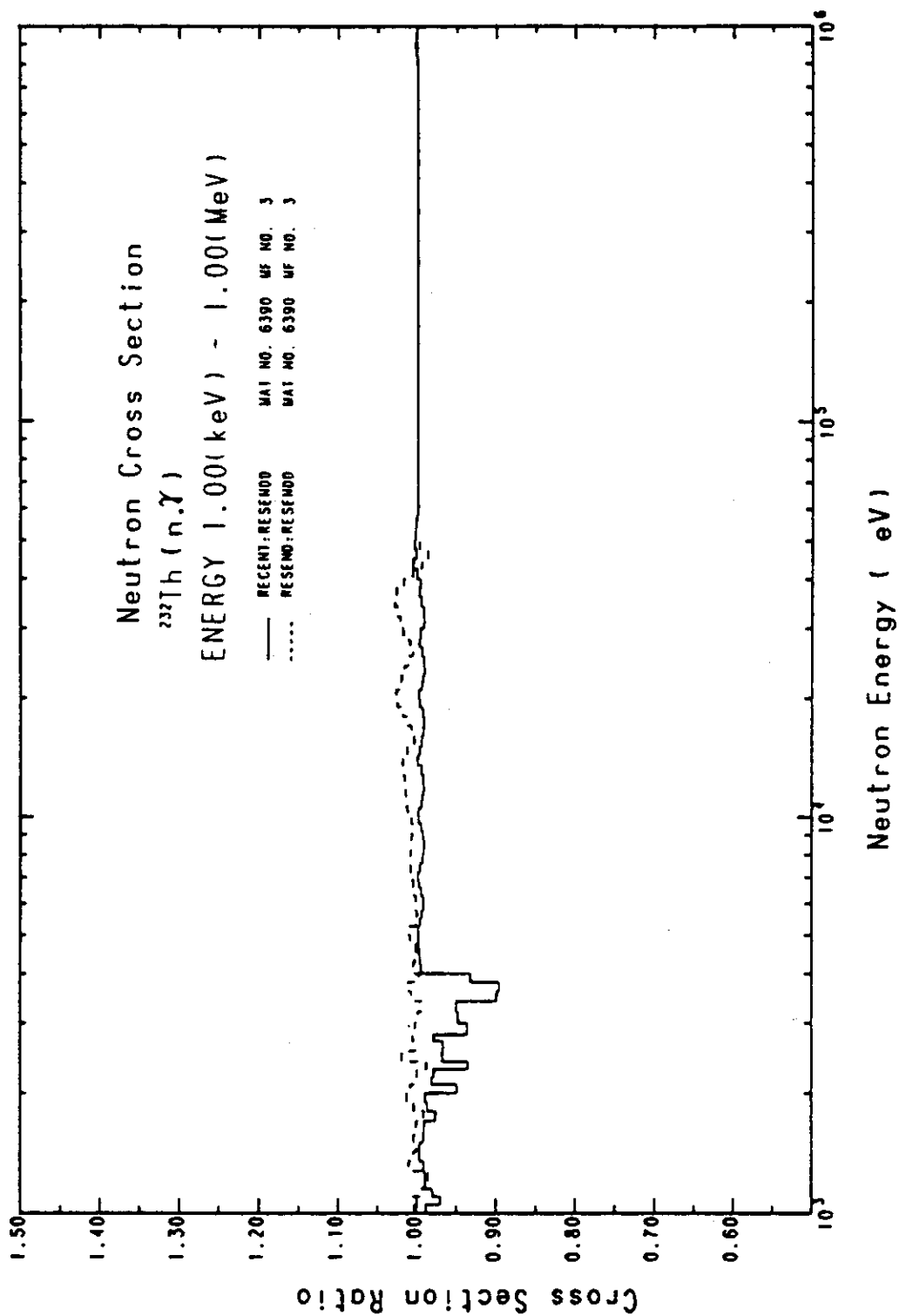


Fig. 3.5 Processed cross-section ratio by RESEND, RESEND code to RECENT one for Th-232 (n, gamma) reaction

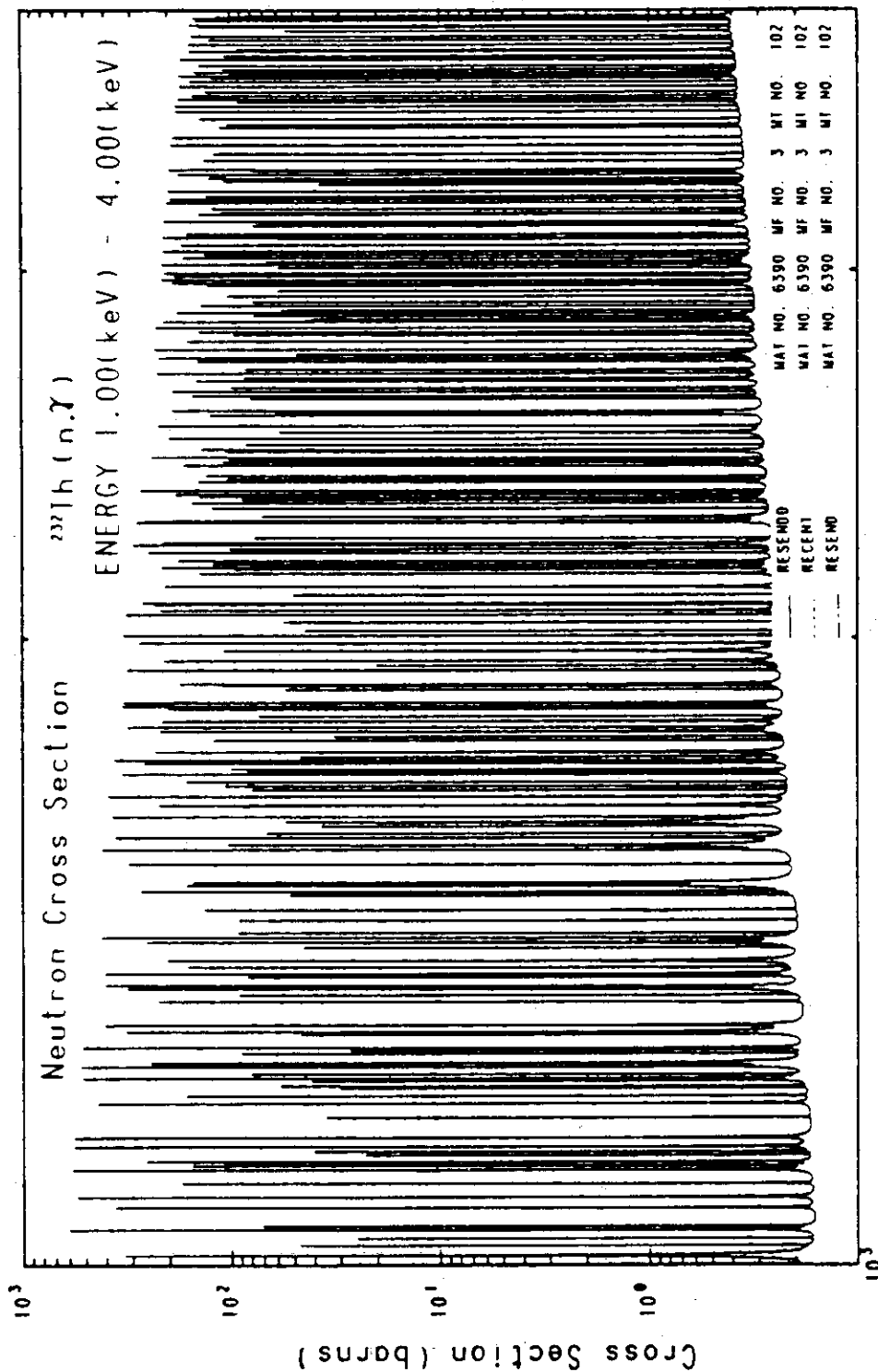


Fig. 3.6 Generated cross-sections by RESEND, RESEND and RECENT code for Th-232 (n, gamma) reaction

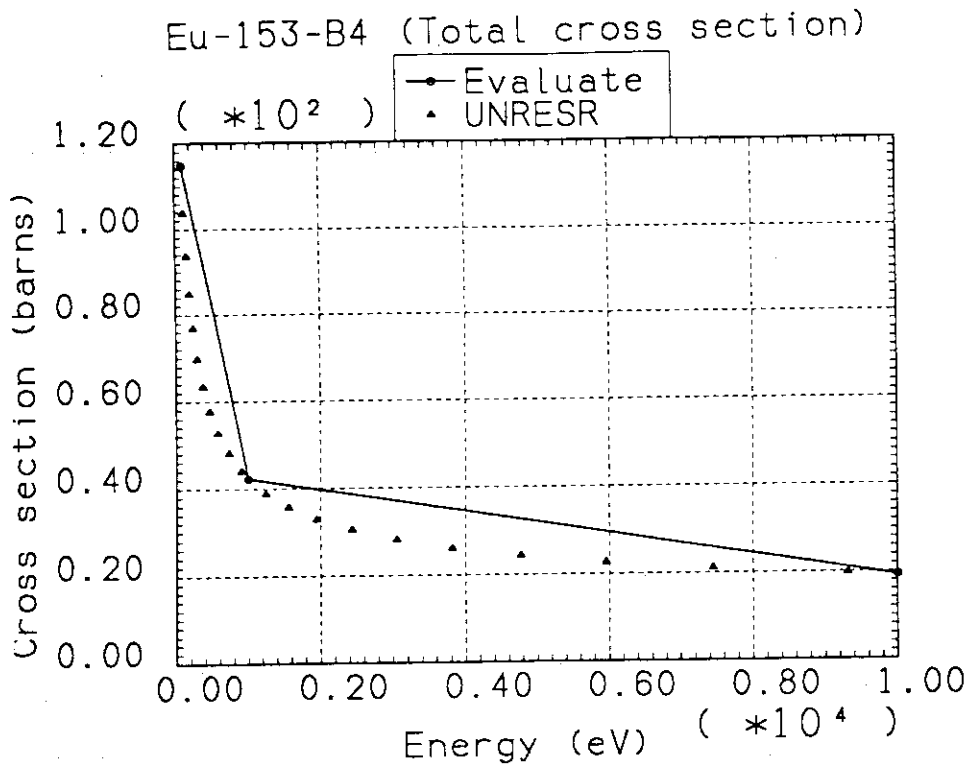


Fig. 3.7 Total cross-sections of Eu-154 (MAT=1291) of ENDF/B-IV generated by UNRESR, solid line show the evaluated points by the definition of ENDF/B

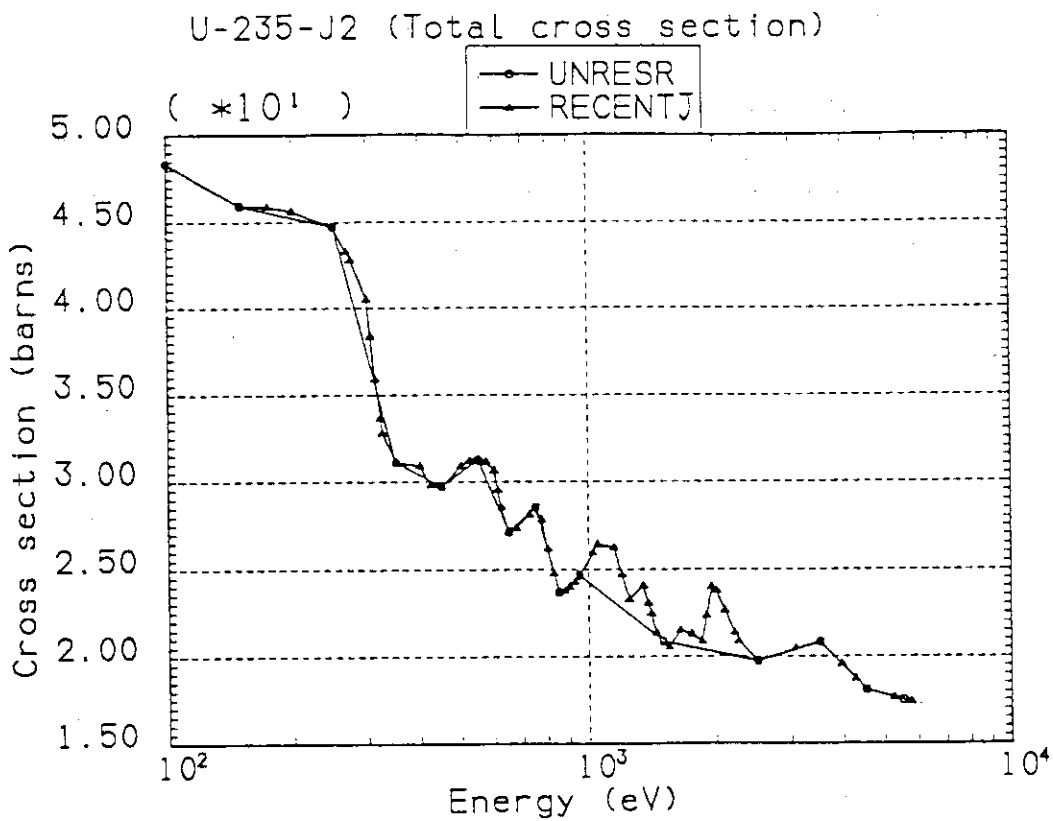


Fig. 3.8 Comparison of generated total cross sections between UNRESR and RECENTJ for U-235 (MAT=2923) of JENDL-2, circle points show the results from UNRESR and triangular points show the results from RECENTJ

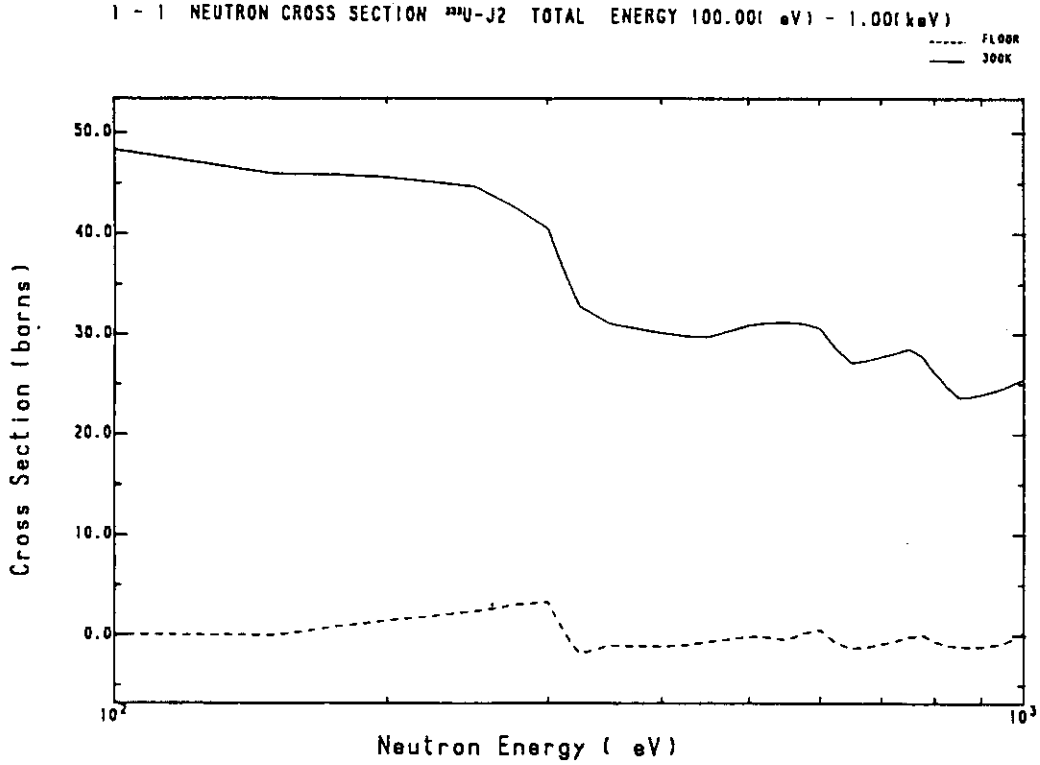


Fig. 3.9 Total cross-sections generated by RECENTJ and its floor cross-sections of U-235 (MAT=2923) of JENDL-2 for energy range from 100 eV to 1 keV (1)

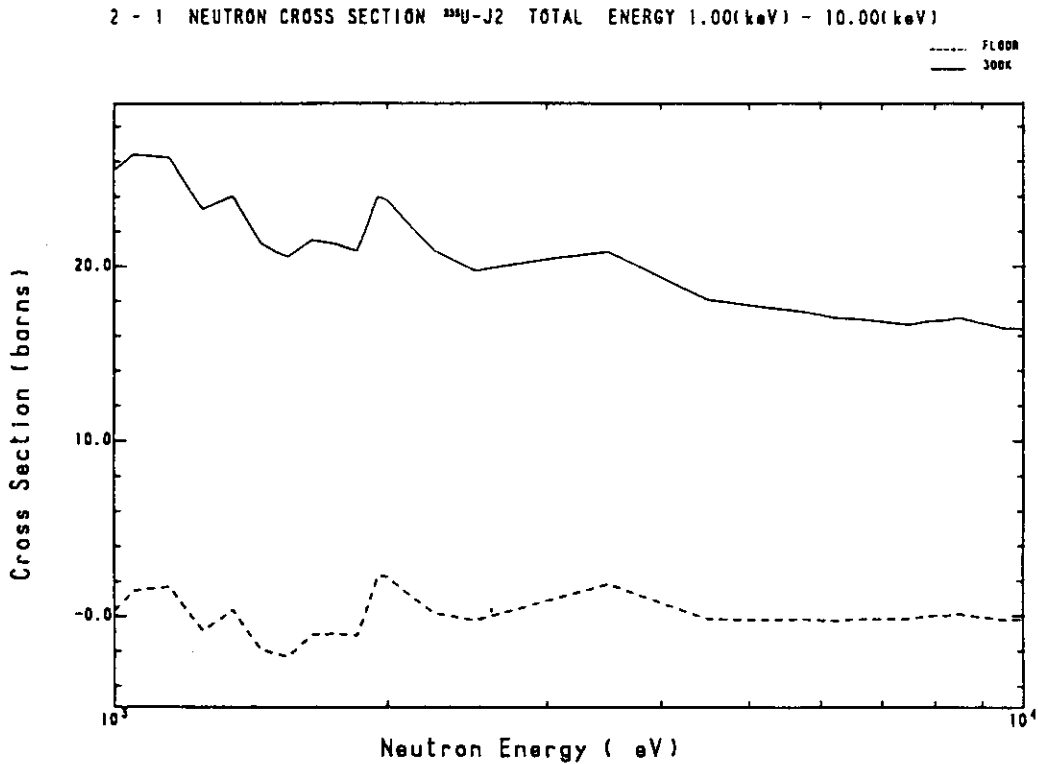


Fig. 3.10 Total cross-sections generated by RECENTJ and its floor cross-sections of U-235 (MAT=2923) of JENDL-2 for energy range from 1 keV to 10 keV (2)

4. Double Differential Neutron Emission Cross Sections at 14 MeV Measured at OKTAVIAN

Akito Takahashi

Department of Nuclear Engineering, Osaka University
Yamadaoka 2-1, Suita, Osaka-565, Japan

A review is given for double differential neutron emission cross sections at 14 MeV, measured at OKTAVIAN since 1981. Pertaining to fusion reactor neutronics, the present status of evaluated nuclear data libraries (ENDF/B-IV and JENDL-3PR1) is shown by comparing with the measured data. As a result, insufficient secondary neutron data are given in ENDF/B-IV for D, Li, Be, B, C, F, Na, Cl, Ti, Cr, Mn, Ni, Cu, Zr, Nb, Mo, W and Pb, although the data for N, O, Si, Al and Fe are fairly well evaluated. Significant improvements are seen in JENDL-3PR1 & -3PR2.

1. Introduction

It has been pointed out¹⁻⁴⁾ that double differential neutron emission cross sections are quite useful in fusion neutronics transport calculations as well as in re-evaluations of secondary neutron data for fusion-oriented nuclear data libraries. At the intense 14 MeV neutron source facility OKTAVIAN of Osaka University, double differential neutron emission cross sections have been measured since 1981, for 25 natural elements; D, Li, Be, B, C, N, O, F, Na, Al, Si, S, Cl, Ti, Cr, Mn, Fe, Ni, Cu, Zr, Nb, Mo, W, Pb and Bi. The measured data have been mainly compared with the ENDF/B-IV data. Some of the results were reported elsewhere⁵⁻⁸⁾. Tabulated numerical data are available in Ref.5 or from the NEA Data Bank, for D, Li, Be, C, O, Al, Si, Cr, Fe, Ni, Cu, Nb, Mo and Pb.

In the present paper, a brief review is first given for the older works as reported in Ref.5-7 and recent results are shown in comparison with the ENDF/B-IV data in most cases. The status of the latest evaluated data JENDL-3PR1 and -3PR2 is shown by comparing with the measured data for Li, Be, Cr, Fe and Ni. A plan in future work will be mentioned at the end.

2. Experimental

A ring geometry & TOF method has been used as shown in Fig.1⁵⁾. In order to vary scattering angle, a ring sample (2 cm in minor diameter and 20 cm in major diameter for most samples) is moved along the accelerator beam line. Incident neutron energy changes from 14.8 MeV to 13.5 MeV, corresponding to the change of scattering angle from 10 deg to 160 deg. Therefore, neutron flight path changes around 9.5 m.

Pulsed D-T neutrons are generated with 1.5-3 ns width at the air-cooled TiT target. Source neutron spectrum and angular dependence of yield are given in Ref.6. Pulse repetition rate has been changed from 2 MHz to 125 kHz, according to a set bias of a 5" dia 2" NE213 neutron detector.

Three kinds of bias setting have been tried for the n- γ pulse shape discrimination circuits⁶⁾; i) For the highest bias 2 MeV, single pulse shape discrimination was used, ii) for the intermediate bias 0.3 MeV, two parallel discrimination circuits having "low" and "high" gain respectively were active and iii) for the lowest bias 0.05 MeV, three parallel discrimination circuits could cover a wide dynamic range. Energy-dependent detector efficiencies were experimentally determined by using a polyethylene scatterer and a Cf-252 spontaneous fission source, for the highest and the intermediate bias, and a 30 cm dia graphite sphere was used in addition, for the lowest bias⁶⁾.

Absolute values of double differential cross sections were calibrated by the elastic scattering of hydrogen using the polyethylene ring scatterer⁶⁾.

Scattering samples of chemical compounds were prepared for D, N, O, F, Na and Cl, while metal samples were available for others. The experimental condition of good statistics and high resolution made it possible to apply a subtraction method to reduce an emission spectrum at specified angle for a pure element from that of a compound molecule.

For correcting multiple scattering effect, a simple method based on the one-point collision probability was used in the older works^{5,6)}, but the method was revised to use the multi-point collision probability⁷⁾. The correction often encountered with difficulty when the measured spectrum was drastically different from the used secondary neutron spectrum data (namely, ENDF/B-IV), and became meaningless. However, in most cases the corrections were within 10 % differences from uncorrected data, which could already be used for comparison with calculated double differential cross sections from, e. g., ENDF/B-IV. The revised method of multi-point collision probability gives larger corrections at back-ward elastic scattering, while smaller ones for low energy neutrons in the 0.3-2 MeV range.

3. Brief Review of the Older Experiments^{5,6)}

Typical results are shown in Fig.2 through Fig.12, for important elements ; lithium (tritium breeder), beryllium (neutron multiplier), graphite (reflector), lead (neutron multiplier), chromium, iron and nickel (structural).

Natural lithium ; As shown in Fig.2, measured DDX cannot be reproduced at all by ENDF/B-IV which ignores the discrete level excitation of 4.63 MeV and the kinematics of continuum neutrons from ${}^7\text{Li}(n,n't)$ reaction. In low energy part where (n,2n) neutrons are dominant, experimental data are significantly higher than the ENDF/B-IV data, as shown in Figs. 3 and 4.

Beryllium ; Emission spectra from ${}^9\text{Be}(n,2n)$ reaction are very different from those of ENDF/B-IV, as shown in Fig.5. The excitation of 1.68 MeV state is not seen in the experiment. The experimental peak corresponding to the 6.76 MeV discrete level excitation is very broadened and no distinct peak is seen at 11.28 MeV state. The recent evaluation by Shibata⁹⁾ in JENDL-3PR1 seems better than that of ENDF/B-IV, but there remains significant discrepancy, as shown in Fig.6. The latest reevaluation in LLNL¹⁰⁾ fits our data very well. Four sequential processes are taken into account for ${}^9\text{Be}(n,2n)$ reaction in Ref.10, while only two in the JENDL-3PR1 evaluation. The agreement is considerable in the lower energy part than 0.5 MeV, as shown in Fig.7.

Carbon ; The ENDF/B-IV data cannot reproduce at all the measured spectra except the elastic and the 4.43 MeV state peak, because the 7.65 and 9.63 MeV level excitations are ignored. The ENDF/B-V data are much better, but disagreement is seen in the lower energy part than 5 MeV at backward angle, as shown in Fig.8. Angle-differential cross sections at 4.43 MeV state (integrated value for the 4.43 MeV state peak in DDX) by experiment are somewhat higher than those of ENDF/B-V in forward angles. The newly evaluated data in JENDL-3PR1 are as good as ENDF/B-V.

Lead ; As shown in Fig.9, the ENDF/B-IV data give too soft spectrum for the (n,2n) reaction and too high cross sections for the (n,3n) reaction. Pb(n,2n) cross sections around 14 MeV should be re-checked since the integral multiplication experiments¹¹⁾ have shown larger multiplication factors than calculated ones by ENDF/B-IV.

Chromium ; A new evaluation is made in JENDL-3PR1¹²⁾ which reproduces nicely the measured DDX, in contrast with drastic discrepancies given by ENDF/B-IV and JENDL-2, as shown in Fig.10¹²⁾.

Iron ; The JENDL-3PR1 data (solid curve in Fig.11) as well as the ENDF/B-IV data show good agreement with the experiment¹²⁾

Nickel ; As shown in Fig.12, significant improvement is made by JENDL-3-

PR1¹²⁾, compared with the ENDF/B-IV data which give flat spectrum in the 4-11 MeV range and the JENDL-2 data which do not include the direct and precompound contributions.

3. Recent Results

3.1 High Resolution Measurements

The results of the older measurements have shown that the main causes of disagreements with ENDF/B-IV data are attributed to the ignorance or insufficient evaluation of the direct and precompound processes in inelastic scattering. Especially, the experimental data have shown that there exist many distinct excitations of discrete levels in medium and heavy elements. However, identification of levels has been still difficult due to poor resolution and insufficient statistics. Hence, the succeeded measurements after the older ones have been conducted with the condition of better resolution and statistics¹³⁾.

In order to study the spectral structures of inelastically scattered neutrons in higher secondary neutron energy range, DDX measurements were carried out for pure or nearly pure isotope elements; sulfur (95.02 % ³²S), ²⁷Al, Iron (91.8 % ⁵⁶Fe), ⁵⁵Mn, ⁹³Nb and ²⁰⁹Bi. Observed isolated peaks were analyzed by comparing with excitation levels given in Nuclear Data Sheet¹⁴⁾. As a result, it has become clear that the observed peak energies are corresponding to some particular excitation levels in many given levels¹³⁾.

Examples of measured DDX data are shown in Fig.13 through Fig.16, respectively for S, Al, Fe and Bi. For ³²S in Fig.13, 2.23, 4.46 and 5.01 MeV state peaks can be corresponded to the 2⁺ state (one phonon quadrupole vibration), sum peak of the 2⁺ and 4⁺ states (two phonon quadrupole vibration) and the 3⁻ state (one phonon octapole vibration). However, higher peaks (6.58, 8.27 and 9.20 MeV state) are not identified yet. Probably, all the peaks are attributed to collective excitations. For ²⁷Al, three peaks of 0.91, 2.17 and 2.99 MeV state can be corresponded to one phonon quadrupole vibrations, i. e., 3/2⁺, 7/2⁺ and 9/2⁺ state, but higher levels of 4.64, 5.54, 6.64, 7.45, 8.24 and 8.64 as seen in Fig.14 are not identified yet. Identification becomes difficult for odd mass isotopes because of phonon coupling with ground state having non-zero spin. For ⁵⁶Fe, one phonon quadrupole vibration (0.82 MeV state 2⁺) and one phonon octapole vibration (4.58 MeV state, 3⁻) are taken into account in JENDL-3PR1¹²⁾. In addition, peaks can be separated at 3.23, 5.29, 6.09, 6.49 and 7.94 MeV state. It is interesting that the 3.23 MeV is close to

the pairing energy if the pairing vibration is excited. As shown in Fig.16, discrete excitations at selected levels are seen even for heavy nucleus like ^{209}Bi which must have more than hundreds of levels by statistical theory. Observed peaks at 1.73, 2.68, 4.28 and 6.53 MeV state seem to be collective excitations by either surface vibration or rotation of nucleus.

3.2 Comparison with Evaluated Data for Other Elements

High resolution measurements have been additionally carried out for light elements (Li, B and N), medium ones (Na, Cl and Zr) and heavy one (W), and compared with ENDF/B-IV, JENDL-3PR1 and -3PR2.

Lithium ; Measured DDX data are compared with JENDL-3PR1¹⁵⁾ in Figs. 17 and 18, respectively for 45 deg and 135 deg. Peak at $Q = -2.15$ MeV is coming from the first excited state of inelastic scattering of ^6Li . JENDL-3PR1 data reproduce well the experimental up to the $Q = -4.63$ MeV state of $^7\text{Li}(n,n't)$ reaction, below which disagreement is obvious and the experimental shows two additional discrete level excitations, i. e., 6.68 and 7.47 MeV level. Hence, the continuum spectra of $^7\text{Li}(n,n't)$ neutrons in JENDL-3PR1 should be altered. Comparisons with the latest JENDL-3PR2 data¹⁶⁾ are shown in Figs. 19-a, b, c and d. JENDL-3PR2 data are reproducing quite well the measured data for every scattering angle, in contrast with the disagreement with the ENDF/B-IV data.

Boron ; An example is shown in Fig.20. The experiment clearly shows that emission spectra are expressed by gathering discrete level excitations; 2.12, 4.45, 5.02, 6.74, 9.19, 10.6 and 11.5 MeV level excitations by $^{11}\text{B}(n,n')$ are distinguished by the experiment. The ENDF/B-IV data are unreasonable due to the statistical model calculation.

Nitrogen ; To make a ring scatterer, ZrN powder is contained in a ring case of thin aluminum. DDX data for nitrogen are obtained by subtracting the contributions of Zr and Al, as shown in Fig.21. The results are compared with the ENDF/B-IV data, as shown in Figs. 22-a, b and c for three angles. By experiment, 5 discrete-level excitations could be distinguished; 2.3, 3.9, 5.0, 5.7 and 7.0 MeV state. For these levels, the evaluation of ENDF/B-IV seems to be satisfactory, though the experiment gives higher values for the integrated values within the energy interval from 8 to 13 MeV at forward angles (see Fig. 22-a). Below the 7.0 MeV state, disagreement between the experiment and the ENDF/B-IV data should be marked.

Sodium ; An example of measured DDX at 60 deg is given in Fig.23, in comparison with the ENDF/B-IV data. Drastic disagreement in the 6-13 MeV range is due to the neglect of direct and semi-direct processes in ENDF/B-IV.

Chlorine ; A ring sample of CCl_4 contained in a thin Al case was used. By subtracting carbon DDX, sufficiently accurate DDX data for chlorine were obtained. An example at 45 deg is shown in Fig.24, in comparison with the ENDF/B-IV data which are unsatisfactory except the elastic peak.

Zirconium ; An example of the results is shown in Fig.25. Since the multiple scattering correction is difficult in the 8-13 MeV range, it is better to adopt the uncorrected data (black dots) in this range and corrected data can be adopted for others. Three distinct peaks (2.186, 2.748 and 4.04 MeV state) in the experimental data seem to be coming from the collective excitation of ^{90}Zr which is existing by 51.5 % in natural sample. Due to the effect of other isotopes like ^{91}Zr (11.2 %), ^{92}Zr (17.1 %) and ^{94}Zr (17.4 %), other possible peaks than the three are not separable. Evaluation of these collective excitations is not done in ENDF/B-IV, which reproduces very different DDX from the experimental one as shown in Fig.25.

Wolfram ; The result for wolfram brings us similar discussions to the discussions for zirconium, as seen from Fig.26. Since there is no dominant isotope in a natural wolfram sample ($^{182}\text{W} = 26.3\%$, $^{183}\text{W} = 14.3\%$, $^{184}\text{W} = 30.7\%$ and $^{186}\text{W} = 28.6\%$), no distinct peaks are obvious in the measured spectrum. However, it can be predicted from the results of pure isotope samples like ^{209}Bi that the structure of measured spectrum in the 8-13 MeV range reflects the superposition of many collective states of 4 wolfram isotopes. Hence the missing data in ENDF/B-IV in that energy range should be added by evaluating the direct process of collective excitation, rather than the precompound process which may contributes a little.

4. Concluding Remarks

DDX data around 14 MeV incident neutron energy have been measured for 25 elements at the OKTAVIAN facility. These data have been quite useful to point out guide lines for re-evaluating evaluated nuclear data libraries like ENDF/B-IV and JENDL-2, although the incident neutron energy varies with the change of scattering angle. Through the comparison work with available evaluated nuclear data libraries, we can say the following for the status of ENDF/B-IV and JENDL-3PRL;

Status of ENDF/B-IV:

- a) Sufficient; Al and Fe
- b) Fairly well; N, O and Si
- c) Insufficient; D, Li, Be, B, C, F, Na, S, Cl, Ti, Cr, Mn, Ni, Cu, Zr,

Nb, Mo, W, Pb and Bi.

Status of JENDL-3PR1;

- a) Close to sufficient; C, Cr, Fe and Ni
- b) Fairly well; Li and Be

Status of JENDL-3PR2 for Li is satisfactory.

It has become clear that the direct and semi-direct processes are important for the secondary neutron emission data at 14 MeV. For heavier elements, excitations of discrete and collective levels by inelastic scattering should be further investigated. It is expected to collect angular differential data for individual levels at specified incident neutron energy. For light elements, angle-energy correlation data (DDX) are important for continuum neutrons. Hence, a high resolution DDX measurement with fixed incident energy will be required. A 90 deg 8 m TOF system is nearly completed for this purpose at the OKTAVIAN facility. Using this system, re-measurements will be done for some of the 25 elements and new measurements will be started for other elements than the 25.

References

- 1) Takahashi, A., Rusch, D. : KFK-2832/I & II (1979)
- 2) Ebisuya, M., et al. : JAERI-M 8135 (1979)
- 3) Yamamoto, J., et al. : J. Nucl. Sci. Technol., 19 [4], 276 (1982)
- 4) Takahashi, A. : J. At. Energy Soc. Jpn. (in Japanese), 21[12], 903 (1979)
- 5) Takahashi, A., et al. : Proc. Conf. Nuclear Data for Science and Technology Antwerp, 1982, p.360 (1983), Reidel Publ. OKTAVIAN Rep. A8301, Osaka U. (1983)
- 6) Takahashi, A., et al. : J. Nucl. Sci. Technol., 21[8], 577 (1984)
- 7) Yamamoto, J., Takahashi, A. : JAERI-M 84-010, p.391 (1984)
- 8) Takahashi, A. : J. At. Energy Soc. Jpn. , 26[3], 182 (1984)
- 9) Shibata, K. : JAERI-M 84-226 (1984)
- 10) Perkins, S. T., et al. : UCRL-91276 (1984)
- 11) Yanagi, Y., Takahashi, A. : OKTAVIAN Rep. A-8402 (1984)
- 12) Kikuchi, Y., et al. : J. Nucl. Sci. Technol., 22[6], 499 (1985)
- 13) Takahashi, A., et al. : OKTAVIAN Rep. A-8308 (1983)
- 14) Nuclear Data Sheets : Fe; 20[3], 253 (1977), Bi; 5[3] (1973)
Nucl. Phys., A214[1] (1973) for Al
- 15) Shibata, K. : JAERI-M 84-204 (1984)
- 16) Chiba, S. : Private communication

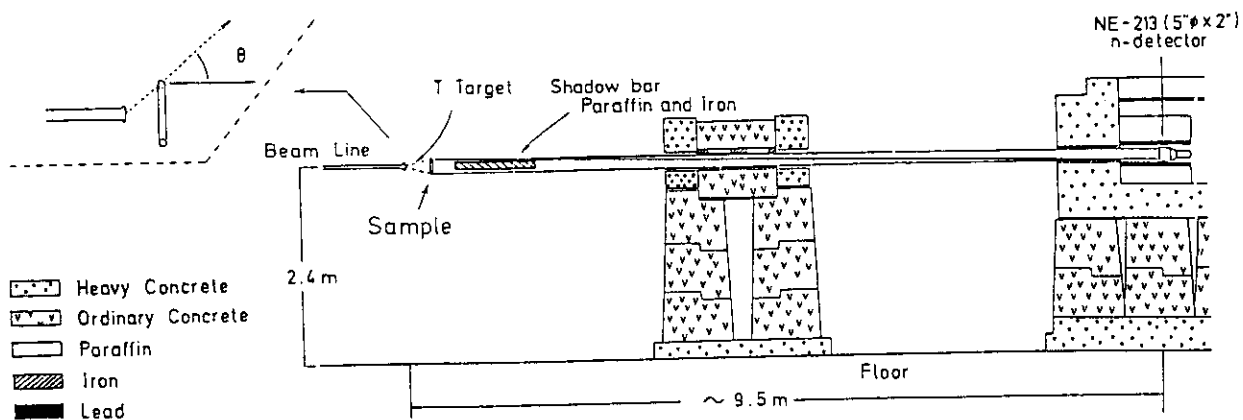


Fig.1 Schematic arrangement for DDX experiment at OKTAVIAN

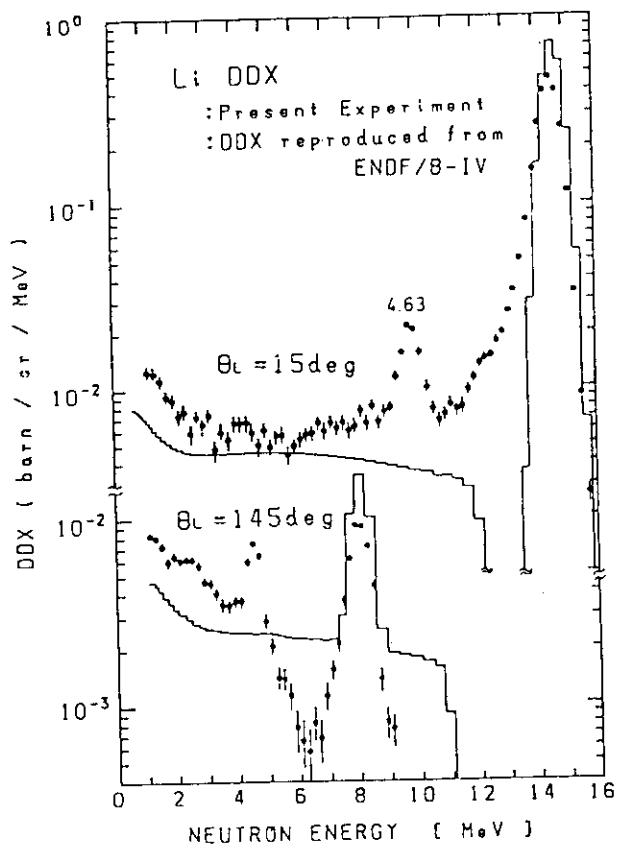


Fig.2 DDX of natural lithium, compared with ENDF/B-IV

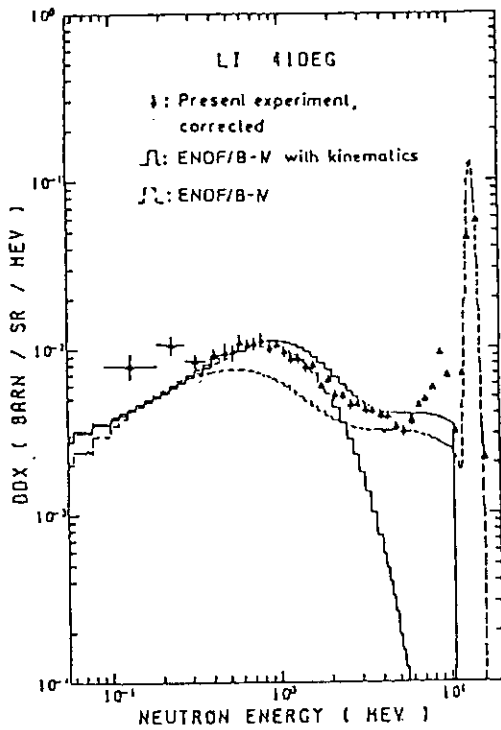


Fig.3 Low energy part of Li DDX at 41 deg; broken curve, ENDF/B-IV

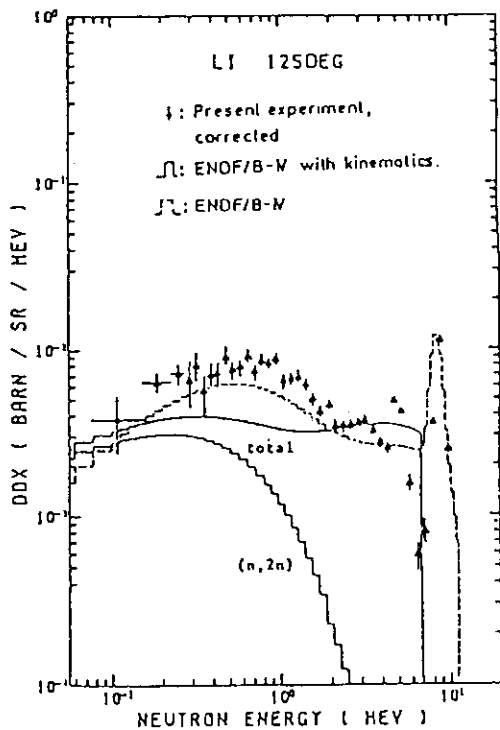


Fig.4 Low energy part of Li DDX at 125 deg; broken curve, ENDF/B-IV

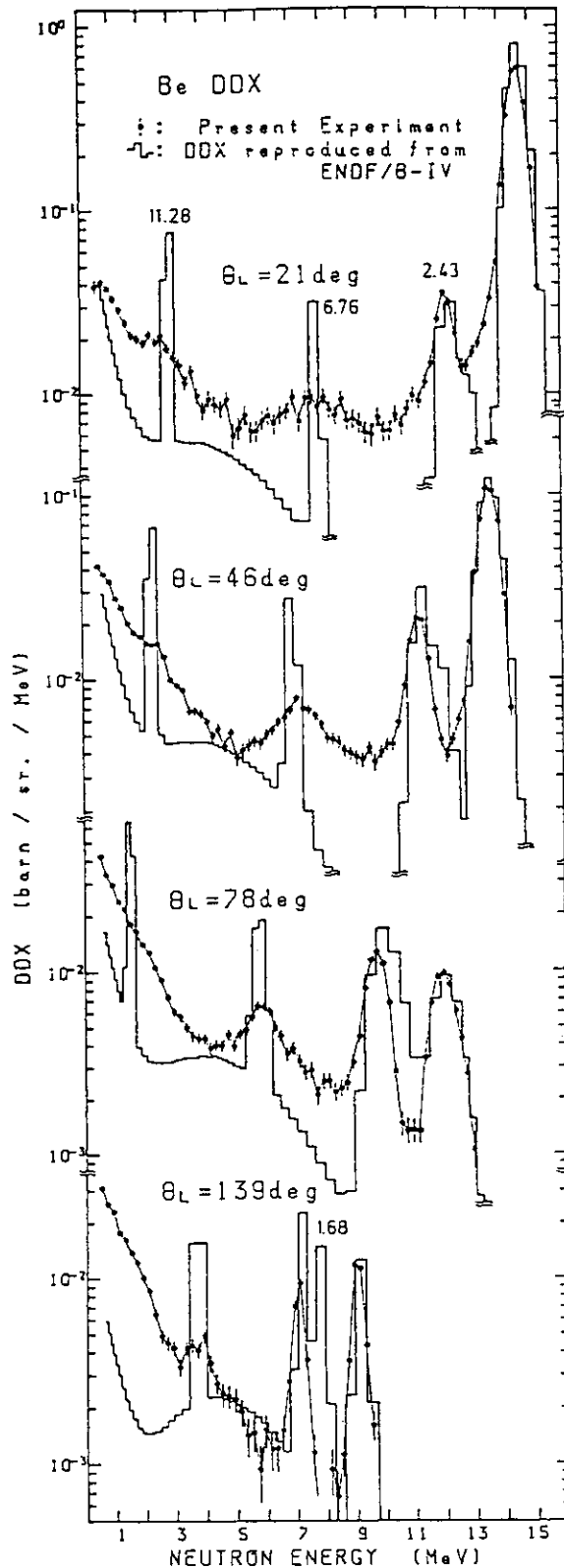


Fig.5 DDX of beryllium, compared with ENDF/B-IV

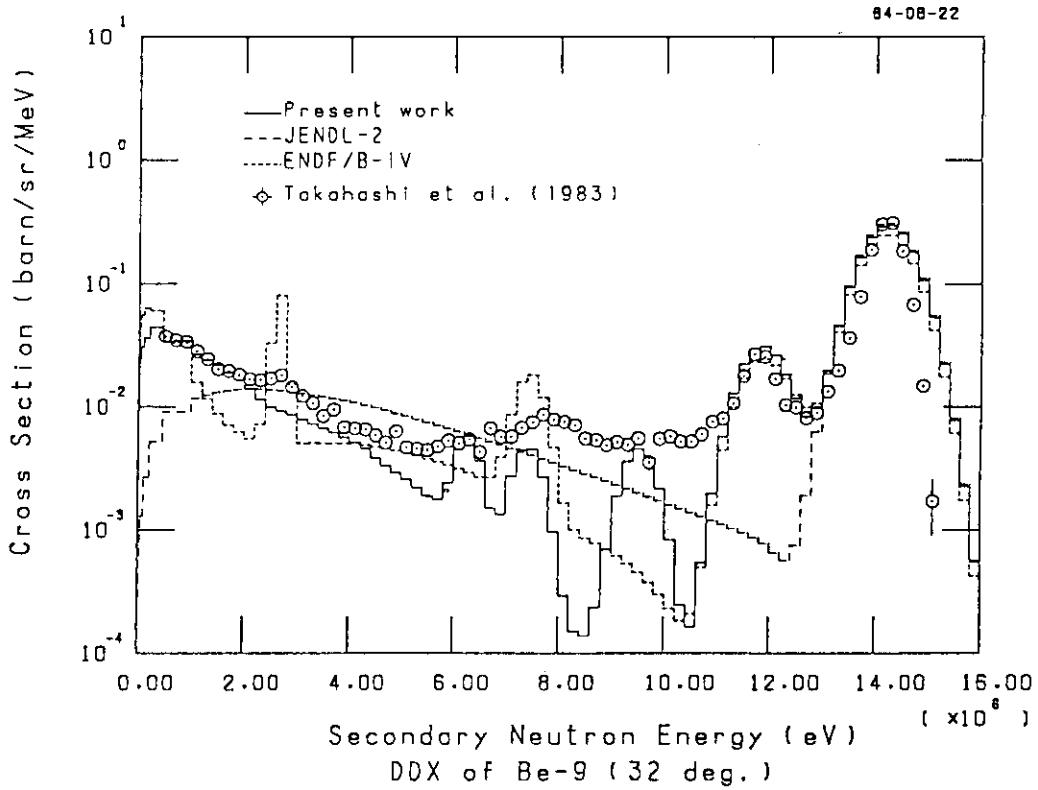


Fig.6 DDX of Be-9 at 32 deg, compared with JENDL-3P1 (solid curve)⁹⁾

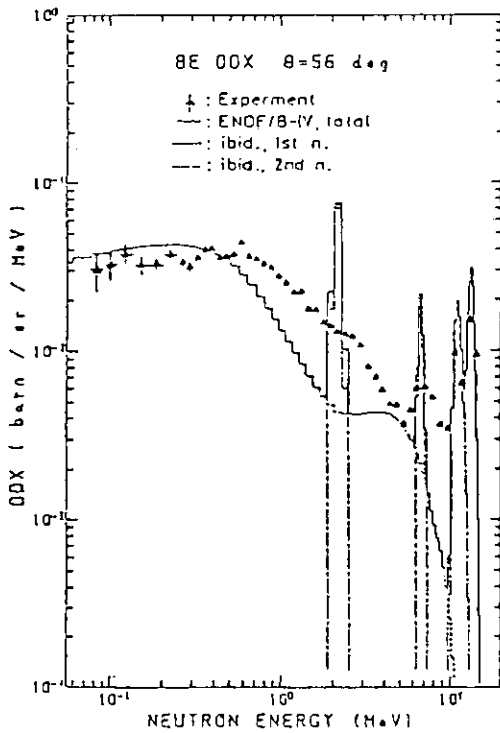


Fig.7 Low energy part of Be-9 DDX at 56 deg; compared with ENDF/B-IV

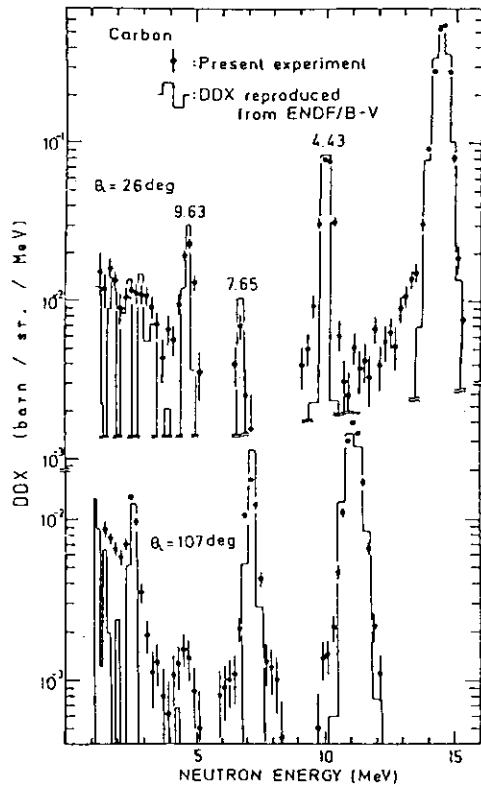


Fig.8 DDX of C-12, compared with ENDF/B-IV (solid histogram)

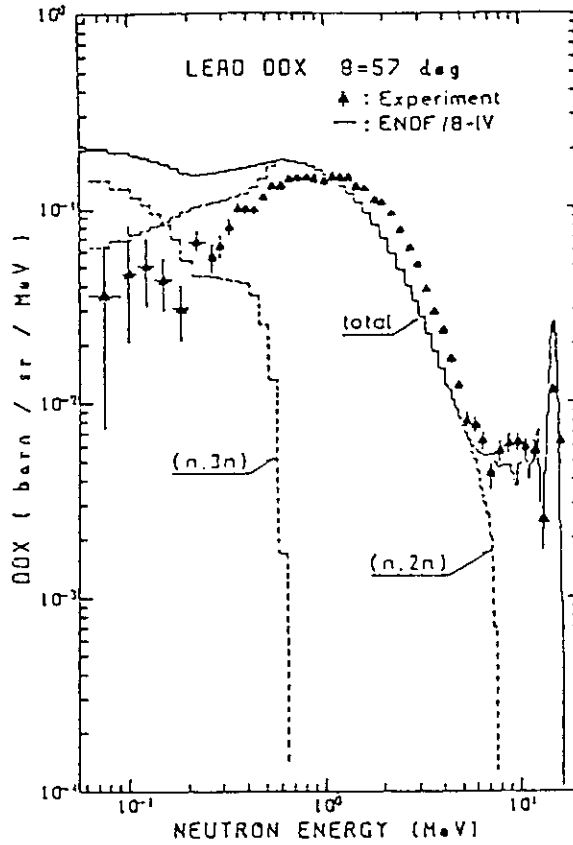


Fig.9 DDX of lead, compared with ENDF/B-IV

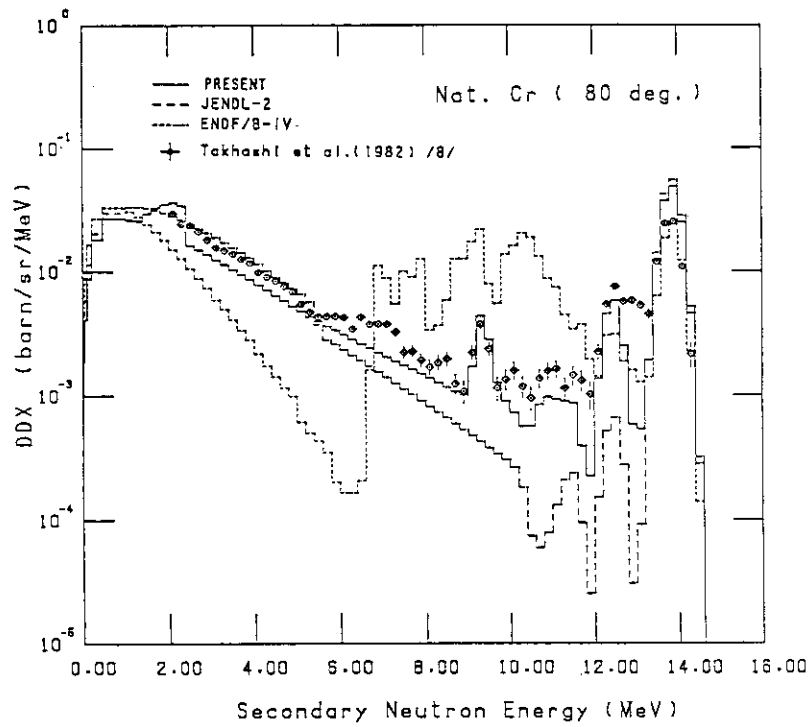


Fig.10 DDX of natural-chromium¹²⁾; solid histogram, JENDL-3PR1

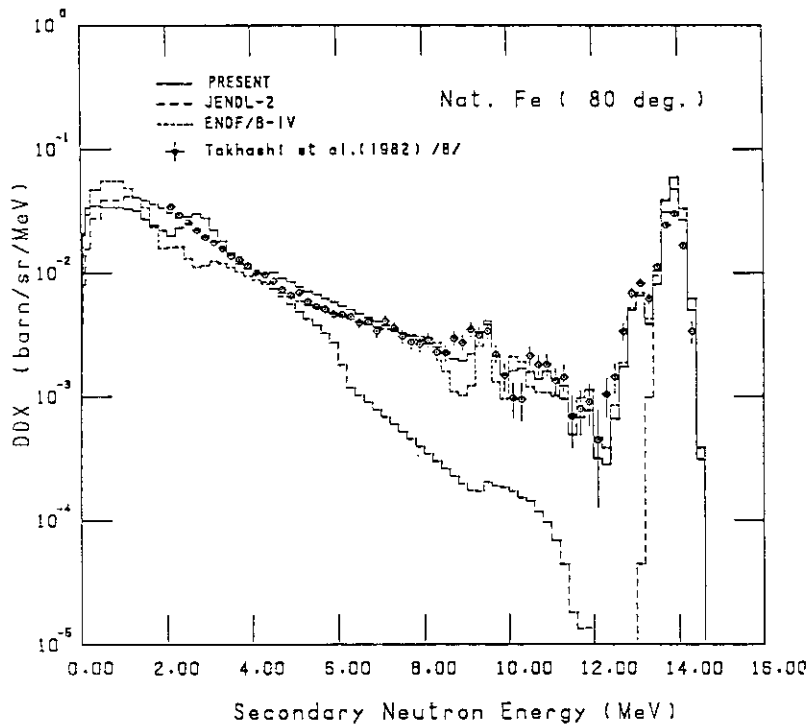


Fig.11 DDX of natural-iron¹²⁾; solid histogram, JENDL-3PR1

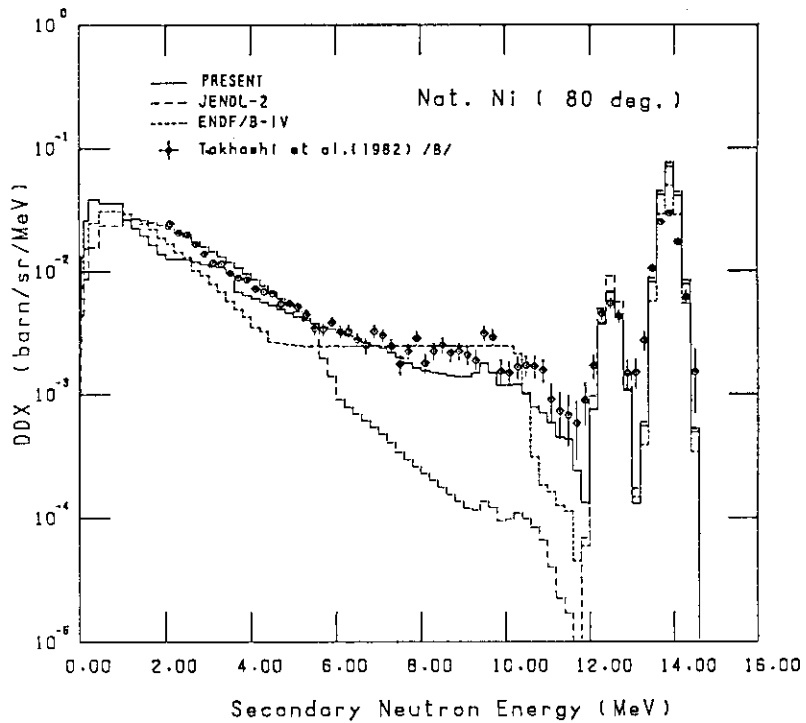


Fig.12 DDX of natural-nickel¹²⁾; solid histogram, JENDL-3PR1

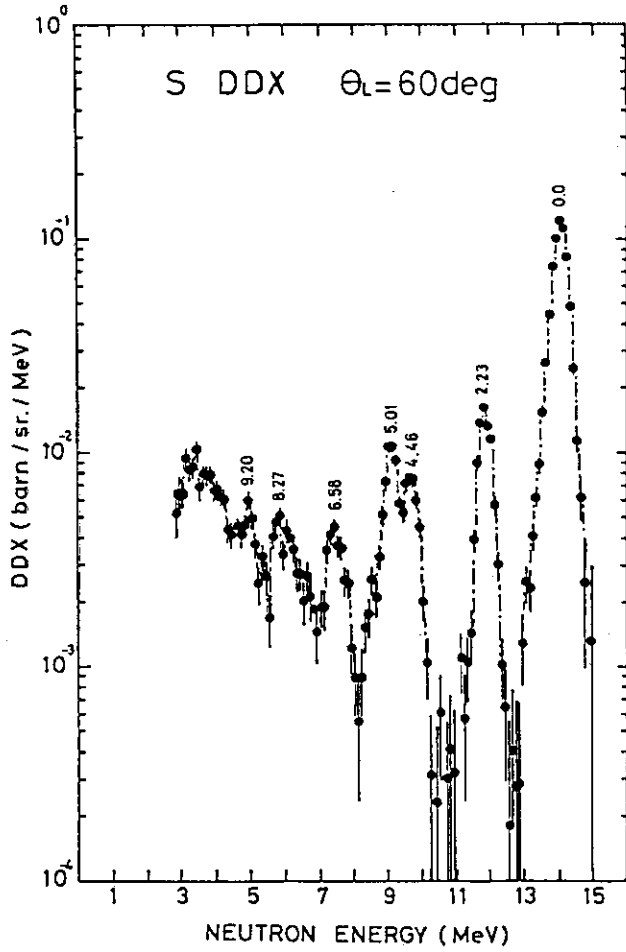


Fig.13 DDX of sulfur at 60 deg

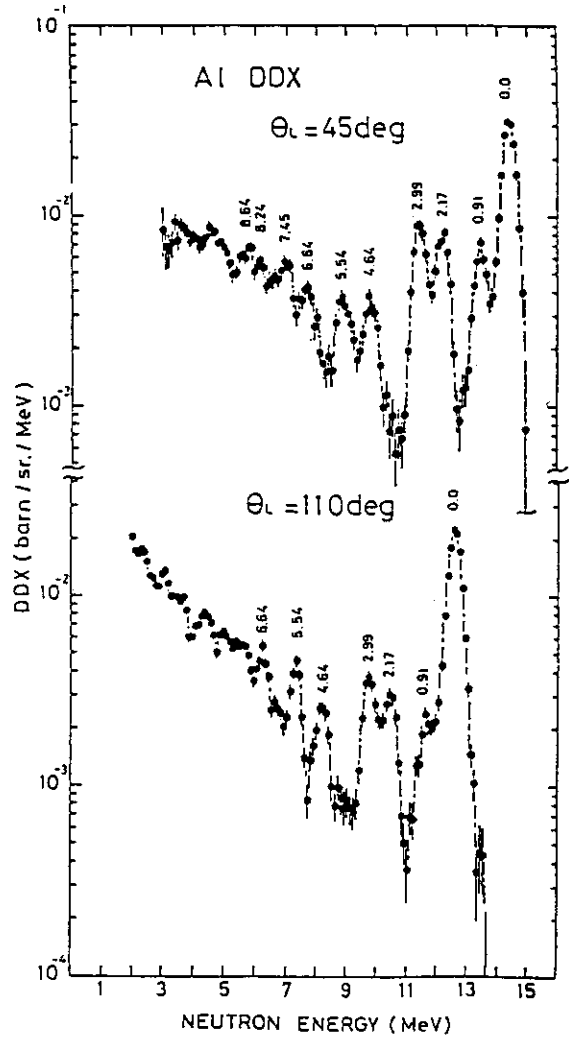


Fig.14 DDX of Al-27

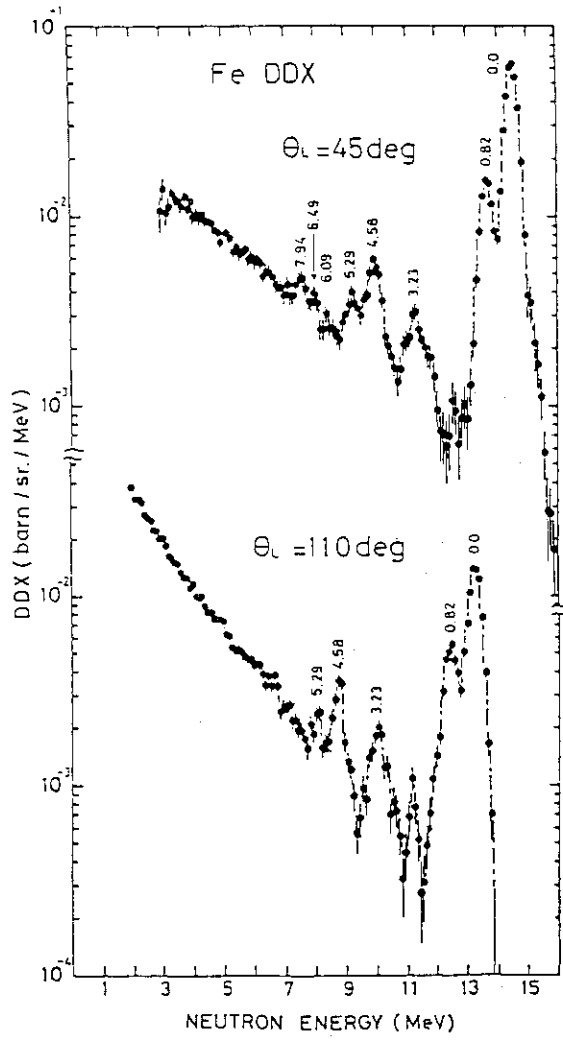


Fig.15 DDX of natural iron

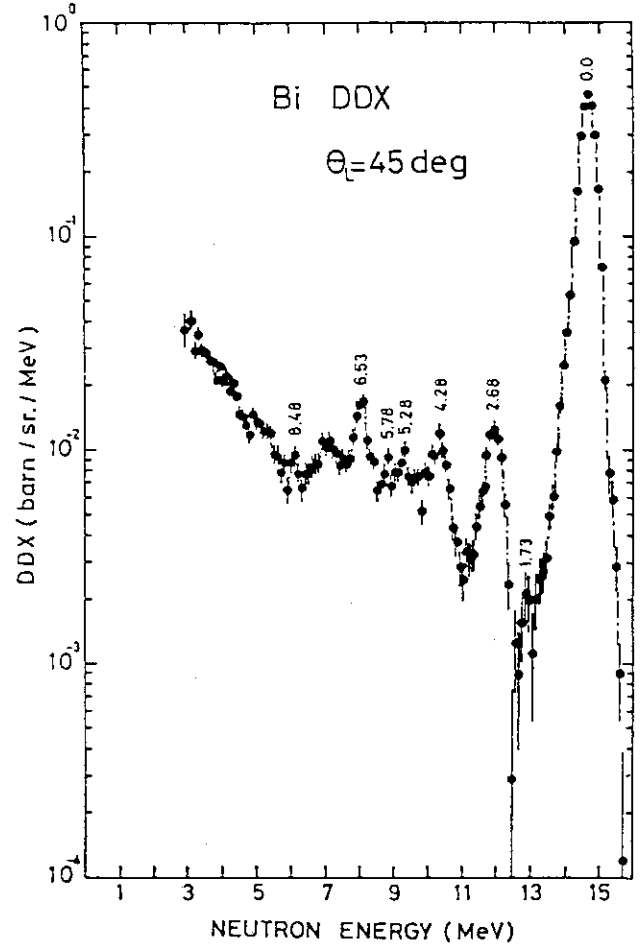


Fig.16 DDX of Bi-209

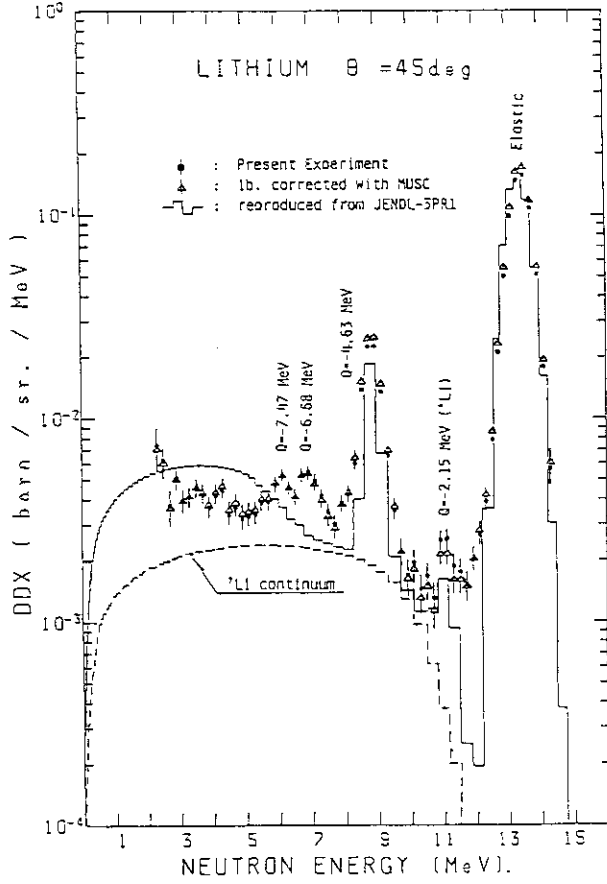


Fig.17

DDX of natural lithium at 45 deg, compared with JENDL-3PR1

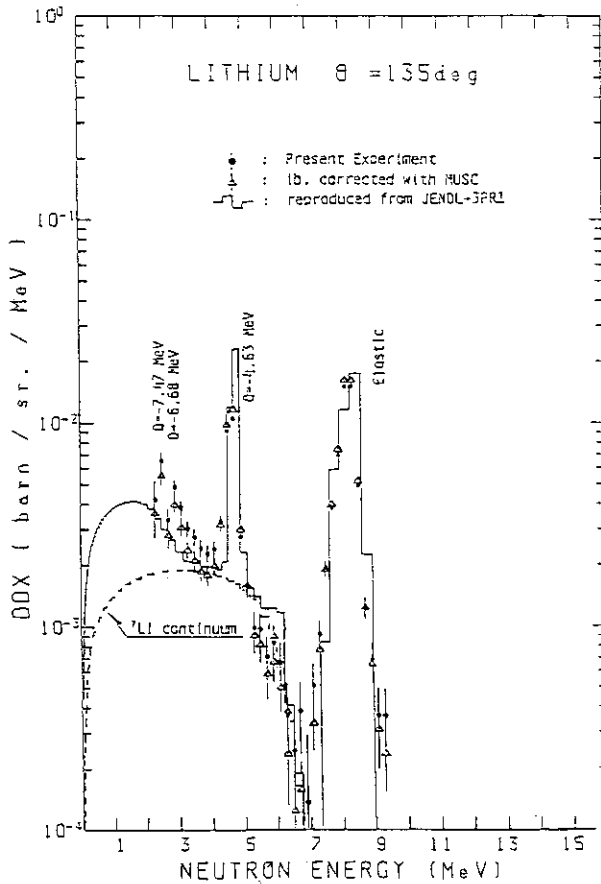
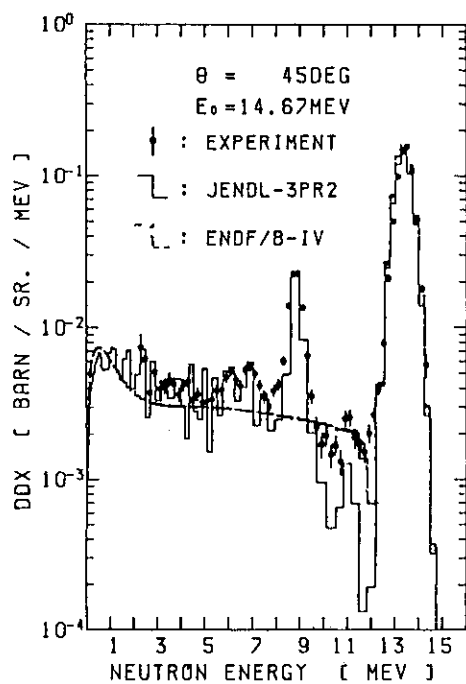
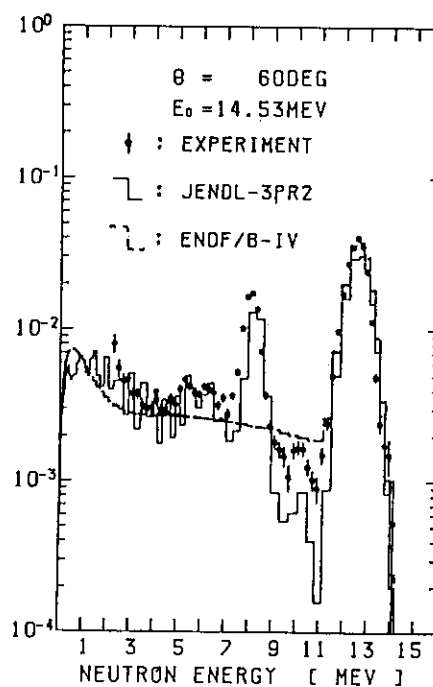


Fig.18

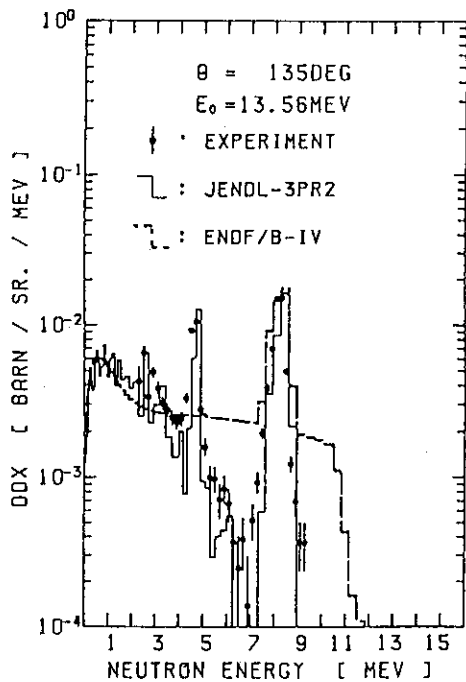
DDX of natural lithium at 135 deg, compared with JENDL-3PR1



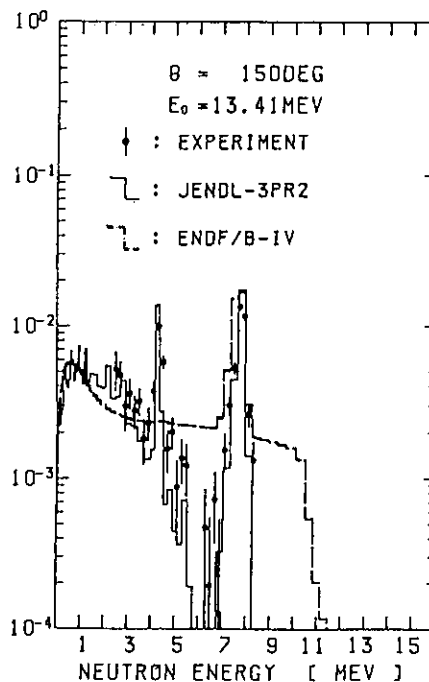
a) 45 deg



b) 60 deg



c) 135 deg



d) 150 deg

Fig.19 DDX of natural lithium, compared with JENDL-3PR2

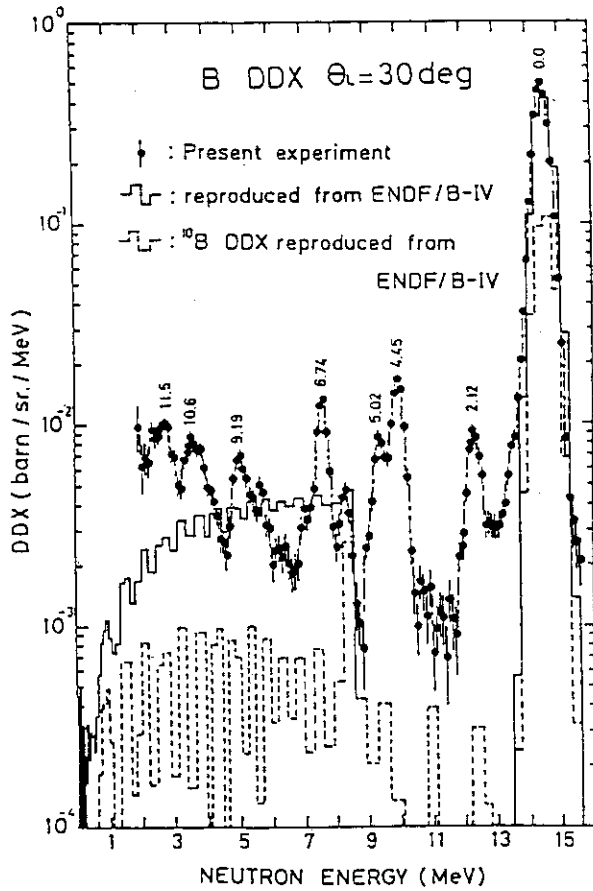


Fig.20
DDX of natural boron,
compared with ENDF/B-
IV

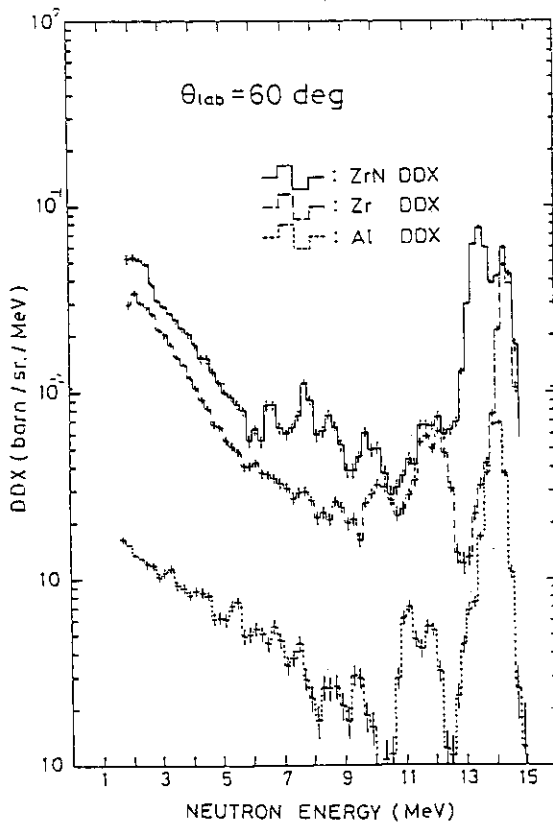
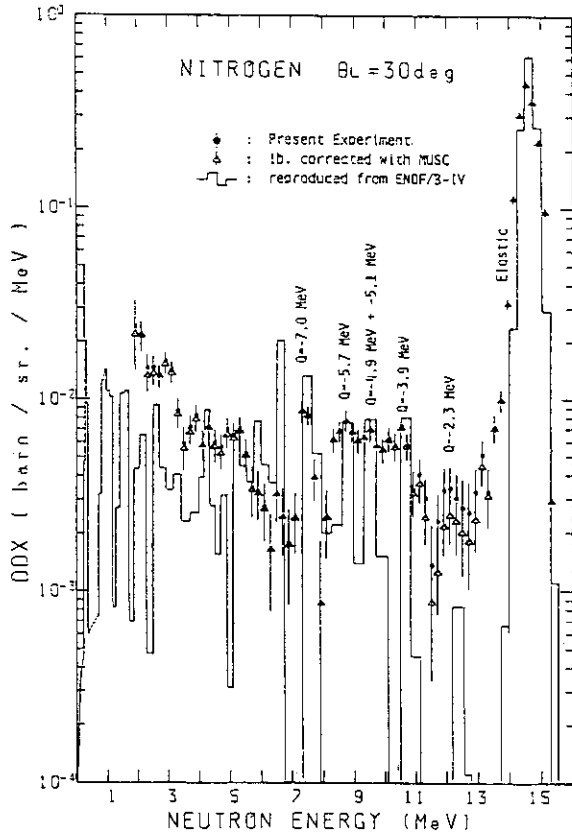
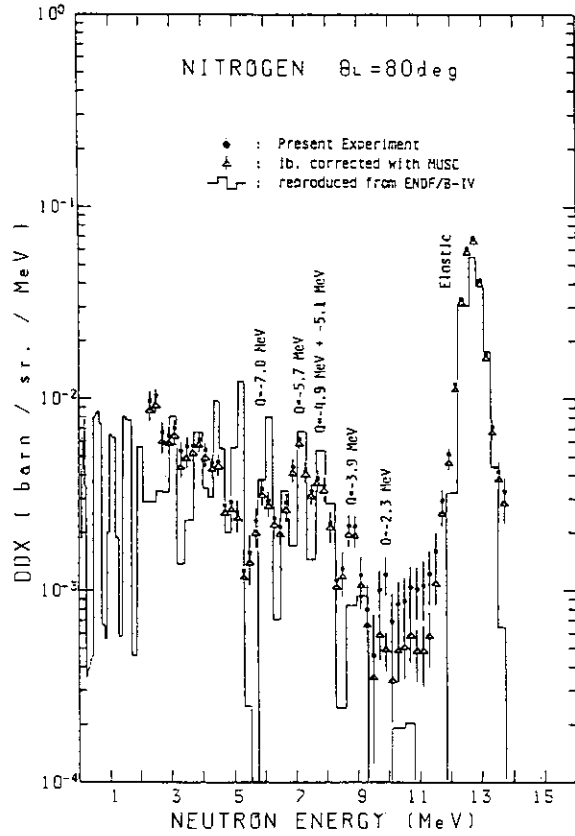


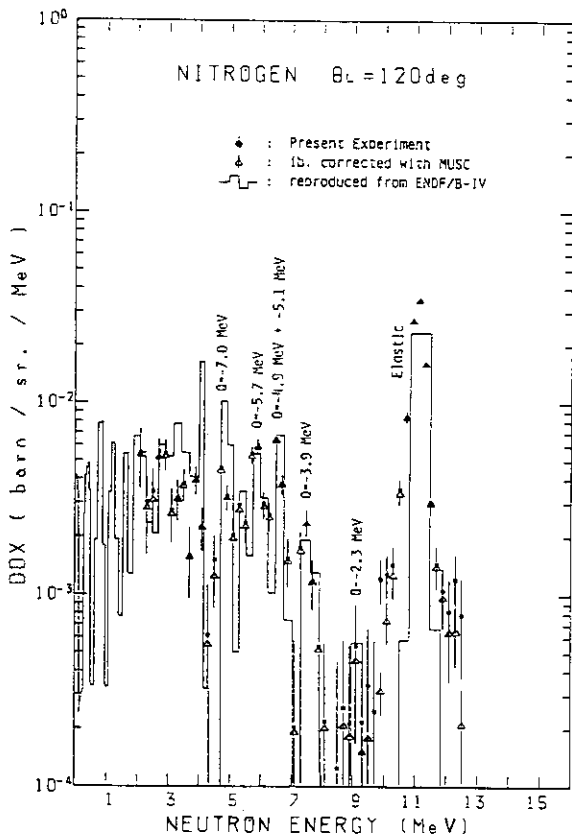
Fig.21
DDX data of ZrN, Zr and
Al, to obtain DDX of
nitrogen



a) 30 deg



b) 80 deg



c) 120 deg

Fig.22
DDX of nitrogen,
compared with
ENDF/B-IV

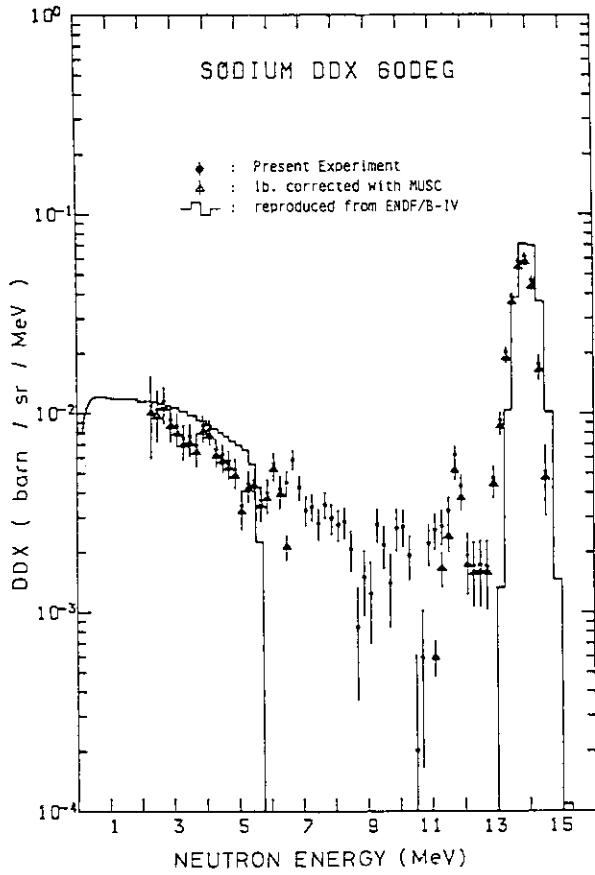


Fig.23
DDX of sodium,
compared with
ENDF/B-IV

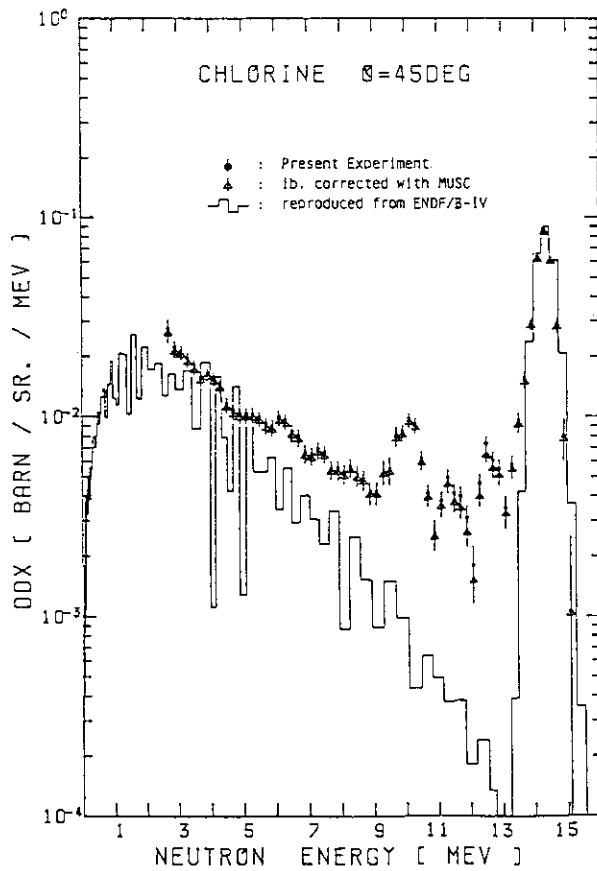


Fig.24
DDX of chroline,
compared with
ENDF/B-IV

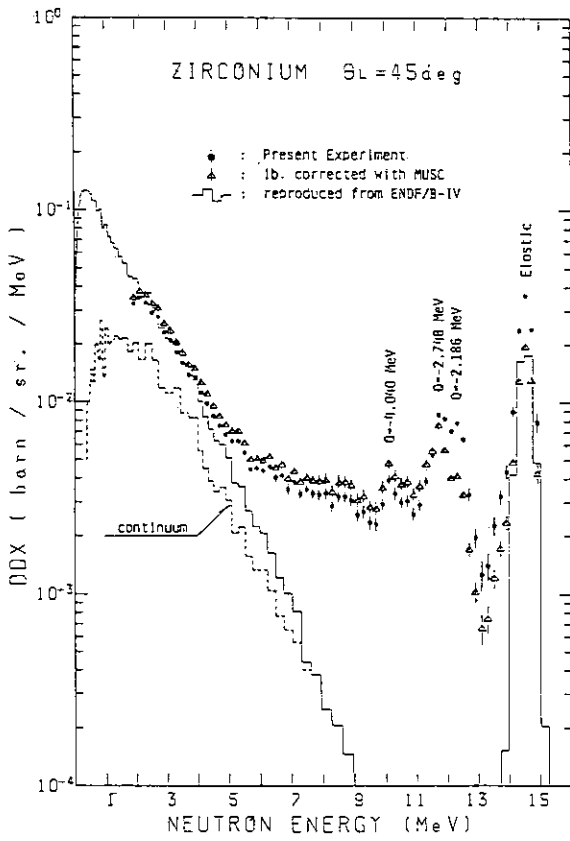


Fig.25
DDX of zirconium,
at 45 deg, compared
with ENDF/B-IV

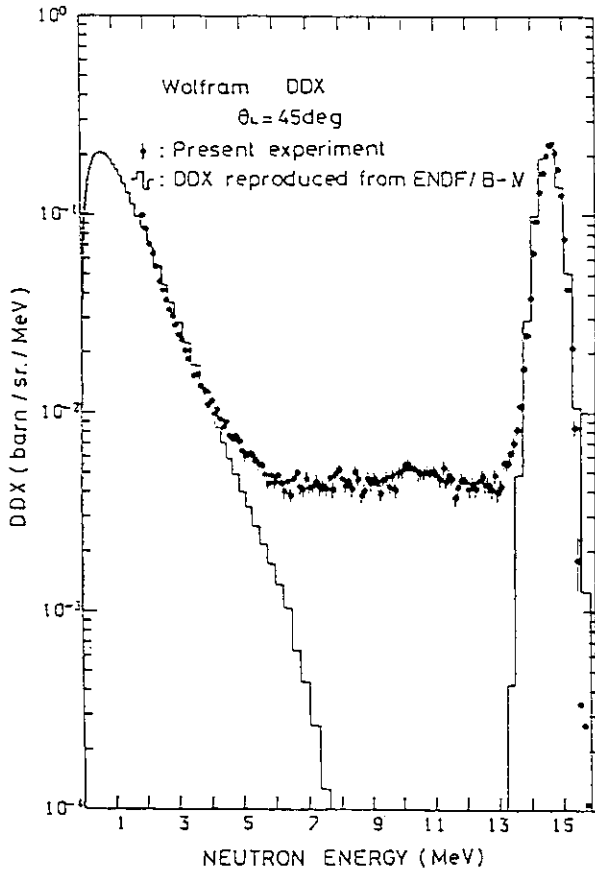


Fig.26
DDX of natural-
wolfram at 45
deg, compared
with ENDF/B-IV

5. Measurements of Double-Differential Neutron Emission
Cross Sections at Tohoku University

M.Baba

Department of Nuclear Engineering, Tohoku University
Aoba, Aramaki, Sendai

A brief summary is presented for measurements and analyses of double-differential neutron emission cross sections for fusion reactor materials performed at the Tohoku University Dynamitron facility. The experiments and the typical results are described for ${}^6,7\text{Li}$, ${}^9\text{Be}$, C, O, Fe, Ni and Pb. The experimental results for emission spectra and scattering cross sections are discussed in comparison with JENDL-3PR1.

1. Introduction

The energy-angular double-differential neutron emission cross sections (DDX) of fusion reactor materials are of prime importance as the basic nuclear data in fusion reactor neutronics studies, since they provide detailed informations for neutron scattering processes required for neutron transport calculations. For light elements of ${}^6,7\text{Li}$, beryllium and carbon, the scattered neutrons exhibit strong energy-angle correlation, so that precise DDX data are required. However, the experimental data are very sparse, and theoretical calculations are not successful in predicting either the energy distribution or cross section. As for medium and heavy nuclei, while a certain amount of experimental data have been reported, the agreements among the

experimental data are not satisfactory owing partly to differences in experimental condition such as incident energy and its dispersion. Therefore, more experimental data with definite experimental conditions are required in order to improve the data reliability.

We have promoted a series of DDX measurements for fusion reactor candidate materials using a time-of-flight spectrometer with a 4.5 MV Dynamitron accelerator as pulsed neutron source. Table-1 presents the summary of the measurements performed at the facility: the incident energy ranges from several MeV to 20 MeV including 14 MeV.

In this reports, we deal with the experiments and results that will be of interest for the JENDL-3PR1 evaluation.

2. Experiments and Data Analyses

The experimental details have been described previously^{1,2,3,4)}, and are only outlined here.

The Tohoku University 4.5 MV Dynamitron accelerator provided pulsed proton and deuteron beam, about 2-nsec duration and 1 or 2 MHz repetition rate, for neutron production. The primary neutrons were obtained via the p+T and d+D reaction using a Ti-T and deuterium gas target, respectively, at MeV region and the d+T reaction at 14 to 20 MeV.

In Fig.1, schematics of our experimental setup are shown. The upper one shows that used for 14.1 MeV measurements: the sample and neutron detector were placed on the plane perpendicular to the incident beam axis, the scattering angle was varied by rotating the sample around the target. In this geometry, the neutrons incident on the sample have well defined energy of 14.1 ± 0.15 MeV, which is the mean energy of the neutrons emitted from the d-T fusion reaction. The lower one is the usual neutron scattering geometry and was employed for measurements at energies other than 14.1 MeV. The flight path length was 4 to 8 m.

The secondary neutrons are detected by a massively shielded NE-213 scintillator, 5" in dia. and 2" thick, equipped with a pulse shape discriminator (PSD). A standard T-O-F electronics setup was employed for measurements using a timing discriminator and a PSD with pulse-height dynamic range of 1000 and 400, respectively, to permit measurements from 300 keV to 20 MeV in a single run. The T-O-F data were accumulated with a two-bias⁴⁾ or dynamic biasing⁵⁾ method to obtain a smooth detector efficiency curve, and improved timing resolution and S/N ratio in high energy region.

The scattering samples were of right cylinder, 4-cm long and 2.5 to 3.5-cm in diameter. The absolute value of cross section was determined relative to the hydrogen scattering cross section.⁶⁾

The measured T-O-F data were corrected for backgrounds, detector efficiency and sample-size effects. For the background correction, the following contributions were taken into consideration: 1) sample-out background, 2) background due to parasitic source neutrons, 3) the effects of degraded neutrons via the scattering by the target assembly and shadow bar. The neutron target was designed to be of low-mass construction to reduce the neutron scattering at the target; it produced negligibly small backgrounds by target scattering. The effects of shadow bar scattering proved to be very small from the measurements of the emission spectra from hydrogen and carbon which emit no or very little neutrons of continuum. The data correction for sample-size effects was performed using the Monte-Carlo⁷⁾ and analytic method⁸⁾. It was noted, however, the simulation based on the currently available evaluated data did not necessarily provide realistic results: therefore, it was necessary to prepare a data sets on the basis of our or other experimental data in order to improve the simulation and correction.

Finally, partial values of scattering cross sections and spectrum

shape parameters were extracted from the emission spectra through the data analysis using the spectrum fitting programs RANSER⁹⁾ and SALS¹⁰⁾.

The experimental uncertainty was evaluated considering the contributions from 1) counting statistics (2-30%), 2) absolute normalization (4-5%), 3) detector efficiency (5%), and from 4) sample-size correction (1-10%).

3. Results and Discussion

In this section, we present typical results of measurements and analyses, and compare them with the corresponding values derived from the JENDL-3PR1. The present experimental results at 14 MeV were in general agreements with the ring-sample data at OKTAVIAN¹¹⁾ of Osaka University.

(1) ${}^6,7\text{Li}$ 2,4,12)

The present results of emission spectra and partial values for ${}^6,7\text{Li}$ are illustrated in Fig.2-5, compared with the evaluated values. The JENDL-3PR1 evaluation gives much improved reproduction than ENDF/B-IV and JENDL-2, however, appreciable disagreements with the experiments are still found as the following: 1) the evaluated energy spectra at 14 MeV are markedly harder than the experimental ones, 2) MeV DDXs show similar features, 3) the evaluated angular distribution and magnitude of inelastic-scattering cross sections are not consistent with the measurements, and 4) the experiments indicated excitation of higher levels not considered in JENDL-3PR1.

The continuum emission spectra are composed of neutrons via the $(n,n'\alpha)$ and $(n,2n)$ reactions, and the enhancement of low energy neutrons in the experimental spectra is considered owing to $(n,2n)$ reaction. In JENDL-3PR1, ordinary phase-space distribution is assumed for the neutron spectra of these reaction. As shown in Fig.4, the emission

spectra are interpreted much better by adopting a Coulomb distorted phase-space model¹³⁾ and a evaporation spectrum for $(n,n'X)\alpha$ and $(n,2n)$ neutrons, respectively, in place of phase-space model in JENDL-3PR1. The angular distributions of inelastic-scattering cross sections were found to be analysed successfully with a coupled channel optical model over wide range of incident energy.^{4,12)} The problems cited above will be taken into consideration in the new evaluation for JENDL-3PR2, and the evaluation details will be described by S.Chiba in this proceedings.

(2) Beryllium¹⁾

The measured DDXs and partial cross sections are presented in Fig.6-8, along with the evaluated values. The beryllium emission spectra are characterized by a large amount of continuum neutrons due to multi-particle decay processes reaching to $(n,2n)$ reaction. As shown in Fig.6, there appear discrepancies between the experiments and JENDL-3PR1.

1) The inelastic-scattering from the "1.7 MeV level" was not observed in the experiment, whereas substantial cross section is given to this branching in the evaluation, 2) The experiments indicate notable excitation of 3.0 MeV level, while it is neglected in the evaluation, 3) In the experimental spectra at 14-MeV by Takahashi et al¹¹⁾, the discrete inelastic peaks from levels higher than 4 MeV are greatly smeared compared with the evaluated ones. These differences are not attributed to the problem in energy resolution, but are likely due to inherent nature of the reaction. Taking accounts of level width of these levels and of simultaneous break-up process would lead to improvement. The inclusion of level width has been performed in recent LLNL evaluation¹⁴⁾ resulting in very good agreements with the experiments.

(3) Carbon ^{15,16)}

The experimental results of DDXs at 14.1 and 18.2 MeV are compared with the JENDL-3PR1 and ENDF/B-V evaluation in Fig.9. In lower energy region of energy spectra, there appear "continuum" neutrons produced via the break-up processes resulting in $(n,n')\alpha$ reaction. From the data comparison, the following problems can be pointed out for the evaluated data.

1) The low energy parts of emission spectra are not described satisfactorily by either JENDL-3PR1 or ENDF/B-V. The problem will be reduced to, 2) the cross sections of the second ($Q=-7.6$ MeV) and third ($Q=-9.6$ MeV) level, and 3) the spectra and cross sections of "continuum" neutrons. Fig.10 shows the evaluated inelastic-scattering cross sections for the second and third levels are in marked disagreements with the measurements. In particular, JENDL-3PR1 evaluation overemphasizes the third level cross section considerably at 14.1 MeV. The "continuum" parts of respective spectrum are fitted with a evaporation spectrum assumed in JENDL-3PR1. The experimentally deduced temperature, however, varies significantly with scattering angle probably because of energy-angle correlation. Therefore, pseudo-level presentation adopted in ENDF/B-V seems preferable for consistent description of these neutrons.

4) As shown in Fig.11, the present values of the first level cross section at 18.2 MeV largely differ from the evaluation, while they are in good agreements with those by Thum et al.¹⁷⁾ The coupled channel calculations shown in Fig.12 give much better results than evaluation and seems useful for cross section evaluation. 5) The present results at 14 MeV for the elastic-scattering and first level cross sections, are respectively about 10 and 30 % higher than those by Haouat et al.¹⁸⁾, while they are in fair agreements with those by Glasgow et al.¹⁹⁾. The reason for these discrepancies has not been well traced, whereas the cross section fluctuation observed in the (p,p) , (p,p') reactions might be of some concern.

(4) Oxygen ^{15,16)}

The results of DDX and inelastic-scattering cross sections are shown in Fig.13-14, together with the evaluated data. From the data comparison, the following can be pointed out.

1) In the energy region lower than 2 MeV, the measured DDX are notably higher than the evaluated values, probably because of break-up neutrons not considered in the evaluation.

2) Distinct disagreements are seen in the inelastic scattering cross sections from the (6.05+6.13) MeV and (6.92+7.12) MeV levels. The present values are considerably smaller especially for (6.92+7.12) MeV levels. In addition, the experimental angular distribution shows forward rise more than the JENDL-3PR1 values. The present elastic-scattering cross section is in fair agreement with that of JENDL-3PR1 and Glendinning et al.²⁰⁾.

(5) Fe, Ni

For these structural materials, new evaluation of JENDL-3PR1²¹⁾ provided much improved prediction of DDXs than previous ones. However, it showed appreciable disagreements with the data at OKTAVIAN¹¹⁾, in the angular dependence of emission neutrons. The present results of DDX and angular distribution of emission neutrons are shown in Fig.15,16. They are in fair agreements with the data at OKTAVIAN¹¹⁾, and show similar but a little milder forward rise even for the low energy neutrons. Therefore, the present data also show disagreements with JENDL-3PR1, although they not final yet and may receive a slight revision. Final results and detailed discussion will be presented later.

(6) Lead ²²⁾

Lead is expected to be a major neutron multiplier in fusion reactor blankets, so that the cross sections are required to be established urgently. In particular, the cross sections and emission spectra of

(n,2n) reaction are of interest. As seen in Fig.17,18, the evaluated values for lead largely differ from each other, and none of them reproduce satisfactorily the experimental cross sections and energy spectra of (n,2n) reaction.

In the present study, therefore, DDX measurements and the theoretical calculation were performed to determine the emission spectra and cross sections of (n,2n) reaction. The calculation was made using the code "GNASH" to take the preequilibrium process into accounts. The emission spectra by the present measurements and (n,2n) cross sections measured by Frehaut et al.²³⁾ were analysed with the calculation. As shown in Fig.17,18, the calculation using the optical model potential by Fu & Perey²⁴⁾ and the back-shifted Fermi-gas level density,²⁵⁾ reproduced successfully both the (n,2n) cross sections and the emission spectra. It was noted that the calculated neutron energy spectra were sensitive to the level density function and parameters.

4. Summary and Conclusion

The measurements and analyses of double-differential neutron emission cross sections for fusion reactor materials at Tohoku University were reviewed and discussed in comparison with the JENDL-3PR1 and other evaluations. The double-differential data proved to be useful to obtain a variety of informations for neutron emission spectra and scattering cross sections. The data in JENDL-3PR1 showed several discrepancies with the measurements in neutron emission spectra and inelastic-scattering cross sections, which should be solved in the new version of the evaluation.

The DDXs for light elements are characteristic of individual nucleus and are difficult to be followed with a unified model; the experimental informations are essential. The energy-angle correlation plays an important

role and is to be considered exclusively for DDXs for light nuclei. Optical model calculations were applied with success to Li isotopes, carbon and seem to be useful for high energy cross section evaluation, even though the physical ground is not sound for application to light nuclei. The angle dependence of emission spectra observed for Fe and Ni will be interesting from the theoretical point of view, and will be traced in more detail. The measurements and analyses for lead brought an improved interpretation; this procedure will be worthwhile for further data refinement.

Acknowledgement

The present work was performed in cooperation with S.Iwasaki, S.Chiba*, M.Ono**, H.Nakashima*, N.Yabuta, T.Kikuch and previous members of neutron scattering group of Tohoku University. We appreciate Dr. K.Shibata and Dr. Y.Kikuchi of JAERI for many valuable discussions and informations. The present work was partly supported by the Grand-in-Aid, Ministry of Education, Science and Culture (Fusion and Energy project).

References

- 1) M.Baba et al.: Proc. Int. Conf. "Neutron Physics/Nuclear Data" Harwell 1978, p.198 (1979)
- 2) M.Baba et al.: Proc. Int. Conf. "Nuclear Cross Section/Technology" Knoxville 1979, p.43 (1980)
- 3) M.Baba et al.: The Technology Report/Tohoku University, 50 1(1985)
- 4) S.Chiba et al.: J. Nucl. Sci. Technol., 22 (10) to be published

* present address; Japan Atomic Energy Research Institute

** present address; Hitachi Co., Ltd.

- 5) J.D.Brandenberger and T.Grandy: Nucl. Instr. Meth., 93, 495 (1971)
- 6) J.C.Hopkins and G.Breit: Nuclear Data Table, A9, 137 (1971)
- 7) T.Sakase: Tohoku University 1978, unpublished
- 8) W.K.Kinney: Nucl. Instr. Meth., 83, 15 (1970)
- 9) M.Kitamura et al.: Nucl. Instr. Meth., 136, 363 (1976)
- 10) T.Nakagawa and Y.Oyanagi: Recent developments in Statistical Influence and Data Analysis, 221 (1980) North-Holland
- 11) A.Takahashi et al.: J. Nucl. Sci. Technol., 21, 577 (1984)
- 12) S.Chiba et al.: Proc. Int. Conf. "Nuclear Data for Basic/Applied Science" Santa Fe (1985) JA-50
- 13) R.E.Holland et al.: Phys. Rev., C19, 592 (1979)
- 14) S.T.Perkins et al.: Nucl. Sci. Eng., 90, 83 (1985)
- 15) M.Baba et al.: Proc. Int. Conf. "Nuclear Data for Basic/Applied Science" Santa Fe (1985) JA-49
- 16) M.Ono et al.: NETU-46, Nuclear Engineering, Tohoku University (1985)
- 17) M.Thumm et al.: Nucl. Phys., A344, 446 (1980)
- 18) G.Haouat et al.: Nucl. Sci. Eng., 65, 331 (1978)
- 19) D.W.Glasgow et al.: Nucl. Sci. Eng., 61, 521 (1976)
- 20) S.G.Glendinging et al.: Nucl. Sci. Eng., 82, 393 (1982)
- 21) Y.Kikuchi et al.: J. Nucl. Sci. Technol., 22, 499 (1985)
- 22) S.Iwasaki et al.: Proc. Int. Conf. "Nuclear Data for Basic/Applied Science" Santa Fe (1985) JA-41
- 23) J.Frehaut et al.: BNL-NCS-51245, 399 (1980)
- 24) C.Y.Fu and F.G.Perey: Atomic Data and Nuclear Data Tables, 16, 409 (1975)
- 25) W.Dilig et al.: Nucl. Phys., A217, 260 (1973)

Table 1 Summary of DDX measurements performed at Tohoku University Dynamitron facility.

Nucleus	Incident Neutron Energy (MeV)	Sample
⁶ Li	4.2, 5.4, 14.1	⁶ Li-95%
⁷ Li	5.4, 6.0, 14.1	⁷ Li-99%
⁹ Be	4.5, 6.4, 7.0, 15.4	¹⁰ B-90%
¹⁰ B	14.1	
¹¹ B	14.1	B-nat
C	14.1, 18.2	Si ₃ N ₄
N	14.1	
O	14.1	
F	14.1	
Al	5.5, 6.2, 7.0, 14.1	SiO ₂
Si	14.1	
Ti	15.0	CF ₂
Cr	14.1	
Fe	5.5, 6.2, 7.0, 14.1	
Ni	5.5, 6.2, 7.0, 14.1	
Nb	15.0	
Mo	15.0	
Pb	15.0, 16.0, 18.0, 20.0	
Th	15.0,	

- d+d, p+t ----- d+t

Sample; (2-3,5) cm dia. (3-5) cm long

DDX Measurements at Tohoku University

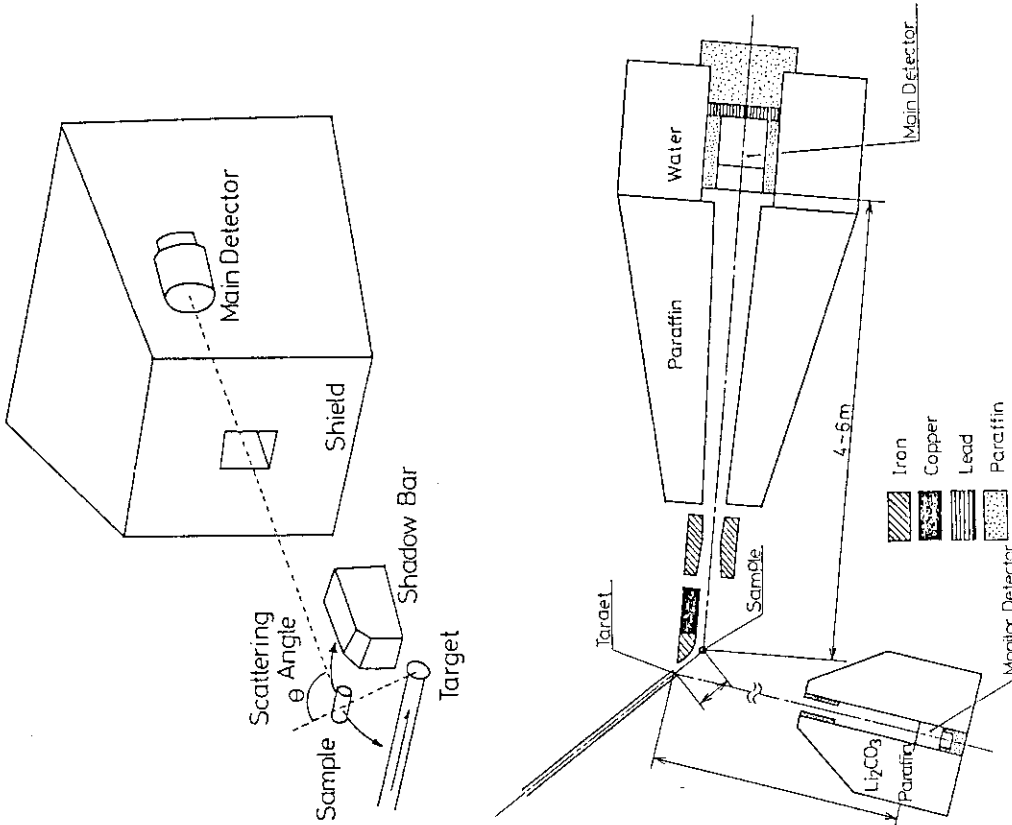


Fig.1 Experimental setup for DDX measurements. The upper one was employed only for 14.1MeV measurements.

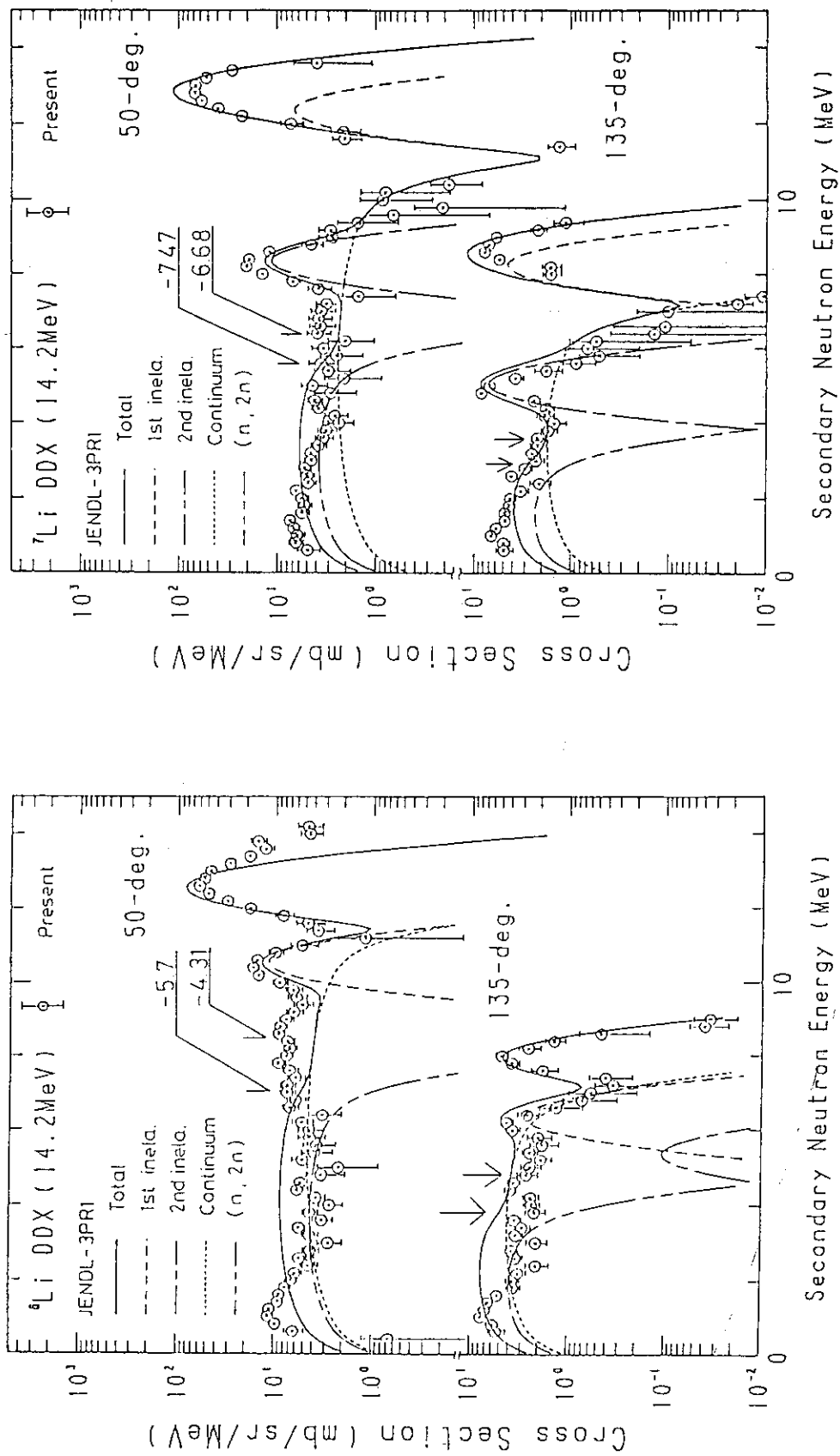


Fig.2 The results of DDX measurements for ${}^6,7\text{Li}$ at 14.2 MeV.

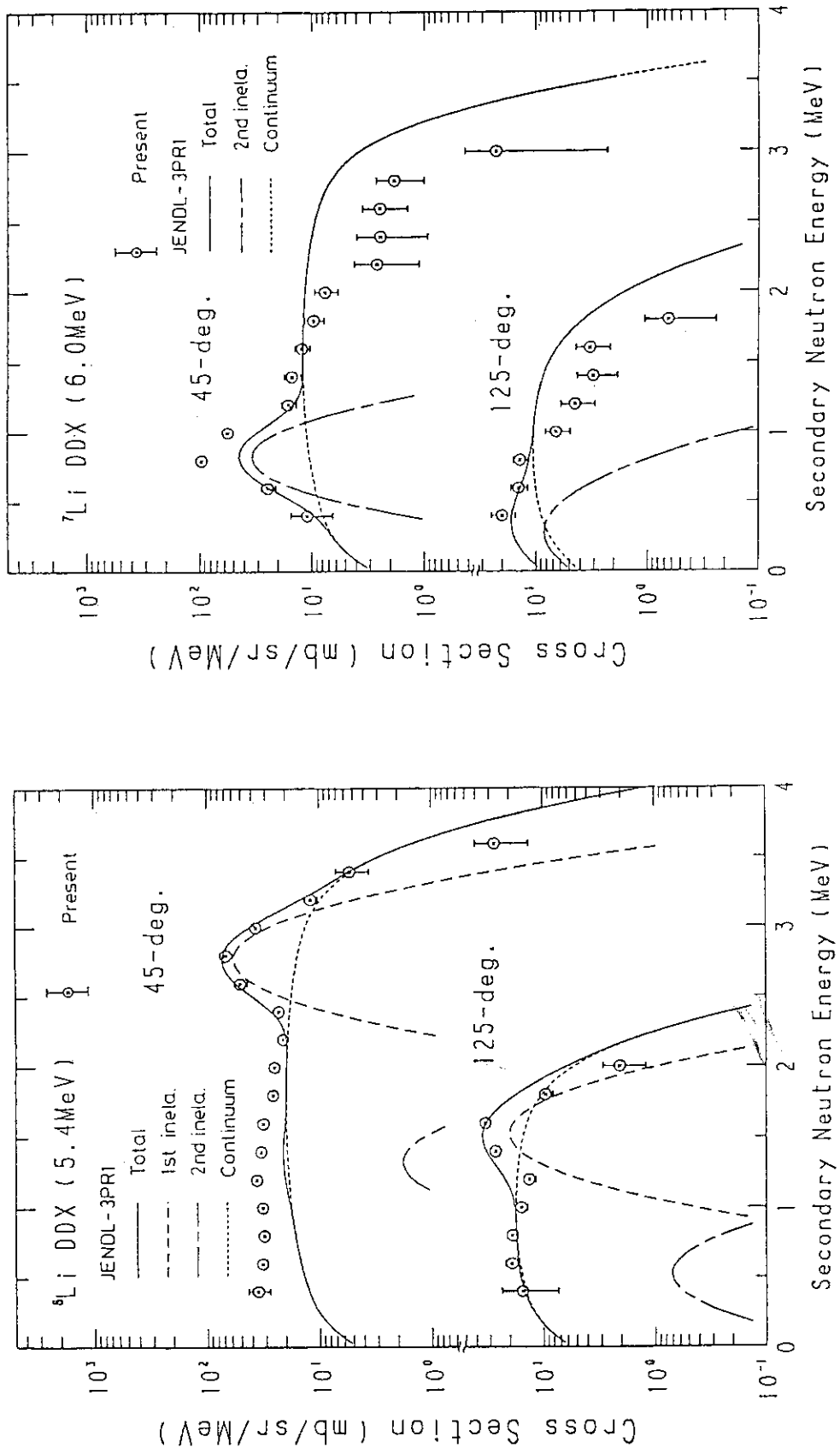


Fig.3 The DDX results for ${}^6,{}^7\text{Li}$ at MeV region.

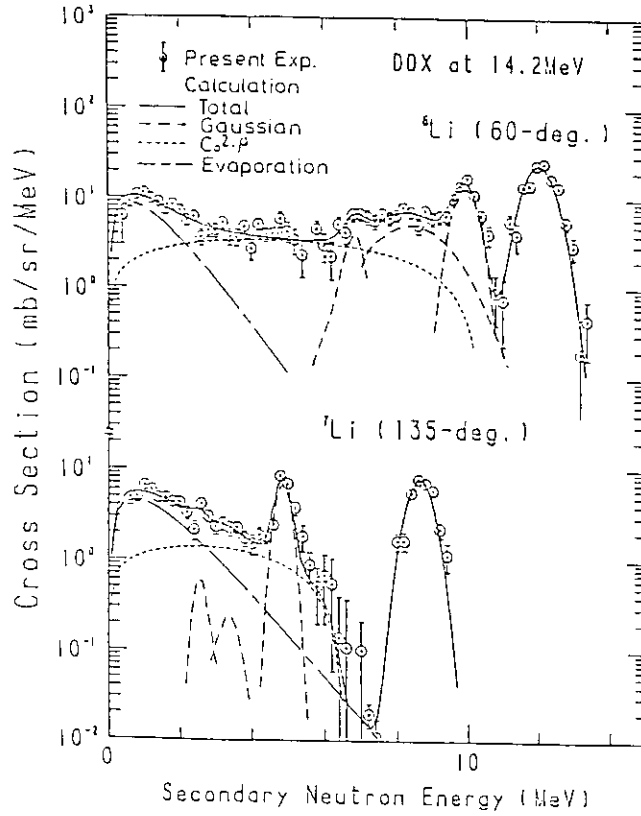


Fig.4 The results of the present analysis of ${}^6,{}^7\text{Li}$ DDXs.

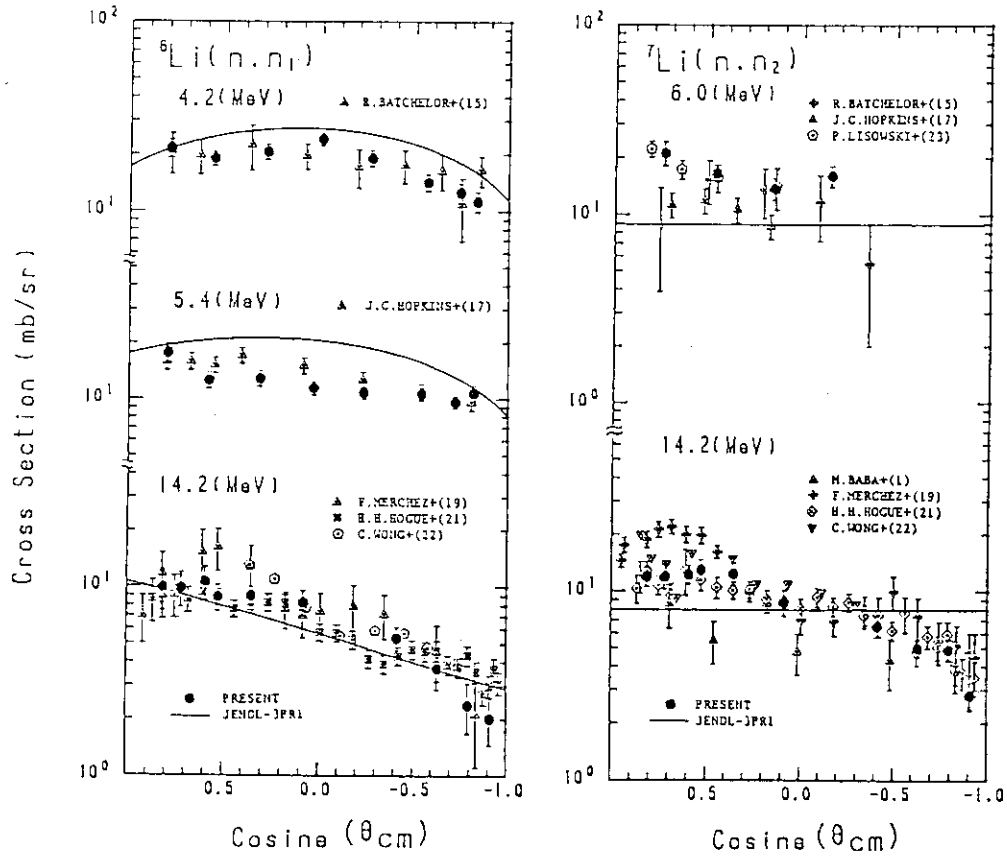


Fig.5 The inelastic-scattering cross sections of ${}^6,{}^7\text{Li}$.

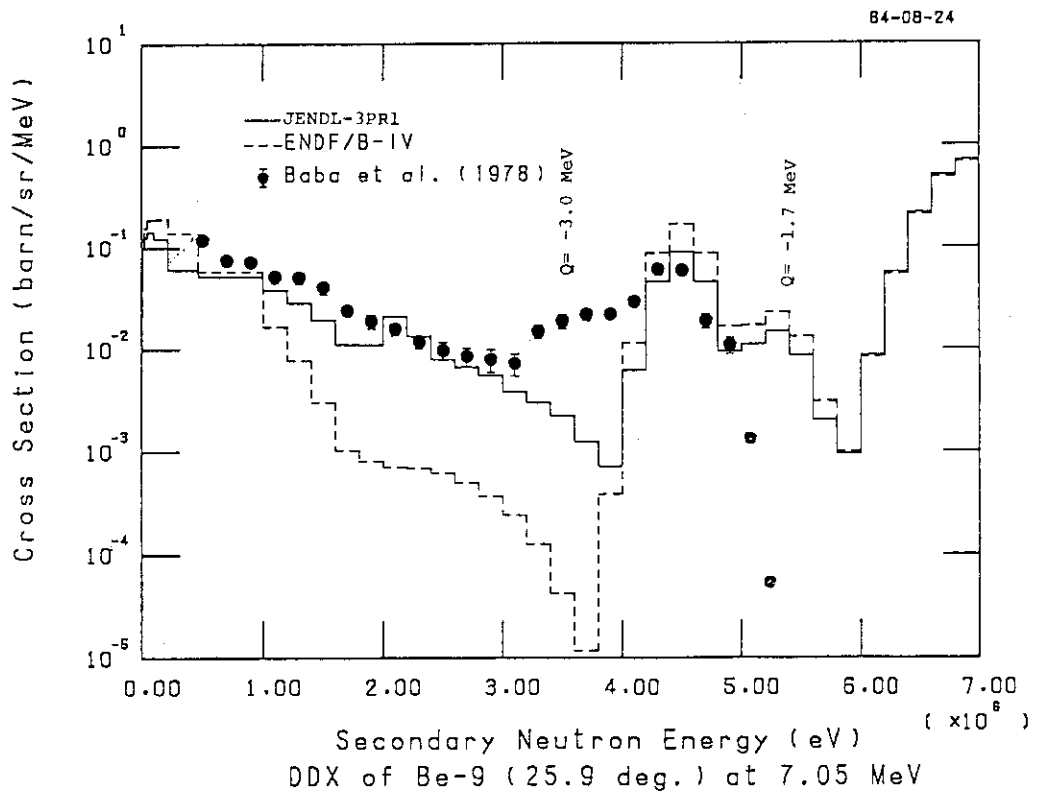
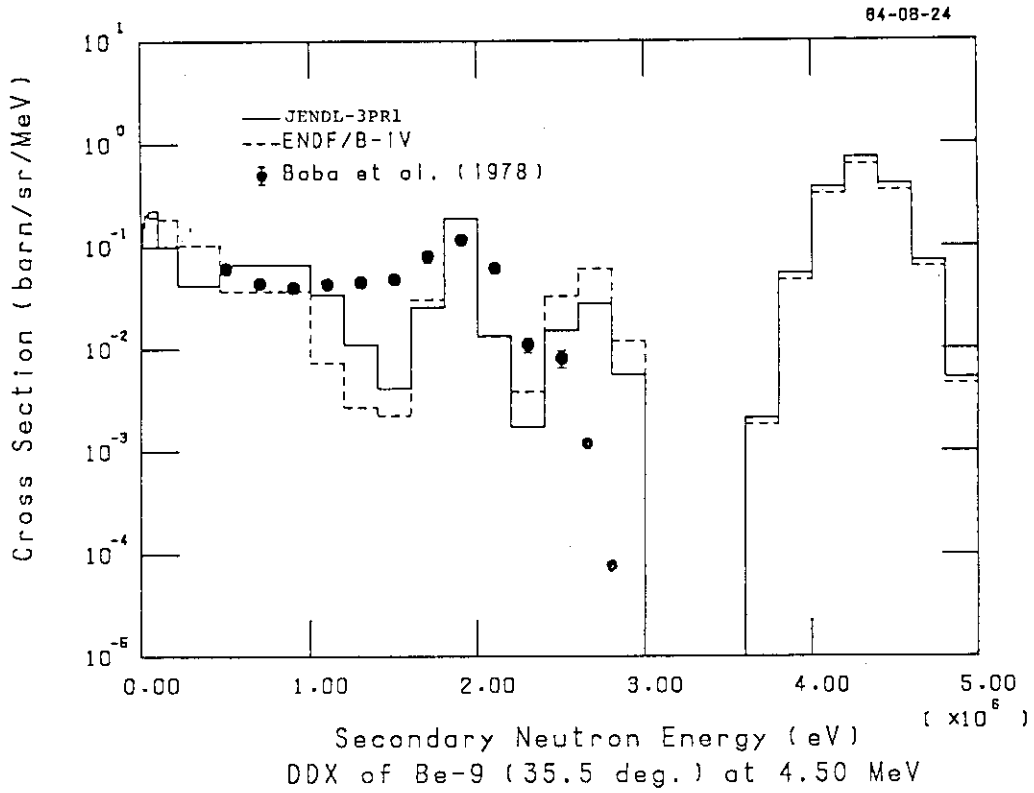


Fig.6 The DDX results of Be.

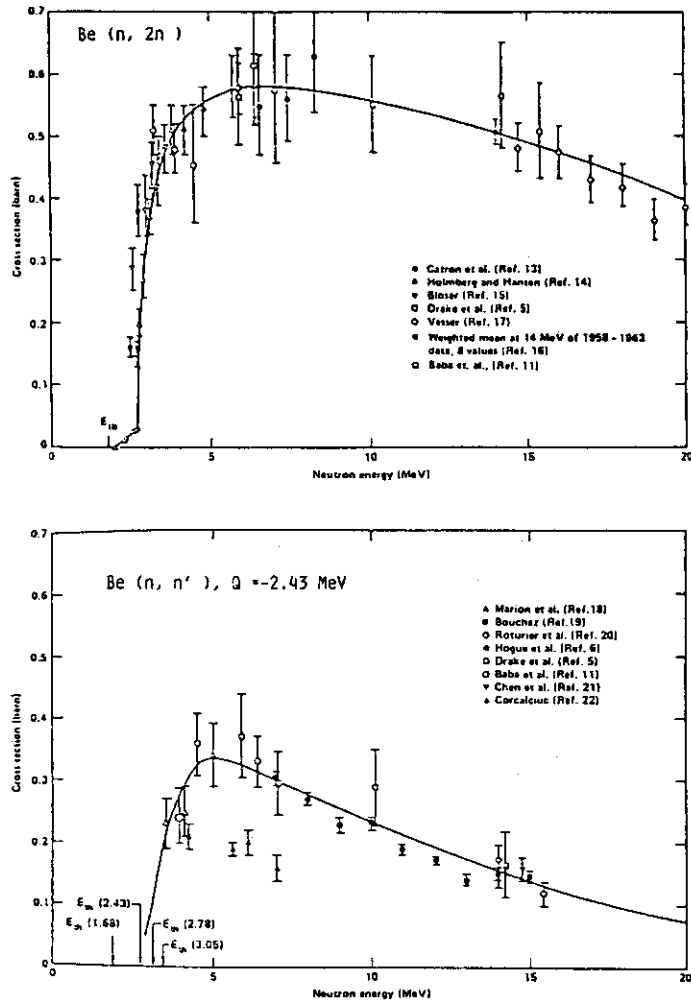


Fig.7 The partial cross sections of Be. The solid line shows the LLNL evaluation.¹⁴⁾

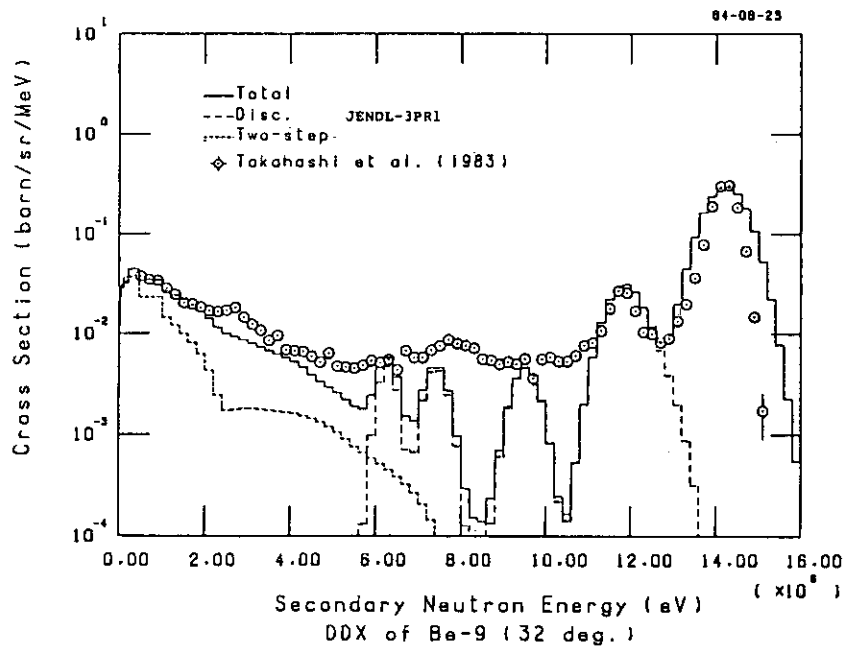


Fig.8 DDX of Be at 14 MeV. The JENDL-3P1 data are compared with the measurements by Takahashi et al.¹¹⁾

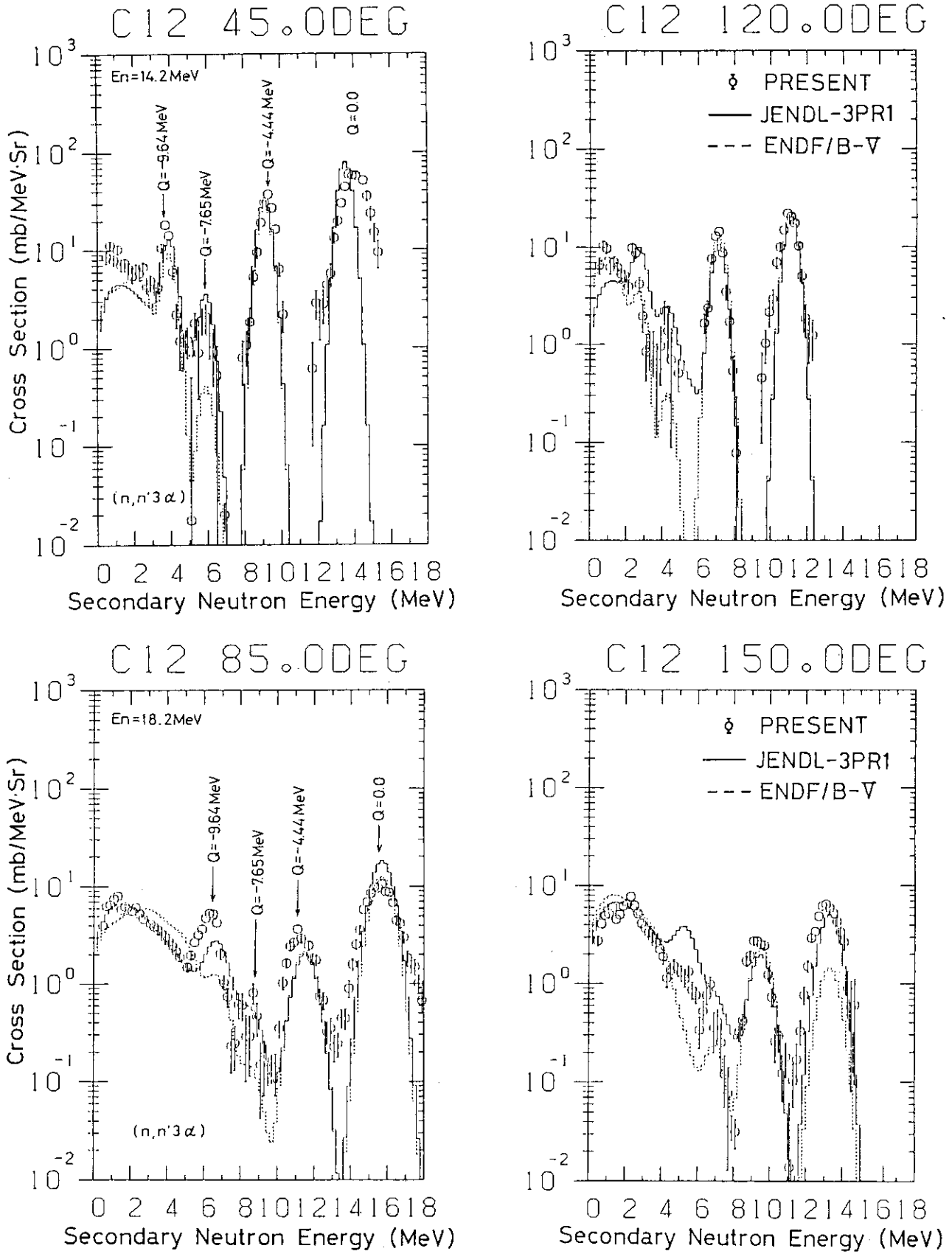


Fig.9 DDX of carbon. The measurements are compared with the evaluation.

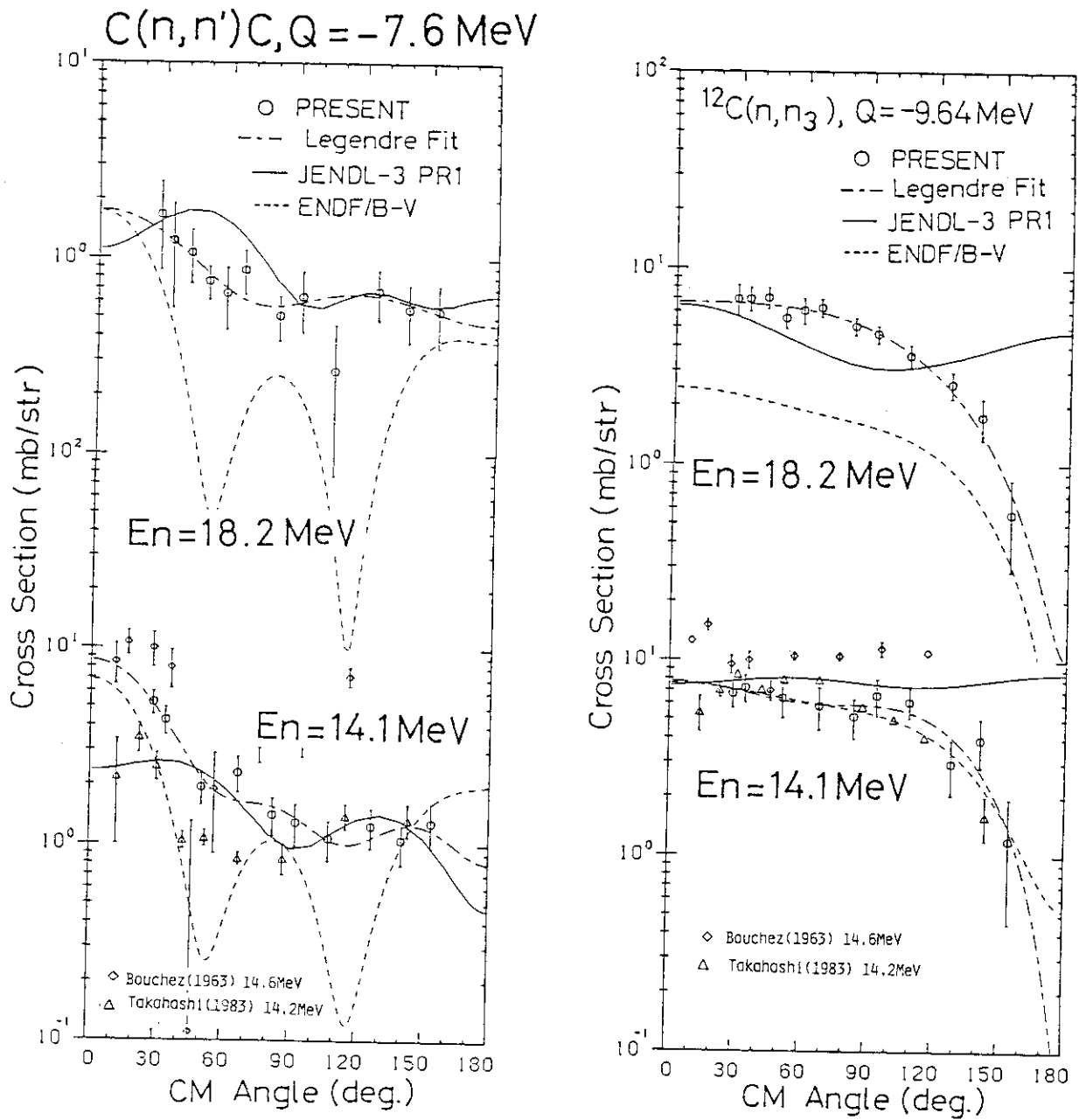


Fig.10 The inelastic-scattering cross sections of carbon.

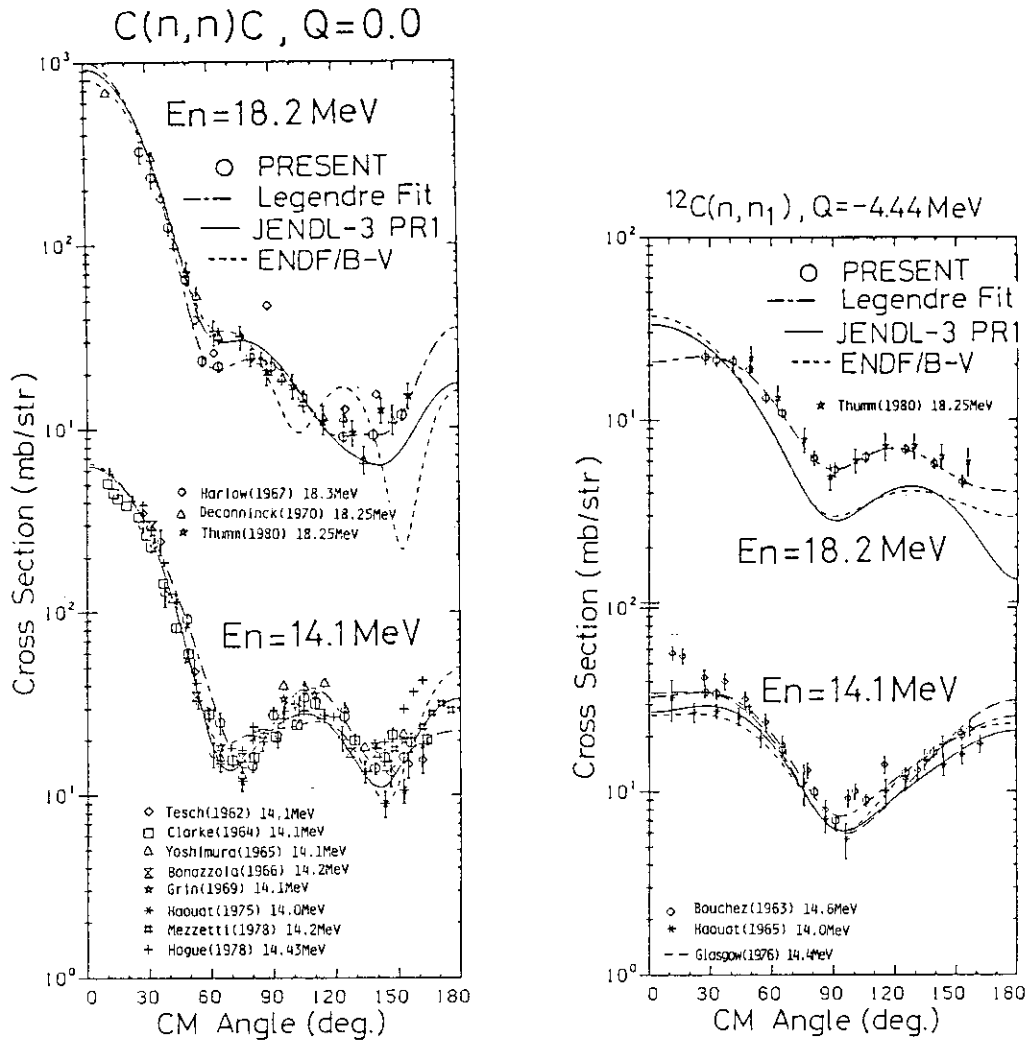


Fig.11 The elastic-scattering and first level cross sections of carbon.

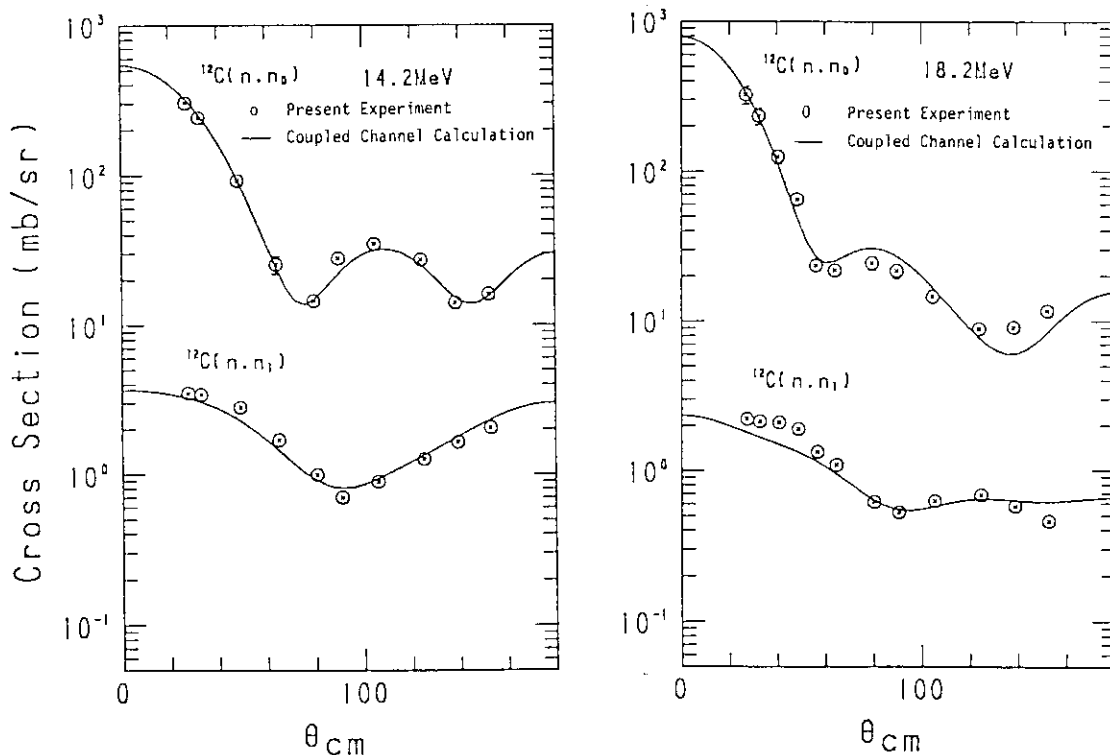


Fig.12 Coupled channel analyses of carbon scattering cross sections.

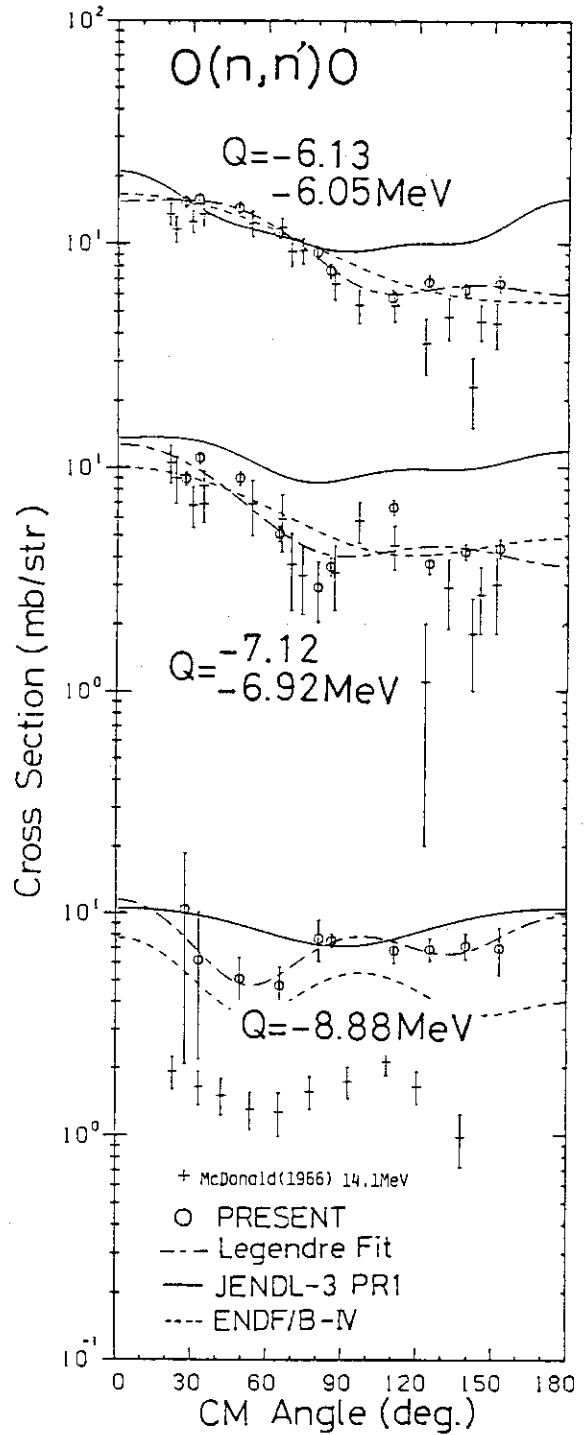
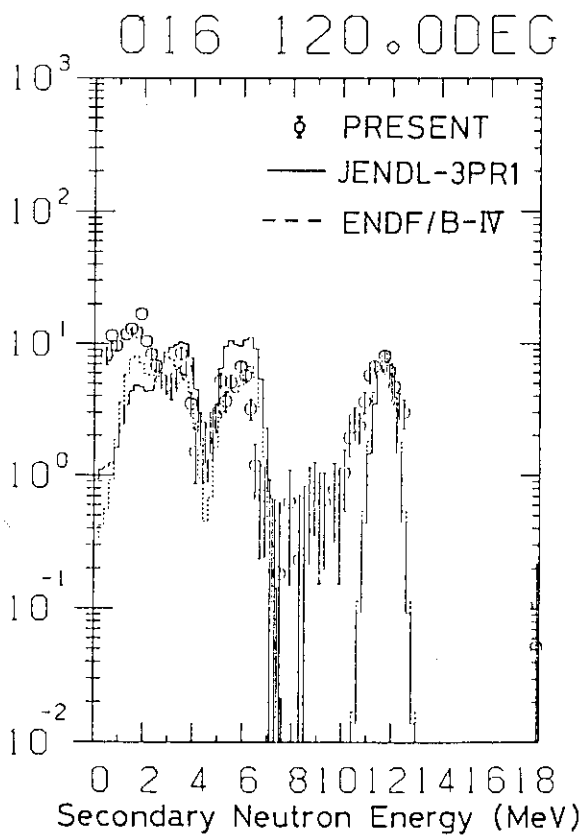
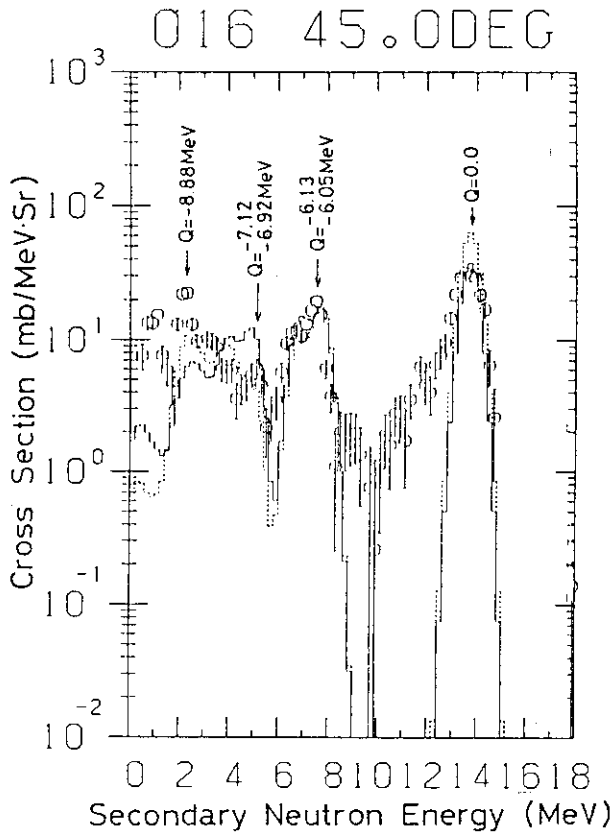


Fig.13 The DDX results of oxygen.

Fig.14 The inelastic-scattering cross sections of oxygen.

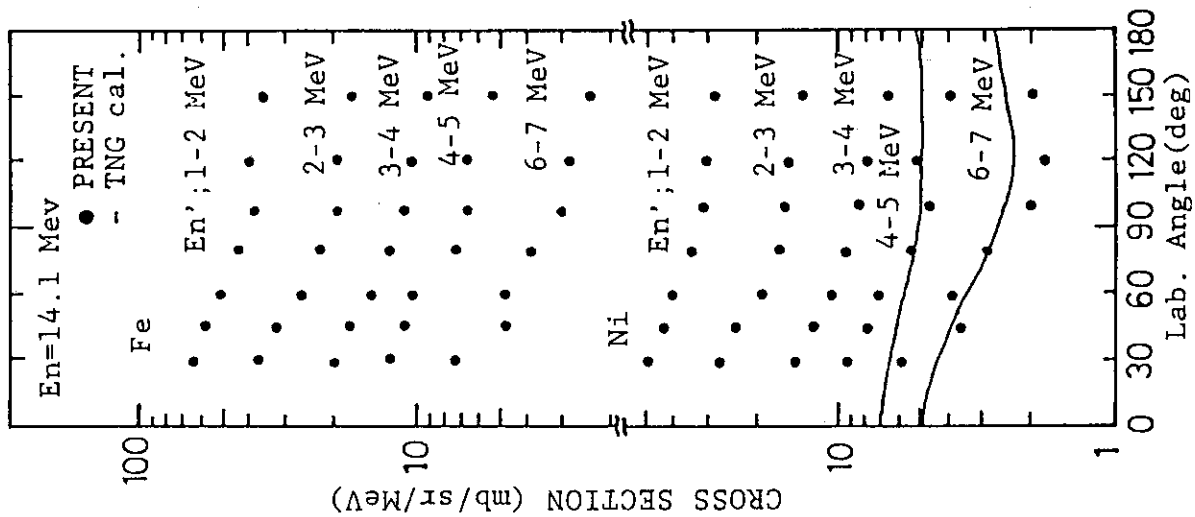


Fig.16 Angular dependence of emission neutrons from Fe and Ni.

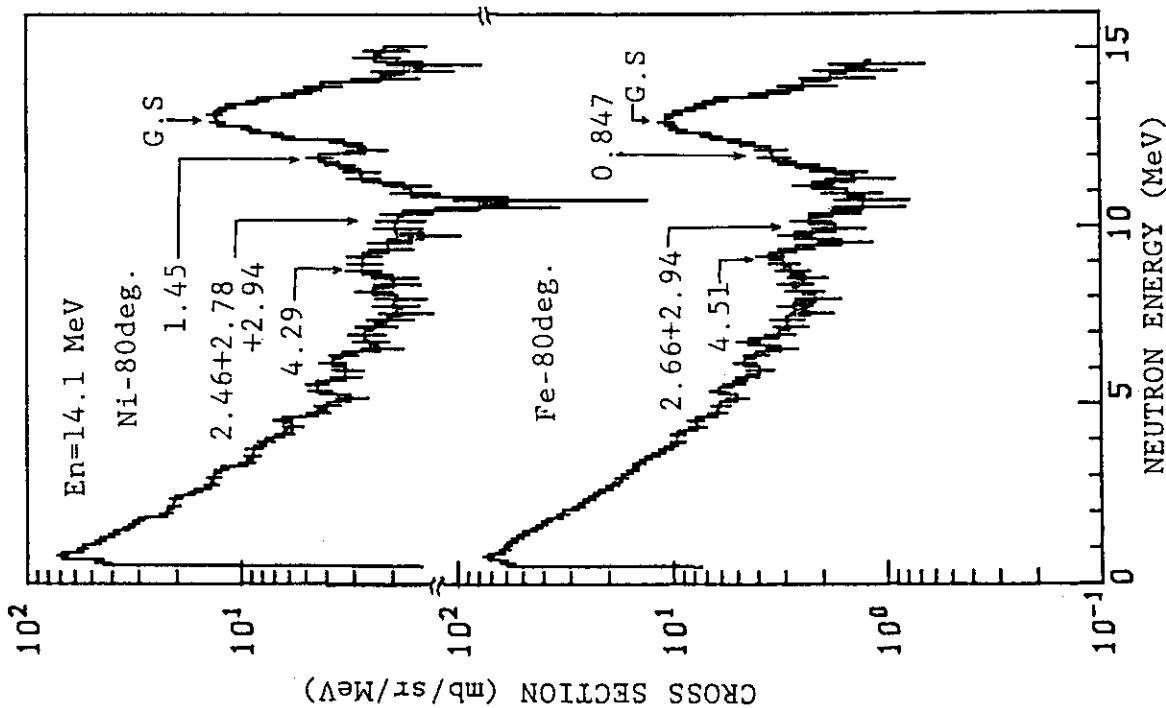


Fig.15 The DDX results for Ni and Fe.

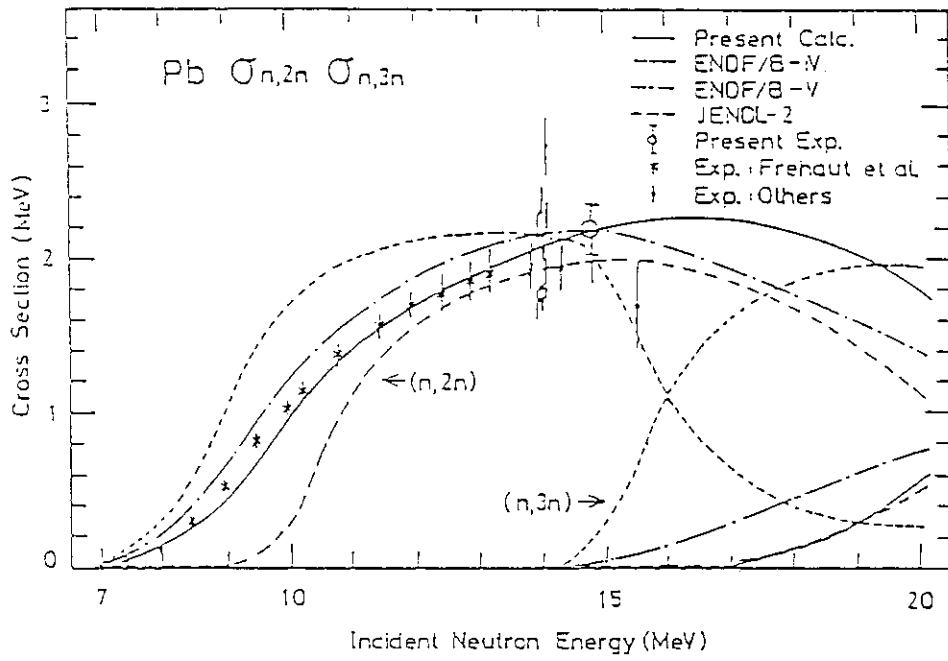


Fig.17 The (n,2n) and (n,3n) cross sections of Pb.

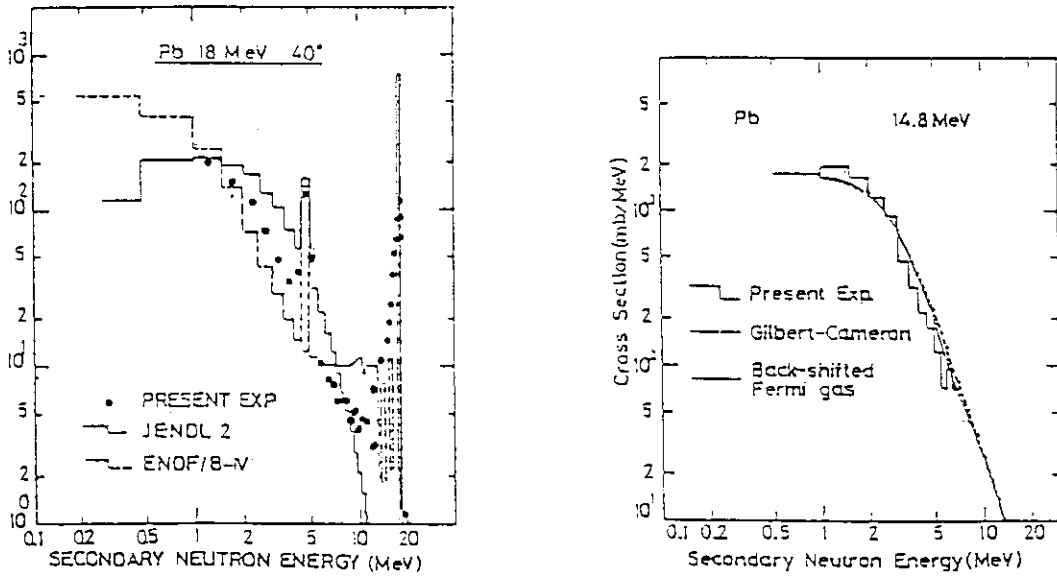


Fig.18 The DDX of Pb at 18 and 14.8 MeV.

III. Integral Experiments: Experimental Results and Analyses

1. Nuclear Data Testing on Integral Experiments of Lithium Spheres

K. Sugiyama, J. Yamamoto* and T. Iguchi**

Department of Nuclear Engineering, Tohoku University
Aramaki-Aoba, Sendai

Uncertainty on the neutron nuclear data of lithium isotopes is discussed concerning with integral experiments using two kinds of lithium spheres, 40cm and 120cm in diameter. Experimental results of neutron leakage spectra and tritium production rates indicate that the cross section of ${}^7\text{Li}(n,n'\alpha)\text{T}$ in the data file JENDL-3 PR2 is preferred in comparison with the values in ENDF/B-IV, and there are some discrepancies for the (n,2n) cross sections of lithium in both files.

1. Introduction

Joint study of university faculties in Japan were programed concerning the measurements of the basic blanket parameters for controlled thermonuclear reactor such as tritium production rates, nuclear heating rates and so on, using 14 MeV intense neutron source facility OKTAVIAN¹⁾ at Osaka university. Results from these experiments provide also for testing the accuracy of the cross sections for neutron induced reactions in lithium isotopes (${}^6\text{Li}$ and ${}^7\text{Li}$) as well as neutron transport calculations. For the purpose, two kinds of spherical assemblies contained natural lithium which are 40cm and 120cm in diameter, were designed and constructed. The details of the assemblies and the experimental arrangements have been reported elsewhere.²⁾ Present paper describes the results on the nuclear data deduced from the integral experiments such as neutron leakage spectra using neutron time-of-flight and tritium production rates at lithium samples in the sphere.

2. Experimental Results

2.1 Neutron leakage spectra from the spheres

Measurements of neutrons leaked from the each sphere have been carried out using a

* Department of Nuclear Engineering, Osaka University

** Department of Nuclear Engineering, Tokyo University

time-of-flight technique in experimental arrangement as shown in Fig. 1. Experimental results are illustrated in Fig. 2 for 40cm sphere and Fig. 3 for 120cm sphere, along with calculational results using transport code NITRAN³⁾ with ENDF/B-IV and JENDL-3 PR 2.

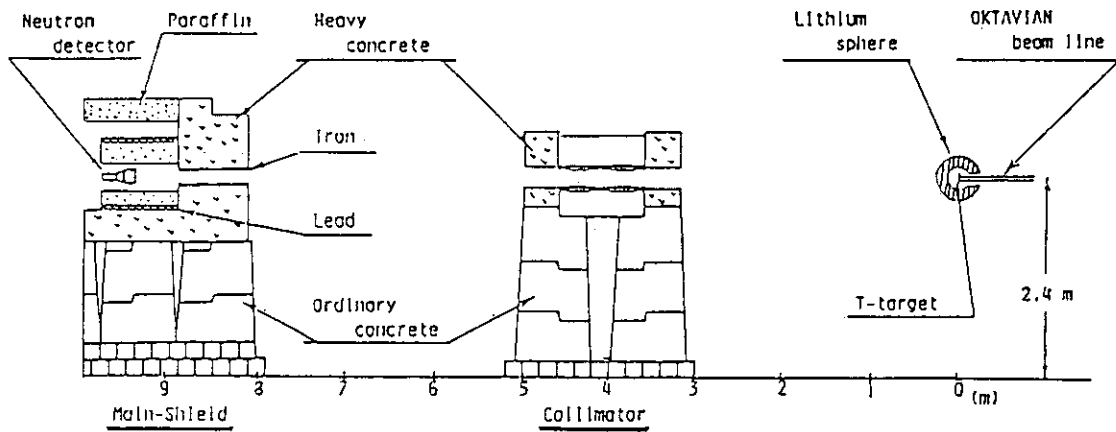


Fig. 1. Experimental arrangement for measurements of neutron leakage spectra.

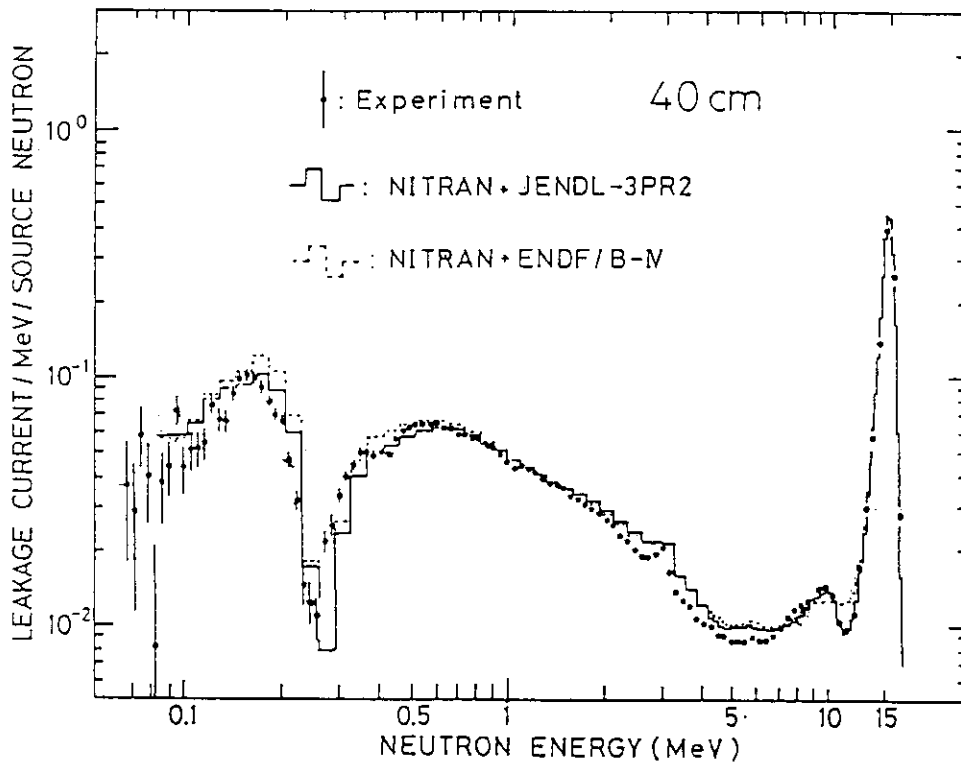


Fig. 2. Neutron leakage spectra from the 40cm lithium sphere.

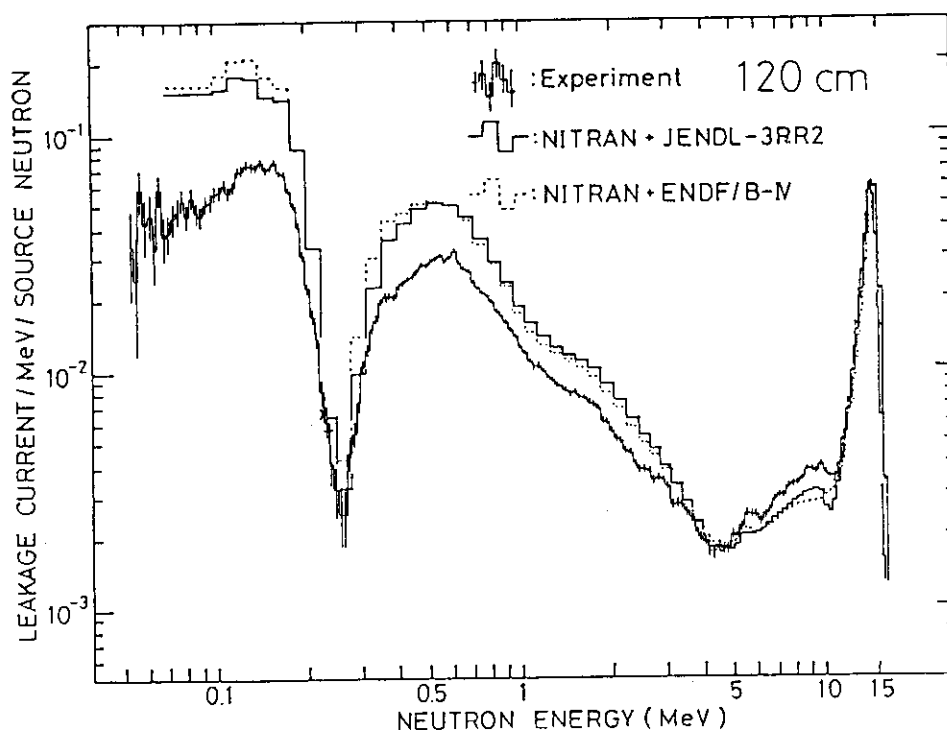


Fig. 3. Neutron leakage spectra from the 120cm lithium sphere.

There are generally agreements between the measured and the calculated spectra. For detailed comparison of these results, it is interested to illustrate the ratio of both values as Figs. 4 and 5. It is found that there are some discrepancies between the measured and the calculated values at the regions of the elastic and the resonance scattering. For 40cm sphere, the inelastic peak through the 4.63 MeV state of ${}^7\text{Li}$ which is important for tritium production is obviously improved in the JENDL-3 PR1 evaluation, and difference at the low energy region would be caused by inadequate cross section for the $(n,2n)$ reaction. Peak around 3 MeV is caused by d-d neutrons. For 120cm sphere, large difference are found in the region around 8 MeV, 1 MeV and below 0.2 MeV. Although any attempts of interpretations for these discrepancies were made, they are not yet clear. Experimental arrangement which has been detected neutrons leaked from limited area in the front of sphere by a precollimator, and its calculation by neutron transport code should be checked. The result would be influent on inadequacies of nuclear data such as angular dependence of neutrons from the scattering and the $(n,2n)$ reactions.

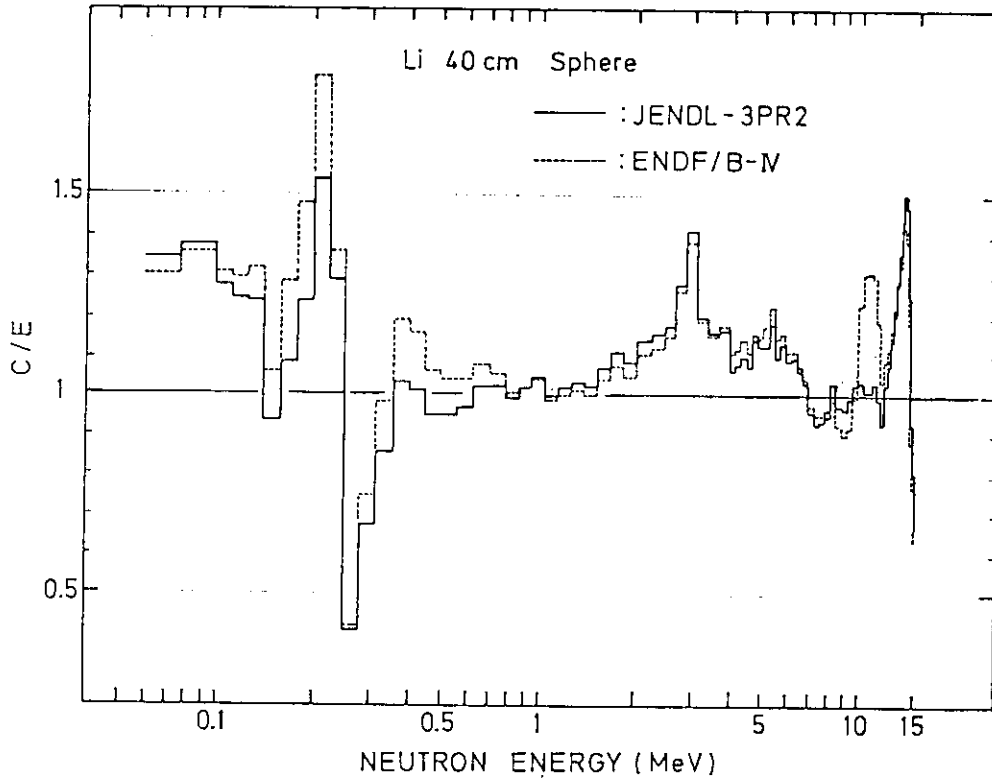


Fig. 4. Calculated / Measured on leakage neutrons from 40cm sphere.

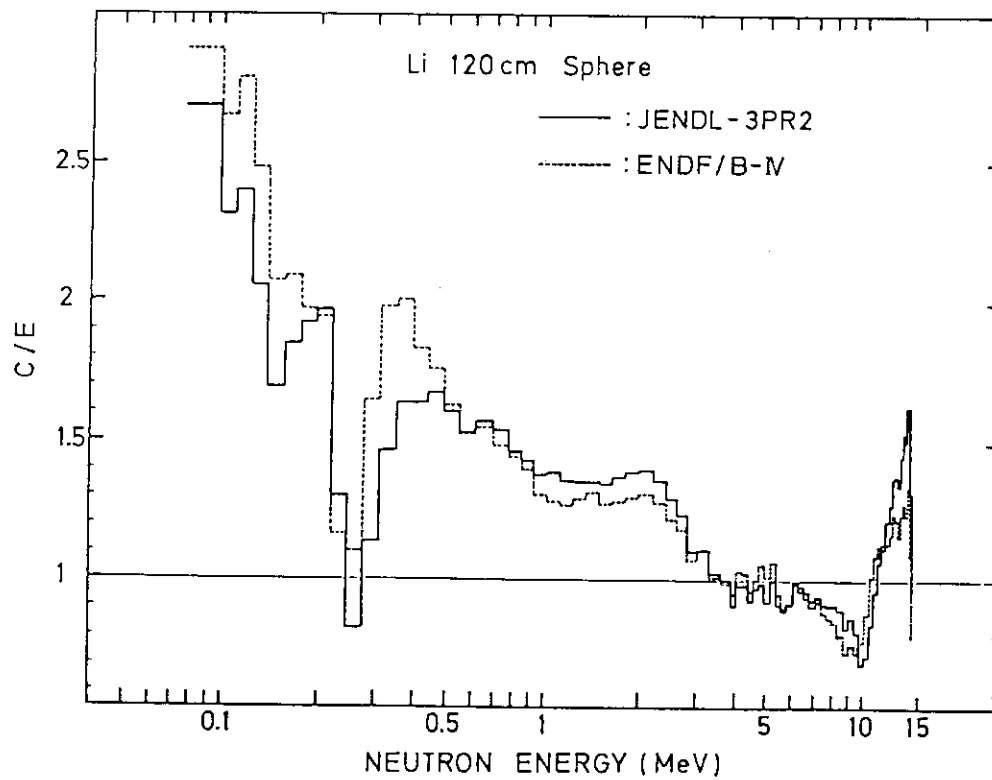


Fig. 5. Calculated / Measured on leakage neutrons from 120cm sphere.

2.2 Activation rates in the lithium sphere

Activation rates have been measured for several kinds of foils and lithium carbonate pellets in the 120cm lithium sphere. These samples were embedded at the radial positions directed to 0°, 45° and 90° with respect to deuteron beam incident into tritium target in the assembly.²⁾ The calculations have also been made by the Monte Carlo code MCNP⁴⁾ with pointwise cross section libraries produced from ENDF/B-V dosimetry file for the reactions $^{115}\text{In}(n,n)$, $^{27}\text{Al}(n,\alpha)$, $^{90}\text{Zr}(n,2n)$ and $^{93}\text{Nb}(n,2n)$, but ENDF/B-IV and JENDL-3 PR1 for the $^{6,7}\text{Li}(n,n'\alpha)$ t reactions. In these computations, one-dimensional spherical geometry has been adopted, where the input source neutron spectrum has been changed depending on each direction to be compared. Results are illustrated in Figs. 6(a) to 6(f), as reaction-rate ratio in order to reduce the neutron source anisotropy effects. It reveals that agreements between the measured and calculated results are fairly good except the $^7\text{Li}(n,n'\alpha)$ t reaction based on ENDF/B-IV cross sections. This disagreement on the reaction is improved by using the JENDL-3 PR1 cross sections.

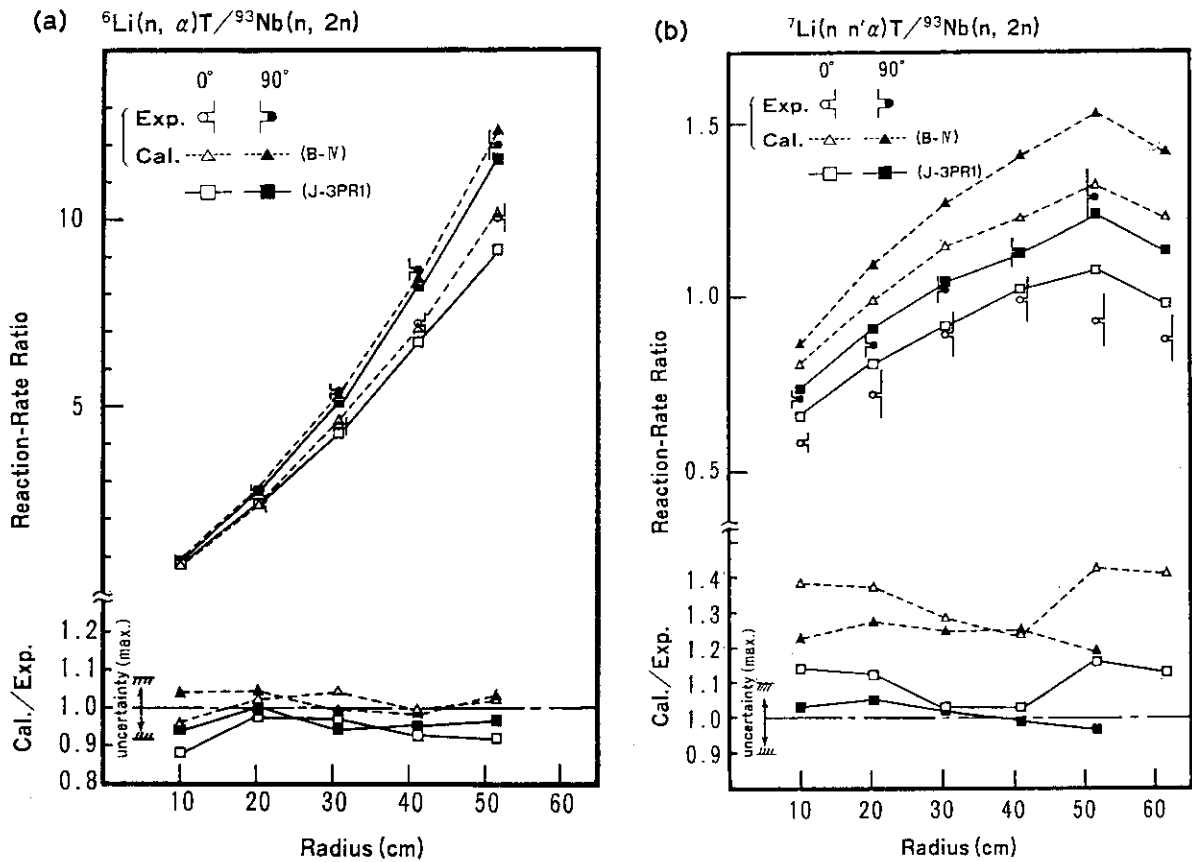


Fig. 6. Reaction-rate ratio in the lithium assembly.

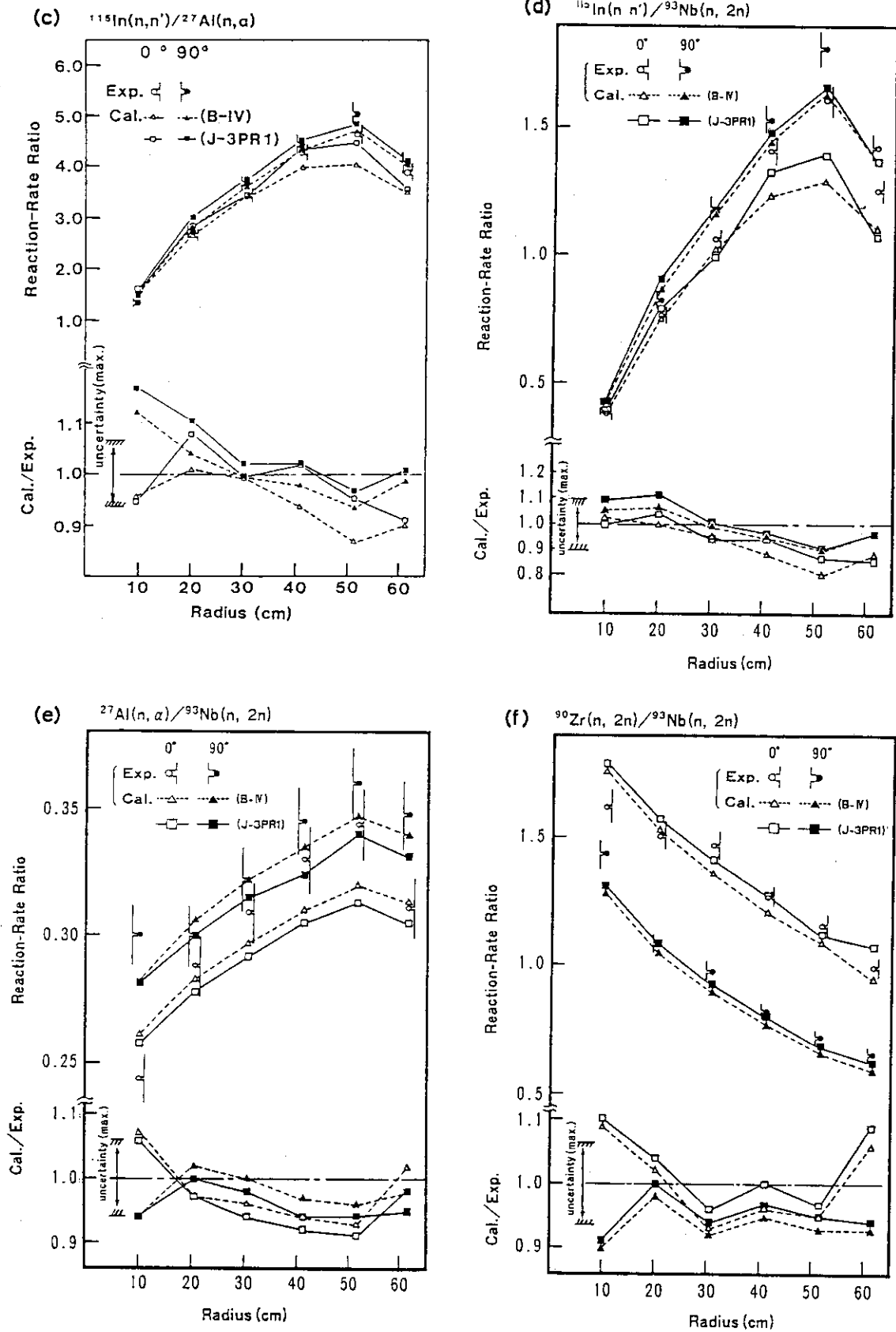


Fig. 6. Reaction-rate ratio in the lithium assembly.

2.3 Tritium breeding ratio

Tritium breeding ratio in the 120cm lithium sphere has been deduced from the tritium production rates measured on the lithium carbonate pellets at the radial positions in the assembly. The calculations have also been performed using neutron transport codes, ANISN and NITRAN, associated with nuclear data, ENDF/B-IV, GICX-FNS⁵⁾ and JENDL-3 PR1. Results are presented in Table 1.

Table 1. Tritium breeding ratio in the 120cm dia (50cm thick) lithium sphere.

	Experiment*	Cal-1 (C/E)	Cal-2 (C/E)	Cal-3 (C/E)
T-6	0.239 ± 0.014	0.252 (1.05)	0.262 (1.09)	0.249 (1.04)
T-7	0.495 ± 0.030	0.526 (1.06)	0.606 (1.22)	0.507 (1.02)
Total	0.734 ± 0.050	0.778 (1.06)	0.863 (1.18)	0.756 (1.03)

* Averaged value of 0 and 90 deg line measurement

Cal-1; GICX-FNS + ANISN

Cal-2; ENDF/B-IV + NITRAN

Cal-3; JENDL-3PR1 + NITRAN

3. Conclusions

Precise comparisons between the measured and calculated values have been carried out on the neutron leakage spectra and the reaction-rate ratio data and tritium breeding ratio in the 120cm lithium sphere, in addition to the neutron spectrum leaked from the 40cm lithium sphere. It is obviously concluded that use of nuclear data JENDL-3 PR1 or PR2 is preferable to predict the tritium breeding ratio in the lithium assembly rather than the use of ENDF/B-IV. We expect more improvement for the cross section and angular distributions in the elastic scattering and the (n,2n) reactions in lithium nuclides.

REFERENCES

- 1) K. Sumita, A. Takahashi, T. Iida, J. Yamamoto, S. Imoto and K. Matsuda, Proc. 12th SOFT held on September 1982, at Juerich [Fusion Technology 1982, Pergamon Press] p. 675.
- 2) K. Sugiyama, K. Kanda, S. Iwasaki, M. Nakazawa, H. Hashikura, T. Iguchi, H. Sekimoto, S. Itoh, K. Sumita, A. Takahashi and J. Yamamoto, Proc. 13th SOFT held on September 1984, at Verase, Italy [Fusion Technology 1984, Pergamon Press] p. 1375, Proc. 6th ANS Topical Meeting on Fusion Energy held on March 1985, at San Fransisco [Fusion Technology, in print 1985], J. Yamamoto, A. Takahashi, K. Kanda, S. Itoh, K. Yugami, K. Sugiyama and K. Sumita, Proc. Int. Conf. Nuclear Data for Basic and Applied Science held on May 1985, at Santa Fe, NM [Radiation Effects, in print 1985], T. Iguchi, M. Nakazawa, H.Hashikura, J. Yamamoto, A. Takahashi, K. Sumita, K. Sugiyama, K. Kanda, S. Itagaki, S. Itoh and Y. Hino, *ibid.*
- 3) A. Takahashi and D. Rusch, KfK-2832/ I, II (1979).
- 4) LASL Graoup X-6, La-7396-M (1979).
- 5) Y. Seki, JAERI-M 83-061 (1983).

2. 14 MeV Integral Experiment at OKTAVIAN to Check Differential Data of Secondary Neutrons

J. Yamamoto

Department of Nuclear Engineering
Faculty of Engineering, Osaka University
Yamadaoka, Suita-shi, Osaka 565, Japan

Differential data for Fe and Pb in ENDF/B-IV, ^{12}C in B-V, and ^7Li in B-IV, JENDL-3PR1 and PR2 were checked with regard to secondary neutron spectra from (n,n') and (n,2n) reactions by 14 MeV neutrons. This verification was done by making use of neutron energy spectra measured in 14 MeV integral experiments at the OKTAVIAN facility of Osaka University. In comparison with transport calculations by 1-D Sn code NITRAN, it was pointed out that there are some uncertainty in emission spectra from (n,2n) reaction with high energy threshold.

1. Introduction

Integral experiments have been carrying out focusing on two fundamental measurements: reaction rate and neutron energy spectrum, since fusion neutronics studies using 14 MeV neutron source OKTAVIAN were started in 1981. Recent works in the integral experiments will be reviewed in the following and the results until the first half of 1984 can be referred in OKTAVIAN reports^(1,2). Measurements of neutron spectra and tritium production rates in a natural-lithium sphere of 120 cm in diameter have been performed as a inter-universities program in Japan⁽³⁾. Analyses by transport codes have been done using the nuclear data files of JENDL-3PR1 and ENDF/B-IV⁽⁴⁾. Another measurement of tritium production rates has been done using a natural-lithium slab with graphite reflector and compared with transport calculations by the B-IV and the JENDL-3PR1 libraries⁽⁵⁾.

A measurement of neutron energy spectrum in the OKTAVIAN facility has been performing by almost using a pulsed neutron source and neutron time of flight technique. Some neutron spectra measured in a integral experiment with simple configuration give the useful information for the verification of nuclear differential data concerning the energy- and angle-distributions of emission neutrons from 14 MeV neutron-induced reactions. Such spectrum measurements will be introduced in the following chapter and the differential data in ENDF/B-IV, B-V, JENDL-3PR1 and PR2 will be discussed

in comparison between the measurements and the transport calculations.

2. Measurements of leakage neutron spectra

Experimental arrangements for the measurements of leakage spectra are shown in Fig.1, where (a) shows the arrangement for a spherical assembly and (b) for slab one. In Fig.1-(a), "leakage current spectrum" integrated over some emission angles on the surface of the sphere can be measured as given in the following equation.

$$M(E) = \eta(E) \int_{\mu_0}^1 \frac{Sd}{4\pi(L_0 - \mu R)^2} f(R, \mu, E) 2\pi \mu d\mu \cdot 4\pi R^2$$

where $f(R, \mu, E)$ is the angular flux spectrum on the surface of sphere, Sd the cross-sectional area of the neutron detector, L_0 the flight path length from the center of the sphere to the detector, μ the cosine of the emission angle θ , $M(E)$ the energy spectrum measured by the neutron detector. Figure 1-(b) shows a setup for the measurement of "angular flux spectrum" emitted from a slab.

The leakage spectra measured by the above arrangements generally will have the specific structure to be sensitive to energy spectra and angular dependences of secondary neutrons emitted from 14 MeV neutron-induced reactions, if the TOF measurement will be done under the experimental condition as follows:

- (i) Test assembly with simple configuration and single component material,
- (ii) A test layer corresponding to the thickness of 0.5 up to 5 times as long as mean free path (mfp) for a 14 MeV neutron,
- (iii) Approximately mono-energetic neutron source,
- (iv) Fast neutron spectrometry ranging from the order of keV up to 15 MeV.

The examples of neutron spectra measured under the condition are presented in Figs. 2 and 3, where the secondary neutrons from elastic and non-elastic scattering are dominant in measured spectra. Figure 2 shows the angular flux spectrum for 0 degree from a graphite slab, of which cross-sectional area was 50 cm x 50 cm and 30 cm in thickness corresponding to 3.4 mfp. The structure appears as peaks by secondary neutrons from discrete level inelastic scattering of ^{12}C by 14 MeV incident neutrons. The peak at 10, 7 and 5 MeV respectively results from secondary neutrons

from 4.43, 7.66 and 9.63 MeV excited states.

Figure 3 shows leakage current spectrum from a natural lithium sphere of 40 cm in diameter. Natural lithium is contained with stainless steel shell of 2 mm in thickness, and the thickness of lithium layer is 10 cm (0.7 mfp). As for the secondary neutrons by discrete level excitations, only one neutron peak by 4.63 MeV excited state of ${}^7\text{Li}$ appears around 10 MeV. This leakage spectrum is just characterized by the energy distribution of secondary neutrons from (n,2n) reaction of ${}^7\text{Li}$ with 7.25 MeV threshold energy other than (n,n') reactions. Spectrometry of low energy neutrons will be naturally required in the measurement of secondary neutrons with increasing threshold energy. Bulk experiment by a sphere with "thin layer", therefore, will be available to check secondary neutron spectra from high-threshold reactions because of the advantage to get the good ratio of signal to noise (S-N ratio) in a TOF spectrum even at the low energy region by surrounding the neutron source with the sphere.

3. Comparison between measured and calculated spectra

Table 1 lists the kinds of slabs and spheres used in the TOF measurements. Some differential data for ${}^7\text{Li}$, ${}^{12}\text{C}$, Fe and Pb will be discussed respectively by the comparison work between measured and calculated leakage spectra from a natural lithium, graphite, iron and lead assembly. Transport calculations of angular flux spectra and leakage current ones have been done by 1-D Sn transport code NITRAN⁽⁶⁾ using 135 group cross section sets of DDX type. Nuclear data were provided from ENDF/B-IV⁽⁷⁾ for Fe and Pb, and B-V⁽⁸⁾ for ${}^{12}\text{C}$. Energy spectra from lithium assemblies were calculated with B-IV, JENDL-3PR1⁽⁹⁾ and PR2⁽¹⁰⁾, respectively.

Figures 4 and 5 present the neutron spectra calculated with B-IV in comparison with measured spectra. The angular flux spectra are shown in Fig.4 for iron slab and Fig.5 for lead slab, of which sizes were 40 cm x 40 cm and 10 cm in thickness. No obvious angular dependence can be observed between the spectra for the emission angles of 45 and 135 degrees in Fig.4 except elastic scattering peak. Two calculated spectra for 45 and 135 degrees are in fairly good agreement with measured ones. Slight undercalculation, however, can be seen in the energy range from 3 to 10 MeV, where secondary neutrons contribute from discrete level inelastic scattering. Q-value of (n,2n) reaction of Pb is -6.73 MeV, so the secondary neutrons from the reaction are distributed in the energy range

below 5 MeV on the angular spectra in Fig.5. The energy spectrum measured at 45 and 135 degrees is respectively harder than calculated one. It can be, therefore, pointed out that the nuclear temperature of (n,2n) reaction should be estimated to be higher than that derived from the energy distribution evaluated in B-IV. The same result can be confirmed by another measurement shown in Fig.6, in which leakage current spectrum from a lead sphere is compared with calculated one. Neutron multiplication factor by (n,2n) reaction of Pb could be obtained from this TOF measurement (11) and the value for the sphere, of which diameter was 38 cm and lead layer was 9 cm in thickness, was 1.50 ± 0.09 . The factor by transport calculation with B-IV was valued at 1.29, which undercalculated the experimental value by 14 %. As for the differential data for lead in B-IV, there are much uncertainty in both the cross section value of (n,2n) reaction and the secondary neutron spectrum at 14 MeV.

Figure 7 shows the angular flux spectra from a graphite slab. Transport calculations were done by using the ENDF/B-V data instead of the B-IV data, in which only the angle-dependent cross section data for 1-st excited level ($Q=-4.43$ MeV) are evaluated as discrete level inelastic scattering. Good agreement can be obtained between measurements and calculations by the B-V data evaluated in consideration of several branch channels for (n,n' 3 alpha) reaction of ^{12}C .

The JENDL-3PR2 library, which is a revised version of PR1, shows the improvement for differential data of non-elastic scattering of ^7Li . PR2 gives the anisotropic angle-dependent cross sections for discrete level inelastic scattering of 0.478, 4.63 and 6.68 MeV excited states. The other levels, that are pseudo levels binned in 0.5 MeV, are almost treated as isotropic scattering. Figure 8 shows the ratio of calculated values to experimental one for leakage current spectrum from the 40 cm lithium sphere as shown in Fig.3. Drastic improvement can be seen around 10 MeV in the leakage spectrum calculated by PR2. Figure 9 shows the comparison among measurements and calculations by B-IV, PR1 and PR2. Computational model of angular flux spectra was a natural lithium slab of 20 cm in thickness(1.4 mfp). It is assumed that angular dependent cross sections for -4.63 MeV in PR2 slightly underestimated at forward scattering angles as shown around 10 MeV in Fig.9-(a). Those in PR1 are evaluated as isotropic scattering in CM system, so the considerable overcalculation can be seen in backward spectra of 135 degrees and undercalculation in forward one. Furthermore angular spectra by PR1 overcalculated the measurements

below 5 MeV at both emission angles of 45 and 135 degrees. The reason can be illustrated with Fig.10, which shows the energy spectra from (n,2n) reaction of ${}^7\text{Li}$ by a 15 MeV incident neutron. The spectrum in PR1 is estimated rather harder than that in B-IV. Even the calculated spectra by PR2 slightly overestimate the measured ones below 5 MeV as can be seen in Figs.3 and 9.

References

- (1) Takahashi, A.: OKTAVIAN Report B-8301 (1982)
- (2) Takahashi, A.: ibid B-8401 (1984)
- (3) Sugiyama, K., et al.: Proc. 13-th SOFT, pp1375(1984)
- (4) Iguchi, T., et al.: Int. Conf. Nucl. Data for Basic and Appl. Sci. (1985)
- (5) Takahashi, A.: ibid
- (6) Takahashi, A. and Rusch, D.: KFK-2832/I & II (1979)
- (7) ENDF/B Summary documentation, BNL-NCS-17541 (2-nd Edition) (1975)
 ${}^7\text{Li}$ (MAT 1272), evaluated by R. J. Labauue, L. Stewart and M. Battat (LASL)
Fe(MAT 1192), evaluated by F. G. Perey, C. Y. Fu, S. K. Penny, W. E. Kinney and R.Q. Wright (ORNL)
Pb(MAT 1288 MOD 5), evaluated by C. Y. Fu and F. G. Perey (ORNL)
- (8) ENDF/B Summary documentation, BNL-NCS-17541 (3-rd Edition) (1979)
 ${}^{12}\text{C}$ (MAT 1306), evaluated by C. Y. Fu and P.G. Perey (ORNL)
- (9) Shibata, K.: JAERI-M 84-204 (1984)
- (10) Shibata, K. and Chiba H.: Private communication
- (11) Takahashi, A., et al.: Proc. 12-th SOFT, pp687(1982)

Table 1 List of slabs and spheres for TOF measurement

Assembly	(Element)	Slab (Emission angle[degree])	Sphere (Radius[cm])	Nuclear data file
Natural Lithium	(⁶ Li, ⁷ Li (S.S.))	0, 45, 135	20, 60*	PR1, PR2, B-N
Graphite	(¹² C)	0, 30, 45, 135	15, 45	B-W, B-V (PR1)
Iron	(Fe)	0, 30, 45, 135	—	B-W (PR1)
Lead	(Pb)	0, 30, 45, 135	13, 16,	B-W
Concrete	(H, C, O, Al, Si, Ca, Fe, etc.)	0	—	B-W, B-V(C) (PR1)
Stainless steel-316	(Cr, Fe, Ni, etc.)	0	—	B-W (PR1)
Water	(H, O)	0	—	B-W (PR1)

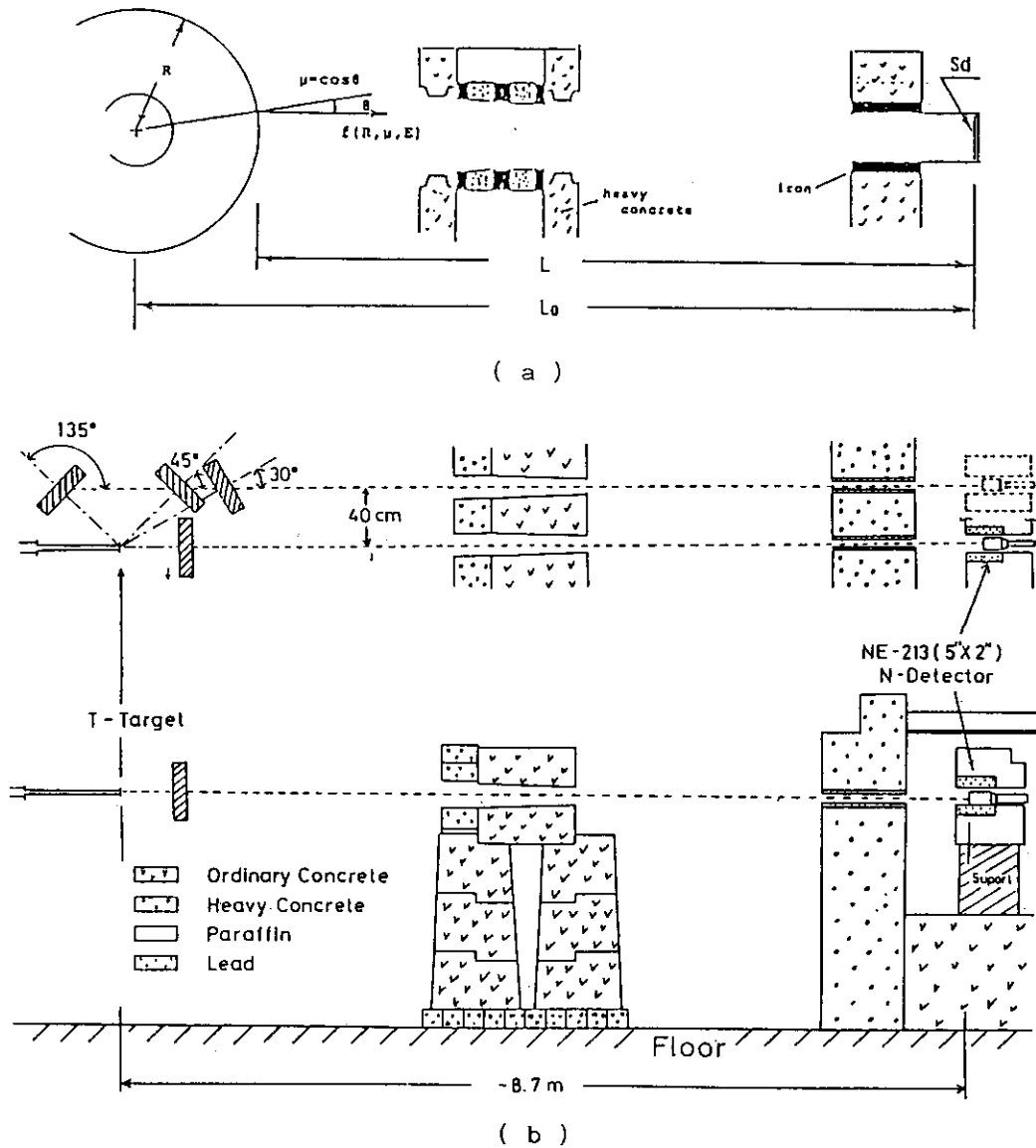


Fig.1 Experimental arrangements for TOF measurement

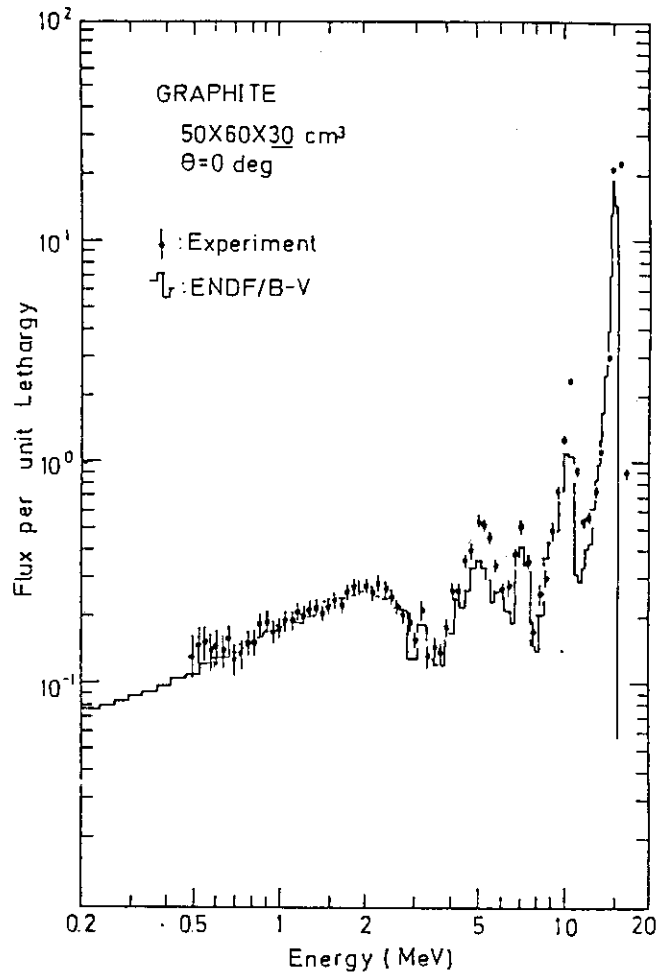


Fig.2 Angular flux spectrum for 0 degree from a graphite slab

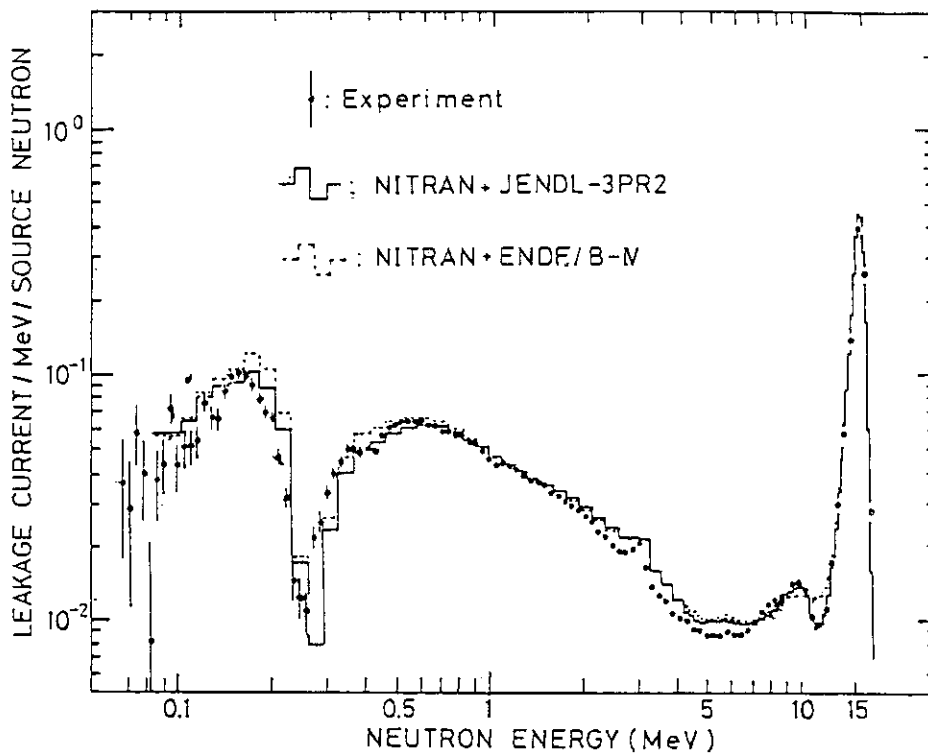


Fig.3 Leakage current spectrum from a natural lithium sphere of 40 cm in diameter

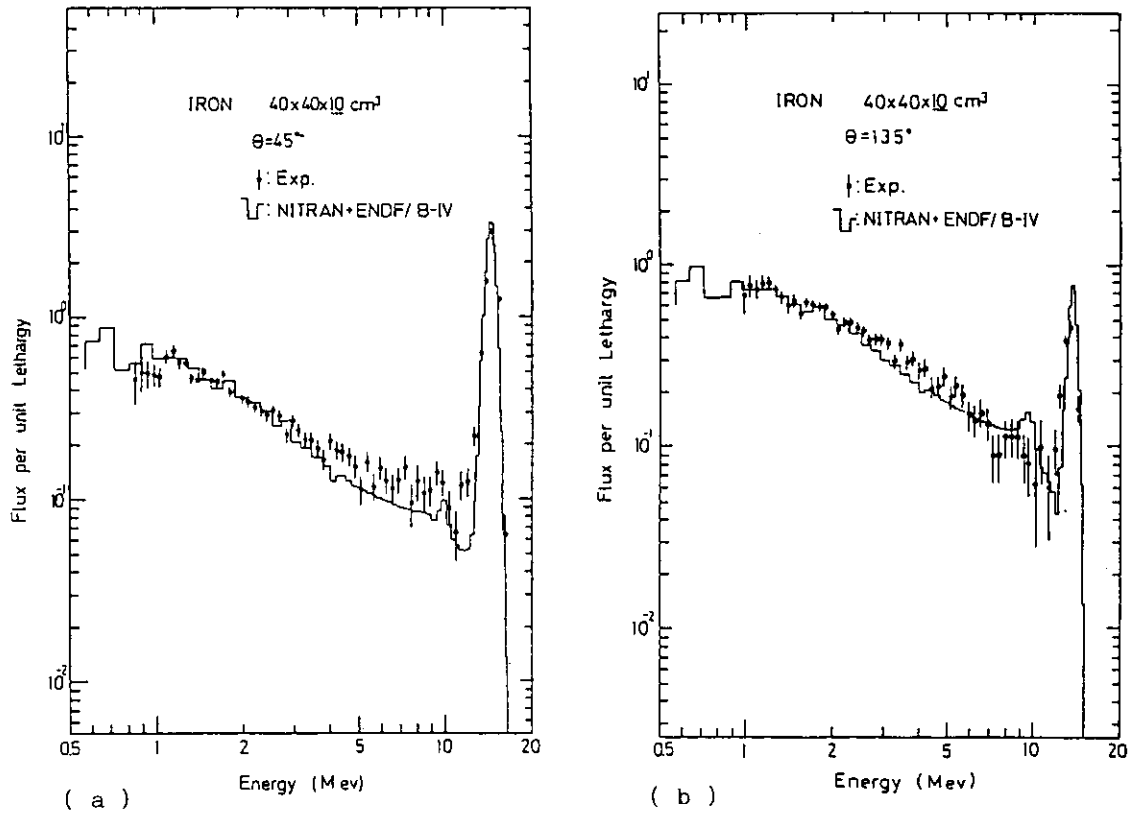


Fig.4 Angular spectra for 45 and 135 degrees from a iron slab in comparison with transport calculations

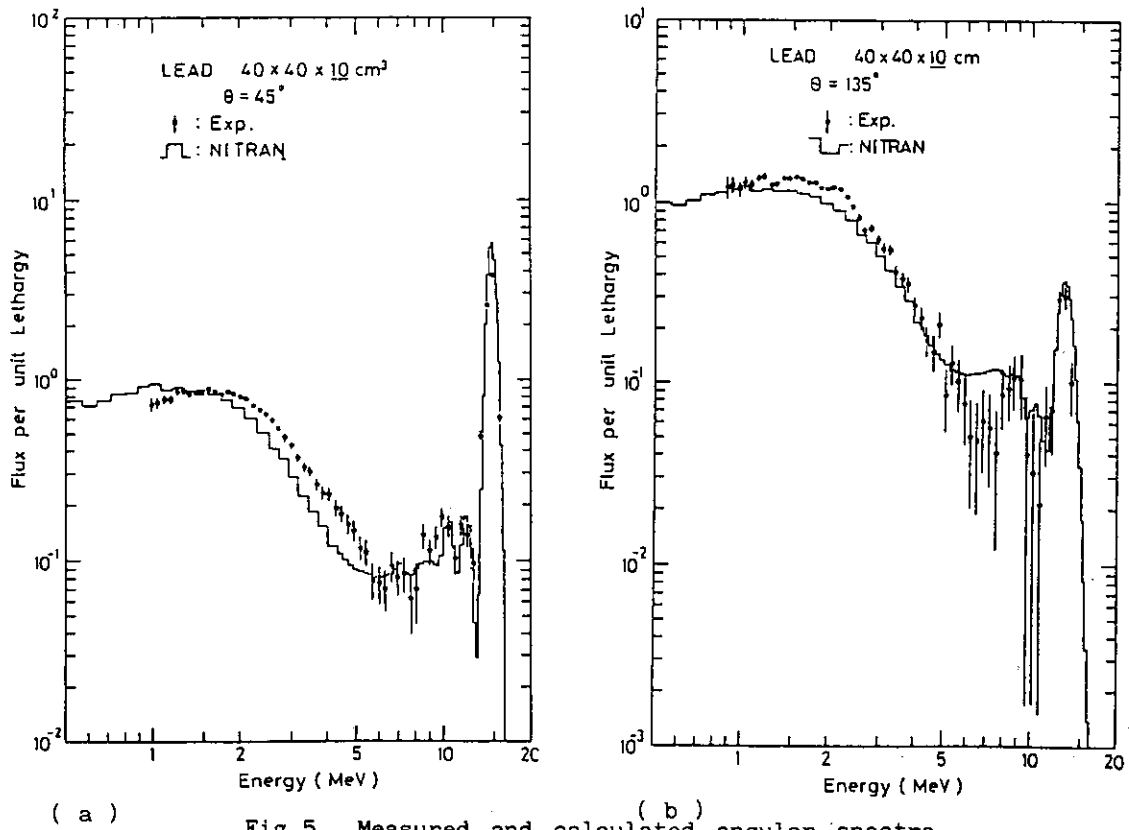


Fig.5 Measured and calculated angular spectra for 45 and 135 degrees from a lead slab

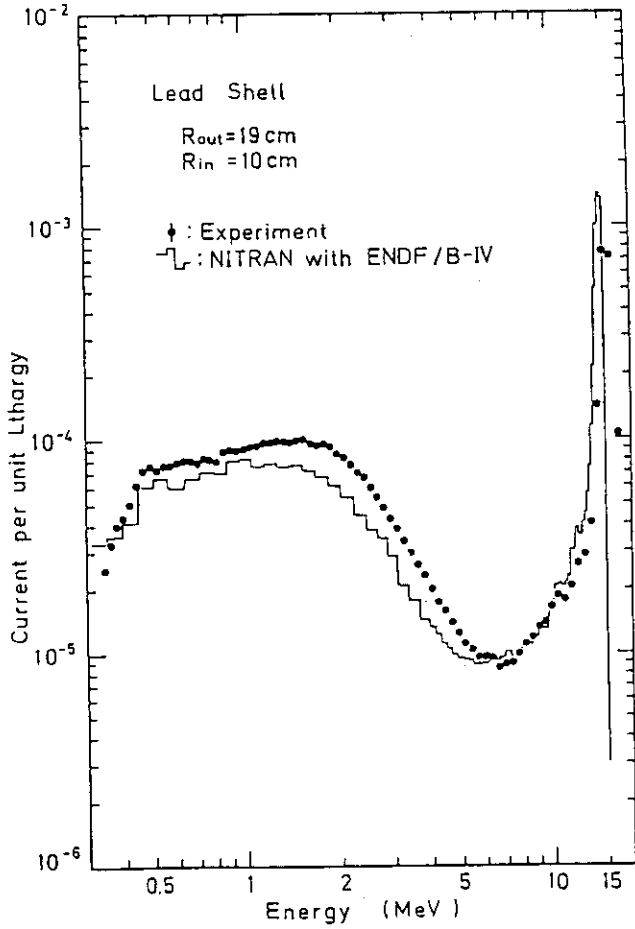
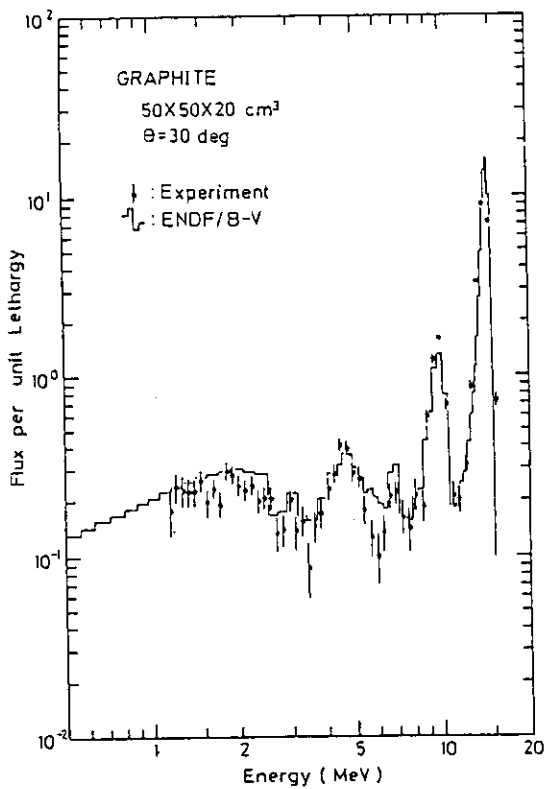
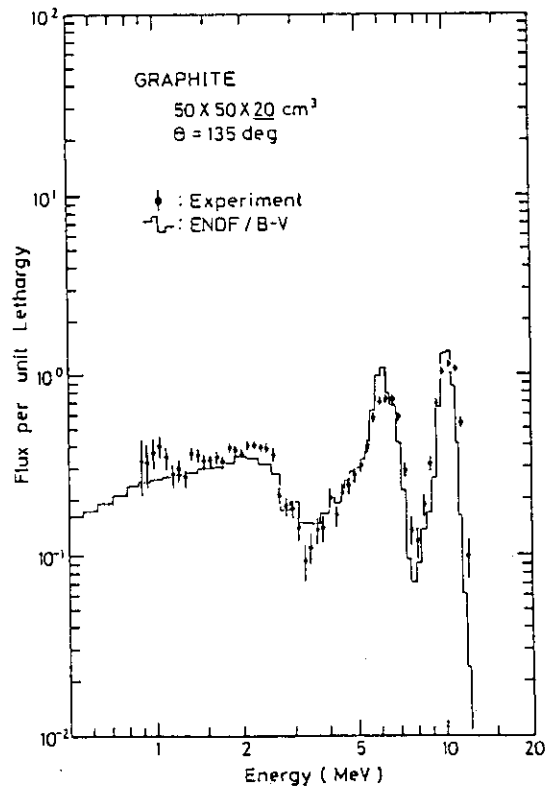


Fig.6 Leakage spectra from a 38 cm diam. lead sphere



(a)



(b)

Fig.7 Angular spectra for 45 and 135 degrees from a graphite slab

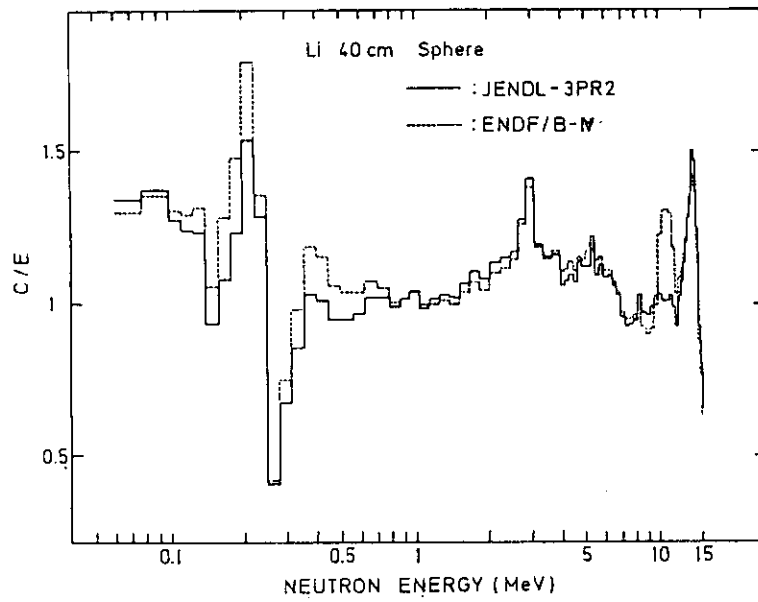
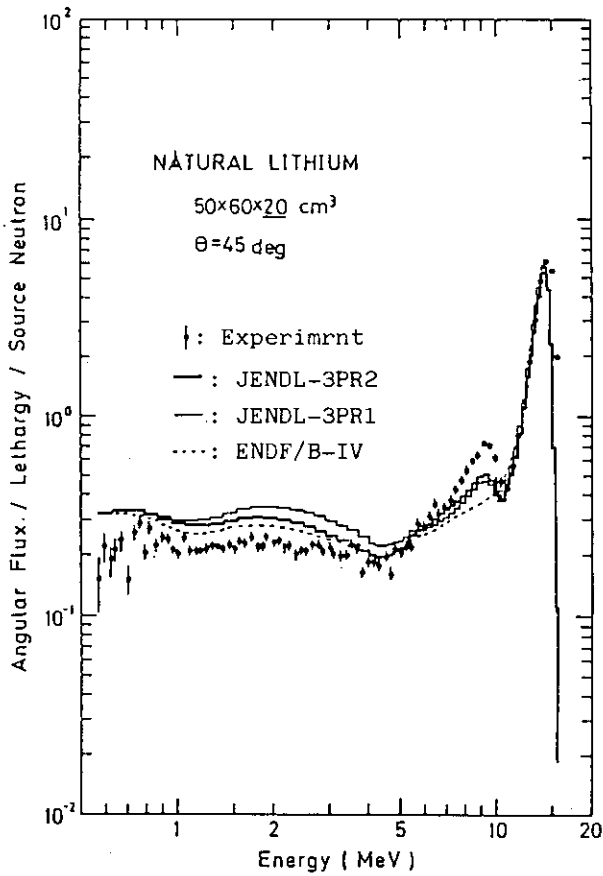
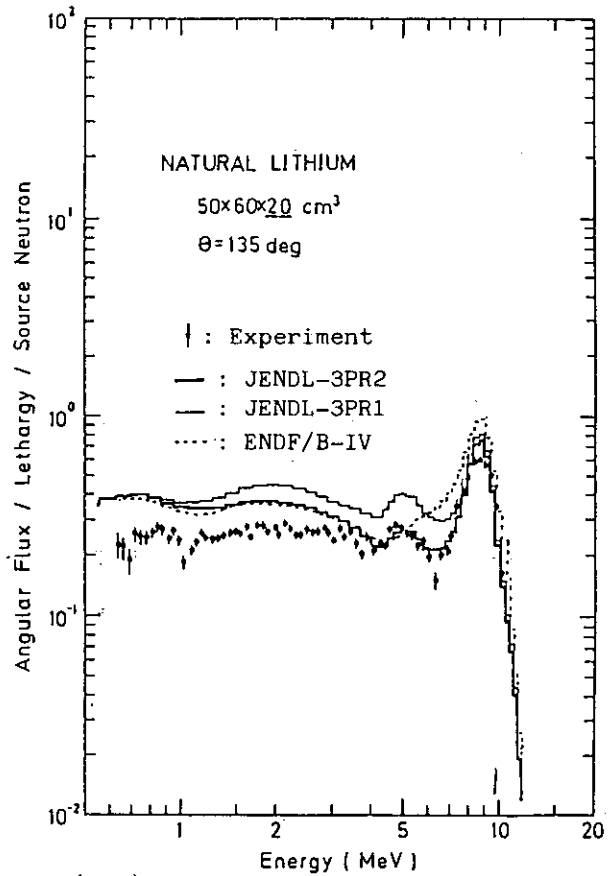


Fig.8 C/E for leakage spectrum from a 40 cm diam. lithium sphere



(a)



(b)

Fig.9 Angular flux spectra for 45 and 135 degrees from a natural lithium slab

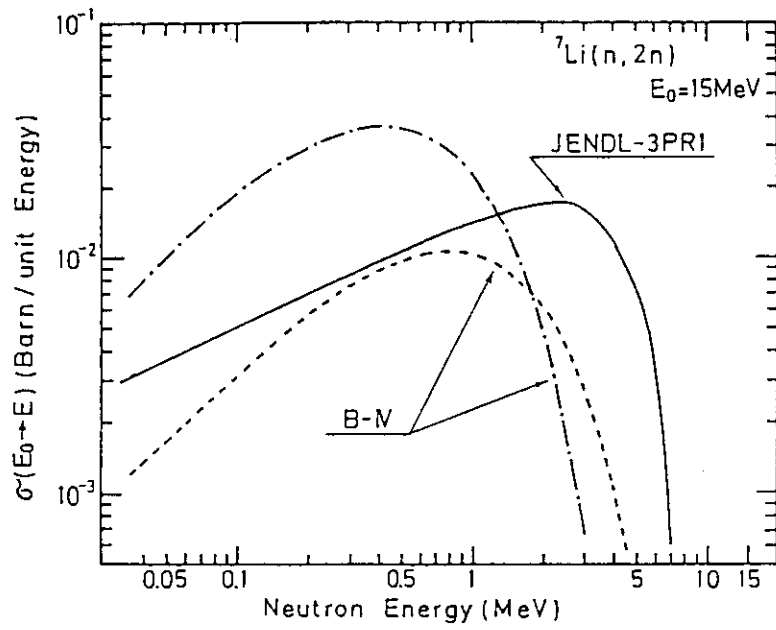


Fig.10 Energy spectra from (n,2n) reaction of ${}^7\text{Li}$ evaluated in ENDF/B-IV and JENDL-3PRI

3. Comparison between measurements of the Neutron Spectra from Materials used in Fusion Reactors and Calculations using JENDL-3PR1

Hiroyuki Hashikura, Yoshiaki Oka,
and Shunsuke Kondo
Nuclear Engineering Research Laboratory,
University of Tokyo
Tokai-mura, Naka-gun, Ibaraki

JENDL-3PR1 which includes very important nuclides for analysis of fusion blanket experiments has been already released. The accuracy of the nuclear data has been checked by the comparison of the integral measurements with the calculational results using JENDL-3PR1. Several problems are pointed out.

1. Introduction

Double differential neutron emission cross sections (DDX) for many elements have been recently measured at Osaka and Tohoku University. The measured DDX data were compared with the calculations based on ENDF/B-IV and JENDL-3PR1.¹⁾ Nuclear data should be also checked by the comparison between the integral measurements and the calculations since there are often large uncertainties in the differential cross sections. The integral measurements of neutron spectra are very useful to detect specific energy range where the data are adequate or not. The measurements of neutron spectra can complement the differential cross section measurements.

The pulsed sphere experiments that were carried out by L.F. Hansen et al.²⁾ and H. Hashikura et al.³⁾ have been used as the cross section benchmark tests.⁴⁻⁹⁾ These experiments measured the neutron spectra emitted from spherical targets

bombarded with a central D-T neutron source. In this paper, calculations are compared with the measurements from 2 to 15 MeV on C, ^6Li , ^7Li , O, Fe, and Ni. All calculations have been made with the continuous-energy Monte Carlo code MCNP.¹⁰⁾

2. Experiment

The measurements have been carried out using the time-of-flight techniques at LLNL and Osaka University. D-T neutrons are obtained from the $\text{T}(d,n)^4\text{He}$ reactions. A tritium-titanium target was positioned at the center of the spheres. The spectra measurements between 2 and 15 MeV were made using NE-213 scintillators. A tabulation of the spherical assemblies which has been analysed for the checking the nuclear data is presented in Table 1.

3. Calculation

The calculations were carried out by the continuous energy Monte Carlo code, MCNP with the fine energy structure of the nuclear cross sections. Processing of JENDL-3PR1-formatted data into MCNP - format was made using NJOY¹¹⁾. The advantage of MCNP are that the multigroup approximations are not required, all the reactions described in the nuclear data are accounted for and the geometries of the spherical assemblies are accurately included in the calculations.

4. Results and discussion

carbon

The measured and calculated energy spectra are compared in Fig. 1. The good agreement is shown in the energy interval of 12 to 15 MeV. The calculation slightly overestimates the measured flux around 5 MeV which corresponds to the inelastic scattering to 9.64 MeV level. The (n,n') cross section to 9.64 MeV level is shown in Fig. 2, with the measured data. The data

of JENDL-3PR1 agree well with the measured data by Antolkovic but overestimate the measurement by Baba.¹²⁾ The analysis of the integral measurement suggests that the measured data by Baba is more realible.

lithium-6

Comparison between the measurement and calculation is given in Fig. 3. The calculation shows good agreement with the measurement above 8 MeV but overestimates it below 8 MeV. It has been already pointed out that the reason the discrepancy is attributed to the secondary neutron distribution from the (n,n') continuum and (n,2n) reactions. The lithium-6 of JENDL-3PR1 has been revised and released as JENDL-3PR2.¹³⁾

lithium-7

The result is shown in Fig. 4. The calculation agrees well with the measured flux above 7 MeV and overestimates it below 7 MeV. This shows the same result as that of lithium-6 in JENDL-3PR1. Lithium-7 of JENDL-3PR1 has been already revised and released as JENDL-3PR2.

oxygen

Comparison between the measurement and the calculation is shown in Fig. 5. Calculated result using ENDF/B-IV is also shown in Fig. 6. Calculated results overestimate the measured flux in the energy region below 7 MeV. Cross sections at 15 MeV are listed in Table 2. Hansen pointed out⁶⁾ that, in ENDF/B-IV, the total (n,n') cross section was right but distribution of the cross sections among 21 levels was incorrect and in particular, too much cross section was assigned to the levels between 6- and 10- MeV excitation energy. In JENDL-3PR1, smaller value of the total (n,n') cross section has been assigned but the calculation overestimates the measured flux. This indicates that, in JENDL-3PR1, the distribution of the cross sections is incorrect and too much cross section is assigned to the levels between 6- and 10-MeV.

iron

Fig. 7 shows the comparison between the measurement and the calculation. The calculated result underestimates the measured flux in the energy region between 10 MeV and 5 MeV and an evident peak is observed around 9 MeV. Secondary neutron spectra from the (n, n') continuum reaction are shown in Fig. 8, with those of JENDL-3P1 and ENDF/B-IV. The small peak which is observed in Fig. 7 corresponds to that in Fig. 8. This indicates that the secondary neutron distribution from the (n,n') continuum is incorrect.

nickel

The result is shown in Fig. 9. The calculated spectrum agrees well with the measurement except for the energy region around 13 MeV. The discrepancy is attributed to the large values of the inelastic scattering cross sections to 1.33- and 1.45-MeV levels.

5. Conclusion

The analysis of the integral measurements has been carried out using the continuous energy Monte Carlo code, MCNP. Some discrepancies have been found by the comparison of the measurements with the calculations. The present results should be considered for the final version of JENDL-3.

Acknowledgement

The experiment of nickel was made as a cooperative work between Osaka and Tokyo University. The authors wish to thank Dr. A. Takahashi and Dr. J. Yamamoto for their assistance. The present work has been partially supported by Grant-in-Aid, Ministry of Education, Science and Culture.

References

- 1) Kikuchi, Y., et al: J. Nucl. Sci. Technol., **22**, 499 (1985).
- 2) Hansen, L.F., et al: UCID-19604 (1982).
- 3) Hashikura, H., et al: Submitted to J. Nucl. Sci. Technol.
- 4) Hansen, L.F., et al: Nucl. Sci. and Eng., **35**, 227 (1969).
- 5) Hansen, L.F., et al: ibid., **51**, 278 (1973).
- 6) Hansen, L.F., et al: ibid., **60**, 27 (1976).
- 7) Hansen, L.F., et al: ibid., **72**, 35 (1979).
- 8) Estes, G.P., et al: Trans. Am. Nucl. Society., **33**, 679 (1979).
- 9) Estes, G.P., et al: ibid., **35**, 460 (1980).
- 10) Los Alamos Radiation Transport Group (X-6), "MCNP - A General Monte Carlo Code for Neutron and Photon Transport", LA-7396-M, Revised (1981).
- 11) MacFarlane, R.E., et al: "The NJOY Nuclear Data Processing System: User's Manual", LA-9303-M.
- 12) Baba, M. : private communication.
- 13) Chiba, T. : private communication.

Table 1 Assemblies used for analyses.

Material	Radius (cm)
Li-6	25.52
Li-7	25.52
C-Nat	20.96
O-Nat	10.50
Fe-Nat	22.30
Ni	16.0

Table 2 Point Cross Sections at 15 MeV for ^{16}O .

	JENDL-3PR1	ENDF/B4
total	1.76281	1.759
elastic	1.12148	1.068
nonelastic	6.40929-1	
(n,d)	1.58-2	1.222-2
(n,p)	3.53-2	3.8178-2
(n, α)	8.500-2	1.0745-1
(n, γ)	7.7867-9	9.9133-9
inelastic	5.08329-1	5.4033-1
6.049	2.5616-2	3.900-2
6.1300	9.800-2	6.99-2
6.917	7.84403-2	2.3604-2
7.1169	3.05039-2	3.2982-2
8.872	6.49018-2	5.1268-2
9.63	3.28008-2	2.627-2
9.847	2.68765-2	3.336-2
10.36	1.9919-2	3.3906-2
10.96	6.8336-3	7.0902-3
11.08	1.81005-2	3.5178-2
11.10	1.50041-2	3.0179-2
11.26		6.6357-3
11.44		3.9814-2
11.52	8.629-3	2.2361-2
11.60	2.89597-2	3.3997-2
12.05	1.98311-3	2.9088-3
12.44	5.94501-3	4.9995-3
12.53	1.06532-2	7.0902-3
12.80	1.27127-3	9.09-4
12.97	5.94993-3	
13.02	2.24-38-3	3.36-3
13.09	2.73778-3	1.4632-2
13.12	8.87787-3	
13.26	8.13476-3	
13.45		1.1689-2
13.66	1.27149-3	
13.75		7.409-3
13.87	1.05653-3	
13.98	1.86-3	
14.3	3.0956-4	
14.1	1.38015-3	1.7207-3

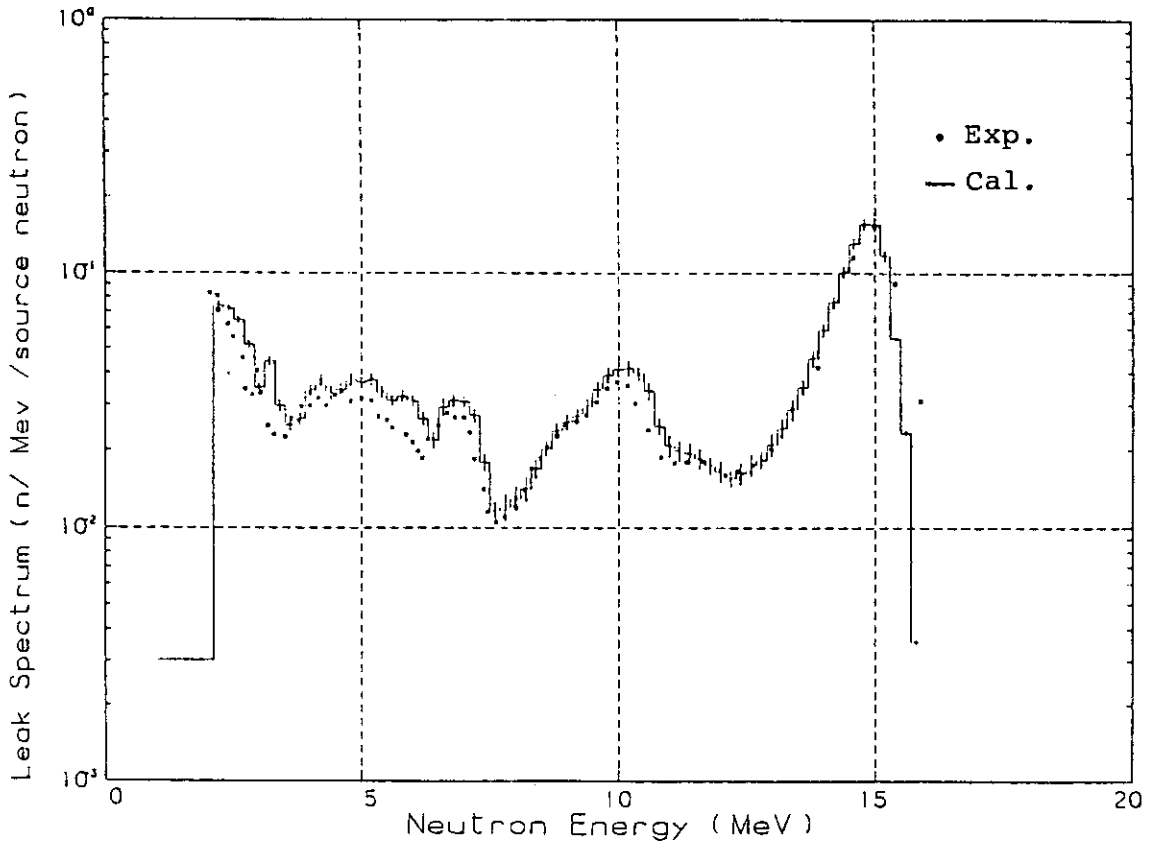


Fig. 1 Measured and calculated energy spectra for Carbon.

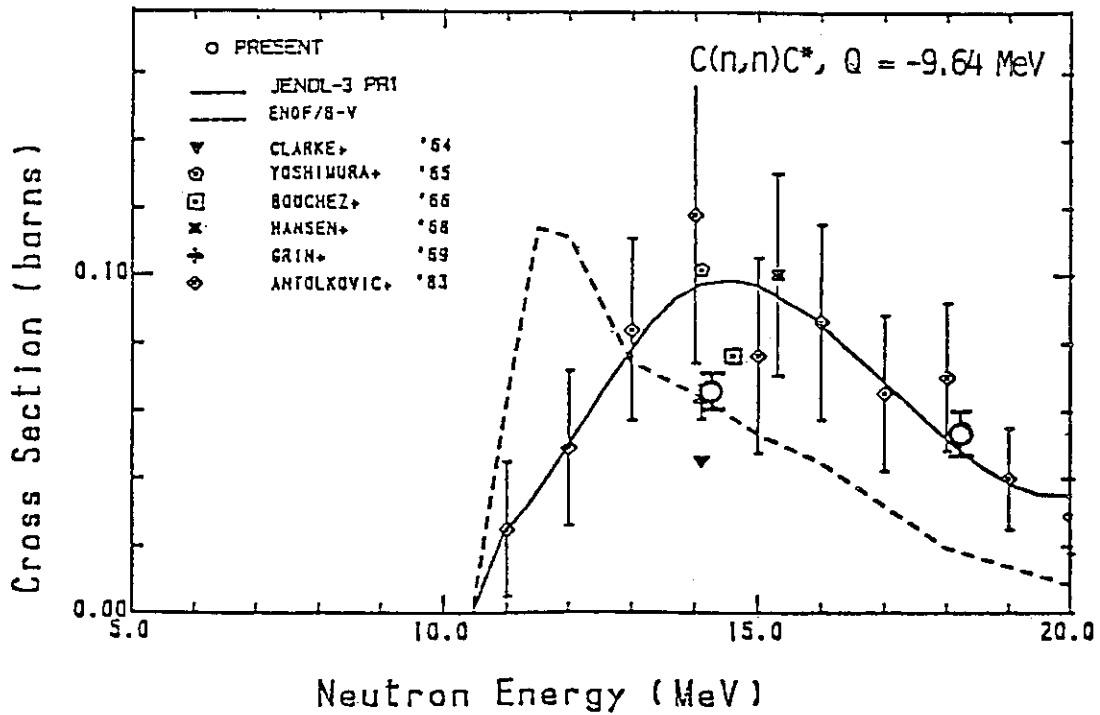


Fig. 2 Inelastic scattering cross section to 9.64 MeV level.¹²⁾

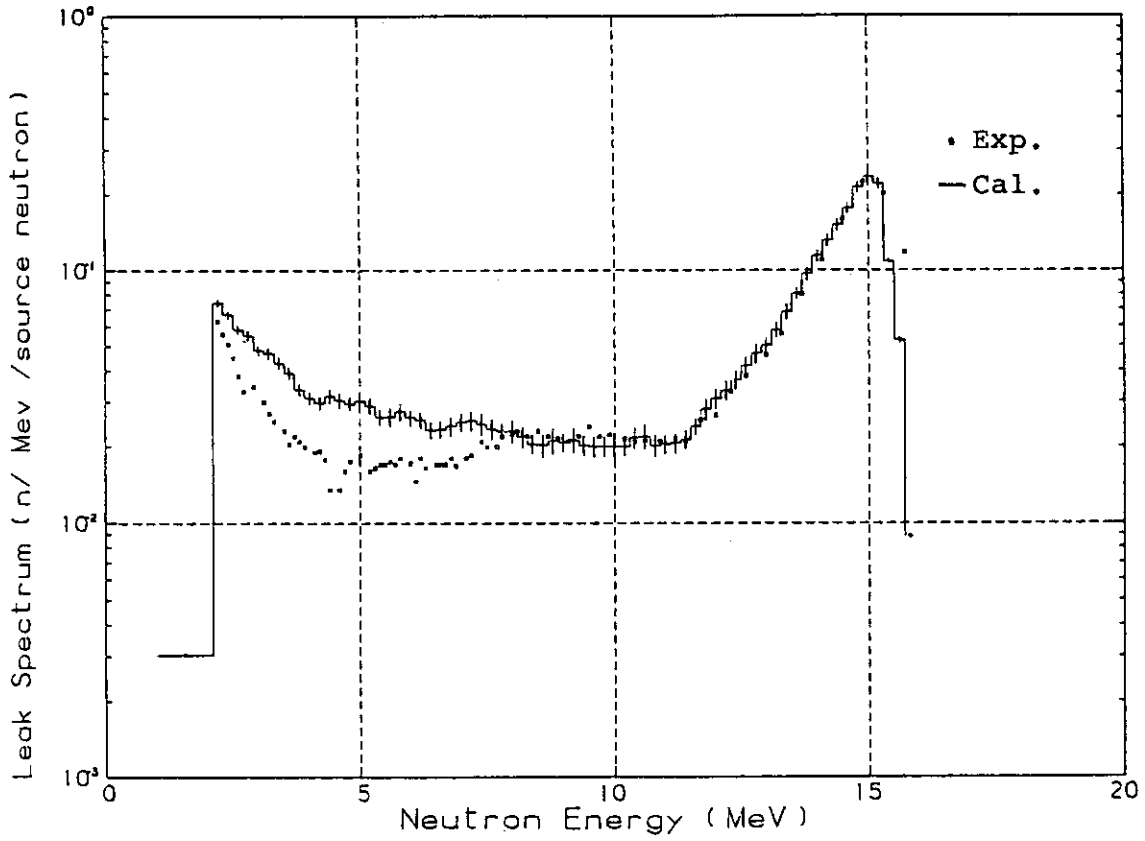


Fig. 3 Measured and calculated energy spectra for Lithium-6.

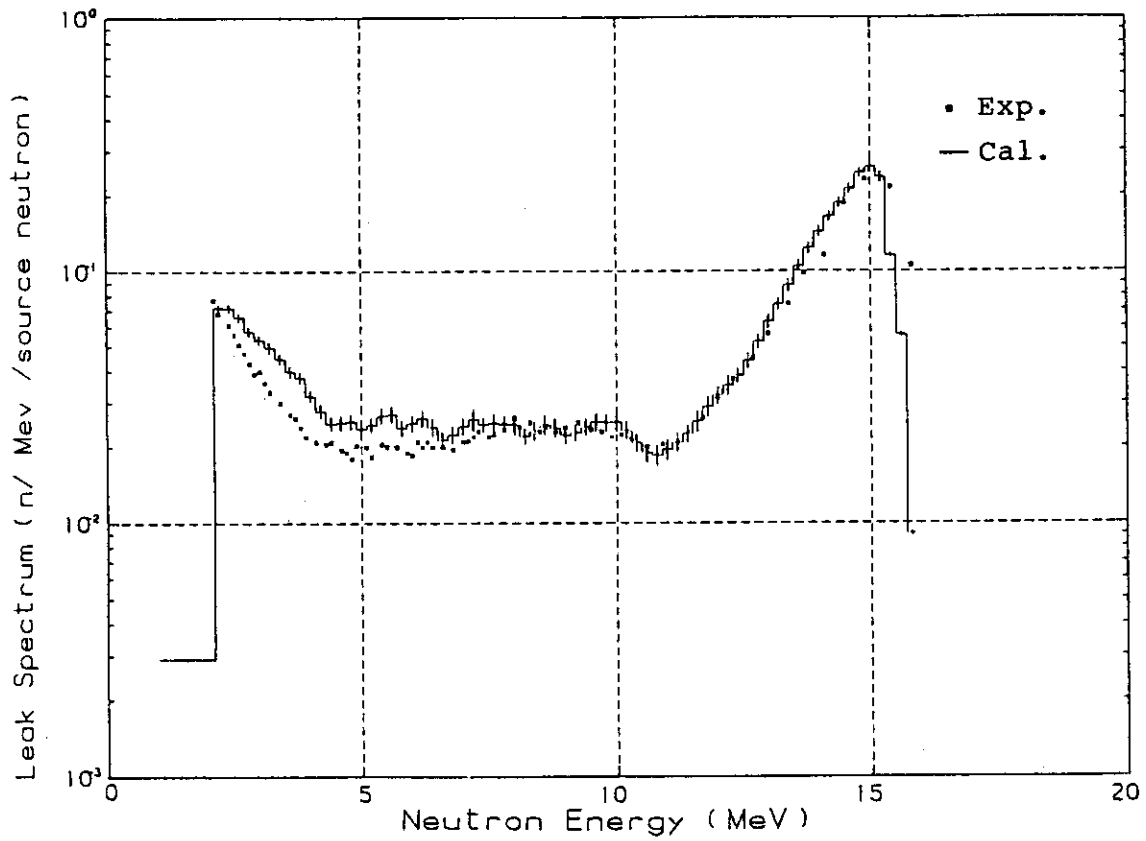


Fig. 4 Measured and calculated energy spectra for Lithium-7.

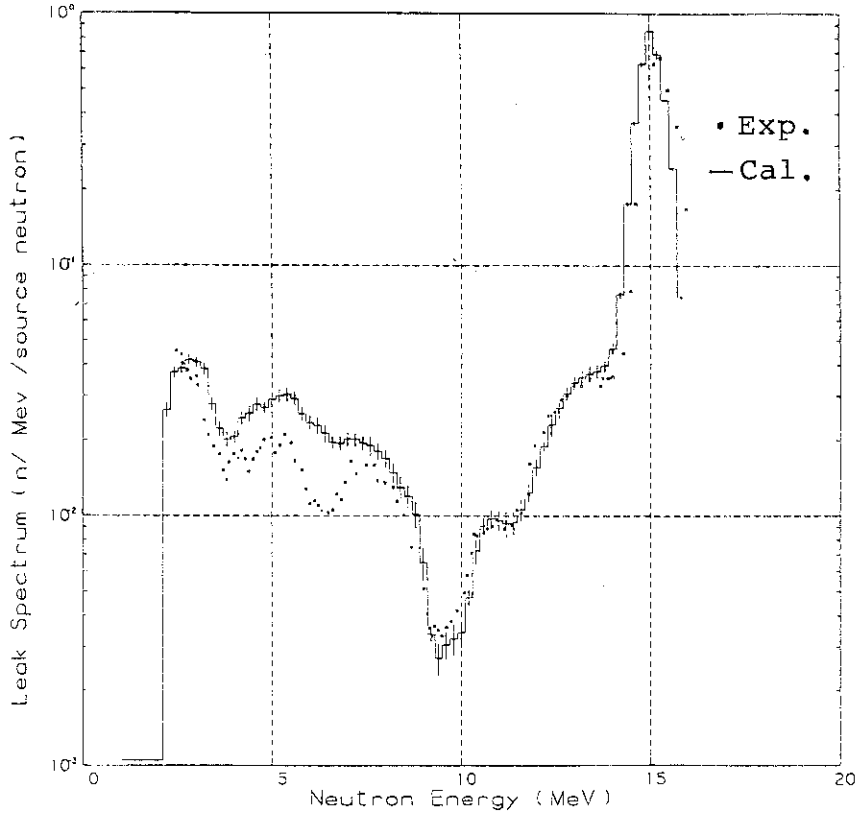


Fig. 5 Measured and calculated energy spectra using JENDL-3PR1 for Oxygen.

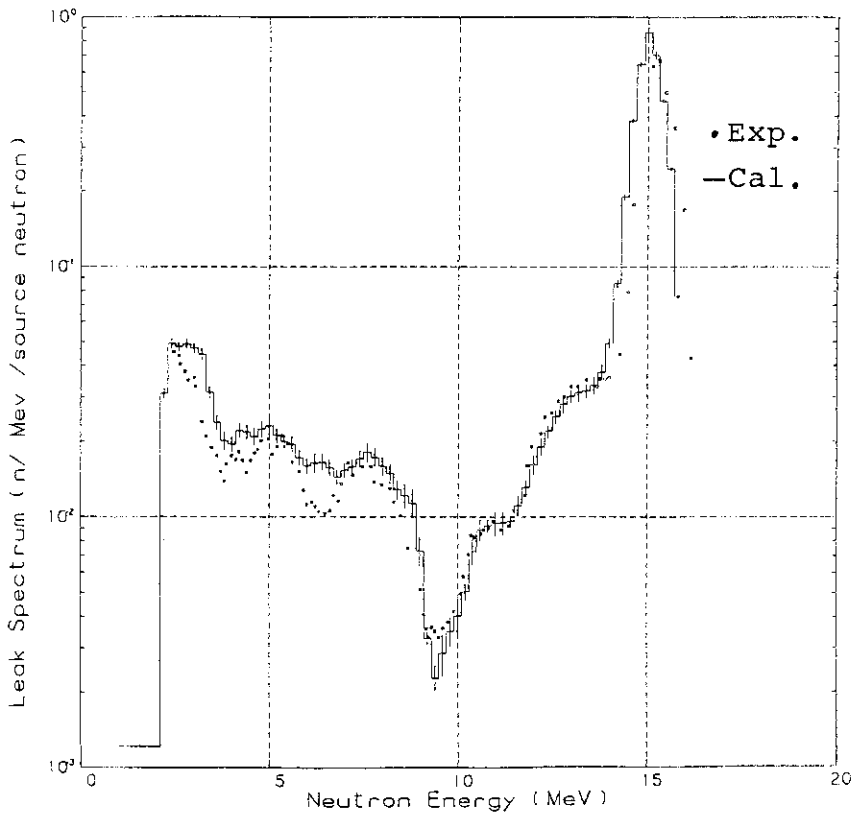


Fig. 6 Measured and calculated energy spectra using ENDF/B-IV for Oxygen.

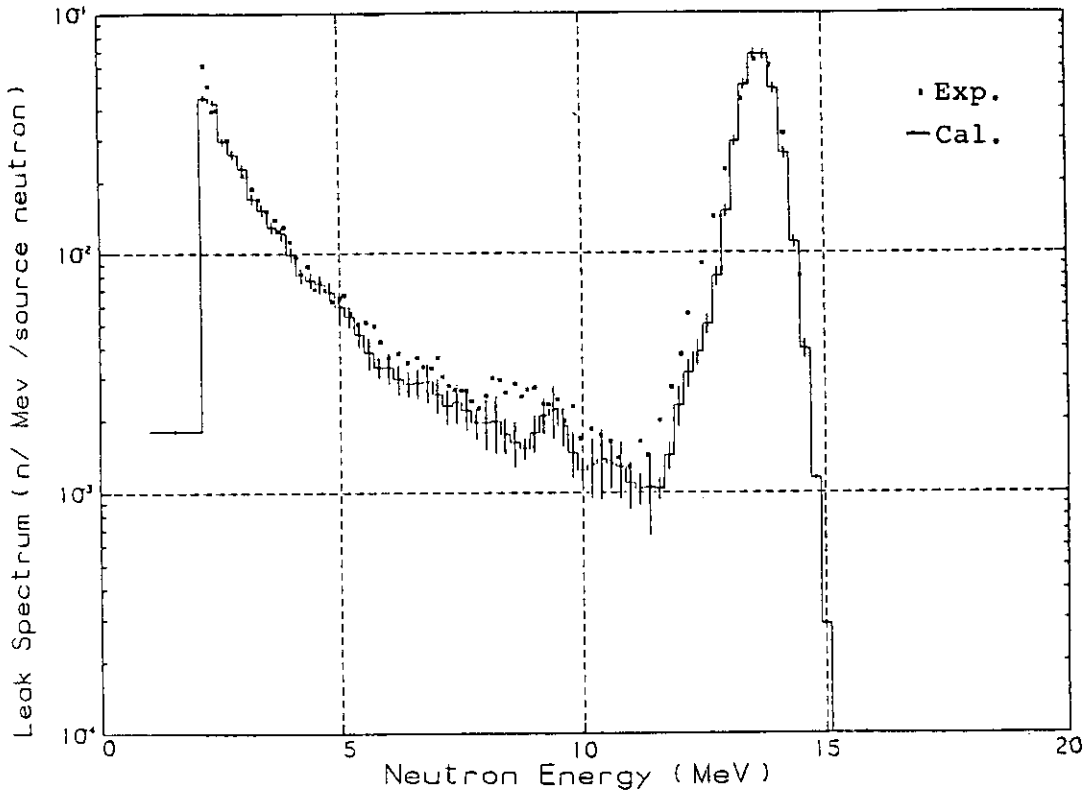


Fig. 7 Measured and calculated energy spectra for Iron.

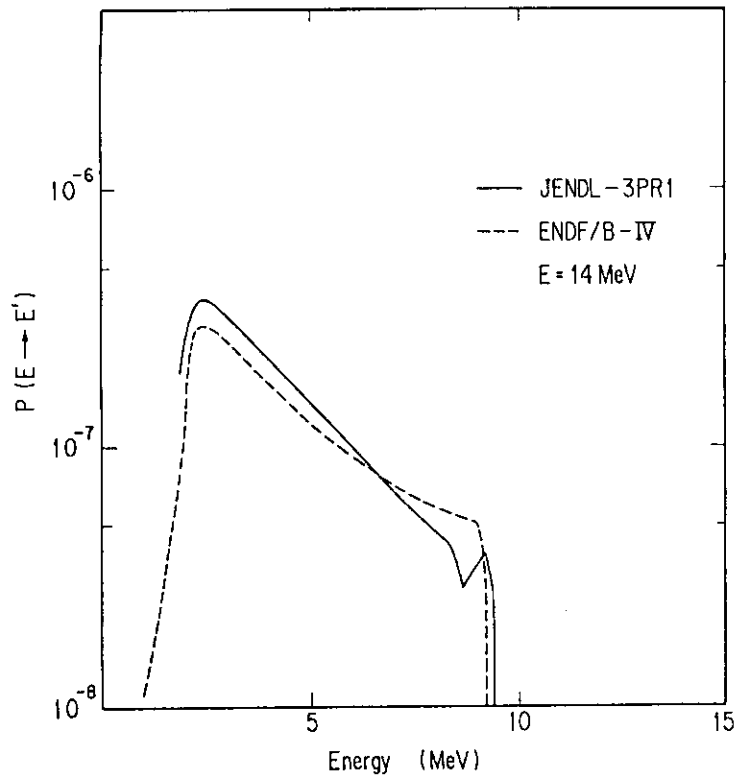


Fig. 8 Secondary neutron spectra from inelastic scattering to the continuum level in JENDL-3PR1 and ENDF/B-IV.

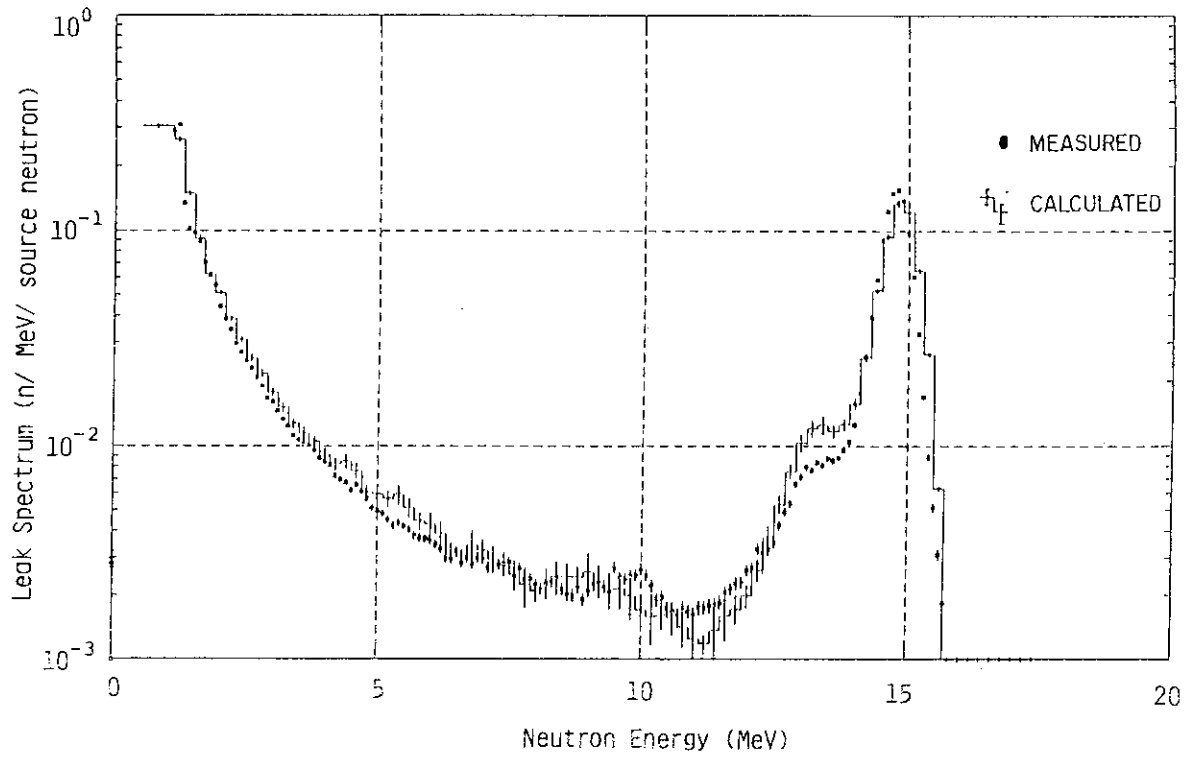


Fig. 9 Measured and calculated energy spectra for Nickel.

4. Clean Benchmark Experiments and Analyses at FNS

Hiroshu Maekawa

Japan Atomic Energy Research Institute
Tokai-mura, Naka-Gun, Ibaraki-ken

Two types of clean benchmark experiments have been carried out at the FNS (Fusion Neutronics Source) facility. They are integral experiments and time-of-flight experiments. The former includes integral experiments on cylindrical assemblies with: (1) 60-cm thick lithium oxide (Li_2O), (2) 60-cm thick graphite, and (3) 40-cm thick Li_2O followed by 20-cm thick graphite. Various reaction rates such as tritium production rate and neutron spectra were measured in these experiments. The time-of-flight experiments were conducted to measure angle-dependent neutron spectra leaking from: (1) Li_2O , (2) graphite, and (3) lithium-metal slab assemblies. These experiments were numerically analyzed by making use of the DOT3.5 transport code with newly processed 125-group cross-section sets, i.e., JENDL-3PR1, JENDL-3PR2, ENDF/B-IV, and ENDF/B-V (^{12}C only). It was found that the calculations based on JENDL-3PR1 and JENDL-3PR2 predicted tritium production rates of ^6Li and ^7Li better than those based on ENDF/B-IV. These analytical results are expected to provide useful information for the future development of the JENDL-3 nuclear data file.

1. Introduction

Experimental examinations are required to verify the accuracy of both calculational methods and nuclear data which are used in nuclear design and analysis of a fusion reactor. The most suitable experiments for this type of method/data verification are clean benchmark experiments on a simple geometry with simple material compositions. Analyses of the experimental results are expected to identify the accuracy as well as the deficiencies in the currently available methods and nuclear data.

In this report the outlines of integral experiments and time-of-flight experiments that were carried out using the powerful D-T neutron source FNS are described, and comparisons are made with numerical analyses. The numerical analyses by DOT3.5 utilize multi-group cross-section sets. Upon the generation of the group cross sections, two types of weighting spectra, viz, $1/E$ and flat weighting functions, were used. Effects of these two different weighting spectra will be also discussed.

2. Clean Benchmark Experiments

The clean benchmark experiments conducted at FNS include: (a) integral experiments -- measurement of reaction-rate distributions and neutron spectra in an assembly, and (b) time-of-flight (TOF) experiments -- measurement of angle-dependent neutron spectra leaking from a slab assembly.

The integral experiments have been carried out on the following three assemblies:

- (1) 60-cm thick Li_2O cylindrical slab assembly (Li_2O assembly)
- (2) 60-cm thick graphite cylindrical slab assembly (C assembly)
- (3) 40-cm thick Li_2O cylindrical slab assembly followed by 20-cm thick graphite reflector (Li_2O -C assembly).

Measured quantities and their methods are summarized in Table I. As the experimental results and comparison with pre-experimental analyses were previously reported at meeting (such as the annual meeting of the Japan Atomic Energy Society), the experimental details are not described here. Experimental reports including digital data will be presented in a JAERI-M publication.⁽¹⁾

Several observations have been made regarding the integral experiments. They are as follows:

- (1) The geometries of the experimental assemblies were simple enough to be accurately modeled for calculations.
- (2) Measured data were absolute values; experimental data can be directly compared with calculated results.
- (3) Various measured values, such as reaction rates having different energy responses, give a lot of information.
- (4) The experimental data were consistent to each other; measured data are reliable.

As with the TOF experiments, measurements of Li_2O , graphite and lithium-metal slab assemblies have been done. They are summarized in Table II. The work on the Li_2O slabs⁽²⁾ and its analysis⁽³⁾ using DOT3.5 transport code⁽⁴⁾ with the ENDF/B-IV nuclear data file has been published. A report on the graphite slab experiment is in progress. In the case of the lithium-metal experiment, the lower limit of measured energy was extended from 500 keV to 50 keV and the detector efficiency below 200 keV was required to process the

measured data. An additional experiment is planned in the near future to measure the efficiency curve. The final result will be obtained using this efficiency curve.

3. Analyses of Experiments

In the present analyses for both the integral and TOF experiments, the DOT3.5 code was used with the P_5-S_{16} approximation. The cross-section sets used were obtained from the nuclear data files of JENDL-3PR1, JENDL-3PR2, ENDF/B-IV, and ENDF/B-V (only for carbon data) using the processing code PROF-GROUCH-G/B (Ref. 5). These features are shown in Table III along with the cross-section sets used in the pre-experimental analyses. As the weighting function, a Maxwellian distribution was used for the thermal group (125th group) and a $1/E$ distribution was used for the other groups in the JENGIX and ENDGIX sets. A flat distribution was assumed in the JEFIX set for 1 ~ 124 groups.)

The source neutron spectrum calculated by a Monte Carlo method⁽⁶⁾ was adopted in the analysis of the integral experiments. On the other hand, the measured source spectra were used in the TOF experiments. The GRTUNCL code was used to calculate the first collision source for the succeeding DOT calculations.

4. Results

4.1 Integral Experiments

The ratios of calculated-to-experimental values (C/E) for the tritium production rate (TPR) of ${}^6\text{Li}$ in the Li_2O assembly are shown in Fig. 1. The experimental values have been corrected for self-shielding and room-return effects. The calculation based on JENDL-3PR1 predicted the experimental values very well. The calculated value based on JENDL-3PR2 was a little higher than that based on JENDL-3PR1. On the other hand, the result obtained with ENDF/B-IV overestimated the experiment due largely to the incorrect ${}^7\text{Li}(n,n'\alpha)\text{T}$ cross section in this data file. The effect of the difference in the weighting function between the flat and $1/E$ was, however, small and within 1%.

The C/E values for TPR of ${}^7\text{Li}$ in the Li_2O assembly are shown in Fig. 2. The results calculated with both JENDL files agree very well with those of the experiment. It is clearly observed that those with ENDF/B-IV overestimated the experiment by about 20%. The result using the spectrum calculated with

ENDF/B-IV and the ${}^7\text{Li}(n,n'\alpha)\text{T}$ cross section in JENDL was close to that using JENDL itself. Therefore, the difference in the ${}^7\text{Li}$ cross section has little effect in the higher energy region.

As a typical example of high-energy threshold reactions, the C/E values for the ${}^{27}\text{Al}(n,\alpha){}^{24}\text{Na}$ reaction are shown in Fig. 3. Results calculated using the cross-section set generated with the flat weighting function were smaller than that using the $1/E$ by up to 3%. In the case of ${}^{58}\text{Ni}(n,2n){}^{57}\text{Ni}$, the calculation for the flat weighting function was smaller than that for $1/E$ by 2 ~ 5%. This fact suggests that the D-T source neutron spectrum should be used for the weighting function in the higher-energy region.

The tendency of the C/E curve of ${}^{238}\text{U}(n,f)$ is similar to that of ${}^{27}\text{Al}(n,\alpha){}^{24}\text{Na}$, though the measuring method for them were quite different and the data were obtained independently. The same tendencies are found in the cases of the C and Li_2O -C assemblies. The distributions of C/E value for energy-integrated neutron spectra also show the same tendency. It can be concluded that the experimental data are consistent to each other.

In the case of ${}^{235}\text{U}(n,f)$ which has a strong sensitivity to low energy neutrons, it becomes clear that the calculated result depends on the weighting function. The C/E values for ${}^{235}\text{U}(n,f)$ in the C and Li_2O -C assemblies are shown in Fig. 4 and 5, respectively. It is clearly seen that the differences between the two cross-section sets are more than 15% in the graphite regions. The differences in the Li_2O assembly are small in the case of ${}^6\text{Li}(n,\alpha)\text{T}$. Because the neutron population in the energy range below 250 keV is very small in this assembly, the following observations can be made from the present analysis:

- (1) The calculated results using the JENDL-3PR1 and JENDL-3PR2 data sets agree well with the measured tritium production rates of both ${}^6\text{Li}$ and ${}^7\text{Li}$.
- (2) The impact of the difference in the weighting spectrum is small except some special cases such as ${}^{235}\text{U}(n,f)$. The calculation is expected to give fairly good values when it is made with a cross-section set using the weighting function of a D-T neutron source spectrum in a higher-energy region, a Maxwellian distribution in a thermal region, and a typical fusion reactor blanket spectrum in the region between them.

4.2 Time-of-Flight Experiment

Figure 6 shows the measured spectrum for the Li_2O slab of thickness 5.06 cm and 24.9 deg along with the calculated spectra with JENDL-3PR1 and ENDF/B-IV. Figure 7 shows the results calculated with JENDL-3PR1 and JENDL-3PR2. The results with the three nuclear data files are almost the same except near the peak at ~ 9 MeV. The peak corresponds to the first level of inelastic scattering for ${}^7\text{Li}$. It is clearly seen that the spectrum calculated with JENDL-3PR2 substantially improves the accuracy and is almost satisfactory in the region corresponding to the first level. The same tendencies are seen in the other thickness and angles. There are some discrepancies in the regions of elastic peak (14 MeV), near 4 and 1.5 MeV. Further examinations should be carried out for the evaluation of these nuclear data.

For the graphite slabs, experimental results for 5.06-cm thickness and 2.49-deg angle are shown in Fig. 8 along with the calculated ones for ENDF/B-IV and ENDF/B-V, and in Fig. 9 for JENDL-3PR1 and JENDL-3PR2. In the case of ENDF/B-IV, there exists only the peak corresponding to the first level of inelastic scattering for ${}^{12}\text{C}$ due to the lack of data for other levels. Even though the spectra calculated by the other three nuclear data files show the peaks which correspond to the first, second, and third levels, the values of these peaks are slightly different from the experiments. This fact suggests that re-evaluation is required for the nuclear data of these levels including the angular distribution of secondary neutrons. Among the nuclear data files used, there are some differences in the calculated spectra below 2 MeV depending on thickness and angle. Further examination remains to be done for the data such as the angular distribution that is important to the determination of the spectrum in these energy regions.

5. Concluding Remarks

The results of analyses for the integral experiments on the three assemblies and the time-of-flight experiments on the two materials were discussed. The results shown in this paper, however, cover only part of the data that have been obtained. Further evaluations and examinations of all results will be very useful for the development of the JENDL-3 nuclear data file. Mutual communication between our experimentalists and nuclear data evaluators should be profitable to complete the JENDL-3 nuclear data file.

References

- (1) Maekawa H., et al.: "Fusion Blanket Benchmark Experiments on a 60-cm Thick, Li₂O Cylindrical Assembly," JAERI-M report (to be published).
- (2) Oyama Y., Maekawa H.: JAERI-M 83-195 (1983).
- (3) Oyama Y., Yamaguchi S., Maekawa H.: JAERI-M 85-031 (1985).
- (4) Rhodes W. A., Mynatt F. R.: ORNL/TM-4280 (1973).
- (5) Hasegawa A.: to be published.
- (6) Seki Y., et al., J. Nucl. Sci. Technol. 20, 686 (1983).

Table I. Measured quantities and their methods for integral experiments.

-
- (1) Tritium production rates of ${}^6\text{Li}$ and ${}^7\text{Li}$
- Liquid scintillation method with ${}^6\text{Li}_2\text{O}$ and ${}^7\text{Li}_2\text{O}$ pellets
 - ${}^6\text{Li}$ and ${}^7\text{Li}$ glass scintillators
- (2) Fission rates
- Micro-fission chambers (mfc) (${}^{235}\text{U}$, ${}^{238}\text{U}$, ${}^{237}\text{Np}$, ${}^{232}\text{Th}$)
 - Solid-state track detectors (SSTD) with ${}^{235}\text{U}$, ${}^{238}\text{U}$, and ${}^{232}\text{Th}$ foils
- (3) Reaction rates
- Foil activation method
 - with Al, In, and Ni foils for Li_2O assembly
 - with Al, Au, In, Nb, Ni, and Zr foils for C assembly
 - with Al, Au, Co, Fe, In, Mn, Na, Nb, Ni, Sc, Ti, Zn, and Zr foils for Li_2O C assembly
- (4) Response of PIN diodes
- (5) Response of TLDs (measured in Li_2O and C assemblies)
- TLD-600, -700, -100 ----- LiF
 - UD-110S ----- CaSO_4
 - Mg_2SiO_4 , Sr_2SiO_4 , Ba_2SiO_4
- (6) In-system neutron spectra
- Small sphere NE213 spectrometer
-

Table II. Measurement of angle-dependent leakage spectrum.

-
- Time-of-flight method
 - Thickness:
 - 5, 20, and 40 cm for Li_2O and C slab assemblies
 - 10 and 30 cm for lithium-metal slab assemblies
 - Angle: 0, 12.2, 24.9, 41.8 and 66.8 deg
 - Energy: 0.5 ~ 16 MeV for Li_2O and C slabs
0.5 ~ 16 MeV for lithium-metal slabs
-

Table III. Cross-section sets for DOT3.5.

Name	Group No.	Process Code	Weight	File
GICXFNS ^a	135	NJOY	Flat ^b	ENDF/B-IV
GICXFNS1	135	NJOY	Flat ^b	ENDF/B-IV
JENGIX	125	P-G-G/B ^c	1/E and Maxwell	J-3PR1 & 2 ^e
JEFGIX	125	P-G-G/B ^c	Flat and Maxwell	J-3PR1 & 2 ^e
ENDGIX ^d	125	P-G-G/B ^c	1/E and Maxwell	ENDF/B-IV

^aC: ENDF/B-5, ⁷Li(n,n' α)³T: Young's evaluation.

^bThe thermal group constants were calculated by SRAC code.

^cPROF-GROUCH-G/B.

^dData of carbon in ENDF/B-V are included.

^eJENDL-3PR1 and JENDL-3PR2.

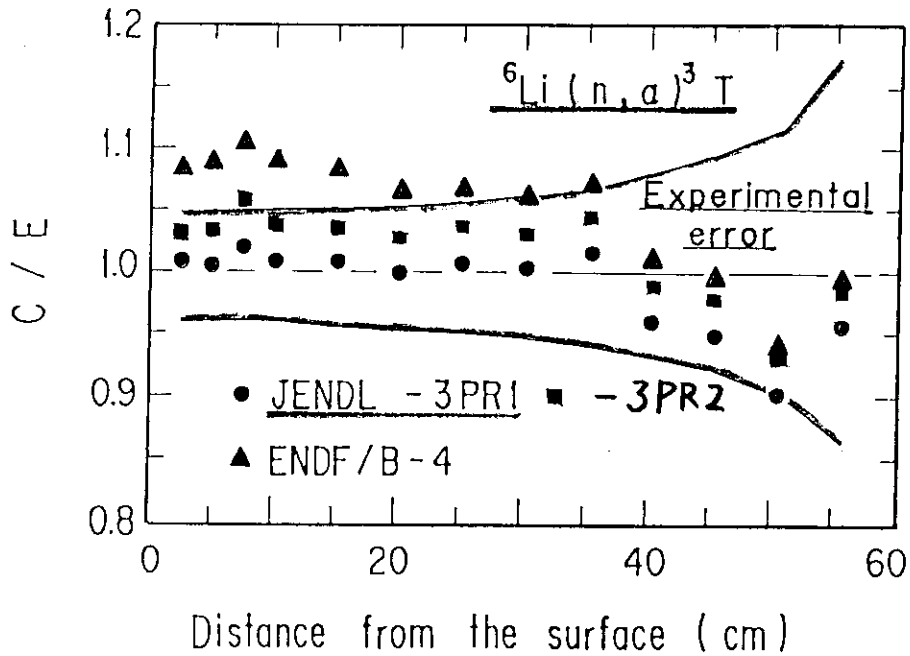


Fig. 1. Comparison of C/E values for tritium production rate of ⁶Li in the Li₂O assembly.

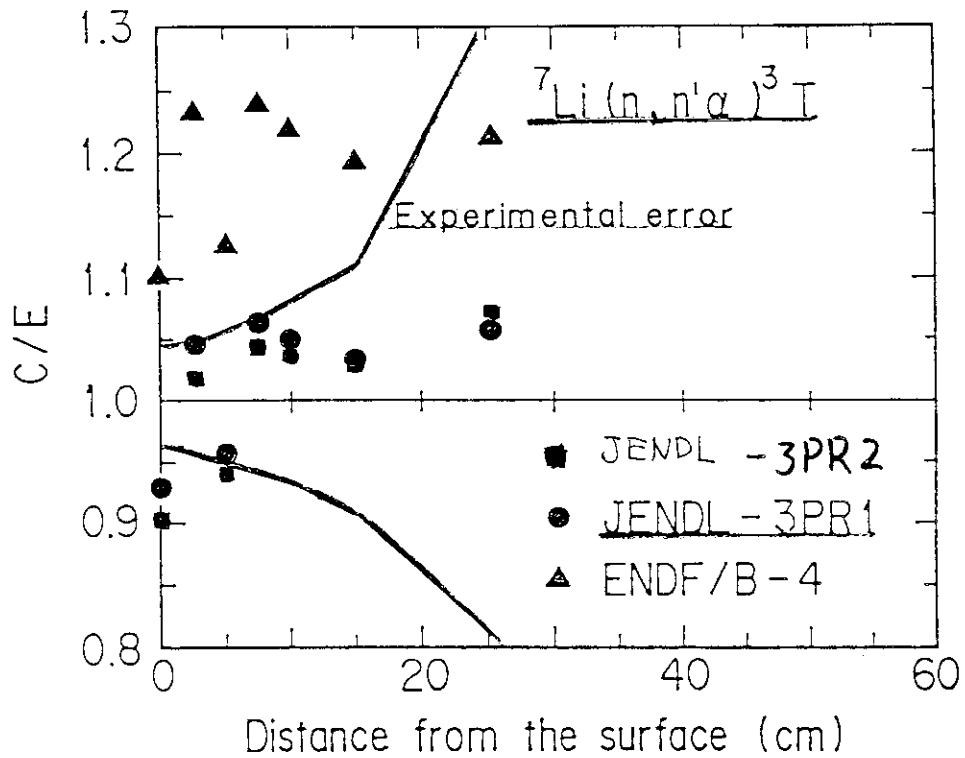


Fig. 2. Comparison of C/E values for tritium production rate of ${}^7\text{Li}$ in the Li_2O assembly.

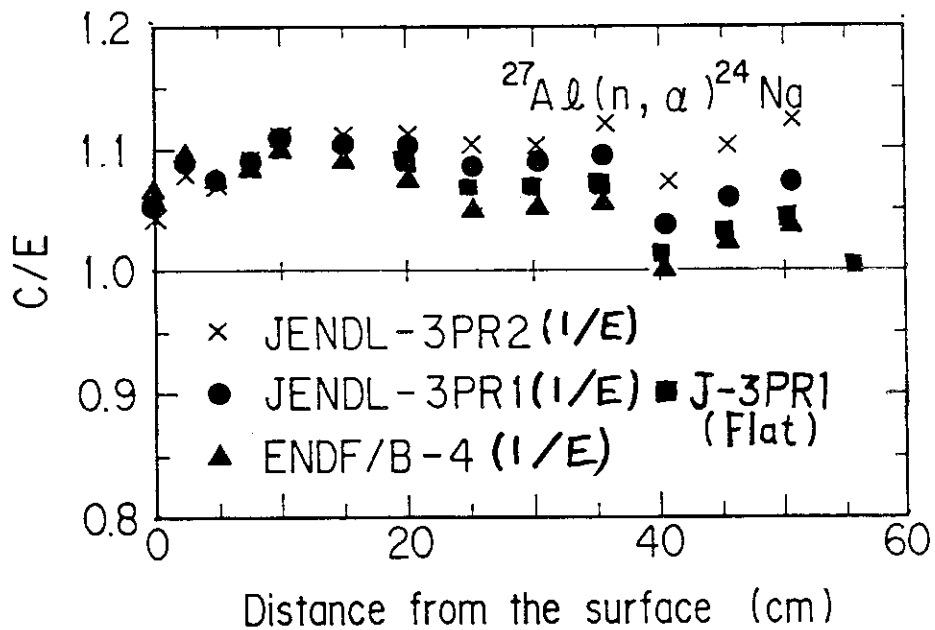


Fig. 3. Comparison of C/E values for ${}^{27}\text{Al}(n,\alpha){}^{24}\text{Na}$ reaction rate in the Li_2O assembly.

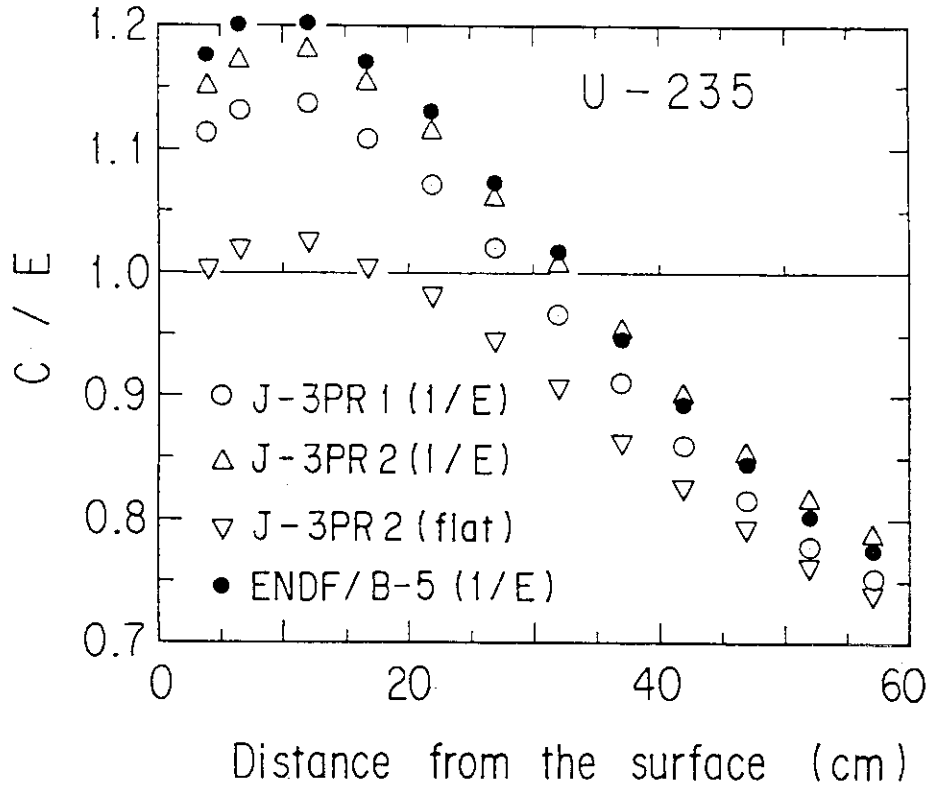


Fig. 4. Comparison of C/E values for $^{235}\text{U}(n,f)$ fission rate in the C assembly.

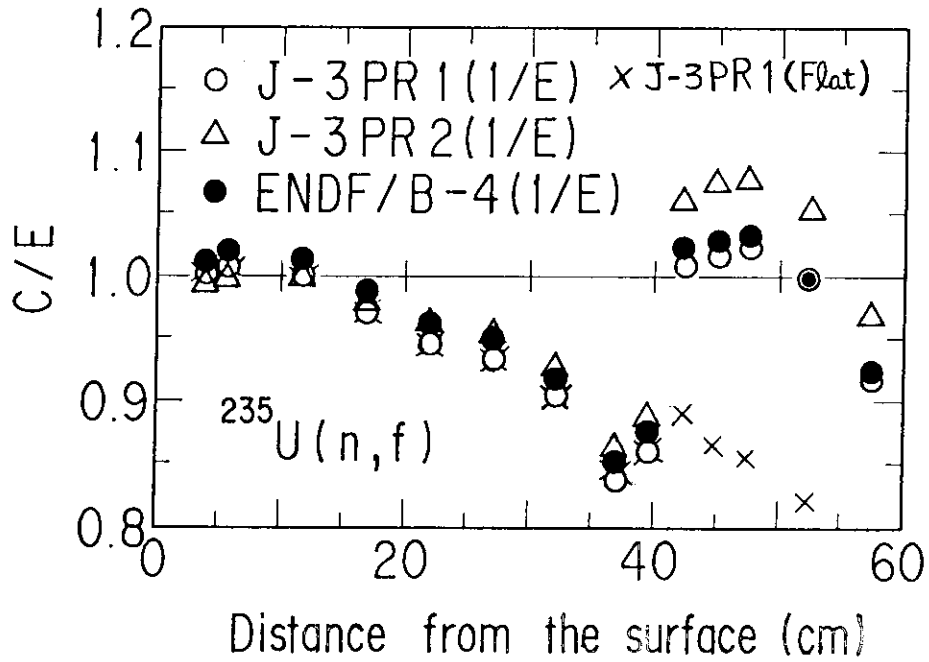


Fig. 5. Comparison of C/E values for $^{235}\text{U}(n,f)$ fission rate in the $\text{Li}_2\text{O-C}$ assembly.

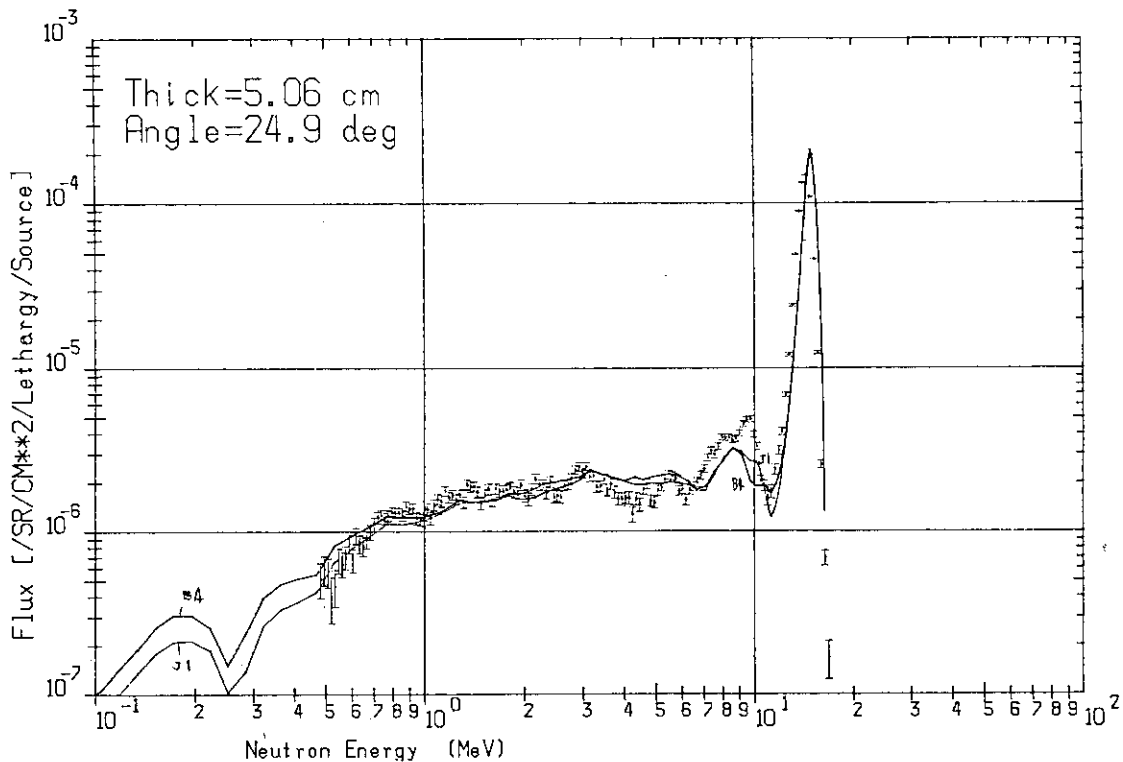


Fig. 6. Measured and calculated leakage spectra from the 5.06-cm thick Li₂O slab.

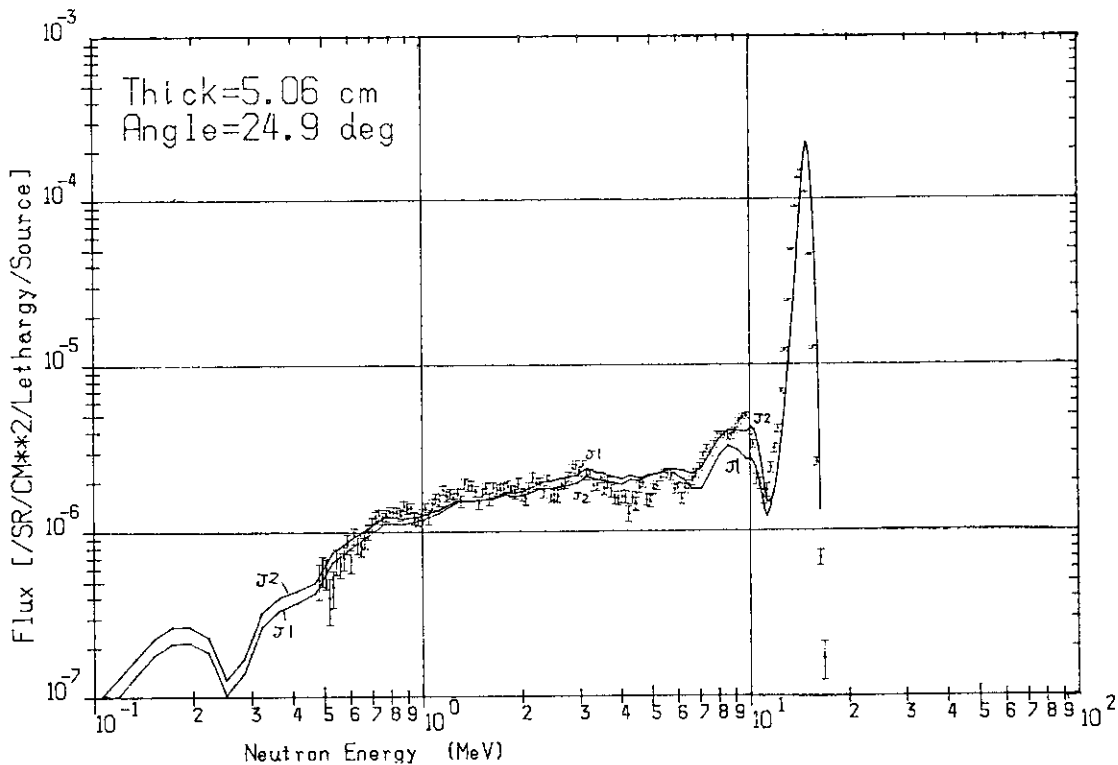


Fig. 7. Measured and calculated leakage spectra from the 5.06-cm thick Li₂O slab.

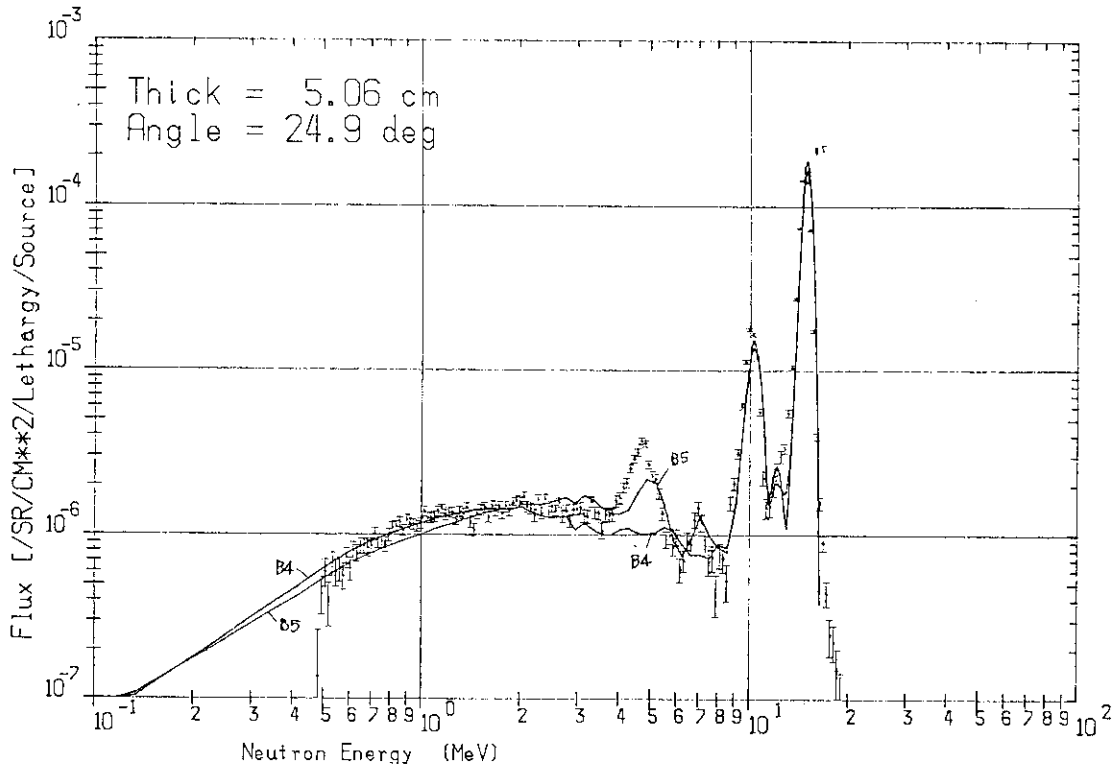


Fig. 8. Measured and calculated leakage spectra from the 5.06-cm thick graphite slab.

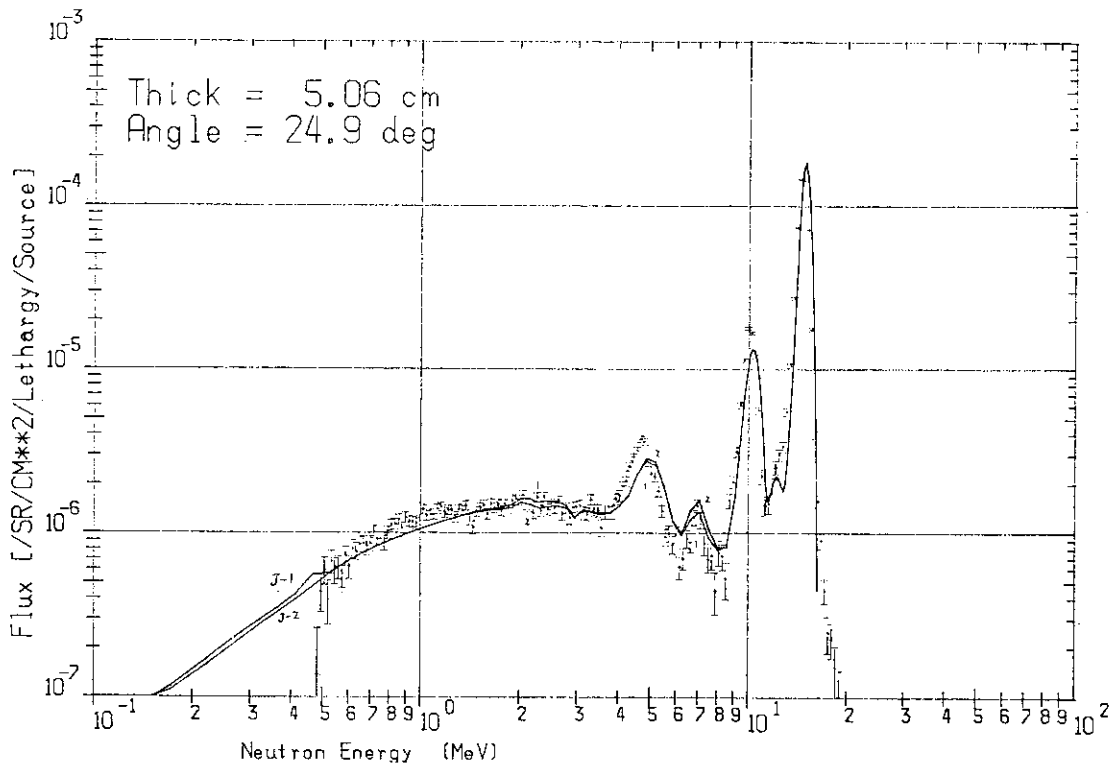


Fig. 9. Measured and calculated leakage spectra from the 5.06-cm thick graphite slab.

5. Fusion Blanket Engineering Benchmark Experiment

Tomoo Nakamura

Japan Atomic Energy Research Institute

1) Introduction

An ordinary benchmark experiment on fusion neutronics is usually so designed as to keep both geometry and composition as simple as possible. This is required to make the point of interest, on nuclear data or calculational methods, to be clear and emphasized, and the comparison between the experimental to calculated values as straightforward as possible. The breeding blankets in many conceptual designs, however, have rather complex configurations. It is not so simple to estimate the accuracies of neutronic parameters in a composite system by superposing the data obtained in individual simple benchmark experiments. Hence, an experimental effort is required to fill up the gap somehow.

In Fusion Blanket Engineering Benchmark Experiments at the FNS, simplified systems of composite configurations are deliberately chosen, experimental data are acquired in parametric way, then, the comparisons are made with various calculational results to point out problems associated with the heterogeneous structure and to assess the overall accuracies of the nuclear calculations.^(1,2) The accumulation of the information thus obtained serves to reduce the uncertainties in interpreting the TBR and other neutronic quantities in the conceptual reactor design, performing a complementary role to the basic benchmark experiments. This program has been selected as one of the joint activities between JAERI and U.S.DOE.

2) Experimental Arrangement

In the arrangement of the Phase-I experiments of the program now in progress, the target room #2 of the FNS is assumed to correspond to the plasma chamber of a fusion reactor and its thick concrete shielding wall to a blanket zone, of which a portion is substituted by a test module of breeding blanket as is shown in Fig. 1. The rotating neutron target (RNT) of the FNS locates at the center of the cavity and simulates the neutron producing plasma. The mixed field of direct and room wall-reflected components is assumed to represent

the fusion neutron field.

The blanket test module is installed in a large experimental hole prepared in the wall. The size of the module is 63 cm in equivalent diameter and 61 cm in length, which allows full-size simulation of radial configuration in breeding blanket. Some candidate configurations for the model module are illustrated in Fig.2.

The test module is composed by assembling blocks of rectangular prism; the basic unit length of the side is 5.06 cm. The breeding material used in the present experiment is lithium oxide of natural abundance, granules of which are cold-pressed to 75 % of theoretical density and encapsuled in a thin-walled case of stainless steel to form a block. The block structure allows modifications of the system readily by placing zones on the front, rear or inside the breeder region. The example for a heterogeneous configuration is shown in Fig.3. Neutronic quantities are measured along the central axis of the module; an experimental channel is provided for this purpose.

Main efforts are put on the measurement of tritium production rate(TPR) and neutron spectrum. New techniques have been developed to meet the requirements of this program on both on-line type and time-integrated type measurements.

3) Neutron Source

The neutron source and field characterization was performed in the first place. It is the most important part in this program, because the experimental arrangement is not so simple as those in the case of basic benchmark experiments. Measurements have been done on neutron yield, angular distribution and neutron spectra for the direct component from the RNT. Figure 4 shows the neutron spectrum emitted in the direction of test module. The spatial distribution and spectrum were measured at the surface plane of the test module to obtain the data on the contribution of the reflected component from the room wall.

Source characteristics was also numerically evaluated by Monte Carlo calculations in which rigorous configurations of the RNT and the room were represented. Good agreement was obtained between the calculation and the experimental value assuring that the Monte Carlo results could be used as the input source for the analysis in the

Phase-1 experiments.

4) Experimental Systems

Three experimental series have been conducted on different configurations so far: a) reference system, b) first-walled system and c) beryllium neutron multiplier system.

The reference system is a single-region breeder that is made up by assembling Li_2O blocks. Since the system is the most simple one, it is used as the base in estimating the effects that are introduced by adding or inserting the regions of other materials.

The first-walled system has a simulated wall layer that is placed on the front surface of the reference system. The changes of TPR distribution in the breeder region were systematically measured for four different first wall patterns that is shown in Fig.5.

In the Be neutron multiplier system, a Be layer is added to the reference system to examine the impact of the neutron multiplying material on the TPR value and its distribution. Three different configurations were composed in this series as are shown in Fig.6

5) Experimental Results

Since the data processing is still being continued, the results obtained up to now is briefly described. Figure 7 shows the tritium production rate distribution of ${}^6\text{Li}$ in the reference system measured by Li-glass scintillation method. Also given is the calculational result of DOT 3.5 R-Z model with a nuclear data set GICXFNS that is based on ENDF/B data file. As is seen, a good agreement is observed for the shape of the TPR distribution. The sharp rise in the front part is the contribution of the low energy neutrons contained in the wall-reflected component. That in the rear is due to the reflection from the back.

In the first wall experiment, the measurements of TPRs were performed successively for the five patterns shown in Fig.6 with the detector fixed at a point; then the procedure was repeated for each measuring point in the breeder region. Hence, the effects on TPRs caused by the insertion of first wall layer were obtained exactly and systematically. The ratios of the measured TPRs of the first-walled to non-walled systems are given in Figs. 8 and 9 for ${}^6\text{Li}$ and ${}^7\text{Li}$ along with the calculated results, respectively. The agreement is

fairly good between experimental and calculational values as a whole, though this calculation underestimates the slowing down effect at the first wall layer.

An example is shown in Fig. 10 on the change of the neutronic quantities by the addition of Be neutron multiplier. Here the ratios, both measured and calculated, are plotted for the TPR of ${}^6\text{Li}$ in the Be system to that in the reference at the same locations in the breeder zone. In this calculation, JENDL-3PR1 was used as the nuclear data. The comparison shows that the calculation underestimates considerably the effect of beryllium in the breeder region following the Be layer. This suggests the nuclear data on Be is to be re-examined including secondary neutron emission data.

6) Summary

Three series of experiments have been carried out in the Phase-1 of Fusion Blanket Engineering Benchmark Experiment Program. Experimental data of high relative accuracy have been obtained for three different configurations. Reasonable accuracy have been achieved in assessing the absolute values, and further efforts are being paid to narrow the range of uncertainties.

The cause of the deviation that is found between the calculated results and the measured one could be concerned with one or some of the many factors involved in the nuclear calculations, not directly related to the nuclear data. However, since the acquisition of a large body of data are pursued systematically in this program by various means, it is expected that the results are effectively utilized to assess and discriminate possible biases in the nuclear data or the calculation method used in the analysis.

References

- 1) T. Nakamura et al. JAERI-M 84-139 4.11 (1984)
- 2) T. Nakamura et al. JAERI-M 85-116 4.10,11 (1985)

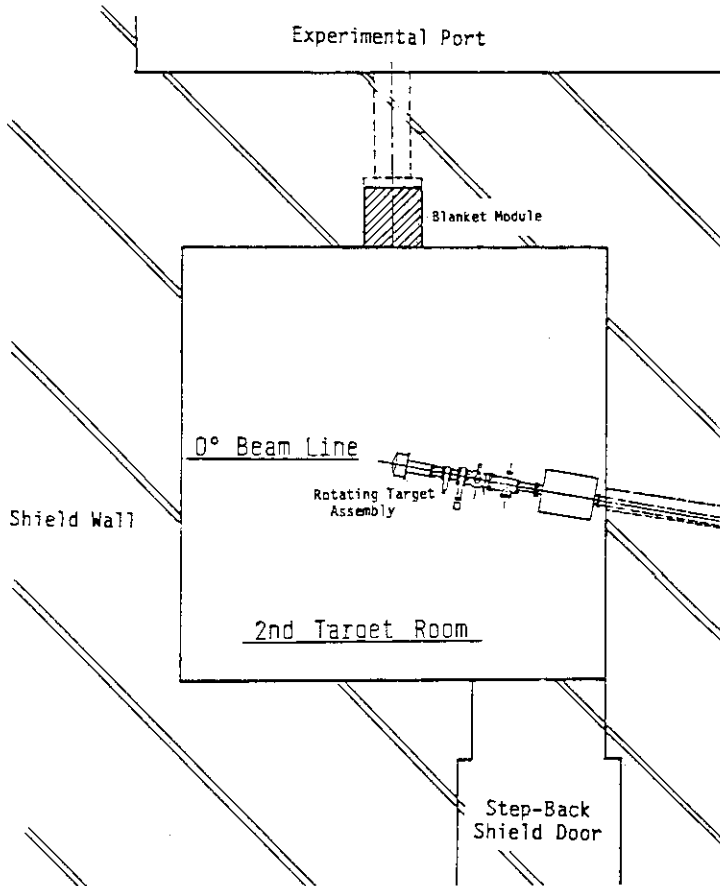


Fig.1 Experimental Arrangement

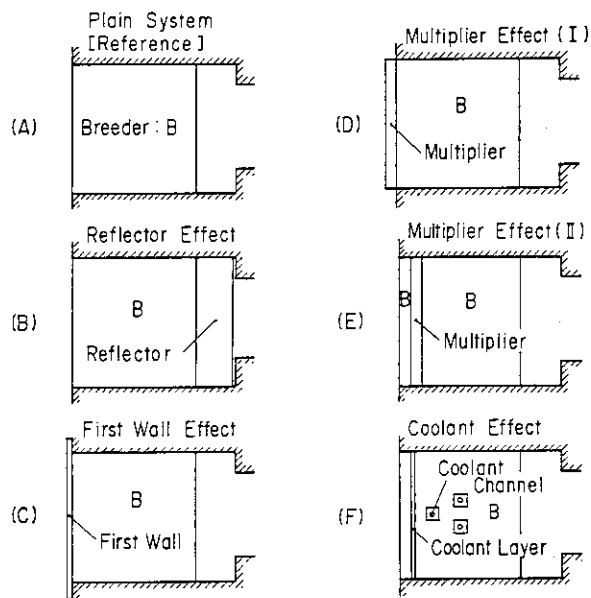


Fig.2 Schematic Drawing of Candidate Experimental Configurations

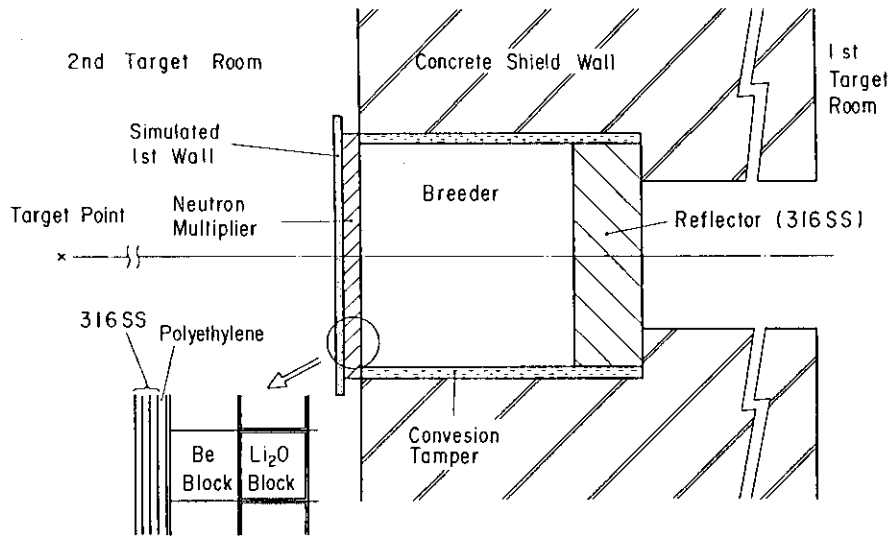


Fig. 3 Typical Configuration in 1st Phase Experiment

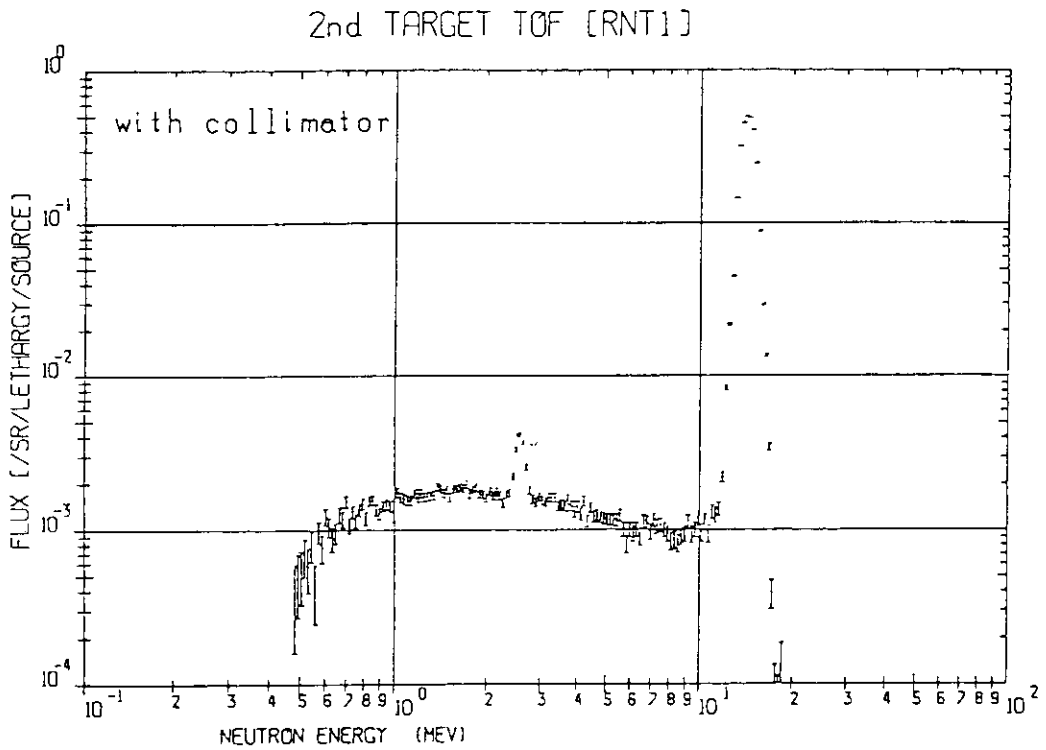


Fig. 4 RNT source neutron spectrum measured by TOF method

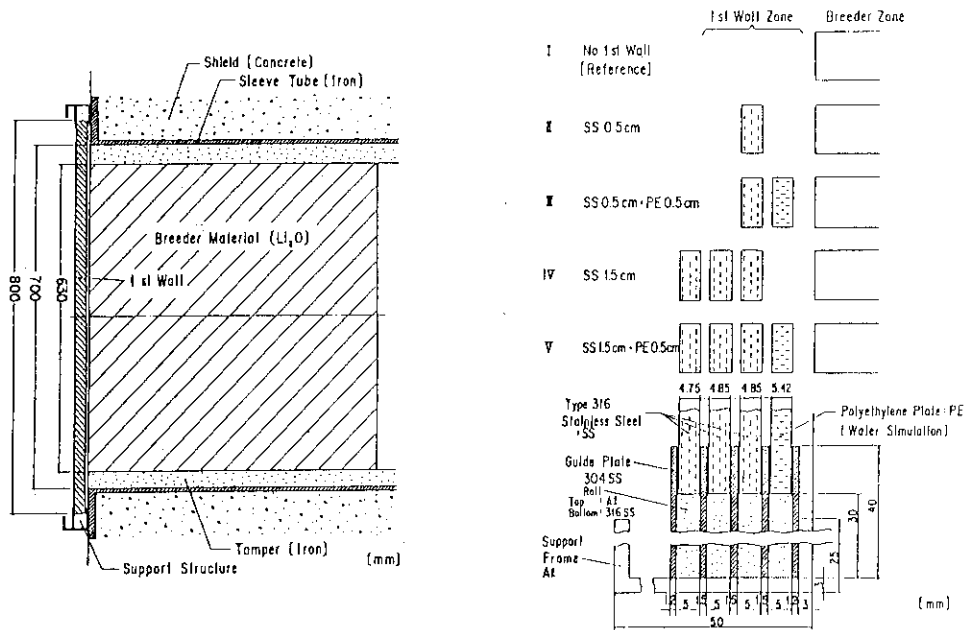


Fig. 5 Configurations for the Experiments on First Wall Effect

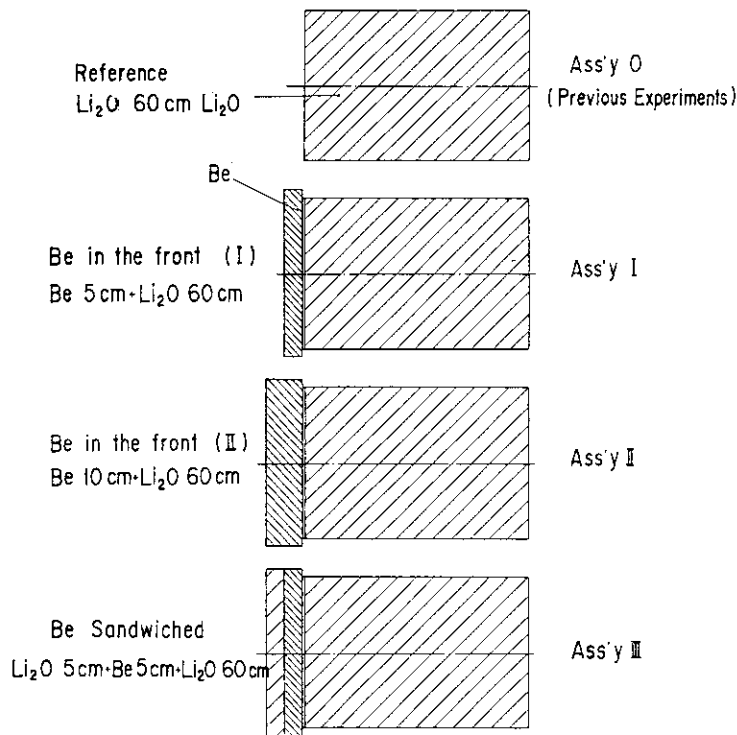


Fig. 6 Assemblies for the Experiments on Neutron Multiplier

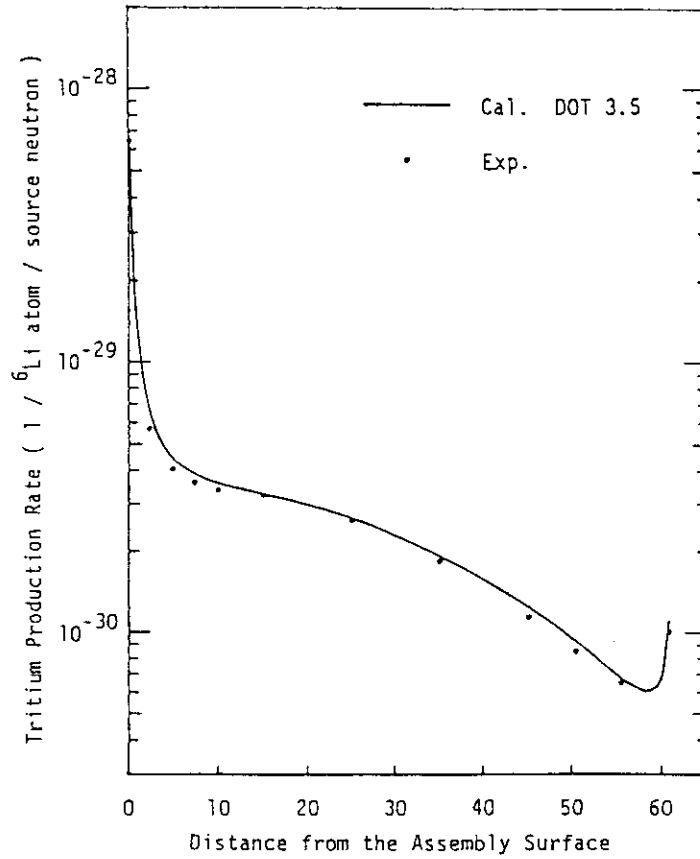


Fig. 7 Tritium production-rate distribution of ${}^6\text{Li}$ in the reference assembly measured by Li-glass scintillator method

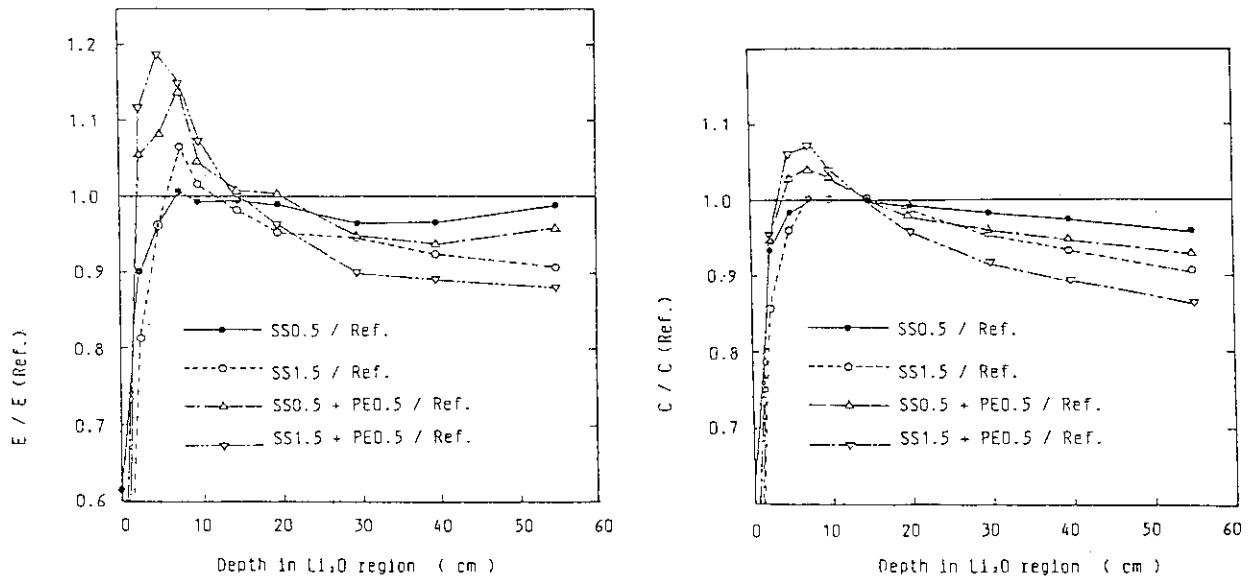


Fig. 8 Ratios of TPR for ${}^6\text{Li}$ of FW System to That of the Reference

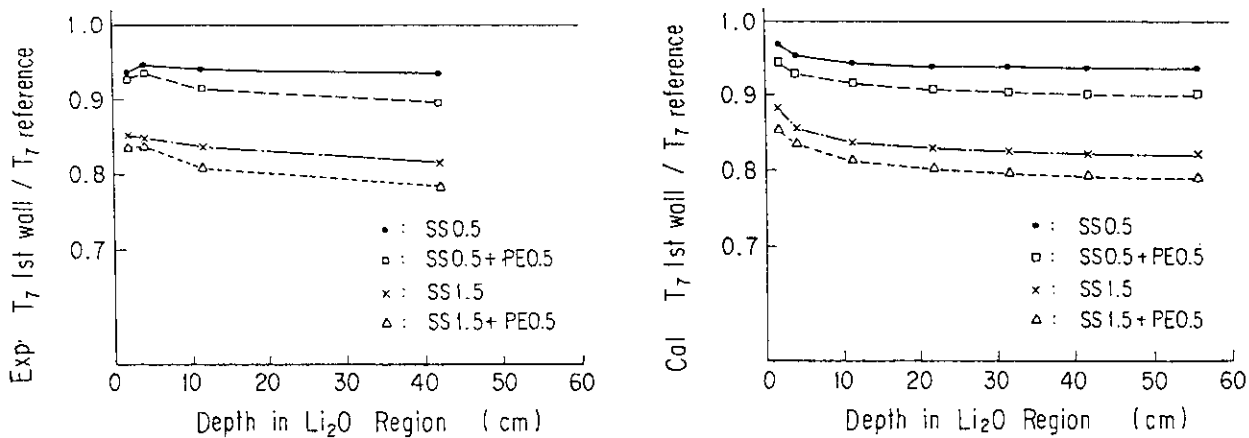


Fig. 9 Ratios of TPR for ⁷Li of FW System to That of the Reference

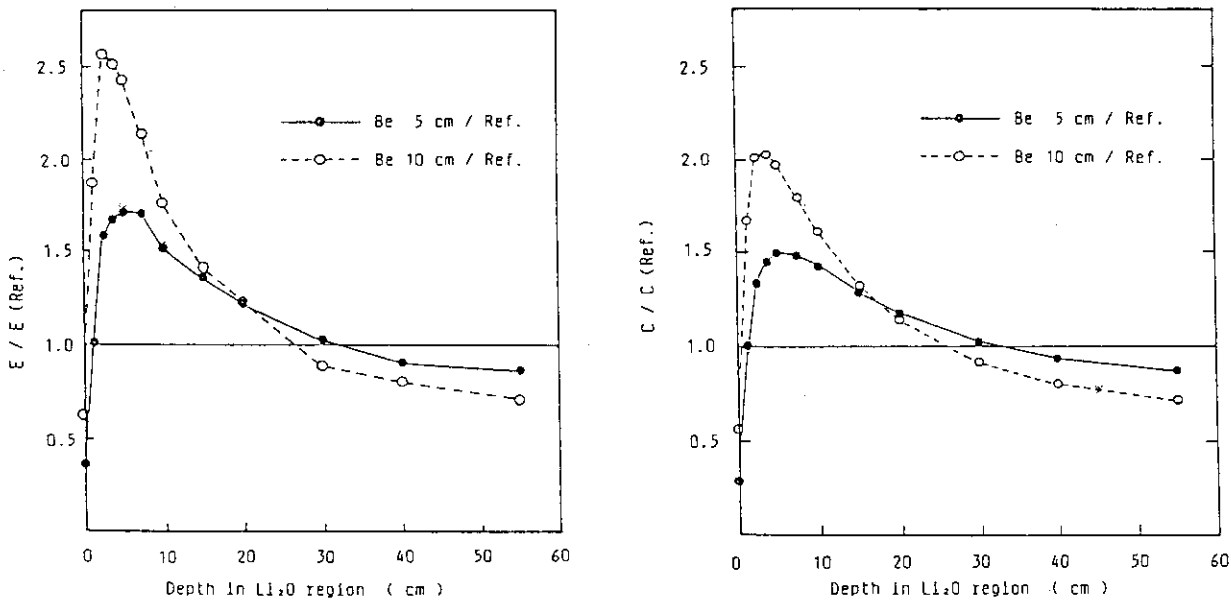


Fig. 10 Ratios of TPR for ⁶Li of Be System to That of the Reference

IV. Conclusions

1. REPORT OF SUBGROUP A

"DATA REQUEST FOR THE JENDL-3"

Group Members: Maekawa H. (leader), Sugiyama K., Baba Y., Maki K., Murata T., Takahashi A., (Sekii Y.)

The first item discussed was the priority of nuclear data to be evaluated in the JENDL-3 within our limited time and knowledge. This is summarized in Table 1. The priority depends on the point of user's field, such as neutronics, dosimetry, damage, etc. As we are primarily engaged in neutronics and/or nuclear design fields, Priorities 0 and 1 were classified by such points of view. The data of "Priority 0" are already included in the JENDL-3PRI and 2, and being examined by analysis of benchmark experiments. These nuclear data need to be checked or re-evaluated by the results of the analyses. The elements of "Priority 1" are mainly used for structural materials, superconductive magnets, neutron multipliers, and hybrid reactors. The data ^{19}F are included in this group because FLIBE is pointed out again as a candidate for blanket material.

We also discussed the status of reactions for each element. The status "S" means that present data seem to be satisfactory. It is desirable to check again, especially for higher energy region.

The main discussions were as follows:

- (1) Re-evaluation is recommended for ^6Li , ^7Li , ^{12}C , and ^{16}O .
- (2) The evaluated data on Pb are required for analysis of a benchmark experiment on Pb assembly. The ENDF/B-IV data are inadequate.
- (3) The photon production cross section for Ni, Fe, Cr, and Cu are required for nuclear design.

- (4) In the case of the hybrid reactor, photon production sections for high energy are required.
- (5) Many neutron emission cross-section data including angular distribution are inadequate or lacking.
- (6) Activation cross sections for Ca, Ti, Mn, Fe, Ni, Zr, Nb, etc. are required for both dosimetry and nuclear design.
- (7) The data of $^{12}\text{C}(n,n')3\alpha$ should be checked.

TABLE 1

Nuclear Data Needs and Status for Fusion Neutronics Study

Nuclide	Priority	σ_{tot}	$\sigma_{\text{n,em}}$	$\sigma_{\text{n,2n}}$	$\sigma_{\text{n,charge}}$	$\sigma_{\gamma,\text{em}}$
¹ H	1	S	S			
² D	2	S	C	S		
³ T						
³ He	3	C	C			
⁴ He	3	C	C			
⁶ Li	0	C	C	C	C	
⁷ Li	0	C	C	C	C	
⁹ Be	0	C	U	U	C	
¹⁰ B	3	S	U			
¹¹ B	3	C	U			
¹² C	0	C	C		C	
¹⁴ N	0	C	C	C		
¹⁶ O	0	C	U		C	
¹⁹ F	2	C	U	U	U	
Na	3	S	U	C	U	
Mg	4	C	U			
²⁷ Al	1	S	C	U	C	
Si	1	S	U		C	
P	4					
S	4					
Cl	4					
Ar	4					
K	3	S	U			
Ca	1	S	U			
Sc	4					
Ti	3	S	U	U	C	
V	2	S	U	U	C	
Cr	0	S	C	C	C	C
Mn	2	S	U	C	C	C
Fe	0	S	C	C	C	C
Co	4					
Ni	0	S	C	C	C	C
Cu	1	S	U	C	C	C
Zr	2	S	U	C	C	
Nb	2	S	U	S(C)	C	
Mo	3	C	U	U	C	
*Sn	2	S	U	U	C	
Ag	4					
Cd	4					
Sb	4					

TABLE 1 (Contd.)

Nuclear Data Needs and Status for Fusion Neutronics Study

Nuclide	Priority	σ_{tot}	$\sigma_{n,em}$	$\sigma_{n,2n}$	$\sigma_{n,charge}$	$\sigma_{\gamma,em}$
Eu	4					
Hf	4					
Ta	4	S	U	U	C	
W	2	C	U	U	C	
Pb	1	C	U	U	C	
Bi	2	C	U	U	C	
²³² Th	2	S	U	U		
²³³ U	2	S	U	U		

Legend

Priority 0: Included in the JENDL-3PR1 and 2; however, it is desirable to check or re-evaluate.

1: Evaluations are needed as soon as possible.

2: Evaluations are needed within six months.

3: Evaluations are needed within one year.

4: To be included in the JENDL-3.

Status S: Present data appears almost satisfactory.

C: Data checking is required.

U: Uncertain; data inadequate.

Blank: No status was discussed.

*There are no plans for this element to be evaluated in JENDL-3.

2. Report of Subgroup B:

WORKING GROUP B) ON THE PROBLEMS OF JENDL ENCOUNTERED IN THE EXPERIMENTAL ANALYSIS, IN THE PROCESSING OF GROUP CONSTANTS AND OF THE FORMAT SPECIFICATIONS

discussion members

ASAMI Testuo

HASEGAWA Akira (group leader)

IGRARASHI Sin-iti

IKEDA Yujiro

KANDA Yukinori

MORI Takamasa

NAKAGAWA Tsuneo

NAKAZAWA Masaharu

1. Introduction

The Working Group on the problems of JENDL encountered in the experimental analysis, in the processing of group constants and of the FORMAT specifications prepared a working group report identifying the problems revealed through this meeting and identifying the recommendations in order to remove these problems or to improve the data quality.

The materials covered in the discussions are very wide from the detailed technical problems to the compilation philosophy of JENDL. And some materials in the recommendation will affect the functions of the board of JNDC (Japanese Nuclear Data Committee).

2. Necessity of error assignment in every steps from nuclear data to experimental analysis

Because errors are inevitable in every steps in the calculation of the experimental analysis, it is necessary to quantify the error involved in each step.

example:

steps

Experiment (experimental accuracy)

Nuclear Data (Data accuracy)

Processing of group constants (processing accuracy)

Modelling for the experimental analysis (Modelling accuracy) Trans-

port calculation (calculation accuracy)

C/E (prediction accuracy==> this depends on all accuracies described above)

3. Preparation of common group constants for the comparisons of common basis

It is requested to prepare common group constants library so as to be used commonly in the fusion community based on JENDL library i.e., JENDL-2, -3 PR1 and -3 PR2. For the moment, as seen from the presentation by A.Hasegawa, processing code and the evaluated data file are tight coupled, thus it is necessary to produce the group library using the authorized processing method or code for the persons not available these codes.

Although for the actual productions, the details of the work such as the man power allocation or the specification of the group library should be left for the adhoc-committee, it is recommended basically to make a group library of about 125 groups similar to the GICXFNS which is frequently used in the fusion community now. And at the same time there is a suggestion to produce two libraries using different weighting functions, (i) Thermal:Maxwell, $1/E$ (or flat), 14-MeV peak (ii) typical realized flux in Li2O assemblies, the former is for the experimental analysis and the latter is for the application oriented one such as for the design of blankets.

4. A handy book summarizing know-hows of using the transport code

It is recommended to summarize know how or utilization technics of transport code in a handy book. Especially for the elementary use of these code, it is necessary a handy book describing the experiences about the parameters which affect the results considerably such as mesh size, P1 order, group structure, Sn order,..etc in the case of actual calculations.

5. Comments for the processing code

It is recommended to perform cross check of the processing codes. And also it is necessary to quantify the processed errors introduced by the numerical calculations. But the processing errors except the effect from weighting functions can be quantified up to some extent.

The group constants production methods, such as selection of weighting functions or selection of group structures..., are probably

the theme for eternal.

6. Problems encountered in the processing of current JENDL file, i.e., JENDL-2, -3 PR1 and -3 PR2.

The detailed discussions were given in the presentation by A.HASEGAWA in the session II. Here only summary is given.

(1). Problems relating to FILE2 : Resonance parameters

a. RESOLVED RESONANCE RANGE

i). J-unknown state problems for MLBW (Multi-level Breit Wigner) formulae.

So many nuclides.

ii). Two resolved resonance range definition.

For Fe-natural of JENDL-2.

b. UNRESOLVED RESONANCE RANGE

i). Floor cross-section for fission MT=18 data for JENDL. UNRESR accepts only MT=19 floor cross-sections for fission.

ii). Problem by detailed floor cross-sections definition finer than the unresolved energy node points.

example: U-235 JENDL-2 (MAT=2923)

iii). Sparse energy node points problem for UNRESR.

In some case, interpolation of the resonance parameters is made. It is forbidden.

iv). Resonance energy range un-matching in isotopes composing of natural element.

Example: Mo natural of JENDL-2.

n.b. in the above expression, i). to iii). are for the problem of UNRESR (NJOY).

(2). Problems relating to FILE4 : Angular distributions

(i). Too much precise File4 angular distribution data

It is recommended in inelastic cross-sections that if anisotropy is less than 5 %, give them as isotropic one.

(3). Problems relating to FILE5 : Energy distributions

(i). Consistency between the energy mesh in the partial sections

In JENDL file, the energy distribution data are frequently

represented by several partial sections, and the energy mesh for each partial sections should be given by the same energy mesh. JENDL violates this law in several times.

- (ii). Representation for the exit neutron energy distribution function

All secondary energy distribution must start and end with zero values for the distribution function. JENDL file sometimes violate this regulation.

- (4). Problems relating to FILE6 : Energy-Angular distributions

In JENDL-2, -3 PR1, -3PR2 files, the adoption of FILE6 data are actualized for the first time in the world. But mixed use of FILE6 data and FILE4 & FILE5 data for the same reaction is taken. But this is a violation to the rule of data uniqueness. Therefore if the FILE6 data are given for some reactions, no data should be given for FILE4 and FILE5.

7. Recommendation for the protocol of JENDL

- (i). Acceptance as JENDL file for an evaluation data

The each evaluated data accepted as JENDL library should be authorized by the relevant board of JNDC (japanese Nuclear Data Committee) by considering the quality of the evaluations submitted by the author. Up to now, an evaluation performed by the author nominated as JENDL file evaluator is automatically called as JENDL file without any authorizations by the board. In some case there exists the evaluation called as JENDL only by the author but not known to the Nuclear Data Center.

- (ii). Problem for the publication of numerical data in a report

It is requested to examine the merit and the demerit in the internal board of JNDC on the publication of the numerical data of evaluations i.e., publishing the listing of a file itself of an evaluation in a report. Recently the evaluated data file is regarded as strategic materials and the availability of the numerical data becomes very difficult. According to these circumstances the numerical data exchange becomes very difficult internationally as seen in the case of ENDF/B-V.

Thus following rather radical opinion is put out in the discussions.

The publication of the numerical data in a report should be avoided, only analogue data like curve in a graph or average values should be allowed. The numerical data must be placed uniquely under the control of the Nuclear Data Center as far as the evaluations named as JENDL data. If this system is adopted then all administrative informations like the data history or revision history or history of data dispatch to the users are completely known to the Center. Therefore JENDL data are uniquely controlled by the Center. But at the same time, the right of numerical data exchange by private communications for the authors of the evaluations should be also protected.

(iii). Opening of JENDL for the general users

It is necessary to clarify the general rules for opening of JENDL file in some board of JNDC. And also there should be an authorization committee for the opening of processed group constants from JENDL file.

(iv). Protocol of JENDL for the general users

- a. Center retain the right to get the feed-back informations when the JENDL data (evaluated data or group constants) are transferred to some users. Thus the user should report the feed back informations to the Center.
- b. User should make a description on the use of JENDL data in any publications as long as JENDL data are used in the results.
- c. It is better to use the name easily understandable to be used the JENDL file for the group constants generated from JENDL-file, for example using the prefix name of JDL etc. And also it is better to inform the generated library name to the Center.

8. Problems on the file making and FORMAT

(i). Necessity for the physical checks for the opening

As both of JENDL-3 PR1 and PR2 are not opened through the official route, physical check and FORMAT check were not completely performed. It is requested to be checked carefully both in format and in physics for the opening through the official route in JNDC.

(ii). Naming of JENDL-3 PR1 and PR2

Naming of JENDL-3 PR1 and PR2 is frozen for the available version

of the two. That is, JENDL-3 PR2 is a version containing Li6, Li7 and C are newly revised ones and the other is the same as in the JENDL-3 PR1 file.

(iii). Recognition of JENDL-3 PR1 and PR2 file

Up to now there are no explicit information about the version identification in the file itself. From now on for the recognition of these version, a mod-field (modified field) index in file1 is used.

(iv). Uniqueness of the route for the information about JENDL

All of the information about the data opened for the publics such as the status of the evaluations, anticipated completion date for the evaluation under progressing, data availability or data file name in the computer, etc., should be completely known to the users uniquely through the Center. For this purpose, computer managements for these information might be required. Although there exists a publication of NUCLEAR DATA NEWS in every 4-months from Nuclear Data Center but it may not be sufficient for the latest information sources. And the current situations of under progressing evaluations should be carefully watched by the working group of file creation of JENDL.

9. Recommendations for forthcoming JENDL-3 file

(i). FORMAT system to be adopted

It is recommended to adopt ENDF/B-VI FORMAT system so as to compete with other new data appearing in the same format, i.e., ENDF/B-VI, JEF or EFF. For the users not acceptable of B-VI format, it is also recommended to produce files of ENDF/B-V FORMAT system. The former is regarded as an official file of JENDL-3 and the latter is produced only for services to the old users.

(ii). No Mixing use of FILE6 and FILE4 & FILE5 for the same reaction data

Mixed use of FILE6 and FILE4 & FILE5 for the same reaction taken in JENDL data is now completely forbidden by the violation of the uniqueness of the data representation.

(iii). Recommendation for using of FILE6 representation

It is strongly recommended to use FILE6 (energy-angular) representa-

tion instead of FILE4 & FILE5 one for the reactions requesting to use its representation. Because by using of FILE6 representation, the actual physical process is presented more precisely. But at the same time for the users who want to use old processing codes, it is also recommended to prepare a service file with no FILE6 data, i.e., composed from FILE4 & FILE5 representation. That is two files are prepared, as an official file where FILE6 representation is taken with ENDF/B-VI FORMAT, as a service file where FILE4 & FILE5 representation is taken with ENDF/B-V FORMAT. This option is taken because several time delay should be inevitable for the acceptance of the FILE6 processing in a majority of the processing codes.

(iv). J-unknown state assignment in MLBW (Multi-level Breit-Wigner) resonance parameters

It is strongly recommended to abandon the problematic adoption of J-unknown state definition in MLBW which is a origin of a greater confusion of the processing code to be used for JENDL processing up to now. In the evaluation for the level of J-unknown states, some value should be assigned by the evaluator to avoid the ambiguity.

(v). Request for the evaluaters about the compilation of the evaluated data

When an evaluator perform the evaluation of some materials it is always requested for him to remind the design philosophy of the evaluated nuclear data files of 'completeness' and 'compactness'. That is, the data represented in the evaluated file should be given as practical/simple as possible. Don't give the data in a complicate way.

(summarized by A.HASEGAWA)

3. Report of the Working Group C on the Feedback of Information from Neutronics Experiments and Their Analyses

Chiba, H.	Nakajima, Y.
Hashikura, H.	Nakamura, T.(chairman)
Iguchi, T.	Oyama, Y.
Kanda, K.	Yamamoto J.

I. Introduction

This working group discussed how to feed the information obtained in the differential or integral neutronic experiments and their analyses back to the data evaluation of JENDL 3. It is often mentioned that the effective communication should be encouraged from the users of the data in neutronics to the nuclear data people. So far, the communication has been limited rather to the private basis and not necessarily well oriented. As the number of experiments, hence, the application of JENDL 3PR to them increases, a better treatment becomes necessary for the efficient and systematic information exchange. The present meeting is the first step toward the goal.

II. Proceedings

Firstly, each member of the working group presented his view point on the subject concerned with his speciality, and then discussion followed on the issues brought up in it. Naturally opinions were diverse and it is not so easy to summarize them as the group consensus. Major points that were talked over during the meeting are summarized in the following.

1) Double differential cross section

In the case of DDX experiment and the analysis, the feedback of the results is rather straightforward. They are directly to be compared with the evaluated nuclear data of interest, and the degree of the agreement in energy and in angle provides useful and direct measure on the accuracies of the evaluation. In fact, the DDX data of Osaka University and Tohoku University had been made most use of in the evaluation of JENDL 3PR1 and 2. It was agreed that DDX experiment should be encouraged more, in wide neutron energy range. It is important, however, to minimize experimental uncertainties; measurements around 0 and 180 degrees are especially difficult. It would be not practical to cover the whole energy and angle by experiment. Rather the DDX data should be utilized to check the evaluation at selected parameter points.

2) Integral benchmark experiment

Integral experiment is concerned with a bulk media; incident neutrons suffer multiple scatterings and the neutron field of broad energy spectrum is formed in the medium. As a matter of fact, the interpretation of experiment and their analysis in view of nuclear data is not as direct as the DDX case, and so is the feed back.

a) TOF experiment in a bulk system

This category of experiments uses the same measuring techniques as in 1), but the size of the system is by far larger than DDX samples, hence it covers wider and continuous energy range in the neutron field. It plays a complementary role to the DDX experiment. Uncertainties are introduced, however, relating to the numerical method of neutron transport, calculational modeling and processing for nuclear data set, if multi-group method were applied, in the comparison of experimental results with the analyses. So, proper care should be taken in referring the results in nuclear data evaluation. Evaluators consider the data in this category are also helpful. The data from the spherical shell experiments at LLL and Oktavian as well as the slab geometry experiment at FNS were utilized in the preparation of JENDL 3PR1 and 2.

b) Integral experiment in a bulk system

Different from the experiment of type a), most of measured quantities are integrated ones over neutron energy in this type of experiment. The experimental value contains cross section information on both the media, i.e., neutron field and on the detector itself. Since nuclear data contribution is folded into one with pertinent weight, it has direct meaning regarding to the quantity of interest such as tritium production rate; it has better experimental accuracy, in general, compared to differential data. In this meaning, the results of integral experiments can be used in verification of the accuracies in evaluated nuclear data. It is important, however, to assess the uncertainties included in the calculated results regarding to the factors mentioned above in a) in the comparison. Extensive works have been conducted in Oktavian and FNS experiments and their analyses. Full utilization of the data in this category is yet to come hereafter.

Most of the discussions were developed on integral experiments.

It was pointed out that the objectives of integral experiments be various. Other than the verification of nuclear data, they include:

- i) examination of calculational method of neutron transport,
- ii) examination of modeling in the calculation,
- iii) establishment of measuring techniques, and
- iv) mock up to assist the nuclear design.

It is required, therefore, to clarify the objectives and the degree of concern to the nuclear data involved in presenting the results of an integral experiment and its analysis.

To examine nuclear data, pertinent design of the experiment is important so as to make the effect of the nuclear data of interest on the measured quantity maximum, while the uncertainties associated to other factors to be minimum. Point Monte Carlo calculation and an experiment suitably designed for that was mentioned of as an example. It was also emphasized that good accuracies of the experimental values be essential.

Opinion was divided in regard to the usefulness of integral experiments for the verification of nuclear data in the area of fusion neutronics. Some were positively in favor of integral experiments, while one of the members gave limited value on them. He had an opinion that accumulation of DDX data be able to solve nuclear data problem related with fusion; the information from fission field could cover the lower energy range.

Views were exchanged on the necessity of the systematic analysis for integral experiments of various types in different organizations. Property common to them can be extracted by doing so excluding possible biases associated with individual experiments. Sensitivity analysis should be encouraged to interpret them. It is, however, questionable whether data adjustment method is as effective in fusion neutronics as it was in fission case.

To make comparisons and evaluations of the data in different organizations more convenient, it was proposed that a reference nuclear data set be prepared basing on JENDL 3PR2 and be used as a common set along with the one characteristic to individual organizations. Admitting the convenience brought in by it, there was an opinion that its introduction be considered deliberately so as not to interfere with the individuality and uniqueness of each experimental plan or organization.

It may occur at times that the same type of experiments in different laboratories show somewhat different results and conclusions giving a confusion to the evaluator in charge. In that case, it would be necessary to examine the data and make an adjustment between experimenters themselves prior to leave them to nuclear data group.

A question was raised whether a system be necessary to coordinate the communication between groups and manage the issues mentioned above. Opinion was diverse and no definite plan was proposed.

III) Recommendations

1) As JENDL3 Preliminary Version is still an intermediate stage to Nuclear Data File JENDL-3, its users should cooperate to the improvement by the feedback of the results obtained through its use in order to make the final version more reliable.

2) In reporting data obtained by an integral experiment, the nature of the experiment, the degree of contribution due to nuclear data separated from other factors and the accuracy of the data should be explained as clearly as possible.

3) The feedback of the data is to be made through proper publications or technical meetings. By the involvement of other people, the action can be treated more objectively avoiding personal bias and exact information transfer can be achieved within the people concerned in fusion cross section and neutronics. So, the holdings of technical meetings like the present one should be encouraged.

4) Upon a consensus of a number of groups, a reference cross section set is recommended to be settled for major nuclides used in fusion neutronics to facilitate the comparison of the results of experiments and their analysis in various groups.

5) Examination of the quality of the data is advisable through the discussions with other related neutronics groups before the data is supplied to nuclear data group as recommendation or reference for modification.

6) Lastly and most important, every neutronics group should make best efforts to provide high-quality data to support the completion of JENDL-3.

4. Discussion on Summary Reports from Three Working Groups

Nakazawa, M. (chairman of session)

Dr. H. Maekawa, the leader of working group on " Data Request for the JENDL-3 ", has given their summary table on " Nuclear Data Needs and Status for Fusion Neutronics Study ", where the nuclear data of fusion relating 48 nuclides have been classified from two points of view of present uncertainties and priorities for re-evaluation.

Several comments have been made from nuclear data evaluators on the present schedule of re-evaluation of these nuclear data.

Dr. A. Hasegawa, the leader of working group on " Problems of JENDL Encountered in Experimental Analysis ", has pointed out many problems and recommendations of current JENDL file. General discussions for the improvements of comparison procedures between experiments and their analysis calculations have been made on several points such as (1) necessity of all uncertainty assignments not only in experimental data but also in every calculational results, (2) standardization of calculational procedures basing on common group constants and on common utilization techniques of actual neutron transport codes.

Dr. T. Nakamura, the leader of working group on " Feedback of Information from Neutronics Experiments and Their Analysis ", has stated that their hot discussions have been made on how to extract and transfer useful informations from integral neutronic experiments for nuclear data verifications. Two important conclusions have been that (1) the discrepancies between integral experiments and their analysis should be analysed as clearly as possible to separate the degree of contribution due to nuclear data from other factors, and (2) the feedback of these information

should be made through proper publications or technical meetings like present one in order to avoid systematic error or personal bias, when some confusing results have been reported for the same type of experiments and their analysis.

Throughout these discussions, necessity and importance of quantitative estimates of uncertainties (accuracies) have been strongly impressed in many fields of nuclear data, experiments and calculations, and also design goal of fusion reactor blanket neutronics. This impression and following actions are expected to encourage more efficient and fruitful discussions among relating researchers. And as a whole, this meeting is concluded to be the first step toward the goal and to be a good mile stone also for the 1988 International Symposium on Nuclear Data to be held in JAPAN.

Plenary Discussions

S. Igarasi and T. Nakamura

A session for free discussion followed the summary reports presented by the group leaders. Many items omitted in this meeting and to be discussed in future meetings were pointed out. They were problems on neutron spectra in some block samples, problems related to the scalar flux, dosimetry, activation and gamma-ray.

Necessity of quantitative presentation for the target accuracy of the nuclear data was discussed. Since requirements of the data accuracy were strongly dependent on different blanket design systems, appropriate benchmark problems should be proposed in order to make sensitivity analyses. The meeting suggested that the fusion neutronics community should set the benchmark problems to explore the nuclear data of which accuracy has influence on the calculations. To clarify that the requested accuracy is achieved, needed is proper methodology with which degree of the achievement is definable. Including this, the meeting asked the community to define the ways of feedback from the benchmark tests to the nuclear data evaluation and measurement.

There was a question about release of the JENDL-3PR1 and JENDL-3PR2 as well as their definition. Some confusions had been occurred in the data users since the JENDL-3PR2 appeared. Definition of the latter was not always clear to many users. A reasonable management system is needed in order to avoid vain confusion and notify smoothly the community of revision of the evaluated data and library. Anxiety was expressed that some information was restrained from circulation, if the management system bound the exchange and circulation of information rigidly. Data and information should be released freely, but exchange of data or information between

individuals would often cause confusion. The meeting suggested that some reasonable rule concerning exchange of information, release of data, revision of evaluated data library, etc. needed to be established.

It was stressed that the nuclear data measurements should be stimulated further in Japan. Double differential cross sections at 7 and 14 MeV have been accumulated. In addition the data between these two energy points are needed. Experiments with the JAERI Tandem accelerator were expected. At present, measurements between 5 and 6 MeV are scheduled at JAERI. The measurements will be expanded gradually to higher energy region in future.

This meeting was the first big occasion that the specialists of nuclear data and their application in the fusion field gathered and exchanged the opinions frankly from the various stand points. The meeting worked effectively to deepen the understanding of the present status in data evaluation, cross section measurements, integral experiments and data needs from the design work in relating to the JENDL-3. It was generally agreed that information exchange and collaboration in this community should be encouraged further. This would be promoted by holding meetings like the present one, for example.